The mechanism of *grk* mRNA localisation during *Drosophila* oogenesis

Nina MacDougall

PhD Thesis
The University of Edinburgh
December 2003

For my parents

ABSTRACT

Cell polarity and identity play important roles in the development of many organisms and the correct localisation of key proteins is vital for proper functioning of multicellular systems. mRNA localisation within the cell provides an important means of delivering proteins to their correct site of function within the cell cytoplasm. The importance of mRNA localisation was first shown almost two decades ago in Ascidian embryos, where the majority of β-Actin mRNA accumulates in the myoplasm. In chicken fibroblast cells Actin mRNA is localised to the leading edge of the cell, later shown to be essential for cell motility. Further studies include yeast and many multicellular organisms, such as *Xenopus*, protozoa, plants and *Drosophila melanogaster*. *Drosophila* development is regulated utilising asymmetric mRNA localisation on many levels and provides the first symmetry-breaking step in the development of the unfertilised egg. In recent years several examples have emerged of mRNA localisation by directed transport along microtubules or Actin using cytoskeletal motors. However, the details of the mechanisms of RNA movement have not been understood fully.

This thesis provides exciting new evidence for the mechanisms of mRNA localisation during *Drosophila* oogenesis and shows that the RNA encoding one key developmental regulator, *grk* mRNA, uses multiple steps involving motor proteins that transport the cargo along ortholog populations of microtubules within the oocyte. Similar mechanisms of transcript localisation are likely to be utilised by many other key mRNAs during many stages of development and by diverse organisms.

DECLARATION

I hereby declare that this thesis is my own work and the experiments described in it were performed by myself, unless otherwise stated. All work was carried out at the Institute of Cell and Molecular Biology, University of Edinburgh.

ACKNOWLEDGEMENTS

I would like to thank my supervisor, Ilan Davis, for all his help and tremendous support during my time as a PhD student and for his encouragement and enthusiasm for science, which helped me so much over the past four years. I would also like to thank my second supervisor, Andrew Jarman, for encouragement and support. I am indebted to the Darwin Trust for their generous financial support during my PhD.

I am grateful to my fellow lab members of the Davis lab. In particular, I would like to thank Hille Tekotte for many fruitful discussions and advice, Alejandra Clark for all the help and the never-ending enthusiasm, which helped me so much with the difficult task of particle analysis and more, Veronique for invaluable advice and knowledge, Renald, Isabel and Richard. I would also like to thank all members of the Jarman lab for advice and also the most interesting information exchange.
I am indebted to members of the Ish-Horowicz lab for invaluable advice and reagents and flystocks, Tom Hays, Trudi Schüpbach and Richard Fehon for flystocks and reagents.

Finally I would like to thank Colin for never giving up hope and listening patiently to my endless complaints about the difficulties of writing, Lena for being perfect and all smiles and pure happiness, and my family and parents, without whom this thesis would have never been finished.

TABLE OF CONTENTS

LIST OF FIGURES AND TABLES

Following Page

ABBREVIATIONS

bcd	*bicoid*
BicD	Bicaudal D
bp	base pair
BRE	Bruno response element
βgal	beta-galactosidase
cDNA	complementary deoxyribonucleic acid
DAPI	4, 6-diamidino-2-phenylindole
DIC	Diffraction interference contrast
DIG	Digoxygenin
Dhc	dynein heavy chain
Dlc	dynein light chain
DNA	Deoxyribonucleic acid
ds	double stranded
EDTA	Ethylenediaminetetraacetic acid
EGF-R	epidermal growth factor receptor
Egl	Egalitarian
EJC	Exon-exon junction complex
EMS	ethyl methane sulphate
Exu	Exuperantia
Flp	Flipase
FRT	Flipase-recognition target sequence
fs	female sterile
ftz	*fushi tarazu*
GFP	Green fluorescent protein
grk	*gurken*
hb	*hunchback*
HRP	Horse radish peroxidase
Hsp	heat shock protein
Kb	kilobase(s)
KDa	kilo Daltons
khc	Kinesin heavy chain
klc	Kinesin light chain
l	lethal
lacZ	beta-galactosidase

mRNA	messenger ribonucleic acid
MT	Microtubule
MTOC	Microtubule-organising centre
mm	millimetre
mM	milliMol
μm	micrometre
ml	millilitre
μl	microlitre
NA	Numerical aperture
NGS	normal goat serum
nls	nuclear localisation signal
nl	nanolitre
nM	nanoMol
osk	*oskar*
PBS	phosphate buffered saline
PBT	PBS/0.1% Tween 20
PBTrx	PBS/0.3% Triton-X 100
PCR	Polymerase chain reaction
pl	picolitre
RNA	Ribonucleic acid
RNAse	Ribonuclease
rpm	Revolutions per minute
RT PCR	reverse transcription PCR
ts	temperature-sensitive
TSA	tyramide signal amplification
TGF-α	Transforming-growth factor alpha
Tris	Tris(hydroxymethyl)-amino-methane
Triton-X 100	Octylphenoxypolyethoxyethanol
Tween 20	Polyoxyethylene sorbitan monolaurate
UV	Ultraviolet
wg	*wingless*
3'UTR	3' untranslated region
5'UTR	5' untranslated region

1

INTRODUCTION

Cytoplasmic mRNA localisation has been shown to be an important mechanism of posttranscriptional gene regulation in many, if not all organisms. Localised mRNAs have been found in many different cell types throughout the animal kingdom, as well as in plants and yeast. During development, mRNA localisation establishes polarities within cells and fulfils important functions in the correct formation of the perpendicular axes. Over 90 localised mRNAs have been found so far with most of them being characterised in *Drosophila* oocytes and embryos, as well as *Xenopus* and yeast. In recent years, considerable progress has been made in the understanding of the mechanisms through which mRNAs are localised. They include the diffusion and anchoring of transcripts as well as selective degradation and protection of mRNAs and motor driven transport along the cytoskeleton. The models proposed for mRNA localisation mechanisms are not mutually exclusive and it is likely that localisation involves multiple steps utilising the proposed mechanisms in concert. Furthermore, transcript localisation involves cis-acting sequences as well as trans-acting factors and directional transport also involves proteins which function as linkers between the RNA complex and the motor protein.

The establishment of cell polarity and cell identity are key aspects of the development of all organisms. One important mechanism used to define regions within the cell is the sorting of proteins and nucleic acids to their site of function within the cytoplasm (St Johnston, 1995). Over the past two decades, asymmetric RNA localisation within the cytoplasm has been detected in many different cell types, and it is likely that it occurs in most, if not all polarised cells (Palacios, 2001). Most asymmetrically localised RNAs have been found in oocytes and embryos of which *Drosophila* has the best-studied system.

Approximately 10% of randomly chosen cDNAs have been found to recognise asymmetrically localised transcripts in *Drosophila* oocytes (Dubowy and Macdonald, 1998). In *Xenopus laevis* oocytes, about 25 mRNAs have been found to localise asymmetrically. At least nine mRNAs have been shown to localise to the vegetal pole of the oocyte. One of them, *Veg-T* mRNA is required for the determination of the endoderm (Mowry and Cote, 1999). It regulates expression of mesoderm inducing factors, such as *derriere* and *Xnr-1, 2* and *4* (Clements et al., 1999; Kofron et al., 1999; Hyde and Old, 2000). Other vegetally localised mRNAs, such as *Xwnt-11* and *Vg1* have been suggested to play a role in axis formation and patterning, although this has not been tested directly. When injected elsewhere in the embryo, however, they have been shown to affect patterning (Ku and Melton, 1993; Thomsen and Melton, 1993). In Ascidians, a number of mRNAs have been shown to localise to the vegetal pole of the egg, then segregate asymmetrically during divisions to become localised in the embryo (Swalla and Jeffery, 1996; Yoshida et al., 1996; Satou, 1999). One of these, *macho1*, has recently been shown to be a determinant for muscle development (Nishida and Sawada, 2001).

The localisation of mRNAs to specify polarities and deposit cytoplasmic determinants has been shown to be required in many different organisms, suggesting that some of these mechanisms are part of a conserved pathway. In *Drosophila*, *nanos* mRNA localisation at the posterior pole of the embryo specifies the development of the pole cells (Ephrussi and Lehmann, 1992), (Forbes and Lehmann, 1998). Three Nanos homologues have been found in *C.elegans* and two of them appear to function in similar ways to Nanos (Shisa et al., 2001). Furthermore, *Xcat-2* mRNA, localised to the vegetal pole in *Xenopus,* associates with the terminal granules and has similarities to *Drosophila* Nanos on the protein level (Mosquera et al., 1993; Kloc and Etkin, 1998; Kloc et al., 2000). Another mRNA, *Xdazl*, also shows localisation to the vegetal pole and has been shown to be involved in the differentiation of the Polar granule cells (PGC). In Ascidian and zebrafish, homologues to the *Drosophila* posterior determinant Vasa have been shown to be localised as mRNAs and be segregated into the germline Olsen et al., 1997; Yoon et al., 1997; Fujimura and Takamura, 2000).

In *Drosophila* the localisation of maternal transcripts during oogenesis initiates both the anteroposterior and dorsoventral axes of the future embryo. Thus, mRNA localisation appears to play a major role in the symmetry breaking steps within the unfertilised *Drosophila* egg. Subsequently, an overview of *Drosophila* oogenesis is given before the mechanisms of mRNA localisation are discussed further.

Drosophila oogenesis

Polarity within the *Drosophila* oocyte

By the time a *Drosophila* egg is laid, the major body axes have already been specified (St Johnston and Nüsslein-Volhard, 1992). Each female *Drosophila* fly has a pair of ovaries containing 16-20 ovarioles with developmentally ordered egg chambers. Oogenesis can be divided into fourteen stages and progresses from the very anterior of the ovariole, the germarium, to the posterior, where the fully developed egg is released (King, 1970; Spradling, 1993). Each egg chamber is an independent unit, which develops from one germline-derived stem cell. This stem cell undergoes an asymmetric division to produce a new stem cell and a cystoblast, the latter undergoing a series of four incomplete cell divisions, leading to a cyst of sixteen interconnected cells. Each cell is connected via actin rich structures, the ring canals (Robinson and Cooley, 1997). Two of the sixteen cells contain four ring canals and they become pro-oocytes prior to one of these cells being chosen to be the oocyte.

The establishment of anteroposterior polarity

Although it is not fully understood how the oocyte is chosen it may involve the asymmetric segregation of the fusome, a vesicular organelle which contains cytoskeletal proteins, such as Cyclin A and Dynein (Yue and Spradling, 1992; McGrail and Hays, 1997). The fusome derives from a spherical structure, the spectrosome, which becomes localised into one daughter cell during the first cystoblast division. During the following rounds of mitosis, the spectrosome forms a

branched structure, connecting all cells, which is referred to as the fusome. The fusome interacts with one spindle pole of each dividing cell at each division and accumulates in their place after disaggregation (Spradling et al., 1997). It is believed that the spectrosome polarises the fusome, which then directs the formation of an active microtubule-organising-centre (MTOC) in a single cell (Lin et al., 1994). Specific mRNAs are believed to be transported along the microtubules (MTs) into the cell containing the active MTOC, therefore selecting this cell to become the oocyte (Theurkauf et al., 1992; Theurkauf et al., 1993; Theurkauf, 1994).

The differentiation of one of the cells to be singled out as the oocyte is MT dependent and requires activity of the two maternal genes *egalitarian* (*egl*) and *bicaudal-D* (*bicD*) (Koch and Spitzer, 1983; Mach and Lehmann, 1997; Theurkauf et al., 1993). Previous work has identified that BicD and Egl localise to the minus ends of oocyte MTs and in recent years, more findings have added other very interesting potential functions for both Egl and BicD. It has been shown in the Blastoderm embryo, that both proteins appear to be involved in recruiting mRNAs to the apical cytoplasm (Bullock and Ish-Horowicz, 2001) and a further role for BicD in midoogenesis has been suggested to provide the polarity for the migrating oocyte nucleus towards the future dorsal side. In addition BicD:GFP protein has been shown to be localised in a focus at the oocyte nucleus, before and while it migrates (Pare and Suter, 2000). The correct localisation has been shown to require activity of the dynein-heavy chain (Dhc) as well as other RNA binding proteins, suggesting the involvement of the minus end directed motor cytoplasmic dynein in the correct cellular localisation of BicD.

Once the oocyte is determined it moves to the posterior of the cyst, a process driven by Cadherin-dependent adhesion (Gonzalez-Reyes and St Johnston, 1998). Correct positioning of the oocyte forms the first symmetry-breaking step during oogenesis as it defines the anteroposterior axis (Gonzalez-Reyes and St Johnston, 1994). The posterior movement of the oocyte is disrupted by several mutants, such as *homeless*, *armadillo*, *dicephalic* and the *spindle* genes-*spindle A-E*, *okra*, *aubergine*, *vasa*, *squash*, *zucchini* and *deadlock* (Gillespie and Berg, 1995; Gonzales-Reyes and St Johnston, 1994; Gonzalez-Reyes and St Johnston, 1998). Mutants in any of these genes also show a disruption of mRNA localisation later on in oogenesis. Molecular analysis of two *spindle* mutants revealed that the complex phenotype is the result of a failure to repair DNA breaks during recombination (Gonzalez-Reyes et al., 1997); (Ghabrial et al., 1998). Other genes have been shown to encode DNA helicases and are most probably involved in translational control of *grk* mRNA later on in oogenesis (Gillespie and Berg, 1995; Styhler et al., 1998; Tinker et al., 1998; Tomancak et al., 1998).

Oocyte growth and maturation

Once the oocyte is determined, the other fifteen cells subsequently endoreplicate to become the polyploid nurse cells. The nurse cells provide the growing oocyte with organelles, proteins and mRNAs that are required for its correct development. Within the germarium, the oocyte becomes surrounded by somatic cells, the follicle cells, which are derived from stem cells located within germarium region 1 and 2. Each egg chamber within the ovariole is initially completely surrounded by follicle cells when the egg chamber buds off the germarium in stage 2 and interconnecting stalk cells form a bridge from one egg chamber to the next. The follicle cells undergo divisions from stage one to six of oogenesis and then cease dividing. There

are more than one thousand follicle cells surrounding each egg chamber at that stage and they provide the growing oocyte with yolk protein, which results in fast increasing oocyte size (Gonzalez-Reyes and St Johnston, 1998).

Although up until stage six, nurse cells and oocyte are the same size, the oocyte grows rapidly and takes up a third of the egg chamber by stage 9. At this stage, most of the follicle cells start migrating over the oocyte and complete their movement by stage 10, when they form a columnal epithelial layer over the oocyte only. In addition, another small group of specialised follicle cells, the border cells, migrates through the nurse cell cluster to reach the anterior boundary, where they are joined by another group of centripetally migrating follicle cells. These migration events lead to the whole oocyte being completely surrounded by follicle cells. As late oogenesis progresses, the nurse cells then start to dump their entire contents through the ring canals into the oocyte, before undergoing apoptosis. The stretched follicle cells that surround the oocyte secrete the egg shell and then also become apoptotic, leaving behind the mature egg surrounded by the chorion. Within the chorion, specialised structures, such as the micropyle, and the dorsal appendages and aeropyle, which are secreted by a group of centripetally migrating follicle cells, provide sperm entry and function as respiratory structures of the embryo.

Initiation of the perpendicular axes in the oocyte

The whole development of the egg chamber from stem cell to the mature egg is accomplished in multiple diverse steps during oogenesis. The first symmetry-breaking event is the decision, which of the cells within the cyst is chosen to become the oocyte. Once the oocyte has been established and moved to the posterior of the cyst within the germarium, bidirectional signalling between the oocyte and the surrounding somatic follicle cells polarises the follicle cell layer along both the anteroposterior as well as the dorsoventral axis. Distinctions amongst initially identical follicle cells are established through two rounds of signalling at different times during oocyte maturation involving the TGF-α homologue Gurken (Grk) in the oocyte and the EGF-R homologue Torpedo in the adjacent follicle cells (Schüpbach et al., 1990; Schüpbach and Roth, 1994; St Johnston, 1995; Shilo et al., 1998; Nilson and Schüpbach, 1999). The restriction of *grk* mRNA and protein in early oogenesis to the posterior of the oocyte from stage1-6 is required to correctly polarise approximately 200 terminal follicle cells through tyrosine kinase signalling to adopt a posterior, rather than anterior fate (Perrimon, 1994; Gonzalez-Reyes and St Johnston, 1998). The posterior follicle cells subsequently send a signal back to the oocyte to polarise the anteroposterior axis (Ruohola-Baker et al., 1994; Gonzalez-Reyes et al., 1995; Roth et al., 1995).

The identity of the polarising signal itself is still unknown, but a number of proteins, such as PKA, Mago nashi, Merlin and Laminin A have been shown to be involved in the process (Lane and Kalderon, 1995; Lane and Kalderon, 1994; Micklem et al., 1997; MacDougall et al., 2001; Deng and Ruohola-Baker, 2000). These factors and their proposed function are discussed in more detail in chapter 3 of this thesis.

Once the unknown signal has been sent, the oocyte MT network reorganises to form an anteroposterior gradient throughout the oocyte. In early oogenesis, MTs within the oocyte are located with their minus ends at the posterior of the oocyte, where the MTOC lies (Theurkauf et al., 1992). The reorganisation leads to the formation of a new, diffuse MTOC along the anterior cortex of the oocyte. The polarisation of the MTs is thought to drive the relocation of the oocyte nucleus from its posterior position to the dorso-anterior corner of the oocyte (Gonzalez-Reyes et al., 1995); (Roth et al., 1995). The anterior MTOC has been visualised using Nod:βgal, a putative MT minus end marker (for more details see chapter 3 of this thesis), the centrosome component Centrosomin, as well as MT nucleating components (Clark et al., 1997; Brendza et al., 2000; Schnorrer et al., 2002). Plus ends of MTs in the oocyte have been visualised using Kin:βgal, which was found to localise to the posterior of the oocyte (Clark et al., 1994). Furthermore, visualisation of MTs in the oocyte using a fusion protein of the bovine MT-binding protein Tau coupled to GFP revealed that MTs are most concentrated along the anterior cortex (Micklem et al., 1997).

At the dorsoanterior corner, *grk* mRNA and protein accumulate between the oocyte nucleus and the adjacent follicle cells. Correct localisation of *grk* mRNA and protein requires the activity of the *fs(1)K10* gene, which encodes a helix-loop-helix DNA

binding protein (Wieschaus et al., 1978), as well as the hnRNP homologue, Squid (Sqd) (Norvell et al., 1999). Grk signalling to the overlying follicle cells determines dorsal rather than ventral cell (Neuman-Silberberg and Schüpbach, 1993). In the follicle cells, Rhomboid expression is induced by EGF-R activation thus activating a positive feedback loop, which amplifies EGF receptor activation in the follicle cells (Sapir et al., 1998; Peri and Roth, 2000). Induction of dorsal fate in the follicle cells prevents activation of the Toll receptor in the embryo, as activation leads to nuclear localisation of the morphogen dorsal, required for ventral fate (Barkai and Shilo, 2002). The dorsal follicle cells subsequently secrete the specialised eggshell structures, such as the micropyle and the dorsal appendages, which perform respiratory functions in the embryo.

In addition to *grk*, other key maternal transcripts are localised asymmetrically within the oocyte to establish the axes of the future embryo. *bicoid* (*bcd*) mRNA is localised to the anterior cortex of the oocyte, leading to a morphogenetic gradient of Bcd protein when it is translated in the fertilised embryo (Driever and Nüsslein-Volhard, 1988). The anterior morphogen *bcd* encodes a transcription factor containing a homeodomain (St Johnston et al., 1989). The Bcd gradient in the embryo is crucial in defining anterior polarity and subsequent patterning. *bcd* mRNA is transcribed by the nurse cells, from where it is transported and localised in the oocyte, a process which is thought to require Exuperantia (Exu) protein and MTs (Macdonald et al., 1991; Cha et al., 2001). Later on in oogenesis, *bcd* RNA localisation in the oocyte requires Swallow (Swa) and Staufen protein (Berleth et al., 1988; Hazelrigg, 1990; Stephenson, 1988) for correct localisation to the anterior.

The localisation of *oskar* (*osk*) mRNA to the posterior of the oocyte defines the posterior of the future embryo (Ephrussi and Lehmann, 1992). *osk* mRNA is transcribed by the nurse cells and initially transported and localised to the anterior of the oocyte, before it moves to the posterior after the repolarisation of the oocyte MTs during stage 7 of oogenesis. Localisation of *osk* mRNA to the posterior is required for recruiting other molecules to the posterior, such as Vasa protein, Staufen and *nanos* mRNA (Curtis et al., 1995; Ephrussi et al., 1991; Ephrussi and Lehmann, 1992). These molecules subsequently play a role in the assembly of pole plasm and formation of pole cells in the embryo (Kim-Ha et al., 1991). Localisation of *osk* is regulated in a complex manner, whereby translation of unlocalised *osk* mRNA is repressed through binding of Bruno to sequences in the 3'UTR of *osk* mRNA, the Bruno response elements (BREs) (Kim-Ha et al., 1995). Other proteins, such as Apontic, p50 and possibly Bicaudal C (Bic-C) have also been implicated to be part of the regulation of translational repression of unlocalised *osk* mRNA (Lie and Macdonald, 1999; Gunkel et al., 1998; Saffman et al., 1998). Furthermore, Staufen protein is required for *osk* mRNA localisation as well as translation in the oocyte (Micklem et al., 2000). Alternative splicing leads to the translation of two different isoforms of Osk protein, short Osk and long Osk, which are localised specifically and are thought to perform different and possibly redundant functions throughout oogenesis and embryogenesis (Markussen, 1995; Johnstone and Lasko, 2001). Recent data revealed that the kinase Par-1, required for polarisation in both *Drosophila* oocytes and *C.elegans* embryos, is involved in the phosphorylation of Osk at the posterior, which regulates Osk protein stability (Riechmann et al., 2002).

The mechanisms of mRNA localisation

To establish the perpendicular axes of the future embryo, *grk*, *bcd* and osk transcripts are localised asymmetrically within the oocyte. While the functions of the three key maternal transcripts have been studied in detail, the mechanism of localisation is not as well understood (Tekotte and Davis, 2002).

In general, various different models have been proposed for how transcripts become localised. Directional export from the nucleus prior to localisation suggests that specific mRNAs may be exported only from one side of the nucleus closest to the localisation site in the cytoplasm. Although not directly shown, it was proposed to be the mechanism for localisation of apically distributed transcripts in the syncytial blastoderm stage of *Drosophila* embryos (Davis et al., 1993; Francis-Lang et al., 1996). However, evidence from recent work suggests that export of pair rule transcripts occurs from all sides of the nucleus and vectorial export does not apply (Wilkie and Davis, 2001).

Vectorial export has also been suggested as a model for localisation of *grk* mRNA in the *Drosophila* oocyte, as the oocyte nucleus may be the site of transcription for *grk* mRNA during some stages of oogenesis (Saunders and Cohen, 1999), although it is not yet clear whether *grk* mRNA transcription occurs in nurse cells or the oocyte nucleus during oogenesis (Thio et al., 2000; Lipshitz and Smibert, 2000). There is also no direct evidence to test vectorial export in the case of *grk* nor in the case of a number of other mRNAs where it has been proposed. Perhaps the only case, which could be said to be best explained by vectorial export is the alga *Clamydomonas*

reinhardtii. It has been shown that in Clamydomonas, the nucleus is polarised with most nuclear pore complexes (NPCs) distributed at the posterior, where *beta2-tubulin* mRNA has been shown to accumulate prior to deflagellation (Colon-Ramos et al., 2003).

Diffusion and anchoring

The diffusion and subsequent anchoring of transcripts as one possible mechanism of mRNA localisation in the cytoplasm has been proposed for the localisation of the maternal transcript *osk* in *Drosophila* oocytes. In experiments using injection of fluorescently labelled *osk* RNA, cytoplasmic streaming in the oocyte, a MT dependent process which mixes the oocyte cytoplasm, has been suggested to facilitate the movement of *osk* RNA to the posterior (Glotzer et al., 1997). Subsequent anchoring is likely to trap the localised RNA at the posterior, as mutations disrupting the protein TropomyosinII (TmII), a protein of the actin cytoskeleton, fail to localise *osk* mRNA at the posterior pole of the oocyte (Erdelyi et al., 1995). However, diffusion and anchoring are suggested to be only part of the mechanism of *osk* mRNA localisation, and recently, active transport involving Kinesin I, a plus-end directed motor protein has also been suggested (Brendza et al., 2000). It is not yet clear whether active transport is directly responsible for *osk* mRNA localisation, or whether Kinesin excludes *osk* mRNA from the cortical regions of the oocyte (Cha et al., 2002; Palacios and Johnston, 2002). However, recent experiments using molecular beacons that fluoresce only when hybridised to endogenous *osk*, was able to follow the movement of *osk* transcripts in real time (Bratu et al., 2003) and direct visualisation of movement of RNAs will allow to distinguish between the different proposed models.

Another localised transcript in the *Drosophila* oocyte, *nanos* mRNA, is also suggested to localise via diffusion and subsequent anchoring, although it cannot be ruled out that active transport may also play a role (Palacios, 2001). Recent data reveal that endogenous *nanos* mRNA when labelled with GFP localises in a diffusion based manner to the posterior where it is subsequently anchored through an Actin dependent process to maintain posterior localisation (Forrest, 2003).

Actin dependent anchoring has also been shown to be required for the localisation of *Vg1* mRNA in *Xenopus* oocytes (Yisraeli et al., 1990). Anchoring of another maternal transcript, *bcd* RNA has been suggested to be facilitated by the double stranded RNA-binding protein, Staufen (Stau) (St Johnston et al., 1991). In the budding yeast, *S. cerevisiae*, anchoring of *Ash1* mRNA to the tip of the bud requires the activity of the two proteins Bni1 and Bud 6, two members of the actin cytoskeleton (Beach, 1999). It is therefore likely that diffusion and Actin-dependent anchoring is used by some mRNAs as the mechanism of localisation.

Selective degradation and protection of localised transcript

Transcript localisation to specific sites within the cytoplasm can be achieved by another mechanism, involving the degradation of unlocalised, and protection of localised, mRNA. In *Drosophila* early embryos, heat-shock protein (*hsp)83* mRNA is degraded after fertilisation in all parts of the embryo except the posterior, where transcripts are protected from degradation (Bashirullah et al., 1999). Hsp83 becomes eventually defined to the pole cells and it is likely that the localised stabilisation of *hsp83* mRNA is facilitated by components of the pole plasm (Ding et al., 1993). Stabilisation of *nanos* mRNA in the early *Drosophila* embryo refines localisation to the posterior, as only a small percentage of *nanos* transcripts are localised in the

embryo and selective stabilisation is therefore needed to efficiently restrict *nanos* mRNA localisation (Bergsten and Gavis, 1999). Unlocalised *nanos* mRNA in the embryo is furthermore degraded (Bashirullah et al., 1999).

Directed transport

Directed transport as a means of localising transcripts asymmetrically within the cytoplasm is probably the best studied mechanism and may be utilised by most localised mRNAs (Jansen, 2001; Tekotte and Davis, 2002). Cytoplasmic transport requires a functional cytoskeleton and motor proteins and recent work has revealed cytoplasmic transport for localisation of mRNAs to be the mechanism in many organisms during development and in many different cell types. In chicken fibroblast cells, localisation of *β-actin* mRNA to the distal lamellae has been shown to require actin microfilaments (Sundell and Singer, 1990).

Actin microfilaments have also been shown to play a role in the localisation of *Ash1* mRNA in the budding yeast, *S.cerevisiae*. *Ash1* encodes for a transcription factor that suppresses mating type switching in the daughter cell (Sil and Herskowitz, 1996; Jansen et al., 1996) and localisation of the RNA requires transport along Actin microfilaments and the activity of the Myosin V class motor (Long et al., 1997; Takizawa et al., 1997). She3p and She2p have been shown to function as linkers between the myosin motor and *Ash1* mRNA (Takizawa and Vale, 2000).

In *Drosophila* embryos, apical localisation of *pair rule* transcripts and *wingless (wg)* mRNA has been shown to require the MT cytoskeleton during blastoderm stage (Wilkie and Davis, 2001; Simmonds et al., 2001). Pair rule genes refine the segmentation pattern of the embryo and are expressed in seven defined stripes (Nüsslein-Volhard and Wieschaus, 1980; Pankratz and Jäckle, 1993). They are part of the hierarchy of segmentation genes and, unlike transcripts of gap genes, which are unlocalised, have been shown to localise to the apical cytoplasm during syncytial blastoderm. Furthermore, a developed in vivo injection assay using in vitro transcribed and with fluorescent UTP labelled RNA in living *Drosophila* embryos revealed the requirement of the minus end directed motor protein cytoplasmic dynein in apical localisation (Wilkie and Davis, 2001). In addition, apical localisation of injected pair rule transcripts were also shown to require the two maternal proteins Egl and BicD, which are suggested to function as linkers or facilitate the linking between the RNA complex and the dynein motor complex (Bullock and Ish-Horowicz, 2001). BicD is thought to bind to the dynein motor and the mammalian homologue, BicD2, interacts with the dynein activity regulating subunit dynactin via its N-terminal domain (Hoogenraad CC, 2001; Hoogenraad CC, 2003).

In the *Drosophila* oocyte, posterior localisation of *osk* mRNA is likely to require the Kinesin I motor for transport to the plus ends of oocyte MTs, as posterior localisation of *osk* mRNA and Staufen protein are disrupted in mutants of *kinesin-heavy chain* (*khc*) (Brendza et al., 2000). However, posterior transport of *osk* mRNA has not yet been visualised directly, so there is also suggestion that Kinesin I may function to exclude *osk* mRNA from the cortex of the oocyte promoting its accumulation in the centre and then subsequent delivery to the posterior (Cha et al., 2002). Kinesin I may also act indirectly in *osk* mRNA localisation by initiating

cytoplasmic flows, which locate the RNA at the posterior where it is subsequently anchored. Cytoplasmic flows have previously been reported to localise injected *osk* RNA in oocytes (Glotzer et al., 1997) and Actin has been suggested to be required for posterior anchoring of *osk* (Erdelyi et al., 1995). Interestingly, the Kinesin light chain (Klc) of Kinesin I is not required for *osk* mRNA localisation to the posterior, suggesting that Kinesin I interacts with *osk* mRNA by a novel mechanism (Palacios and Johnston, 2002). It is likely however, that *osk* mRNA localisation requires a combination of diffusion and anchoring as well as directed transport and translational control (Tekotte and Davis, 2002). The localisation of *bcd* mRNA to the anterior of the oocyte requires the protein Swa, a protein which has been shown to bind dynein-light chain (dlc) in in vitro assays and has therefore been linked to the minus end directed motor dynein (Stephenson, 1998; Schnorrer et al., 2000). Furthermore, Exu, a protein also required for correct anterior localisation of *bcd*, has been shown to colocalise with *bcd* RNA in the nurse cells and be transported from the nurse cells to the oocyte, possibly in a complex with *bcd* RNA (Theurkauf and Hazelrigg, 1998; Cha et al., 2001). More recently, dynein and Kinesin I have been shown to function in *bcd* and *grk* transport to their correct cytoplasmic domain, respectively, suggesting that the two opposite polarity motor proteins have interconnecting functions in localising mRNAs to their respective site in the cytoplasm (Januschke et al., 2002).

Cis- acting elements required for mRNA localisation

mRNAs are known to contain specific sequences that are necessary and sufficient to define their cytoplasmic destination. These so called cis-acting elements, or localisation elements usually reside within the 3' untranslated region (UTR) of transcripts. Although in some cases, for example the case of the maternal mRNA *grk*, sequences have so far been identified within both the 5'UTR, as well as the 3'UTR and coding sequence (Saunders and Cohen, 1999; Thio et al., 2000). The mapping of the cis-acting sequences which define the localisation elements has been performed using transgenic reporter gene fusion constructs with subsequent analysis of their localisation abilities (Davis and Ish-Horowicz, 1991; Thio et al., 2000), as well as microinjection of RNA (Glotzer et al., 1997); for review see (Kloc et al., 2002; Palacios, 2001)

In many cases, localisation sequences have been mapped precisely and different sequences have been shown to facilitate different steps in the process of localisation. The localisation elements of different localised mRNAs often do not appear to have common sequence, but the ability to form certain secondary structures probably plays an important role in the localisation of the RNA. However, defining a consensus secondary structure required for localisation can prove difficult, as has been shown for pair-rule and *wg* transcripts in the embryo (Bullock and Ish-Horowicz, 2001).

Nevertheless, in the case of *bcd* mRNA, the 50 nucleotide localisation element BLE1 in the *bcd* 3'UTR uses two different stem loop structures to drive early anterior localisation. Subsequent anchoring requires an additional stem loop structure within

the 3'UTR (Macdonald and Struhl, 1988; Macdonald and Kerr, 1997). In *Xenopus*, *Xcat2* mRNA also localises using the combination of several localisation elements within the 3'UTR. Initial localisation of the Nanos-related factor to the mitochondrial cloud of the *Xenopus* oocyte is facilitated by one localisation element, whereas localisation to the germinal granules is established with a second localisation sequence (Mosquera et al., 1993; Zhou and King, 1996; Kloc et al., 2000). The modular nature of cis-acting localisation elements therefore provides a complex system facilitating the multiple steps of mRNA localisation in many different systems.

Trans-acting localisation factors

The cis-acting elements within the mRNA sequence are recognised by trans-acting proteins, which determine their correct cytoplasmic destination. However, identification of these factors by biochemical means is a difficult process and has so far only been partly successful in *Drosophila* and *Xenopus* (Yisraeli et al., 1990; Norvell et al., 1999; Wilhelm et al., 2000; Arn et al., 2003). It is thought that at least in the case of *bcd* mRNA and probably more generally, specificity may be provided by binding of multiple low affinity factors to localisation elements rather than a single high affinity and specificity trans-acting factor. Genetical analysis has provided another approach to identify the transacting factors required for mRNA localisation. A number of mutations affecting mRNA localisation in *Drosophila* and yeast have been identified, but so far, their precise roles in mRNA localisation remain poorly understood (for review see Tekotte and Davis, 2002).

The first factor identified to play a role in cytoplasmic mRNA localisation was the double stranded RNA (dsRNA)-binding protein Staufen. Staufen had originally been isolated in a screen identifying factors required for patterning of the *Drosophila* embryo (Schüpbach and Wieschaus, 1986). Recent work has revealed that Staufen is a transacting factor with multiple functions and it is involved in localisation, anchoring and translational control for a variety of mRNAs in several different cell types (for review see Palacios, 2001). In *Drosophila*, Staufen is required for anchoring of *bcd* mRNA to the anterior of the oocyte, for MT-dependent transport of *osk* mRNA to the oocyte posterior and for actin dependent localisation of *prospero* (*pros*) mRNA in neuroblasts during *Drosophila* embryogenesis (Roegiers and Jan, 2000; Kloc et al., 2002). The Staufen protein consists of five dsRNA-binding domains each domain mediating different functions (Micklem et al., 2000). Homologues of Staufen exist in both mammals and *C.elegans* indicating that the function of Staufen in mRNA localisation is conserved. Another trans-acting factor required for mRNA localisation, which shows cross species conservation is actin zip-code-binding protein 1(ZBP-1). In chicken fibroblasts, ZBP-1 binds to the β-actin localisation element (Ross et al., 1997) and the *Xenopus* homologue, Vg1RBP, or Vera, recognises the localisation elements of *Vg1* mRNA (Deshler et al., 1998; Havin et al., 1998). Both homologues share 78% identity, but localise mRNAs through different mechanisms in different species: actin dependent as well as MT dependent localisation. These two highly related proteins mediate, like Staufen, localisation along both types of cytoskeleton.

It has been suggested that the assembly of specific RNA-protein complexes in the nucleus may play a role in the subsequent localisation of mRNAs in the cytoplasm. Work in human cells has shown that in all intron-containing transcripts certain

proteins mark the site at which an intron is removed. The proteins form a complex, called the exon-exon junction complex (EJC) (Palacios, 2002; Farina, 2002). In *Drosophila*, *osk* mRNA localisation in the cytoplasm has been shown to require such a complex, containing Y14 and Mago nashi, as well as Barentz, which is probably recruited to the EJC complex in the cytoplasm (Hachet and Ephrussi, 2001; Micklem et al., 1997; van Eeden et al., 2001). However, the specificity of such complexes which are part of the general nuclear export machinery is not fully resolved and it will be interesting to identify the factors required to perform the specific roles in cytoplasmic mRNA localisation.

Translational control

The localisation of specific mRNAs has often been found to be coupled to translational control, providing a mechanism to restrict proteins to one region of a cell. It is important that the mRNA is not translated before or during localisation, in order to avoid premature protein expression. During *Drosophila* development, many mRNAs that define the body axes have been found to be subject to translational control. Both *osk* and *nanos* mRNA can only be translated if they are correctly localized to the posterior pole and translation of unlocalized mRNAs is prevented by the binding of Bruno to sequences (Bruno response elements – BREs) within the 3'UTR (Gavis and Lehmann, 1994; Kim-Ha et al., 1995; Rongo et al., 1995; Dahanukar and Wharton, 1996; Smibert et al., 1999; Smibert et al., 1996; Dahanukar et al., 1999). Once localized, Bruno is removed allowing translation of *osk* and *nanos* to occur at the posterior. *nanos* translational control is an effective means of restricting Nanos protein to the posterior. Most *nanos* mRNA is unlocalised in the embryo, so translational repression of unlocalised mRNA is essential for targeting the protein to the posterior (Bergsten and Gavis, 1999). Proteins, such as Staufen

(Stau) and Bruno have been shown to be required to translationally regulate *osk* mRNA (Kim-Ha et al., 1991; Lie and Macdonald, 1999; Castagnetti et al., 2000; Webster et al., 1997).

Translational control has also been shown to be important in the localisation of *grk* mRNA in *Drosophila* oocytes. The DNA helicase Vasa as well as the protein K10 have been implicated in regulating translation of *grk* RNA (Tomancak et al., 1998; Saunders and Cohen, 1999). Bruno protein has also been implicated to play a role in the translational regulation of *grk* mRNA during *Drosophila* oogenesis. Furthermore, activity of the *spn*-genes has been suggested to regulate translational activation of *grk* mRNA (Gonzalez-Reyes et al., 1997). Recent data also show that the RNA binding protein Orb regulates translation of localised *grk* mRNA and promotes the synthesis of K10, a key regulator of the dorsoventral signalling pathway (Chang et al., 2001). Interestingly, factors such as Bruno, Vasa, Orb and Staufen have all been implicated in the translational regulation of both *grk* and *osk* mRNA, suggesting a potential overlap in the regulation mechanisms of these two mRNAs (Johnstone and Lasko, 2001). Overall rapid progress in recent years has been made in understanding the link between mRNA localisation and translational control. It has become apparent that in many cases, localisation and translational control are coupled processes utilizing overlapping cis-acting sequences making up this fundamental process which defines polarity within the cellular context.

Aims of this study

Asymmetric localisation of maternal transcripts is required to specify polarities in the developing oocyte during *Drosophila* oogenesis. At the onset of this work, the mechanisms by which one of the key maternal transcripts, *grk* mRNA, is localised had been largely elusive. The aims of this work were to investigate the mechanisms of mRNA localisation and axis specification in the *Drosophila* oocyte to further the understanding how polarity is established during early Drosophila development.

The first chapter investigates the initial symmetry breaking step of early initiation of the anteroposterior axis as facilitated through bidirectional signalling. Localisation of *grk* mRNA to the posterior is required for correct polarity within the follicle cells and one component downstream of Grk/TGF-α signalling had been identified in a genetic screen carried out in the lab before the work was started. The start of this thesis describes the characterisation of the phenotypes of conditional mutants of the ERM protein member Merlin, which show a disruption in anteroposterior axis formation. The role of Merlin in the polarising signal is investigated as well as its indirect function in the localization of *bcd*, *grk* and *osk* RNAs.

The remaining result chapters describe the investigation of the mechanism of *grk* mRNA localisation in the *Drosophila* oocyte. The various possible hypotheses that could explain how *grk* mRNA localisation could occur are tested. It is found that active transport using the dynein motor along MTs to their minus ends is sufficient to explain how *grk* localisation occurs. *grk* RNA moves in two steps, first anteriorly and then dorsally towards the oocyte nucleus.

2

MATERIALS & METHODS

Molecular work

Solutions and reagents

All solutions used were prepared according to descriptions in Molecular Cloning-A Laboratory manual (Sambrook et al., 1989). General chemicals were obtained from SIGMA, BDH and Fisher. Modification enzymes, such as restriction enzymes, Taq polymerase, T7, T3 and SP6 polymerases were obtained from Roche, New England Biolabs (NEB), Promega and Stratagene.

All solutions were prepared in double distilled sterile water, unless otherwise stated. Phosphate buffers Saline (PBS) and Luria Betani mediums (LB) were prepared and autoclaved by the Swann building media kitchen. The composition of solutions is given below;

SOLUTION	COMPOSITION
50X TAE	242g Tris; 57.1ml Acetic Acid; 0.5M EDTA
TE	1mM EDTA (ph8.0), 10mM Tris-HCl (ph7.5)
10X PBS	0.1M Sodium Phosphate (ph7.5), 1.3M Sodium Chloride
Hybridisation solution	50% deionised formamide, 5x SSC, 50μg/ml heparin, 0.1% Tween 20 (v/v) (in nuclease free H_2O ph 6.5 adjusted with conc. HCl
LB medium	1 litre: 10g Difco Bacto Tryptone, 5g Difco Bacto Yeast Extract, 5g Sodium Chloride
L-Agar	1 litre: 16g Difco Bacto Tryptone, 10g Difco Bacto Yeast Extract, 5g Sodium Chloride
Colcemid	1ml:100μg Colcemid; 10% DMSO in nuclease free, double distilled H_2O (w/v)
Cytochalasin D	1ml: 150 μg Cytochalasin D in nuclease free, double distilled H_2O
Injection Buffer	0.1mM Na Phosphate, ph 7.8; 5mM KCl

Bacterial Growth

To amplify plasmid DNA, transformation of the DNA into Calcium Chloride competent cells was performed as follows. A 200µl aliquot of competent cells was thawed on ice and incubated with 1-2 µl of plasmid DNA on ice for 15mins. The mixture was then heatshocked at 42°C for 2minutes. Immediately after heatshock, cells were placed on ice for a further five minutes. 1ml of LB medium was added and incubated at 37°C for 30 mins with gentle shaking. The cells were then spread onto petri-dishes containing L-agar, as well as the appropriate antibiotic for plasmid selection. Plates were incubated at 37°C overnight. Selected colonies were picked and incubated overnight in 5ml LB culture medium. Where larger amounts of plasmid DNA were needed, cultures were grown in 250ml flsks.

Purification of Plasmid DNA

For small scale preparation of plasmid DNA, 1.5ml of plasmid-transformed overnight bacterial culture was pelleted. Plasmid DNA was obtained using the Qiaprep Spin miniprep kit from Qiagen. After lysis of the bacteria and removal of bacterial debris and proteins, the DNA was absorbed onto the Quiaprep membrane and extracted using either TE buffer or nuclease free double distilled sterile H_2O. For larger amounts of DNA, the Quiagen midiprep kit was used and 50ml of the plasmid containing bacterial culture was pelleted prior to the procedure.

DNA and RNA precipitation

DNA was generally purified after PCR, Sequencing reactions or restriction digest. 1/10 volume of Sodium Actetate pH5.2 was added and the mixture vortexed

immediately. 2 volumes of 100% cold Ethanol were then added and incubated at –20°C for 10mins to maximise the efficiency of precipitation. DNA was pelleted by 20mins centrifugation at >15,000xg and washed with 70%Ethanol in nuclease free DEPC H_2O. The DNA was resuspended in either TE buffer or nuclease free double distilled sterile H_2O. RNA was precipitated using 1/5 volumes of ammonium actetate pH 5.2 and 2.5 volumes of 100% cold Ethanol. Subsequent steps were identical to DNA precipitation described above. The RNA pellet was resuspended in nuclease free double distilled sterile H_2O.

Isolation of total RNA from flies

Total RNA was isolated from mer^{ts1} homozygous mutant females as well as yw^{67g} female flies using the Rneasy mini kit from Qiagen. Approximately 30 female flies were shock frozen in liquid nitrogen and homogenized in 350 µl of RLT buffer (Qiagen), using a Polytron (Kinematica) at maximum speed. RNA was eluted in 30 µl DEPC H_2O.

PCR

Standard conditions for a 50µl reaction were:

50ng template DNA, 1XPCR buffer containing 15mM MgCl2 (Roche), 0.2mM Ultrapure dNTPs (Amersham), 1µM primer each (forward and reverse) 2.5 Units Taq polymerase (Roche) and double distilled sterile H_2O to make up the final volume.

The standard program used was 94°C hot start for 5 minutes following 35 cycles of melting at 94°C for 30 seconds, annealing at 50-60°C for 30 seconds (exact temperature was based on the melting temperature (T_m) of the primers used) followed by elongation at 72°C for 30 seconds. A final elongation step was carried out for 8 minutes. The exact primers used are listed in the Appendix. A Biometra thermal cycler was used for all PCR reactions and the lid temperature was set to 110°C

RT PCR

RT PCR was performed using the Titan One tube RT-PCR kit (Roche) according to manufacturer's instructions. 10 Units of RNAse inhibitor (Promega) was added to the reaction and reverse transcription was carried out at 50°C for 30 minutes using approximately 1 ng of fly total RNA as a template, before switching to thermal cycling as described in manufacturer's instructions.

The resulting cDNA was precipitated and resuspended in double distilled H_2O.

DNA sequencing

To sequence DNA, a Big Dye Sequencing kit from Perkin Elmer Applied Biosystems was used according to the manufacturers instructions. The method is based on the dideoxynucleotide DNA sequencing method and uses differently fluorochrome-coupled nucleotides, which can later be read out from the electrophoresis gel by an automatic sequencer. The reactions were 10 µl, containing 4 µl of the Big Dye mix and 1.6pmols of primer. The amounts of template DNA used were 50-100ng for PCR products and 200-300ng for plasmid DNA. The cycle conditions were 25 cycles of melting at 96°C for 30 seconds, following annealing for

30 seconds at 50°C and elongation for 4 minutes at 60°C. The sequencing reactions were precipitated by standard method (see previous) and analysed by the ICMB sequencing service, University of Edinburgh. All sequencing reactions were performed on both strands of DNA and from at least two independent PCR reactions, to minimise errors.

DNA Sequence analysis

Computer analysis of the sequences was performed using the following sequence processor programs.

Gene Jockey

This program written by P.L.Taylor (Cambridge) allows comparison of sequences on both nucleotide and aminoacid level, with alignments showing each nucleotide/aminoacid change. It can also be used to define restriction sites within a certain sequence and allows multiple alignments. This program was used to analyse the sequence of mer^{ts1} cDNA versus the wildtype control, yw^{67g}.

Basic Local Alignment Search tool (BLAST)

This program allows comparison of a given sequence against other sequences in public databases. It can be performed either with a nucleotide sequence (BLASTN search), or a peptide sequence (BLASTP) and was used to identify the published sequence of the *Mer* gene in *Drosophila*, as well as the homologue sequences in mouse, rat and human. The alignment of sequences was finalised using word processing.

Drosophila specific protocols

Drosophila flystocks

All flystrains (see Appendix A) were raised on standard yeasted cornmeal-agar medium at 18, 21 and 25°C (1litre: 25g cornflour, 50g sugar, 17.5g yeast, 10g agar, boiled, cooled to 40°C and poured into bottles or vials to set). Temperature-sensitive flystrains were maintained in several copies at 29°C over the X chromosomal balancer FM7c to prevent reversion of the mutant phenotype. The homozygous stock of mer^{ts1} was kept at 21°C. In experiments involving temperature shifts, adult flies were transferred to fresh food after eclosion and subsequently shifted to the restrictive temperature for 3 days. OrR was used as the wildtype strain, unless otherwise stated. For injections of living egg chambers, nlsGFP flies were used as wildtype control. For a comprehensive list of all flystocks used, see Appendix of this thesis.

Preparation and dissection of *Drosophila* ovaries for staining procedures

Drosophila flies were transferred to fresh yeasted medium after eclosion for at least three days. Ovaries were dissected in PBS and subsequently transferred to 3.7% (w/v) formaldehyde/PBS for 20mins. Ovaries used for staining of oocyte microtubules or microtubule associated components were dissected directly into 3.7% formaldehyde/PBS to prevent depolymerisation of the microtubules prior to fixation. After fixation, ovaries were washed 3x5mins in PBS/0.1% (v/v) Tween and dissected further with tungsteen needles to allow greater penetration of the

antibodies/probes used. Prior to in situ hybridisation, ovaries were stored for at least two hours in 100% Methanol at –20°C. Visualisation of DNA was performed through staining of ovaries with 4", 6-diamidio-2-phenolyndole (DAPI) for 2 minutes, following two washes with PBT. For visualisation of actin, ovaries were washed twice in PBS, then stained with phalloidin-Alexa 546 (Molecular probes) at a dilution of 1:50 in PBS overnight at 4°C. Ovaries were mounted in Vectashield medium containing anti-photobleaching reagents.

RNA in situ hybridisation to *Drosophila* ovaries

Digoxygenin-labelled antisense RNA probes were prepared using the Roche Dig RNA labelling kit, following manufacturers instructions. The *grk* probe was synthesised from approximately 1 μgDNA template, previously subcloned into Bluescript vectors (gift from Trudi Schüpbach). After dilution in hybridisation buffer to achieve approximately 0.5ng/ml concentration, aliquots of the probes were stored at –20°C.

Hybridisation was carried out following the procedure described by Tautz and Pfeifle(1989) with the following modifications: Ovaries were rehydrated through a series of methanol/PBT (1:1) into PBT for at least five minutes each. Ovaries were then postfixed for 8 minutes in 3.7% formaldehyde/PBT and washed 5 times 5 minutes in PBT to remove all traces of fix. Ovaries were then washed in hybridisation mix/PBT (1:1) for ten minutes and transferred into hybridisation mix for another ten minutes. Prehybridisation was carried out afterwards in hybridisation mix with added tRNA and Heparin at 70°C for at least one hour. Hybridisation was carried out overnight at 70°C. Two washes were performed in hybridisation solution for 20mins and one in PBT/hybridisation solution, also for 20mins. Ovaries were

then transferred back to room temperature where they were washed four times in PBT for 20mins. Incubation with anti-Digoxygenin-HRP coupled antibody was performed at room temperature for two hours at a concentration of 1:1000. After three more washes, the ovaries were then incubated with the tyramide solution for five minutes. Following two more washes, DNA and Actin staining were performed as described above.

Immunofluorescence on *Drosophila* ovaries

Drosophila ovaries were dissected and fixed as described above. Three washes were performed in PBS/TritonX100 (PBTrx) for five minutes each. Ovaries were then blocked in 2%BSA (w/v) in PBTrx for two hours minimum. Incubation with the primary antibody was carried out overnight at 4°C. For Nodβgal stainings, a polyclonal anti-rabbit anti βgal antibody was used in a dilution of 1:10000 in PBTrx/0.5%BSA/NGS.

After three subsequent 20mins-washes, ovaries were incubated with a secondary antibody coupled to Alexa 546 or Alexa 567 fluorochromes(Molecular probes). Incubation with the secondary antibody was carried out at room temperature for two hours. Ovaries were mounted in Vectashield medium, containing anti-photobleaching reagents, and stained for Actin and DNA as described above.

Follicle cell clones with FRT/Flp system

To generate follicle cell clones homozygous for the female sterile allele *mer*^{3} in an otherwise heterozygous female fly, the yeast derived FRT/Flp system was used. In this system, certain Flipase-recognition-sites (FRT) had to be recombined proximal

to the mutation onto the X-chromosome. The same FRT element had to be recombined to the marker X-chromosome, in this case carrying nlsGFP. The enzyme flipase recognises the FRT sites and causes double stranded DNA breaks, resulting in high frequency mitotic recombination. To achieve directed mosaics only in the follicle cells, the flipase activity was under control of the UAS/Gal4 system, using the *engrailed*-GAL4 driver to activated the enzyme only in egg chambers. Clones were identified by lack of the marker and heterozygous cells could also be distinguished from the homozygous nlsGFP twin spots, which are a result of mitotic recombination.

Ovaries were dissected and subsequently mounted in Vectashield to be analysed by high resolution microscopy (see also Results chapter3).

RNA labelling and synthesis

In vitro transcribed sense RNA for injection was prepared using the Stratagene mRNA mCAP RNA capping kit with the following modifications:

1-2µg of linearised template DNA were used and sense RNA transcribed using either T7, T3 or SP6 polymerases for two hours at 37°C. The 50µl reaction mix contained 0.4mMATP, 0.4mMCTP, 0.36mMUTP and 0.04 mM AlexaFluor 546-UTP, 0.12mMGTP, 0.3mM7mG('5)ppp(5') CAP analogue and 40Units of RNAse inhibitor (Promega). Subsequently, the remaining DNA template was digested with DNaseI (2Units) for 10 mins at 37°C. Unincorporated nucleotides were removed using a Sephadex G50 RNA spin column (Roche) according to manufacturers instruction. The remaining labelled RNA was then precipitated using 2.5 volumes EtOH and 1/10 volume NH_4Oac. The RNA pellet was resuspended in DEPC nuclease free H_2O.

Quantitation of injected RNA

If the oocyte of a stage 9 egg chamber is presumed to be a sphere of ~70-100 μm diameter, the following calculations give an estimate of the injected volume of RNA:

100μm=0.1mm=0.01cm $4 \times \pi \times r^3 / 3\ cm^3 = ml$

=> radius = 50μm=0.005cm

=> 5.23×10^{-7} ml = 0.523 nl =523 pl

if approximately 2% of the volume of the oocyte is injected, this would mean that each time ~10pl can be injected into the oocyte.

Assumptions:

Injecting 10pl (see above).

Concentration of injected RNA is ~200ng/μl.

Average mass of nucleotide: 305g/mole.

Therefore 1.7kb molecule mass is 518,500 g/mole

---

1) How many grams injected?

1μl contains 200ng

therefore 10pl (=0.00001ml) contains: 0.00001 x 200=0.002ng

therefore 0.002ng of RNA injected and 0.002ng=2 x 10[-12]g

2) How many moles injected?

There are 518500g in 1 mole

therefore there are

2 x 10[-12] grams in (2 x 10[-12])/518500 moles=3.85 x 10[-18] moles

3) How many molecules in this?

1 mole contains 6.022 x 10[23] (Avogardo's number) molecules

therefore, 3.8 x 10[-18] moles has (3.8 x 10[-18] x (6.022 x 10[23]) molecules = approximately 2,3 million molecules injected into each egg chamber. Taking into account the variation in concentration of in vitro transcribed *grk* RNA, the final number of approximately 2.3 million molecules can vary by a factor of 2.

Preparation of ovaries prior to injection

Ovaries of 3-4 day old females were dissected into oxygen-rich halocarbon oil with medium viscosity (Series 95, KMZ chemicals Ltd), which allowed culturing of egg chambers for up to two hours. Dissection was performed on coverslips, Thickness No.1 (BDH) in halocarbon oil. Egg chambers were dissected out and appropriate stages aligned to allow injection of multiple egg chambers during the experiment.

Microinjection of oocytes and nurse cells

Injections into living, cultured oocytes and nurse cells were performed, using Eppendorff femtotip needles. *grk*, *osk* and *bcd* RNA was injected at concentrations of 200-500ng/ml. Colcemid and Cytochalasin D inhibitors were coinjected with RNA at a final concentration of 100μg/ml and 30μg/ml for Colcemid and 150μg/ml for CytochalasinD. The monoclonal antibodies injected were anti-dynein P_1H_4B from Tom Hays against a fragment of *Drosophila* Dhc from residues 128-422 of the N-terminal region, as well as the anti-Dhc antibody against the HUV fragment of *Drosophila* Dhc from David Sharp. The control antibody used was 12CA5 anti HA (Yiota Kafalsla and Joe Lewis). All antibodies were spot dialysed into injection buffer using Millipore 0.025 μm VSWP filters before injection.

Preparation and microinjection of *Drosophila* embryos

Embryos were collected from fruit juice-agar plates after allowing the flies to lay eggs for 2 hours. Embryos were then collected into a sieve and dechorionated for 2-5 minutes at room temperature, using 7%hypochloride solution. Following a wash in H_2O embryos were transferred to a thickness 1 coverslip. Glue, which had been made using sticky tape dissolved in heptane had previously been spread onto the coverslip to allow the embryos to stick to the surface. Embryos were then dehydrated in silica gel for 10 mins at room temperature and subsequently covered with halocarbon oil series 700 (KMZ Chemicals Ltd). Embryos were injected with eppendorff femtotip needles. *grk* RNA was used in the same concentrations as above.

Microscopy

4-D Imaging and deconvolution

Fixed egg chambers were mounted in Vectashield (Vector Laboratories). Imaging was performed on a widefield DeltaVision microscope (Applied Precision) based closely on an original design by John Sedat and David Agard. The microscope consists of an Olympus IX70 inverted microscope with a 12 bit cooled CCD camera (Photometrics). To minimize spherical aberration, immersion oil with an optical index of 1.534 was used with no1thickness coverslips and 100X objective with a numerical aperture of 1.4. To scan through the entire egg chambers, z-sections and out-of-focus light was re-assigned to its point of origin using iterative deconvolution as previously described (Davis, 2000). Up to 5 egg chambers were filmed in parallel, by repeat visiting using a very accurate XYZ motorized stage.

Particles tracking

Particles were tracked using a 100X/NA1.4 objective lens and time-lapse intervals of 1 sec. Moving particles were tracked using DeltaVision (Applied Precision) and Metamorph (Universal Imaging Corporation) image analysis software. Speeds of all particles tracked were calculated in microns per second according to the distance travelled each interval. A vector was taken between the first and last points of each tracked particle to calculate overall directionality. The directions traveled were then calculated with reference to the anteroposterior and dorsoventral axes as visible in brightfield images or nls GFP fluorescence of the injected egg chamber. The directionality of particles moving anteriorly and then dorsolaterally was calculated with vectors representing the anterior as well as the lateral phase. Both directions and speeds of all particles tracked were calculated using Microsoft Excel and plotted onto circles to represent the direction of travel. Anterior moving particles were tracked immediately after injection (30-60 secs). The dorso-anterior phase of the movement towards the nucleus was more difficult to observe as the particles were spread over a wide range of planes of focus after moving from the site of injection to the anterior to the oocyte. Two approaches were used to identify the dorsoanterior phase of movement. Particles were either injected anteriorly or imaged directly, or injected in the centre of the oocyte and imaged after approximately 20 mins at the anterior.

3

THE ERM PROTEIN MERLIN AND ITS ROLE IN *DROSOPHILA* AXIS SPECIFICATION DURING OOGENESIS

Introduction

The formation of the mutually perpendicular anteroposterior and dorsoventral axes in *Drosophila* is initiated during oogenesis, when key maternal mRNAs become localised asymmetrically within the oocyte (St Johnston and Nüsslein-Volhard, 1992; van Eeden and St Johnston, 1999). The polarities within the developing egg are established mainly through bidirectional signalling, specifying certain regions within the oocyte and the overlying somatic follicle cells. Many symmetry-breaking steps take place before the egg is laid and fertilised and it has been of major interest for many years to find out more about the underlying mechanisms leading to a polarised oocyte. However mutations in any of the maternal genes can cause lethality very early on in development and conventional genetic screens for mutations in zygotic genes (Nüsslein-Volhard and Wieschaus, 1980) may not be able to identify them. More recently, the FRT-Flp system has made it possible to study the mutant phenotype of zygotic lethal mutations in germline clones (Chou and Perrimon, 1992), but genes essential during early oogenesis often interfere with development

when mutated. One way to overcome this problem is to use conditional mutants. Temperature-sensitive mutations will only cause the phenotype at the restrictive temperature, but are viable and display no mutant phenotype at their permissive temperature. By shifting to the restrictive temperature at any time in development the mutant phenotype can be studied. Conditional mutations also have the advantage that the phenotype can be studied a very short time after the shift to the restrictive temperature, reducing the chances of observing effects that are not the direct consequence of the failure of the gene function of interest such as non-specific sickness. Maternal effect mutations can be analysed by studying the ovaries of a homozygous mutant female kept at the permissive temperature and then shifted to the restrictive temperature for a certain length of time. Screens for conditional mutants in *Drosophila* were carried out in the 1970s (Suzuki, 1970; Arking, 1975), but problems with reversion of the mutant phenotype lead to this approach not being as widely used as in yeast, which can be frozen.

Recently, a collection of 180 temperature-sensitive (ts) mutant lines has been created by Helen Francis-Lang and William Sullivan. This screen was designed to identify novel factors involved in cell cycle control and the cytoskeleton of the *Drosophila* embryo. The screen takes advantage of the fact that many maternal effect mutations in essential cellular processes are also likely to be essential zygotically. The starting point was therefore to generate a collection of conditional X lethal lines, which are easy to score in hemizygous males. The generation of these lines was not carried out in our lab, but has not been published yet although the first publication containing this collection was MacDougall et al, 2000. The X-linked conditional mutants were created by feeding EMS, a widely used and effective mutagen, to males of the genotype *y*, Df(1)w^{67g}/Y and subsequently mass-crossing these males to

homozygous females carrying the X-linked viable balancer chromosome FM7*a*, *B*, y^{31d}, w^{a}, v^{OF}. The resulting female progeny was subsequently crossed to FM7*a*/Y males in single pair matings to establish independent lines for testing male lethality at 29°C and viability at 21°C. Out of approximately 10,000 crosses, 180 temperature-sensitive mutations were selected on the X-chromosome and crossed to the female sterile balancer FM7*c* to establish a stable stock. To create the homozygous ts mutant flies, the stocks were temporarily transferred to the permissive temperature, where the progeny were selected against the X-chromosomal balancer FM7*c*, which contains the dominant eye marker Bar (MacDougall et al., 2001; Helen Francis-Lang and William Sullivan, unpublished data). The entire collection of ts lines was kindly given to other laboratories to be tested for identification of novel factors in other developmental context. During a two month rotation in the Davis lab, as part of his four year Wellcome PhD studentship, Yatish Lad screened the collection of ts lethal lines for defects in mRNA localisation by in situ hybridisation with probes against *bcd*, *osk* and *grk*.

Results

The mutation in *l(1)ts594* affects oocyte nuclear migration and mRNA localisation

In order to identify novel genes involved in mRNA localisation and polarity in oogenesis, 73 homozygous ts lines which could be grown up as homozygous stocks at the permissive temperature, were examined after shifting of the females to the restrictive temperature for three days. Ovaries of these females were dissected, fixed and kept at -20°C and in situ hybridisation performed against the three key maternal mRNAs *bcd*, *osk* and *grk* (Yatish Lad and Ilan Davis). When the staining was compared to wildtype staining patterns, it was found that one line, *l(1)ts594* failed to localise *grk* mRNA to the dorsal anterior corner after stage 8 due to a defect in migration of the oocyte nucleus. Taking over the project from Yatish Lad, I subsequently carried out the characterisation of the mutant phenotype during the Diploma studies (Ehrenberg, 1998, also available on CD in Appedix of this thesis). I found that at the restrictive temperature, 55 % of oocytes showed a nuclear migration defect with the oocyte nucleus remaining at the posterior. In such oocytes, *grk* mRNA also remained tightly associated with the misplaced oocyte nucleus. Furthermore, localisation of other maternal transcripts were also affected, with 83% of oocytes showing mislocalisation of *bcd* mRNA to the posterior and 89% of oocytes exhibiting delocalisation of *osk* mRNA in a diffuse pattern to the centre of the oocyte (Figure 3-1 A-B) (MacDougall et al., 2001).

The repolarisation of the oocyte MTs is disrupted in *l(1)ts594* egg chambers

In wildtype egg chambers the first symmetry breaking steps, following the selection of the oocyte are facilitated through bidirectional signalling involving the oocyte and the overlying somatically derived follicle cell layer. The best understood protein involved in this signalling is Grk, a TGF-α homologue. *grk* mRNA is localised at the posterior of the oocyte during early oogenesis and the translated Grk protein functions in a tyrosine kinase signalling pathway with 200 adjacent terminal follicle cells. As a result of the signalling, the 200 terminal follicle cells become specified as posterior, rather than default anterior follicle cells (Gonzales-Reyes et al., 1995; Gonzalez-Reyes and St Johnston, 1998). These cells subsequently send a signal back to the germline to initiate the reorganisation of the oocyte MTs.

The exact nature of the signal remains largely unknown, but some components, have already been suggested to play a role in the transmission and reception of the signal. PKA has been suggested to be part of the machinery that receives the signal in the oocyte (Lane and Kalderon, 1995). Mago nashi has been found to play a role in MT repolarisation in the oocyte and *osk* mRNA localisation, but its precise role in the signalling process is not known (Micklem et al., 1997; Newmark et al., 1997). Notch is required for the specification of the posterior follicle cells, giving it an indirect role in the signalling process (Ruohola et al., 1991; Gonzalez-Reyes and St Johnston, 1998). Notch-Delta signalling is required earlier in oogenesis to polarise the cyst (Torres, 2003) and to specify the number of posterior polar follicle cells, expressing the protein FasciclinIII (Larkin et al., 1996). The two neurogenic proteins Brainiac (Brn) and Egghead (Egh) are required for follicle cell integrity and it has been

suggested that they interact with Notch and EGF-signalling (Goode et al., 1996 a; Goode et al., 1996 b). The extracellular Matrix protein Laminin A is required for the posterior polarising signal in the follicle cells (Deng and Ruohola-Baker, 2000). However, so far the identification of the signal itself remains elusive. The subsequent reorganisation of the cytoskeleton is achieved by disassembling the MTOC at the oocyte posterior and the formation of a diffuse MTOC along the entire anterior cortex as has been shown using immunofluorescence with anti-Tubulin antibodies as well as β-galactosidase fusions to MT-dependent motor proteins. (Theurkauf et al., 1992; Clark et al., 1994; Clark et al., 1997). Visualisation in living egg chambers using TauGFP, a bovine protein known to bind to MTs and fused to a maternal promotor also confirmed the observed organisation in oocytes (Micklem et al., 1997).

The defect in oocyte nuclear migration and resulting dorsoventral defects caused by lack of dorsal signalling of *grk* in *l(1)ts594* egg chambers was found to be caused by a disruption of the oocyte MT network. To establish the exact nature of the defect, marker fusion proteins, such as Nod:βgal and Kin:βgal, which have been shown to localise to the minus and plus ends of oocyte MTs, respectively, were crossed into the mutant *l(1)ts594* line. Kin:βgal is a fusion of the plus end motor Kinesin to lacZ, whereas Nod:βgal was created by replacing the motor domain of Kin:βgal with the putative motor domain of the N-terminal region of Nod (Clark et al., 1997). Nod is a kinesin-related protein that is encoded by the *no distributive disjunction (nod)* gene and is required for segregation of nonexchange chromosomes during female meiosis of *Drosophila.* Although Nod has strong similarities with members of the Kinesin-related protein (KRP) superfamily, isolated and purified Nod has not shown motility, so the question whether it is a motor protein, remains. However, recent data have

identified Nod protein as part of a protein complex that recognises a *bcd* mRNA localisation signal and may be involved in localisation of *bcd* mRNA to the anterior of the oocyte, where the MT-minus ends are located (Arn et al., 2003). The Nod:βgal fusion has been shown to localise to the MT minus end in several cell types and to anterior of stage 8-10 oocytes, respectively. In this context, both fusion proteins were therefore used to define MT polarity in mutant egg chambers of *l(1)ts594*. Subsequent analysis of the fusion protein localisation revealed that in *l(1)ts594* egg chambers the MT network does not reorganise to form the anterior-posterior gradient, as it is the case in wildtype egg chambers at stage 6-7 in mid- oogenesis (See Figure 3-1 B). Instead, mutant oocytes of *l(1)ts594* showed MTs to form a symmetric array thus subsequently resulting in mislocalisation of *bcd* and *osk* mRNA (Ehrenberg, 1998; MacDougall et al, 2001). The nuclear migration defect in *l(1)ts594* oocytes was found to most likely be a result of the defect in organisation of the oocyte MTs (Figure 3-1 C).

l(1)ts594 is a conditional allele of *Mer*

To identify the mutant gene causing the observed phenotype, basic recombination and Deficiency mapping was performed to firstly establish the region of mutation on the X-chromosome. The mutation was found to be within two possible regions that were not covered by deficiencies: 18A2-A5, or 18D-18E on the X-chromosome (Ehrenberg, 1998). Complementation analysis using known alleles in this region were performed by crossing the homozygous mutant flies to any available allele in the region and then testing for either lethality as well as enhancement or suppression of the mutant phenotype at the restrictive temperature (for details on the alleles see Ehrenberg, 1998).

One of the alleles used in the complementation test was a mutant allele of the gene *Merlin* (Moesin-Eszrin-Radixin-related protein), encoding for the *Drosophila* homologue of Neurofibromatosis 2, a member of the ERM (Eszrin-Radixin-Moesin) protein family (Mangeat et al., 1999). These proteins are members of the 4.1 family of proteins, thought to function as linkers between F-Actin and transmembrane proteins at the cell membrane (Turunen et al., 1998) and have also been suggested to function in cell signalling (Mangeat et al., 1999). The human homologue NF2 is a tumoursuppressor protein, causing neurofibromatosis 2, resulting in formation of multiple benign tumours. *Drosophila Mer*, the closest homologue of human NF2, had previously been cloned by degenerate PCR (McCartney and Fehon, 1996) and mutations isolated by reverse genetic methods. Alleles of *Drosophila Mer* have been suggested to play a role in signalling during *Drosophila* eye and wing development (McCartney et al., 2000), but no particular function had been assigned during oogenesis although it is expressed in both germline and follicle cells as shown by antibody staining (McCartney and Fehon, 1996).

When the three available recessive lethal alleles Mer^1, Mer^2 and Mer^4 (LaJeunesse et al., 1998) were crossed to the homozygous *l(1)ts594* line, all three alleles failed to complement the lethality of *l(1)ts594*at 29°C. To investigate whether carrying a genomic fragment including the wildtype copy of the *Mer* gene could rescue the *l(1)ts594* phenotype, flies were subsequently crossed to a line carrying a cosmid containing a genomic fragment including a wildtype copy of *Mer* on the second chromosome. The P-element used was also marked with the w^+ gene, resulting in flies with red eye colour. As the original *l(1)ts594* allele had been generated in a w^- genetic background with flies obtaining white eyes, *l(1)ts594* males carrying a copy of wildtype *Mer* could be identified by their red eyecolour. These males were

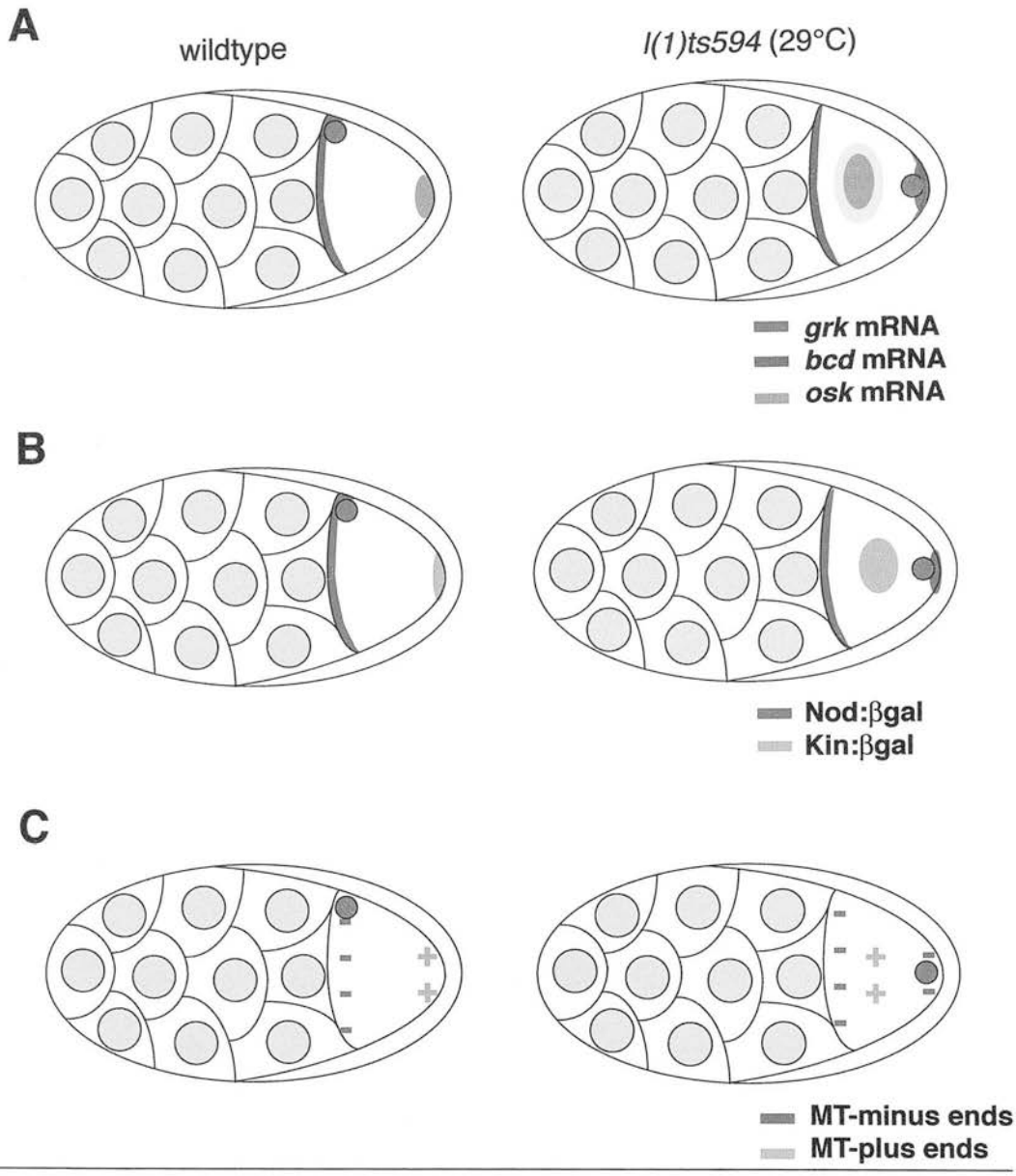

Figure 3-1 *Mer* alleles fail to complement *l(1)ts594*

A Illustrating wildtype stage 9 egg chamber and l(1)ts594. l(1)ts594 show posteriorly misplaced oocyte nucelus and associated posterior grk mRNA. bcd mRNA is mislocalised to the posterior and oskmRNA diffusely localised within oocyte centre.

B Diagram of wildtype and l(1)ts594 egg chambers. NodlacZ, the marker for microtubule minus ends is localised to both anterior and at posterior together with the misplaced oocyte nucleus. Wildtype NodlacZ is distributed along the anterior cortex (see left diagram). KinlacZ, the marker for microtubule plus ends is mislocalised in the oocyte centre instead of posterior localisation as observed in wildtype.

C Illustrating microtubule polarity as suggested for l(1)ts594 versus wildtype. Microtubules form symmetrical array within oocyte instead of anterior posterior gradient.

found to be viable at 29°C. When those males were backcrossed to *l(1)ts594* females, the homozygous *l(1)ts594* female progeny carrying the Mer^{+} containing plasmid was viable and fertile at 29°C and the ovaries had no defect in nuclear migration (data not shown). The cosmid was therefore able to rescue the lethality and sterility of *l(1)ts594*. Another line containing the full length cDNA fragment of *Mer* fused to GFP was also able to rescue lethality and the mutant phenotype. This result suggests that *l(1)ts594* is a novel temperature-sensitive allele of the *Drosophila* homologue *Mer*.

To test this conclusion further, I sequenced the entire coding region of *Mer* in the homozygous mutant *l(1)ts594* flies. To obtain the cDNA, *l(1)ts594* as well as the genetic background line yw^{67g} carrying flies were collected and total mRNA extracted (see Material and Methods chapter of this thesis), and *Mer* mRNA of both lines subsequently reverse transcribed into cDNA using *Mer* specific primers (Appendix). This yielded a fragment of 2.5kb, which was then cloned into a bluescript vector and sequenced using the in house sequencing facility (for details see Material and Methods chapter). When the sequence was analysed and compared to the wildtype sequence of the genetic background of *l(1)ts594*, yw^{67g}, two changes were found, both causing amino acid changes. The resulting amino acid changes were both non-conservative, causing a change of phenylalanine(F) to leucine(L) at position 113 and isoleucine(I) to phenylalanine(F) at position 125 (Figure 3-2). Both changes are located in the conserved N-terminal domain of the protein, thought to be involved in binding to transmembrane proteins (LaJeunesse et al., 1998). It can therefore be strongly concluded that *l(1)ts594* is a novel temperature-sensitive allele of *Mer* and it will from hereon be referred to as Mer^{ts1}

Mer is not required in the germline

It had previously been shown that Mer protein is expressed both in the oocyte and in the posterior follicle cells (McCartney and Fehon, 1996). To investigate whether Mer protein is required in the germline, Mer^{ts1} germline clones were induced using double stranded DNA breaks through exposure to X-ray radiation. This technique takes advantage of the fact that the nurse cells and oocyte derive from the embryonic pole cells, whereas the follicle cells of each egg chambers derive from the embryonic mesoderm. The two cell types separate early in development and mitotic recombination is one technique to create females carrying germ line and follicle cells of distinct genotypes (Wieschaus, 1978).

Mitotic recombination can be induced using X-ray irradiation (Perrimon et al., 1989), or, more commonly the FRT/Flp system derived from yeast, allowing directed mitotic recombination at the FRT sequence. To distinguish between eggs derived from homozygous mutant clones and the wildtype egg chambers, the germ line dependent dominant female sterile mutation *ovoD1* is used. Therefore egg chambers carrying this mutation arrest very early in oogenesis. However, the appropriate *ovoD1*/FRT stocks were not available and the more usual FRT was distal to *Mer*. Therefore, X-ray irradiation was used to create germline clones (Ehrenberg, 1998; MacDougall et al 2000). Out of 1000 crosses, 26 females were found to be mosaic flies and were dissected to obtain the ovaries. Ten ovaries of homozygous mosaic females were used to perform in situ hybridisation against *grk*, *osk* and *bcd* mRNA. All egg chambers showed wildtype localisation of the three maternal mRNA and normal migration of the oocyte nucleus in stage 8-10 egg chambers (Figure 3-3

Figure 3-2

Alignment of Merlin

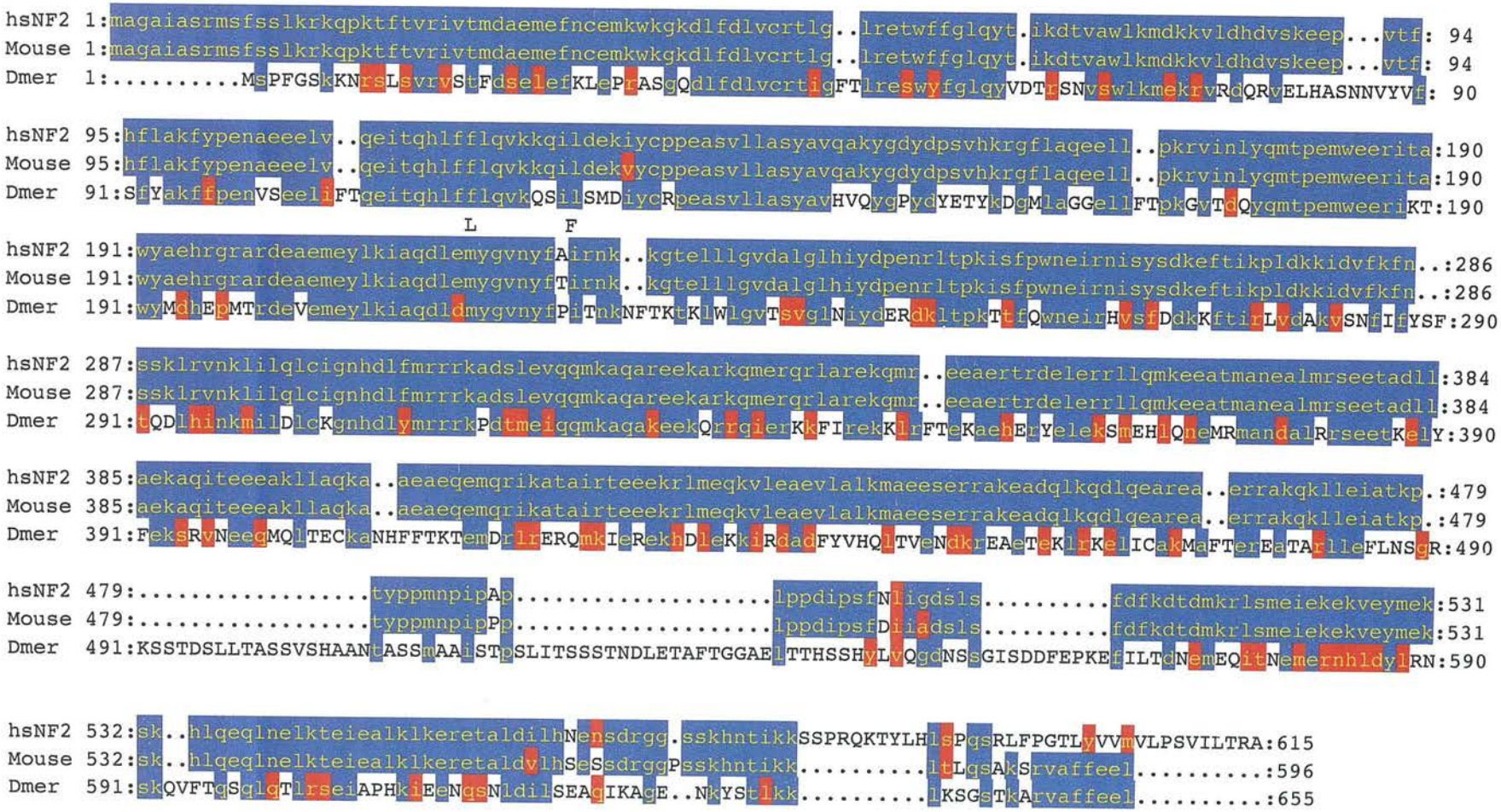

A-C). It could therefore be concluded that Mer is not required in the germline-derived cells during oogenesis.

Mer acts non-autonomously in the posterior follicle cells

To test whether Mer is required in the somatic follicle cells, *Mer* homozygous clones were induced within the follicle cells, using the FRT/Flp system, originally derived from yeast (Chou and Perrimon, 1992), allowing directed mitotic recombination using certain sequences, the Flip-recognition-target sequence, short FRT. To distinguish between the cells homozygous mutant for *Mer* and the surrounding heterozygous cells, the marker nlsGFP (Davis et al., 1995) was used, making the nuclei of all cells which are not part of the clone green fluorescent (see Methods chapter of this thesis). The *Mer* alleles used in this experiment were the viable sterile allele Mer^3 and the strongest lethal allele Mer^1. Due to technical difficulties, Mer^1 clones could not be created and all subsequent results are from follicle cells clones of the viable allele Mer^3.

The mutant follicle cell clones were induced using directed mitotic recombination combining the UAS/Gal4 system with the FRT/Flp (Duffy et al., 1998). To distinguish the homozygous Mer^3 mutant follicle cell clones from the heterozygous cells, nls GFP was used as a marker in these experiments, a modification of green fluorescent protein (GFP) from the jellyfish, *Aequorea victoria*. Transgenic lines carrying a nuclear GFP fusion protein will ubiquitously express nlsGFP, allowing it to be used as a bright and reliable marker. Due to the chromosomal exchange after mitotic recombination, follicle cells carrying the *Mer* mutation on both chromosomes lack fluorescence, because they do not carry the marker nlsGFP. Heterozygous

follicle cell nuclei will fluoresce, carrying one copy of the nlsGFP marker. As a result of mitotic recombination, one half of the daughter follicle cells will also be homozygous for the nlsGFP marker. The nuclei of these cells will fluoresce more intensely and can be visualised and distinguished easily from the heterozygous cell population. Every homozygous mutant clone within the follicle cells will naturally occur together with its twin spot, the cells homozygous for the nlsGFP marker.

To test whether *Mer* is required within the posterior follicle cell layer, follicle cell clones from Mer^3, *FRT/nlsGFP,FRT;en-Gal4, UASFLP* females were examined and 43 interesting egg chambers containing various clones were examined further. 29 of the 43 egg chambers with clonal tissue were analysed in detail. The follicle cell layer of one stage 8 late egg chamber was entirely Mer^3 mutant and this egg chamber showed the *Mer* mutant phenotype. The oocyte nucleus failed to migrate and the posterior follicle cells had formed a multiple layer, just as observed in both Mer^{ts1} and Mer^3 egg chambers. (Figure 3-4 A-C). Three egg chambers had also large clones within the follicle cell layer, covering the entire posterior and displayed the *Mer* mutant phenotype (data not shown). Interestingly, some egg chambers had large Mer^3 mutant clones covering most of the posterior but containing a small population of Mer^3/+ clones (Figure 3-4 D-F).

When these egg chambers were analysed in more detail, it was found that the oocyte nucleus had migrated and that they did not have the double layer of follicle cells within the neighbouring region of the Mer^3/+ follicle cells. This result shows that the follicle cells expressing *Mer* are able to rescue the follicle cell and nuclear migration phenotype in the otherwise Mer^3egg chamber. One very interesting case had one

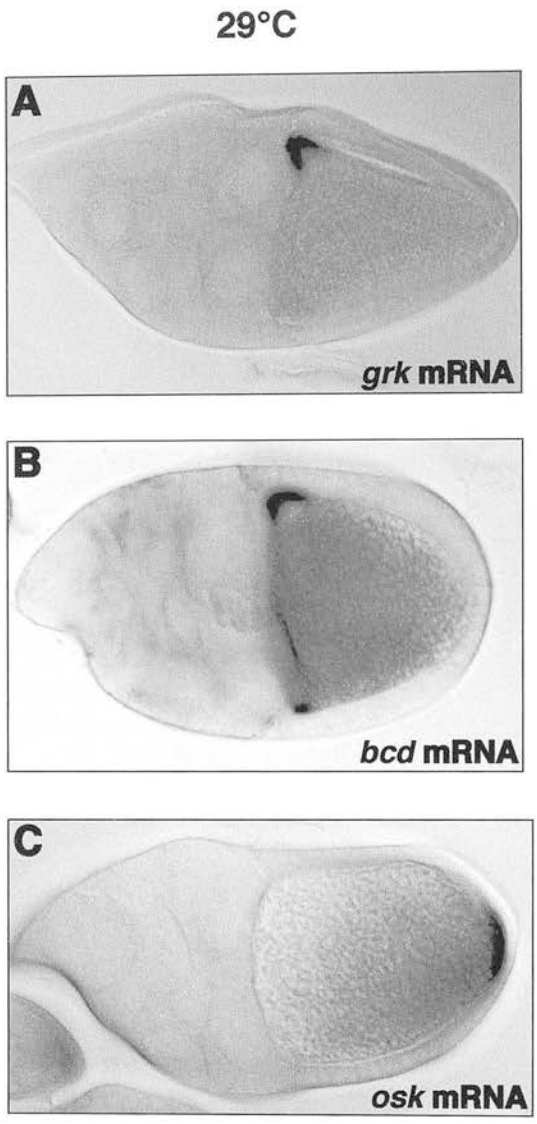

Figure 3-3 Mer^{ts1} germline clones do not show mer mutant phenotype

(A-C) Images of RNA in situ hybridisation on stage 9-10A egg chambers of Mer^{ts1} germline clones using *grk*(A), *bcd*(B) and *osk*(C) probes.

(A) Showing an RNA in situ hybridisation against *grk* mRNA on a germline clone with oocyte and nurse cells mutant for Mer^{ts1}. The oocyte does not show any misplacement of the oocyte nucleus and *grk* mRNA is localised as in wildtype.

(B) *bcd* mRNA in situ hybridisation show normal bcd distribution in Mer^{ts1} germline clone oocytes

(C) *osk* mRNA is localised posteriorly in egg chambers of Mer^{ts1} germline clones, as can be observed in wildtype egg chambers.

All females were kept at the restrictive temperature of 29°C throughout.

single cell at the very posterior of the egg chamber heterozygous Mer^{3}/+ (Figure 3-4 G-H). The follicle cells adjacent to the cell expressing Mer^{3}/+ were arranged in a single layer showing that the single cell expressing wildtype *Mer* was able to rescue the mutant phenotype in 5-6 neighbouring follicle cells, but was unable to rescue the nuclear migration phenotype within the oocyte. It was found that *Mer* producing follicle cells have the ability to rescue the double layer phenotype over a distance of approximately 5-6 cells diameter. It can therefore be concluded that Mer acts in a non-autonomous manner within the posterior follicle cells over a distance of 5-6 cells.

Mer is required for correct posterior follicle cell polarity

In Mer^{ts1} mutant egg chambers, it was found that the posterior follicle cells show a slightly disrupted morphology. This change becomes only apparent after stage 6 and results in the posterior follicle cells forming a double layer. The follicle cells no longer appear regular and columnar, but misplaced around the posterior of the oocyte (MacDougall et al., 2001). When the cell boundaries were highlighted in each follicle cell, using actin staining and visualising the DNA, it was found that the posterior follicle cells form multiple layers (Figure 3-5 A and D). This phenotype is restricted only to the cells in contact with the oocyte.

To determine whether the multiple layers are a result of overproliferation, the cells at the posterior were counted in four separate similar stage 7-8 egg chambers of the genetic background line $Df(1)y,w^{67g}$ and Mer^{ts1} mutant females. Interestingly, it was found that the number of posterior follicle cells increase twofold ($Df(1)y,w^{67g}$:

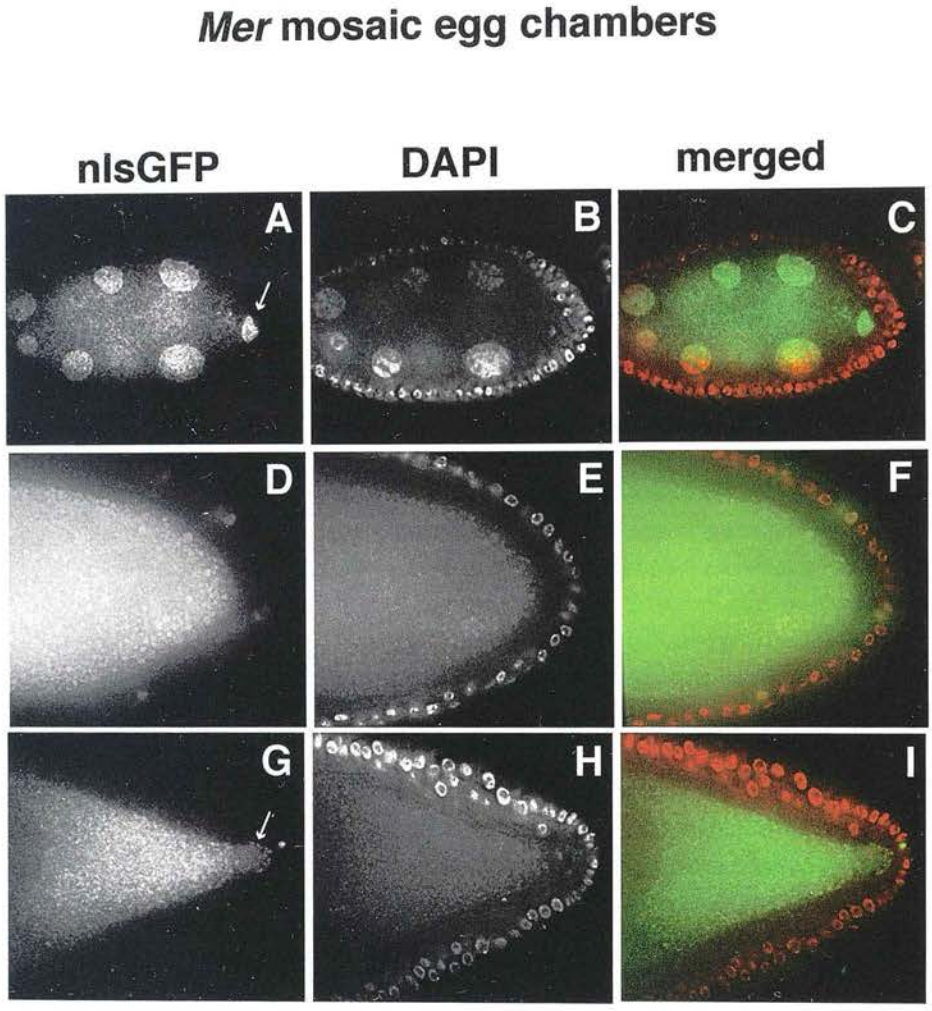

Figure 3-4 Mer is required non-autonomously in the posterior follicle cells

(A-C) Stage 8 egg chamber with all follicle cells Mer^3, but the germline derived cells $Mer^3/+$. The egg chamber is showing the full mutant Mer^3 phenotype, with the oocyte nucleus wrongly positioned at the posterior (see arrowhead) and follicle cells forming multiple layers.

(D-F) Stage 10 egg chamber with four small patches of $Mer^3/+$ cells in an otherwise Mer^3 mutant follicle cell layer. The $Mer^3/+$ cells rescue the mutant phenotype of Mer^3.

(G-I) Stage 10 with one $Mer^3/+$ follicle cell at the posterior in a Mer^3 mutant follicle cell background. The single $Mer^3/+$ cell is able to rescue the mutant phenotype in the neighbouring follicle cells, but fails to rescue the nuclear migration phenotype (see arrowhead).

N=165; Mer^{ts1}: N=287. N= number of follicle cells counted), whereas the number of the other follicle cells remains comparably the same.

To further analyse the posterior follicle cells immunostaining was performed to visualise the centrosomes in each follicle cell, used as an indicator for cell polarity.

When Mer^{ts1} egg chambers were stained for DNA, Actin and γ-Tubulin, which is localised to the centrosomes, Mer^{ts1} egg chambers were shown to have a defect within the posterior follicle cells (Figure 3-5 E and F). Centrosomes in the epithelial follicle cells of wildtype egg chambers are usually located at the apical side of the nucleus, the oocyte facing side (Figure 3-5 B and C), whereas Mer^{ts1} posterior follicle cells often had centrosomes positioned laterally or even posteriorly. Egg chambers were analysed using 0.5μm sections throughout the entire egg chamber and equal numbers of wildtype and Mer^{ts1} stage 6-10A egg chambers were compared. The defect in cell polarity in Mer^{ts1} egg chambers was not observed in earlier stages and only appeared after stage 6.

To find out whether other aspects of the apical- basal polarity in the posterior follicle cells were affected in Mer^{ts1} egg chambers, the distribution of proteins, such as β Spectrin heavy chain (β_H-Spectrin) were studied. (Figure 3-5 G-H). β_H-Spectrin is usually restricted to the apical side of each follicle cell within a Spectrin-based membrane skeleton (Zarnescu and Thomas, 1999). The apical distribution of β_H-Spectrin as well as other markers, such as α-Spectrin was unchanged in Mer^{ts1} mutant egg chambers compared to wildtype. However, only the layer of posterior

follicle cells directly adjacent to the oocyte showed apical localisation of β_H-Spectrin. The double layer of follicle cells in Mer^{ts1} egg chambers showed no detectable β_H-Spectrin in the second layer of follicle cells (Figure 3-5 H). It can therefore be concluded that *Mer* is required for correct MT polarity within the posterior follicle cells, but not in other aspects of cell polarity and that posterior follicle cells contact the oocyte correctly with their apical side.

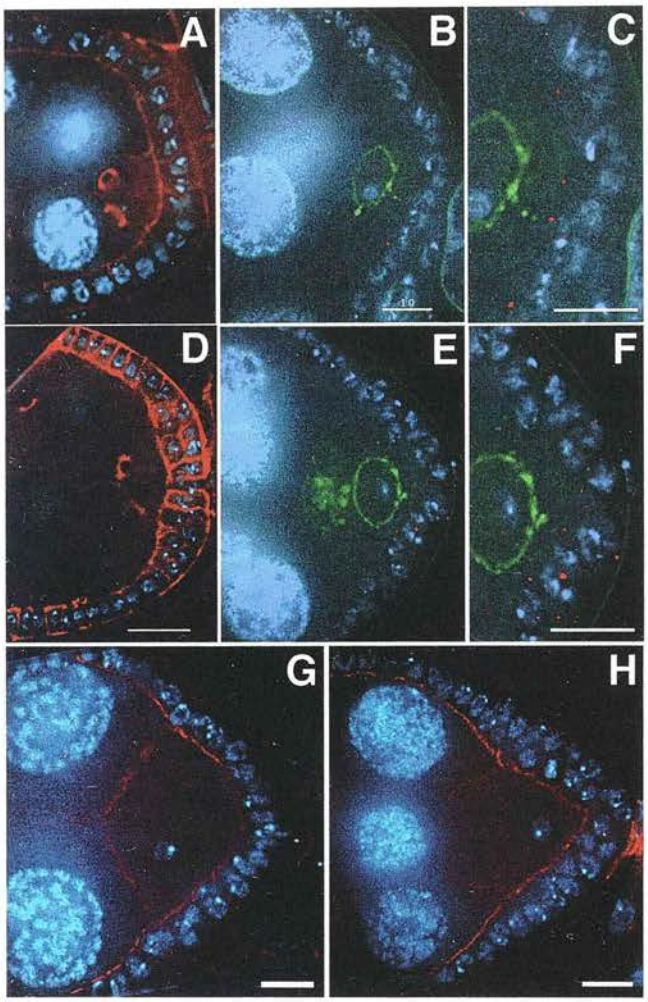

Figure 3-5 Mer is required for correct polarity within the posterior follicle cells

(A and D) Showing the follicle cell morphology visualised by phalloidin-rhodamine staining of actin (red) and DAPI staining of DNA (Cyan). (A) Control showing the columnar layer of posterior follicle cells. (D) *Mer*^{ts1} mutant egg chamber with multiple layers of posterior follicle cells. (B and C) Showing the polarity of posterior follicle of a control egg chamber. Centrosomes (y-tubulin, red) are located at the apical, oocyte facing side of follicle cells . (C) shows a high mignification view of (B). (E and F) In *Mer*^{ts1}egg chambers, posterior follicle cell polarity is disrupted with centrosomes pointing both apically and basally. (F) shows a subregion of (E) in high magnification. (DNA:DAPI(Cyan); nuclear envelope:WGA(green). (G and H) Apical polarity visualised with anti-spectrin β heavy chain (β_H-spectrin) antibody. (G) Control showing apical localisation of β_H-spectrin in the follicle cells. (H) *Mer*^{ts1} egg chamber showing apical localisation of β_H-spectrin in follicle cells adjacent to the oocyte, but not in the second layer of cells.

Scalebars represent 10μm (Image A and D) and 50 μm (Image B, C, E, F, G and H), respectively.

Discussion

The characterisation of a novel temperature-sensitive line of *Drosophila* has revealed that the mutation affects early axis formation. Egg chambers of the line *l(1)ts594* have a defect in oocyte nuclear migration and subsequent dorsoventral signalling mediated by Grk/TGF-α leading to strong patterning defects. Recombination mapping narrowed down the region of mutation and further analysis using known alleles within this region revealed that *l(1)ts594* fails to complement alleles of *Drosophila Mer*. Subsequent sequencing clearly showed that *l(1)ts594* is indeed a novel temperature-sensitive allele of *Drosophila Mer*. The study of the ERM protein member Mer in *Drosophila* oogenesis has revealed that Mer is required for the signal that initiates axis formation within the egg chamber. Mer has been shown to be required for limiting cell proliferation and establishing MT based cell polarity within the posterior follicle cells. The function of Mer has also been shown to be non cell autonomous and appears to be restricted to the posterior follicle cells that are in contact with the oocyte. These cells receive the Grk signal, which in turn activates posterior cell fate. Mer might actually function in apically targeting the follicle cell-oocyte signal, which initiates oocyte MT repolarisation. The current data cannot distinguish between a role of Mer as part of this signal or an indirect role in context of cell polarity. However, Mer clearly is required downstream of posterior Grk signalling and plays a key role in establishing axis initiation. The data provided in this chapter suggest that the effect of Mer on the polarising signal is not indirectly due to overproliferation and changes in the polarity of the posterior follicle cells. Despite changes in the orientation of the centrosomes, the posterior follicle cells of Mer^{ts1} egg chambers distribute β_H-Spectrin correctly in the follicle cells adjacent to

the oocyte. It is therefore likely that these follicle cells are competent to send the polarising signal. It can be concluded from these data that the morphological disruption of the posterior follicle cells in itself is not likely to be responsible for perturbing the unknown signal to the oocyte. Instead, it is proposed that Mer may have a more direct role in targeting the polarising signal to the apical surface of posterior follicle cells.

Drosophila Mer is a member of the ERM protein familiy and the homologue of NF2. ERM proteins have previously been shown to link the actin cytoskeleton to transmembrane proteins, which are involved in signalling. The role of NF2 as a tumour suppressor has also previously been studied in humans and mice and the *Drosophila* overproliferation phenotype, clearly indicates similar functions for Mer in Invertebrates. It is not yet known whether Mer is also required during mammalian oogenesis, but it can be speculated that Mer may function in a similar non-autonomous manner in response to particular signals, such as TGF-α, which is known to be expressed in mammalian oocytes (Vaughan et al., 1992).

The polarising signal sent by the posterior follicle cells to the oocyte defines anteroposterior polarity within the unfertilised egg. The components of the signal are largely unknown, but many factors have been shown to be involved in the bidirectional signalling between the somatic follicle cells and the germline-derived oocyte. Data so far can rule out a direct role for Mer in a number of signalling processes, required during oogenesis. Mer is not required for the identity of polar follicle cells and stalk cells, which suggests that it may not interact directly with Notch-Delta signalling among the posterior follicle cells (Larkin et al., 1996; Ehrenberg, 1998). Mer is also unlikely to be directly involved in the presumptive

Egh/Brn signal, as these proteins are required in the oocyte and not in the follicle cells. However, the similar overproliferation follicle cell phenotype of *brn*, *egh*, *N* and *Mer* mutant egg chambers is intriguing and further analysis should be carried out to explore how these factors are related. So far, no experiments have been conducted to analyse whether any of these alleles are epistatic to Mer and it would be interesting to carry out such an analysis in the future.

Recently, a component of the extracellular matrix, Laminin A, has been shown to be required in the posterior follicle cells for the polarising signal (Deng and Ruohola-Baker, 2000). It could be speculated that Mer and Laminin A could be functionally linked as specialised components required specifically in the posterior follicle cells for the transduction of the polarising signal. Further experiments to test whether both factors are indeed components of one signalling pathway need to be carried out to test this hypothesis. It will be interesting for the future to finally identify all components involved in the polarising signal and to be able to place Mer and its specific function amongst all other known factors.

4

AN INJECTION ASSAY FOR *GRK* mRNA LOCALISATION IN LIVING *DROSOPHILA* EGG CHAMBERS

Introduction

The asymmetric localisation of key maternal transcripts within the developing *Drosophila* oocyte has been shown to be essential for the initiation of the main body axes of the future embryo. Transcript localisation targets proteins function to a particular site, thus establishing the polarity of the oocyte (St Johnston, 1995). Interestingly, both anteroposterior and dorsoventral axes are initiated through the localisation of the maternal transcript, *grk*. Very early on in the development of an unfertilized egg, transcript and protein of the *grk* gene, encoding a homologue of the TGF alpha protein, are localised specifically to the posterior of the oocyte (Neuman-Silberberg and Schüpbach, 1993; Nilson and Schüpbach, 1999). Both *grk* mRNA and protein are present at the posterior cortex of the oocyte, where the transmembrane protein Grk binds to its receptor, torpedo (trp) the *Drosophila* Egf-R, which is located within the follicle cells (for review see Grunert and St Johnston, 1996; Nilson and Schüpbach, 1999). The signal establishes posterior polarity in the adjacent group of 200 terminal follicle cells, which are then activated through an

unknown signal to communicate with the oocyte to establish the reorganisation of the oocyte MTs (Gonzalez-Reyes and St Johnston, 1998; Theurkauf et al., 1992). This reorganisation has been shown to be essential for the subsequent movement of the oocyte nucleus from its posterior position to a lateral anterior position (Gonzalez-Reyes et al., 1995). Subsequently Grk signalling occurs again, this time to establish the dorsoventral polarity within the overlying follicle cells (Neuman-Silberberg and Schüpbach, 1996). Both steps are vital to correctly determine the axes of the future embryo.

grk mRNA has been shown to be involved in the initiation of both, the anteroposterior and dorsoventral axis. The correct localisation of *grk* mRNA and its protein are essential and mislocalisation of *grk* RNA leads to severe formation defects in the embryo, often lethal for the developing embryo. A number of mutant alleles have been shown to affect *grk* mRNA localisation in the oocyte, such as Squid, an hnRNP homologue, as well as fs(1)K10 (Kelley, 1993;Wieschaus et al., 1978; Serano et al., 1995). Both mutants show mislocalisation of *grk* mRNA to the entire anterior cortex instead of the restricted dorsal cap and both mutants lead to dorsalisation of the embryo. More recently, a null allele of the Kinesin heavy chain (KHC) gene has been shown to lead to *grk* mRNA mislocalisation along the anterior cortex with little or no detectable Grk protein leading to ventralisation defects in the embryo (Brendza et al., 2002).

Other mutants, such as the previously described *Mer*, as well as mutants of *mago nashi*, *laminin A* and the *Par* alleles *Par1, Par4, Par3* and *Par5* affect *grk* mRNA localisation through disruption of the organisation of the oocyte MT network. This defect leads subsequently to mRNA mislocalisation of maternal transcripts

(MacDougall et al., 2001; Deng and Ruohola-Baker, 2000; Shulman et al., 2000). The correct localisation of *grk* mRNA to its sites within the oocyte is important for the correct development of *Drosophila*, but the mechanism by which *grk* localisation is established remains largely unknown. However, in recent years important work has established sequences within the *grk* transcript that are essential for its correct localisation. (Saunders and Cohen, 1999; Thio et al., 2000). It has been shown that correct localisation to the dorsal cap depends on the 3'UTR as well as sequences within the ORF of the *grk* gene. The 5'UTR is involved in stability of the RNA. Furthermore, the 3'UTR has been shown to bind to the Squid hnRNP protein in an in vitro assay, which suggests an involvement of Squid in the correct transport and possibly export of the transcribed *grk* RNA (Norvell et al., 1999).

Recent findings implicate the transport of other maternal transcripts, such as *bcd* and *osk*, to require the involvement of motor proteins, such as the minus end-directed cytoplasmic dynein and the plus end- motor protein Kinesin I. Anterior localisation of *bcd* mRNA requires the protein Swa, which has been shown to interact with the dynein light chain (Dlc) of cytoplasmic dynein in vitro and in vivo. It has been suggested that Swa may act as the adaptor linking *bcd* mRNA to dynein in the oocyte (Schnorrer et al., 2000). Furthermore, the formation of a MT dependent complex within the oocyte, containing Exu protein and *bcd* mRNA is required for the anterior specific transport of this maternal transcript (Cha et al., 2001). More recently, a complex recognising a minimal cis-acting localisation signal of *bcd* mRNA has been purified, containing RNA binding proteins, as well as the *bcd* localisation factor Swa and kinesin familiy-member Nod protein (Arn et al., 2003).

The posterior localisation of *osk* mRNA was recently shown to be Kinesin I dependent, as mutants of the motor subunit Kinesin-heavy chain (Khc) displayed mislocalised *osk* transcript. These observations suggest that the plus end directed motor protein Kinesin I transports *osk* mRNA to the posterior after stage 7 of oogenesis (Brendza et al., 2000).

An alternative explanation has been proposed by other studies showing that *osk* is transported to the cortical regions in the absence of of Kinesin function, implying that Kinesin I normally excludes *osk* RNA from the cortex thus allowing it to move to the posterior (Cha et al., 2002). Other studies suggest a model whereby *osk* mRNA localises through cytoplasmic flows within the oocyte and then anchors to maintain posterior localisation (Glotzer et al., 1997).

Recent work analysing the function of Kinesin I on *Drosophila* oocytes suggests that the Khc is required for cytoplasmic streaming within the oocyte and may transport *osk* mRNA by it "hitch-hiking" on a large cargo that drives the Kinesin-dependent cytoplasmic streaming (Palacios and Johnston, 2002). The Actin dependent anchoring has also been shown to play a role in correct *osk* mRNA localisation and one actin binding protein, TropomyosinII, has been identified to have a putative role in *osk* anchoring at the posterior cortex (Erdelyi et al., 1995).

Another protein, Rab11, involved in vesicle transport, has been suggested to be required for *osk* anchoring (Dollar et al., 2002). To clarify the mechanisms, more direct evidence is needed, such as direct observation of the movement of *osk* RNA in vivo. A recent study by Bratu et al. using molecular beacons that fluoresce only when hybridised to endogenous *osk* was able to follow the movement of *osk*

transcripts in real time (Bratu et al., 2003). In the case of osk mRNA localisation to the oocyte posterior the different localisation mechanisms may be used in a complex way and need to all function correctly to establish mRNA localisation in the oocyte (for more details see also chapter 1 of this thesis).

So far, the mechanism of mRNA localisation in the oocyte is not fully understood. As *grk* mRNA initiates both perpendicular axes during oogenesis and is localised firstly to the posterior and then the anterodorsal corner, analysis of the mechanisms underlying this complex localisation pattern is of great interest and would possibly reveal a common mechanism for many of the localised transcripts in *Drosophila*. To better understand the localisation pattern of transcripts requires direct observations of the moving mRNA in vivo. Previously, the maternal transcript *osk* had been injected into oocytes that were cultured, but observation of the path of transcript movement had not been possible, so in depth analysis was limited (Glotzer et al., 1997).

Results

Injected *grk* RNA localises within the oocyte

Our lab had recently developed an assay to inject in vitro transcribed and Alexa UTP labelled transcripts into Blastoderm stage embryos. We improved existing methods by improving the mounting and injection compared with Glotzer et al. and labelled with Alexa-Fluor 546-UTP, or Alexa 488-UTP instead of aminoallyl-UTP and then Fluorescein, which appeared to compromise the motility so that it required addition of nuclear extracts (Lall et al., 1999). When injected, in vitro transcribed and labelled *pair rule* and *wg* transcripts and were shown to localise in a MT and dynein dependent manner (Wilkie and Davis, 2001).

To investigate the localisation of *grk* mRNA within the oocyte, this assay was adapted for use on ovaries. *grk* RNA was in vitro transcribed from the cDNA containing plasmid and labelled with Alexa Fluor 546-UTP, as well as capped with a 7mGGG cap analogue to increase RNA stability (for details, see methods chapter). Ovaries of female flies were then dissected directly into oxygen-rich halocarbon oil and subsequently injected with labelled in vitro transcribed *grk* RNA. As oocytes can only be cultured for approximately two hours before morphological deterioration and cell death, great care was taken to inject them immediately after dissection.

When imaged using timelapse cinematography with one minute-intervals for approximately 1 to 2 hours, *grk* RNA was shown to become localised correctly to the dorsoanterior corner of stage 8-10 oocytes (Figure 4-1 A-H, see also supplementary movies). Localisation of injected *grk* RNA is very efficient with 81% of stage 8-10

oocytes localising *grk* RNA correctly after approximately 1.5 hours (n=96). Earlier stage oocytes seem to be more efficient in localising *grk* RNA, with 87% of stage 8-9 egg chambers localising *grk* RNA correctly (n=47). Stage 10A egg chambers localise *grk* RNA in 83% of cases (n=35), but only 53% of stage 10b oocytes show localisation and the amount of localised *grk* RNA seems to be decreased (n=14) (data not shown). Later stage oocytes do not show any localisation of injected *grk* RNA. The observed decrease in localisation efficiency is probably due to the MT-directed cytoplasmic streaming, which increases five-fold during this stage preventing the injected RNA from localising.

When the injected egg chambers were filmed with time-lapse video microscopy at time lapse intervals of 1-2minutes, it was found that the movement of *grk* RNA to its final destination appears to be bi-phasic. Firstly, *grk* RNA can be seen enriching at the anterior cortex of the oocyte after approximately 10-15 minutes. After 30 minutes, the bulk of injected RNA appears strongly localised to the anterior and already enriches along the dorsal cap. Within approximately one hour the RNA becomes greatly enriched at one side of the oocyte nucleus, in the characteristic pattern seen also with endogenous transcripts.

Interestingly, the origin of *grk* RNA injection within the oocyte does not alter the pattern of localisation observed. When *grk* RNA was injected into the most posterior part of the oocyte instead of the centre, the RNA localised with the same efficiency and the final localisation pattern did not alter (Figure 4-1 E-H). One hour after injection, *grk* RNA predominantly localises to the dorsoanterior cap with only a fraction of the injected RNA remaining along the anterior and particularly in the ventroanterior corner (Figure 4-1D and E).

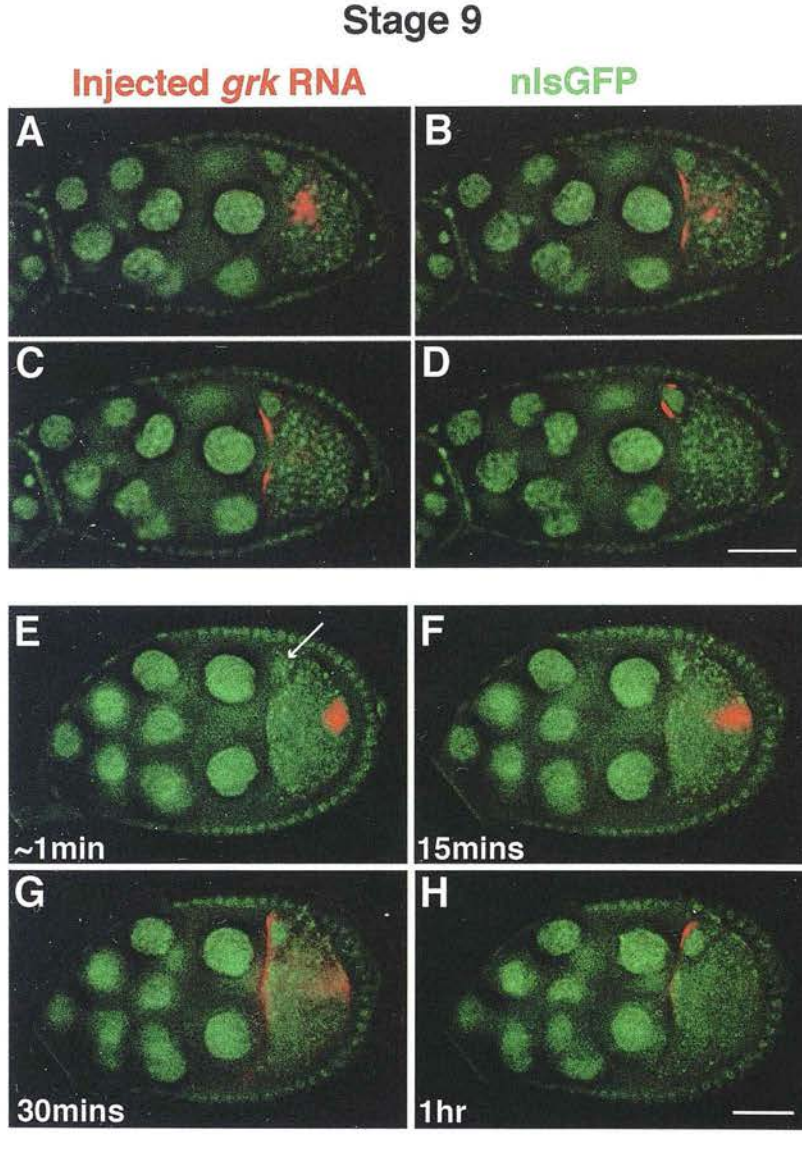

Figure 4-1 Injected *grk* RNA localises to the dorsoanterior of stage 9 oocytes

(A-D) Images taken from timelapse movie of injection of Alexa Fluor 546-UTP-labelled *grk* RNA into a cultured stage 9 egg chamber, expressing nlsGFP.

(A) Showing *grk* RNA injected into the centre of the oocyte one minute after injection.

(B) *grk* RNA partially localises along the anterior cortex of the oocyte fifteen minutes after injection.

(C) Thirty minutes after injection *grk* RNA can be seen localising anteriorly.

(D) One hour after injection, most of the injected *grk* RNA localises in dorsoanterior corner.

(E-H) Images of posteriorly injected *grk* RNA into stage 9 oocyte at successive stages of localisation.

(E) Posteriorly injected *grk* RNA shown one minute after injection.

(F) Fifteen minutes after injection, *grk* RNA has begun to move anteriorly.

(G) Thirty minutes after injection, the majority of injected *grk* RNA localises anteriorly.

(H) One hour after injection, the RNA is predominantly localised at the dorsoanterior cap.

Arrowheads in (A) and (E) indicate the position of the oocyte nucleus, scalebars represent 50 μm.

Final localisation pattern mimics endogenous *grk* mRNA

To investigate whether the localisation pattern of injected *grk* RNA faithfully reflects that of the endogenous *grk* transcript, fluorescent *grk* mRNA in situ hybridisation was performed on comparable stage 9 oocytes (Figure 4-2). Tyramide signal amplification, a highly sensitive enzymatic detection method was used to detect endogenous mRNA (see Material and Methods chapter of this thesis). TSA amplification is based on Horse Radish Peroxidase enzymatic reaction resulting in release of highly reactive fluorochrome species that become covalently bound to surrounding proteins with little visible diffusion.

When *grk* mRNA was imaged and overlayed on a DIC imaging of the egg chamber, it was found that the final localisation of injected *grk* RNA is very similar to that of endogenous transcript (Figure 4-2 A-D). Furthermore, comparison of both injected and endogenous *grk* transcripts by high magnification microscopy show localisation to the dorsoanterior cap in a similar punctate pattern (Figure 4-2E and F). It can therefore be concluded that injected *grk* RNA localises to the same site as endogenous *grk* mRNA approximately 1 hour after injection.

Localisation of injected *grk* RNA is specific

To investigate whether *grk* RNA shows specificity in its ability to localise within the oocyte, another key maternal transcript, *bcd* mRNA, was injected into living egg chambers. Firstly, in vitro transcribed, labelled *bcd* RNA was injected into stage 9 oocytes and its localisation imaged after 1.5 hours. In vivo, *bcd* RNA, which is transcribed in the nurse cells and transported into the oocyte can be found localised in an anterior ring within the oocyte, where it remains localised until fertilisation of

Figure 4-2 Comparison of injected and endogenous *grk* RNA

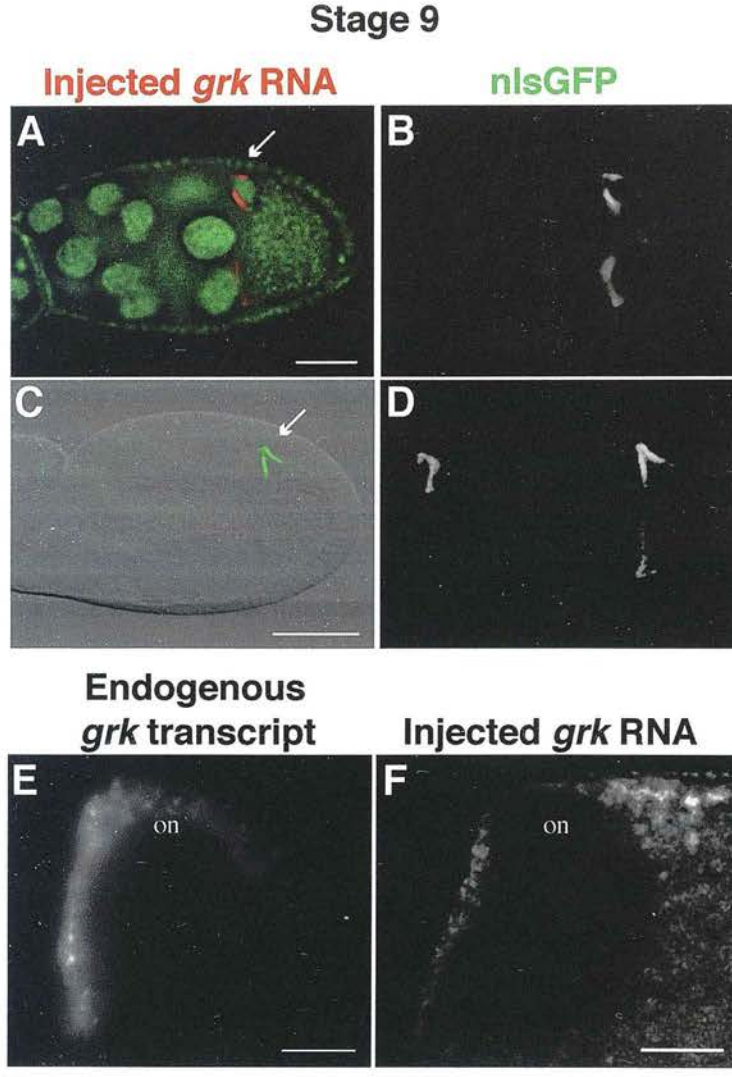

Figure 4-2 Localisation of injected *grk* RNA closely mimics endogenous transcript

(A-D) Stage 9 egg chambers showing a comparison of the final distribution of injected and endogenous *grk* transcripts. Both cases show localisation of the majority of RNA to the dorsoanterior corner with some *grk* RNA at the ventroanterior region of the oocyte cortex.

(A and B) Living stage 9 egg chamber one hour after injection with *grk* RNA.

(C and D) Visualisation of endogenous *grk* mRNA by in situ hybridisation in a fixed stage 9 egg chamber.

(E and F) Showing a comparison of the final distribution of endogenous and injected *grk* RNA at high magnification. Both injected and endogenous *grk* transcripts are localised in a punctate pattern at the dorsoanterior cap.

(E) In situ hybridisation against *grk* transcript in stage 9 egg chamber.

(F) Final distribution of injected *grk* RNA one hour after injection into stage 9 egg chamber.

Scalebars represent 50 μm (A and C) and 10 μm (E and F), respectively.

the egg. *bcd* RNA requires the protein Swa for its anterior localisation, which has been shown to interact with a subunit of cytoplasmic dynein in yeast two hybrid assays (Schnorrer et al., 2000). Furthermore, *bcd* has recently been suggested to localise in large RNA/protein complexes possibly involving motor proteins, such as dynein (Arn et al., 2003). However, no direct proof has been given to date.

When the in vitro transcribed *bcd* RNA was injected, it was found, that it largely did not localise to the anterior. Instead, it was found to adhere to the nearest cortex to the site of injection (Figure 4.3 A-D). Only when injected at the very anterior of the oocyte, did *bcd* RNA localises to the anterior cortex (Figure 4-3 C and D). This finding is in line with recent suggestions that not all machinery for localisation of *bcd* RNA is present in the oocyte, but will need the nurse cell-oocyte transport system and colocalises with proteins, such as Exu, when injected into nurse cells (Cha et al., 2001). It can therefore be concluded, that *bcd*, unlike *grk* RNA cannot localise within the oocyte and does need additional localisation machinery, possibly present within the nurse cells.

In the injection assay, labelled in vitro transcribed *grk* RNA localises in two distinct steps to the anterior and later to the dorsal side of the oocyte nucleus to form the characteristic dorsal cap. To investigate whether this localisation of labelled injected transcripts is specific to *grk* RNA, the anteriorly localised mRNA fs(1)K10 was used for the injection assay. It had previously been shown that the localisation element of K10 mRNA, a 44 nucleotide region residing in the 3'UTR can localise anteriorly in the oocyte when presented as a transgene (Serano and Cohen, 1995). It had also been shown to localise apically in Blastoderm stage embryos when in vitro transcribed, labelled and injected (Bullock and Ish-Horowicz, 2001). To adapt this to the

developed assay within the oocyte, the 44 nt sequence of *K10* mRNA, the *K10-transport/localisation sequence* (*K10tls*) was in vitro transcribed and labelled (Eilidh MacDougall) and injected into stage 9 oocytes. When injected, *K10tls* RNA becomes indeed localised to the anterior, but this localisation is less efficient than localisation of injected *grk* transcripts (Figure 4-3 E). Only 26% of cases injected show clear localisation of the injected *K10* RNA, while the other 64% are unlocalised (n=15). In contrast, a mutant *K10* stem loop previously shown not to localise as a transgene in oocytes and when injected into blastoderm embryos also fails to localise when injected into oocytes (0% anteriorly localised, N=9; Figure 4-3 F) (experiment performed by Alejandra Clark). Furthermore, labelled and injected *hunchback* (*hb*) RNA that is not normally found in the oocyte and is unlocalised in embryos (Davis and Ish-Horowicz, 1991) becomes evenly distributed in the oocyte (Figure 4-3 H). When another embryo-specific RNA, *fushi-tarazu* (*ftz*) was injected into oocytes, a weak localisation to the anterior of the oocyte could be observed (Figure 4-3 G) (44% localise anteriorly n=9). *ftz* mRNA has previously been shown to localise apically in blastoderm embryos and injected transcripts localise similarly to endogenous mRNA, requiring MT- integrity and cytoplasmic dynein (Wilkie and Davis, 2001). Although *ftz* transcripts are not normally present in oocytes, the weak localisation to the anterior suggests that the injected *ftz* transcript may use the localisation machinery in the oocyte, which may use the same components that are present in the embryo. However, it cannot be excluded at this stage that injected *ftz* transcripts localise to the anterior of oocytes by diffusion and anchoring and further experiments would be needed to evaluate the mechanisms of localisation of *ftz* RNA further. The injections of various other labelled transcripts into *Drosophila* oocytes have shown that the anterodorsal localisation of injected *grk* RNA is a specific process.

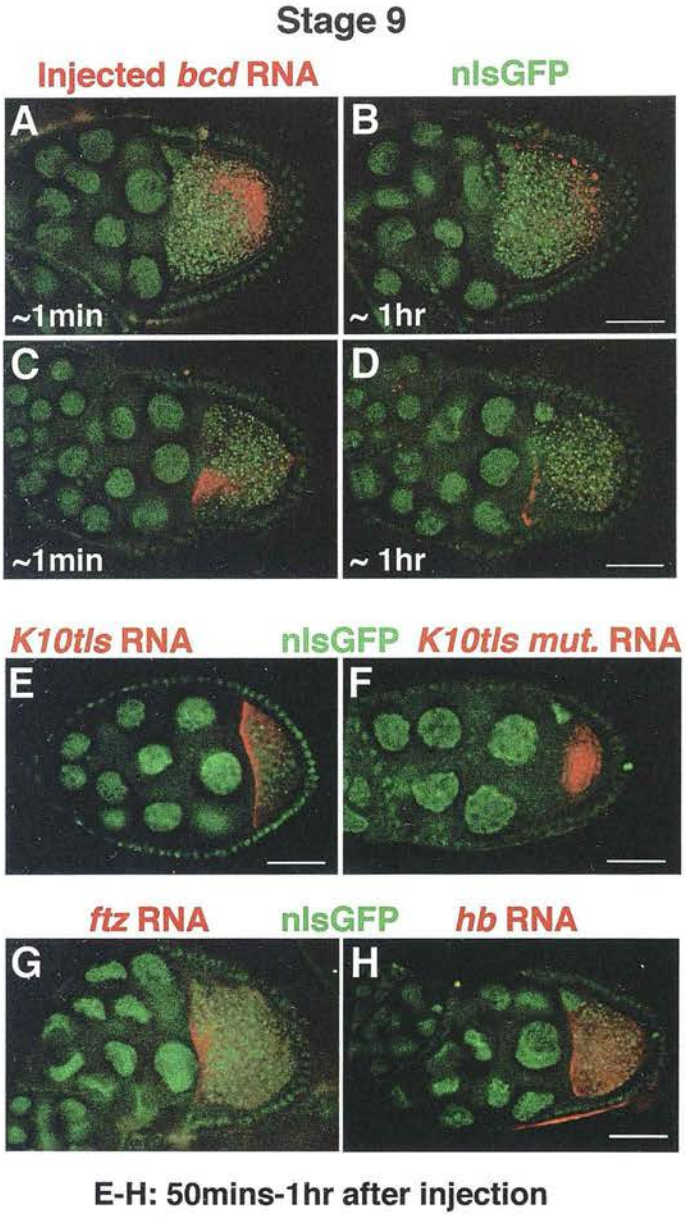

Figure 4-3 Dorsoanterior localisation of *grk* RNA is specific

(A-D) Injection of Alexa Fluor-546-UTP labelled *bcd* RNA into stage 9 oocytes

(A) Stage 9 egg chamber one minute after injection of *bcd* RNA into the oocyte posterior.

(B) One hour after injection, *bcd* RNA localises to the cortex nearest to the injection site.

(C) Showing *bcd* RNA one minute after injection into the anterior part of a stage 9 oocyte.

(D) One hour after injection, *bcd* RNA localises to the anterior cortex nearest the injection site.

(E) Showing a stage 9 egg chamber approximately one hour after injection of *K10tls* RNA into the oocyte. The injected RNA localises to the anterior cortex.

(F) Showing an oocyte injection of the mutated *K10tls* RNA into a stage 9 oocyte approximately one hour after injection. The injected RNA fails to localise and remains near the injection site.

(G) Injected *ftz* RNA weakly localises along the anterior of the oocyte

(H) Injected *hb* RNA fails to localise within the oocyte and diffuses within the ooplasm.

Scalebars represent 50 μm.

Localisation to the dorsoanterior requires Squid

It had previously been shown, that *grk* mRNA localisation requires the hnRNP protein Squid the homologue of heterogeneous nuclear RNA-binding protein (hnRNP) A1. hnRNPs have been implicated in nuclear export and in the processing of RNAs across species. A subset of the hnRNPs, including human hnRNP A1 and A2 have been shown to shuttle between the nucleus and the cytoplasm (Pinol-Roma et al., 1990) and a specific motif in the protein has been shown to facilitate nucleocytoplasmic shuttling (Michael et al., 1995; Siomi and Dreyfuss, 1995). This motif, called M9, is present in the *Drosophila* hnRNP A1 homologue, Squid (Sqd).

In *sqd* mutant oocytes, *grk* RNA is localised to the anterior cortex and fails to localise in the dorsal cap. As a result, the second Grk signal occurs along the entire anterior, leading to strong dorsalisation phenotypes in the embryo. Characteristically, the eggs show a "Squid" like appearance with dorsal appendage material fused at the very anterior of the egg (Kelley, 1993). Sqd protein has been shown to interact with the *grk* 3'UTR in a biochemical UV crosslinking assay. Futhermore, three Sqd protein isoforms (Sqd A, B and S) have been shown to specifically localise within the oocyte. SqdB and SqdS have been detected in nuclei of nurse cells and the oocyte and SqdA has been shown to localise predominantly to the cytoplasm. All three isoforms perform different functions in localisation of *grk* mRNA, with at least one of these isoforms, SqdS, specifically targeting *grk* mRNA localisation (Norvell et al., 1999).

To investigate whether Sqd protein is required for the localisation of injected *grk* RNA in the oocyte, $sqd^{1}/Df(3)urd$ females were dissected and their egg chambers injected with *grk* RNA. The mutation in sqd^{1} affects a germline promotor of *sqd* and eliminates expression of all isoforms during dorsoventral patterning in oogenesis. Heterozygous balanced *Sqd1* females were crossed to the Deficiency uncovering the region including the *sqd* gene.

When *grk* RNA was injected into stage 9 squid mutant oocytes, it localised correctly to the anterior, but always failed to enrich in the dorsoanterior corner (Figure 4-4 A-C). Further injections of *grk* RNA into the $sqd^{1}/Df(3)urd$ females performed together with Alejandra Clark, a postgraduate student in our lab, revealed that 75% of cases show clear anterior localisation (n=8), but no oocytes were found to localise *grk* at the dorsoanterior cap. The localisation of injected *grk* transcripts is very similar to the distribution of *grk* mRNA found in *sqd* mutant oocytes. It can therefore be concluded that injected *grk* RNA, as well as the endogenous *grk* transcript require Sqd protein for correct localisation.

Figure 4-4 Injection of *grk* RNA into *squid* mutant oocytes

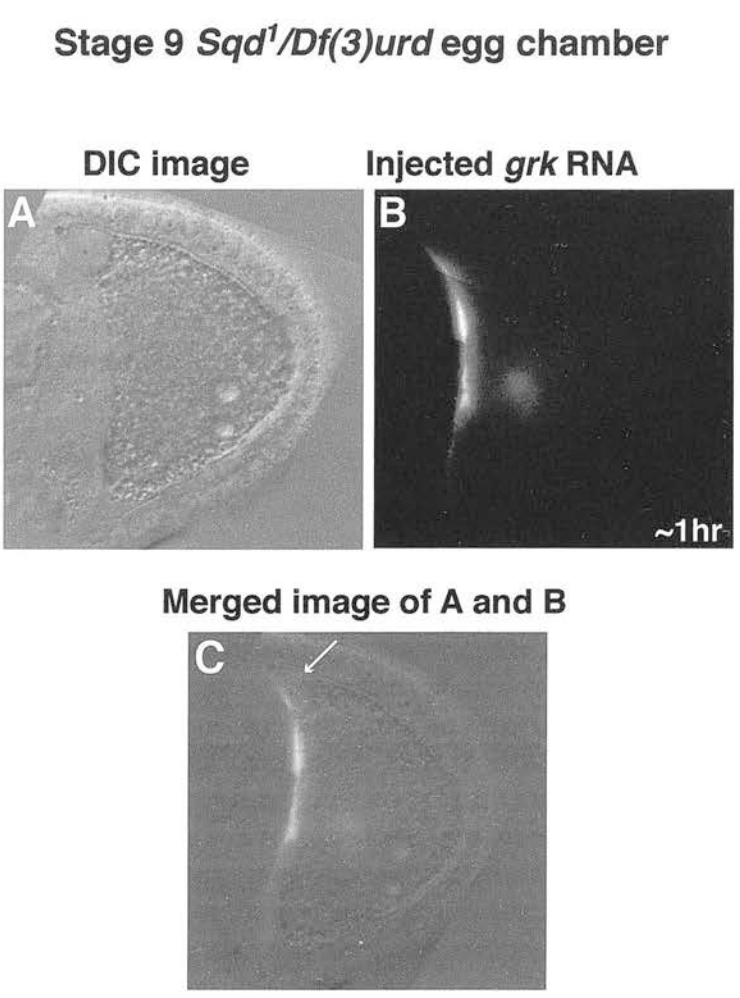

Figure 4-4 Injected *grk* RNA fails to localise to the dorsal cap in *squid* mutant egg chambers

(A) Showing a high resolution DIC image of a stage 9 *sqd*^{1}*/Df(3)urd* (Norvell et al., 1999) egg chamber in vivo. The arrowhead indicates the position of the oocyte nucleus.

(B) Image of injected *grk* RNA into stage 9 egg chamber (A) one hour after injection, The majority of *grk* RNA has localised to teh anterior cortex, but fails to localise to the dorsoanterior cap.

(C) Image of (A) and (B) superimposed to illustrate the final *grk* RNA localisation.

Note: All images were taken at high resolution and delta vision sofware was used to compile several images into one.

Discussion

Injections of in vitro transcribed and labelled *grk* transcripts into cultured oocytes have faithfully reflected the specificity of endogenous *grk* mRNA localisation. Correct localisation of *grk* RNA to the dorsoanterior corner of oocytes requires localisation machinery present within the oocyte. This differs from other maternal transcripts, such as *bcd*, which could not localise correctly when injected into the oocyte. In the case of injected *grk* RNA however, localisation to the dorsoanterior of the oocyte occurred regardless of the injection site within the oocyte. All areas of the oocyte, even the very posterior are able to provide the localisation machinery required for correct *grk* transcript localisation (see Figure 4-1).

When *grk* RNA was injected and imaged using low powered objective lenses and timelapse cinematography, it was observed that localisation occurred in two steps. Firstly, most of the injected *grk* RNA could be seen to move towards the posterior within the first 10-30 minutes. Transiently, when most RNA was located at the anterior, enrichment at the dorsoanterior was also observed. This increased dramatically over the following 30 –60 minutes, with decreasing mRNA along the anterior cortex. This suggests that *grk* RNA localises actively to the dorsoanterior corner within 1-1.5 hrs after injection. The final stage of *grk* RNA localisation was also shown to resemble the endogenous transcript, as visualised by in situ hybridisation. The specificity of *grk* RNA to localise was further supported by injection of the localisation element of *K10* RNA, *K10tls*, which had previously been shown to localise to the anterior within the oocyte. In the assay, this RNA also localised to the anterior. When a mutated form was injected, it failed to localise

within the oocyte, an observation supported by previous findings when this mutated RNA was injected into blastoderm stage embryos. However, localisation of the *K10tls* into oocytes appeared to be reduced, and most oocytes showed aggregation of the injected RNA. The small size of this transcript may increase the probability of aggregation and therefore inhibit localisation in many cases. It will therefore be of interest to inject a larger transcript, possibly the entire 3' UTR into oocytes. *fs(1)K10* mutant oocytes also show similar mutant phenotypes to *Sqd* mutant oocytes, with *grk* RNA failing to localise to the dorsoanterior, but localising at the anterior cortex. When Squid mutant oocytes were injected with *grk* RNA, the same localisation pattern was observed as for the endogenous transcript. It would be interesting to confirm this result with injections of *grk* RNA into *fs(1)K10* mutant oocytes. However, the result of injections into *Sqd* mutants already strongly supports that the developed assay truthfully represents endogenous *grk* transcript localisation.

Other in vitro transcribed and injected RNAs that are not localised and are not specific for the oocyte, such as *hb* RNA, also showed no localisation within the oocyte, further supporting the idea that injected *grk* RNA in the oocyte specifically localises using localisation machinery present in the ooplasm. Interestingly, the injection of the pair rule RNA *ftz* showed weak localisation to the anterior cortex of the oocyte. As this RNA is not normally present in the oocyte, but only transcribed and localised in the blastoderm embryo, this raises the question of a link between the localisation machinery in the embryo and in the oocyte.

Recent data have established a link between the maternal proteins Egalitarian (Egl) and Bicaudal-D (BicD) and localisation of apically localised transcripts within the embryo (Bullock and Ish-Horowicz, 2001). Both Egl and BicD are required for oocyte differentiation and RNA accumulation in the oocyte during oogenesis. They have been shown to colocalise to the minus end of MTs and mutants of both genes show disruption of oocyte MT-integrity and RNA mislocalisation (Mach and Lehmann, 1997; Bolivar et al., 2001). In the embryo, both proteins have been shown to be selectively recruited and co-transported by apically localising transcripts. It would be possible that Egl and BicD and similar proteins could functions as linkers not only in the embryo, but also in the oocyte. Other not yet identified proteins could be involved in both oocyte and embryo mRNA transport. However the decreased efficiency in localisation and the limited use of embryonic patterning transcripts does not yet provide an answer to this observation.

When injected, *grk* RNA is able to localise within the oocyte to the dorsoanterior corner in a similar pattern to endogenous *grk* mRNA. It can therefore be concluded that all the localisation machinery required is present within the oocyte and can be recruited by the injected RNA. When *bcd* RNA was injected into oocytes of cultured egg chambers, it was only able to localise to the nearest cortex. This finding is in line with recent published data, which showed a requirement for *bcd* RNA to associate with factors from the nurse cells in order to achieve anterior localisation in the oocyte (Cha et al., 2001). *bcd* mRNA has been shown to be transcribed by the nurse cells and associates in a complex before transport and localisation into the oocyte. To date, the site of transcription for *grk* RNA is not known, but so far it has been proposed that *grk* may be transcribed by the nurse cells during early oogenesis and other work suggests a transcription possibly by the oocyte nucleus (Saunders and

Cohen, 1999; Thio et al., 2000). However, this data is based on expression of a version of the *grk* transgene lacking certain cis-acting sequences, as well as on colcemid feeding experiments. So far individual endogenous nascent *grk* transcripts have not been detected by in situ hybridisation, as it does not provide the sensitivity to detect very low level transcripts. Although the injection assay shows that all required factors are present within the ooplasm when *grk* RNA was injected, it cannot distinguish between the two possibilities of either oocyte or nurse cell-transcription. Whatever the site of transcription, the mechanism and dynamics of *grk* RNA localisation and movement within the oocyte provide new insights into the delivery of *grk* RNA to its final localisation site. If *grk* is synthesised by the nurse cell cluster, the two-phase movement observed during timelapse cinematography of injected *grk* RNA could resemble nurse cell-oocyte transport and dorsoanterior localisation. If synthesised by the oocyte nucleus, the same two steps are able to deliver the *grk* transcript at its final destination at the dorsal cap.

5

ANALYSIS OF THE MOVEMENT OF *GRK* RNA PARTICLES AFTER OOCYTE INJECTION

Introduction

In vitro transcribed and fluorescently labelled *grk* RNA has been shown to localise when injected into the oocyte cytoplasm of stage 8-10 oocytes in vivo (see chapter 4). Furthermore, all the necessary localisation machinery appears to be present within the cytoplasm to localise *grk* RNA. In chapter 4 of this thesis, it was shown that injected *grk* RNA localises to the dorsoanterior within 1-1.5 hours after injection into the oocyte. Initial movement to the anterior was observed shortly after injection and the second phase of movement to the dorsoanterior corner of the oocyte localised the majority of injected *grk* RNA with the final localisation closely mimicking the endogenous transcript. However, how cytoplasmic localisation of mRNAs is achieved remains not fully understood, although in recent work a number of different possible mechanisms have been proposed and some have been shown to operate in specific cases (for review, see Lipshitz and Smibert, 2000; Tekotte and Davis, 2002).

The first possibility is the specific degradation of unlocalised transcripts and selective stabilization of the localized transcripts (Bashirullah et al., 1999). This mechanism has been shown to be used to localise maternally supplied hsp83 mRNA to the posterior pole of early *Drosophila* embryos (Ding et al., 1993). Alternatively, general diffusion and selective anchoring of transcripts could lead to the localisation of a specific RNA, as has been proposed for *osk* transcripts within the oocyte (Glotzer et al., 1997). Finally, localisation of transcripts could be achieved by directed transport along the cytoskeleton using molecular motor proteins (Tekotte and Davis, 2002). To facilitate mRNA localisation mRNA appears to localise in particles containing motor proteins as well as other transacting localisation factors (Tekotte and Davis, 2002; Arn et al., 2003; Bullock and Ish-Horowicz, 2001). Previous work in our lab has revealed that localisation of apically localised *pair rule* transcripts and *wg* in *Drosophila* embryos is MT and dynein dependent (Wilkie and Davis, 2001). Injected RNA has also been shown to localise into particles prior to localisation with particles containing multiple RNAs.

When in vitro transcribed and fluorescently labelled *grk* RNA was injected into cultured *Drosophila* oocytes, small particles could occasionally be observed even with low powered objectives. Imaging of RNA particles is of great importance for the further understanding of the exact dynamics and mechanisms of RNA localisation. Particle visualisation allows thorough investigation of the speed and direction movement, thus allowing to distinguish between the different models proposed for cytoplasmic mRNA localisation. To investigate whether the particles observed within the ooplasm are aggregates of RNA or whether they have the ability to localise, further timelapse cinematography was performed, both on low and high magnification.

Results

Injected *grk* RNA forms particles in the oocyte

When in vitro transcribed and labelled *grk* RNA was injected into stage 9 oocytes and imaged using time-lapse cinematography using a low powered (20x) objective, small particles of RNA could frequently be observed within the ooplasm (Figure 5-1 A-B). Particles were visualised within minutes after injection close to the injection site (Figure 5-1C). Many of the visible particles appeared to move firstly to the anterior of the oocyte (Figure 5-1D), but tracking their path was made difficult due to the relatively low resolution of images, which only allowed imaging of the very brightest RNA particles.

To determine the precise path of movement of the observed RNA particles, high magnification imaging using high numerical aperture objectives and short interval time-lapse cinematography was therefore used. Typically, injected oocytes were imaged using a 100X objective and imaging was performed at one frame per second for 300 time points. Longer intervals up to one frame per ten seconds were also used, but tracking of particles was found to be more difficult with longer time intervals, as many particles moved out of the focal plane in between two images captured and different particles would apparently cross paths and cannot be uniquely distinguished. However, at time-lapse intervals of 1 frame per second, the tracks of different particles could usually be distinguished. Interestingly, when oocytes were injected with *grk* RNA into the centre and imaged immediately afterwards in one second intervals, particles were found to form approximately 30-60 seconds after injection. Not all injected RNA was visible as particles and the number of visible

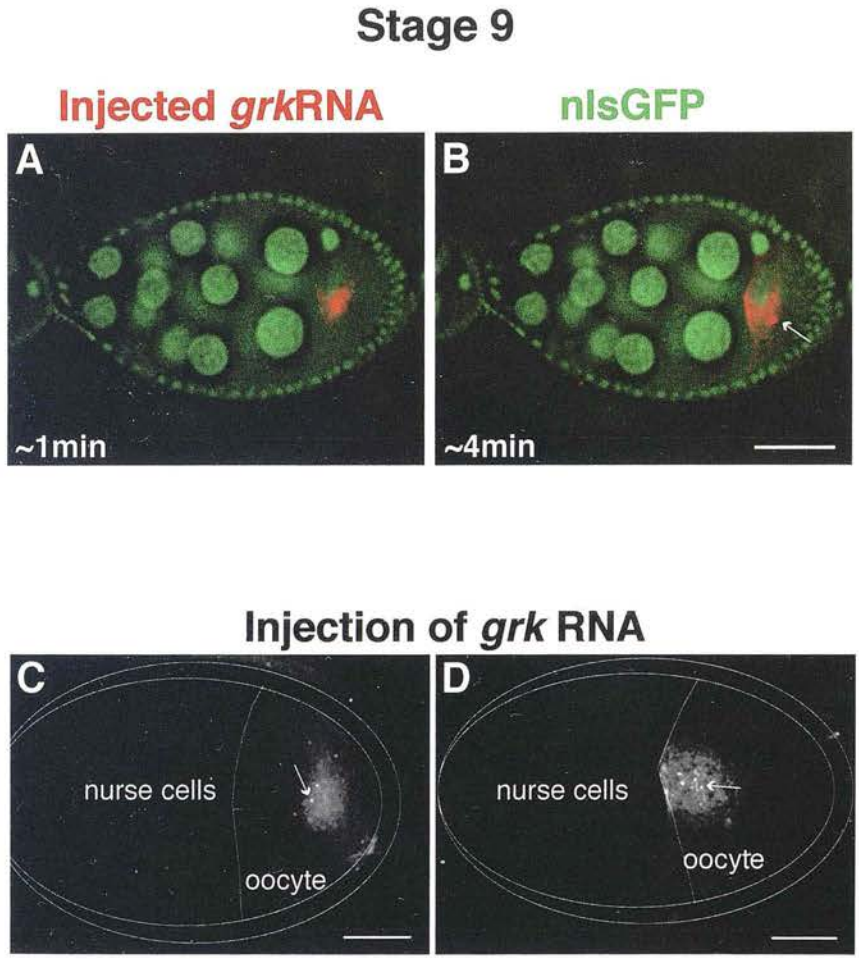

Figure 5-1 Injected *grk* RNA forms particles visible at low magnification

(A and B) Injection of *grk* RNA into the oocyte of an early stage 9 cultured egg chamber.

(A) Showing the egg chamber one minute after injection of *grk* RNA into the oocyte.

(B) Four minutes after injection, *grk* RNA can be seen to form particles (arrowhead). Localisation to the anterior has begun.

(C) Stage 9 egg chamber approximately 1-2minutes after *grk* RNA injection into the centre of the oocyte. Particles have already formed close to the injection site (arrowhead).

(D) Stage 9 egg chamber approximately ten minutes after *grk* RNA injection into the oocyte. Particles can be seen close to the anterior (arrowhead) and localisation along the anterior of the oocyte has begun. Note: white line represents the outline of the egg chambers and follicle cells in (C) and (D). Scalebars represent 50μm.

particles varied, but the size of particles and their behaviour was found to be similar in all experiments carried out. On average, 27% of particles were found to move distinctly anteriorly or dorsally, whereas 31% do not appear to move great distances during the experiment. The remaining 42% of particles visualised could not be tracked as they moved out of focus quickly after formation (n=214). As the experiment only visualised particles in one focal plane, it could not be determined whether the disappearing and reappearing particles followed similar localisation paths, but the dynamics of localisation and increase of RNA along the anterior and the dorsoanterior corner suggest that all particles eventually localise to their correct position. However, localisation of *grk* RNA takes place over one hour or more and it is therefore likely that only a fraction of RNA particles move actively at any given time and that all particles go through periods of rapid movement interspersed by periods of stasis.

Development during oogenesis takes place over a much longer period of time than, for example, during the Blastoderm stages of embryogenesis and the movement of particles is likely to vary. It is therefore not necessary to provide highly efficient and very fast localisation processes, as long as localisation of RNAs is controlled in a sufficient way. It is also possible that the large quantities of *grk* RNA injected into the oocyte during any experiment cannot be localised as efficiently as the endogenous RNA and therefore prolongs localisation. It has previously been suggested that the amount of *grk* mRNA present in the oocyte can affect efficiency of localisation. When multiple copies of the *grk* transgene were presented in female flies, *grk* RNA localisation failed to be precise and *grk* RNA acccumulated along the anterior cortex as well as the cap (Hawkins et al., 1997).

In the above experiments, the amounts of *grk* RNA injected would exceed the total concentration of *grk* transcript, but the exact amounts injected cannot be determined. However, a rough estimate is that 100pl of *grk* RNA at a concentration of 20ng/μl were injected, which amounts to approximately 2.3 million molecules of RNA (for calculations see Methods chapter). It can be concluded that the machinery required to localise endogenous *grk* is present in a large excess compared with the RNA, so that excess of RNA can still be localised efficiently.

When *pair rule* and *wg* transcripts were injected into embryos, the amount of injected RNA could be compared to endogenous transcript through in situ hybridisation on whole mount embryos, which had previously been injected (Wilkie and Davis, 2001). So far it is not possible to perform in situ hybridisation on the injected egg chambers after injection, due to technical difficulties that do not allow the collection of fixation of injected egg chambers. It can therefore be concluded that a huge excess of *grk* RNA is injected, but comparison to endogenous transcript is not possible.

The speed of *grk* RNA particles can reach over 1μm per second

During their phase of movement, particles were found to be travelling at an average speed of 0.25/-0.013 μm/sec, with speed reaching a maximum of 1.25μm/secs. These speeds together with the directionality of the particle movement suggest active transport, rather than diffusion and anchoring of *grk* RNA within the oocyte. However, due to the high resolution imaging with 100X objectives and rapid time-lapse assays with typically 300 images per experiment, it was not possible to track

particles within the entire oocyte over the whole length of time of localisation. Typically, particles were tracked for 5 minutes and sometimes up to ten minutes, which represents only a fraction of the entire RNA localisation path. Attempts to image RNA particles over longer periods of time failed, as imaging at high magnification for longer periods of time compromised particles motility most probably due to photo damage of the cellular machinery required for localisation, presumably by oxygen radicals created by excitation of fluorescent molecules.

The movement of *grk* RNA particles occurs in two distinct phases

A set of experiments was used to try and reconstruct the entire path of *grk* RNA particle movement within the oocyte, as imaging one oocyte at high magnification could not be performed during the entire phase of localisation, due to photo-induced damage and loss of motility of *grk* RNA particles. In order to analyse particle movement, experiments were performed during specific timepoints of localisation and the results used to reconstruct the path of any given particle during the phase of localisation. In one type of experiment, *grk* RNA was injected centrally into the oocyte while imaging with a 100X/NA1.4 objective. Egg chambers had to be injected individually, as multiple injections and imaging would not have been possible with rapid time-lapse imaging. The injected oocytes were then imaged immediately, usually within 30-60 seconds, at the centre of the RNA clouds where most particles tend to form. Sometimes the focal plane used was adjusted prior to imaging in order to capture the maximum amount of particles within the cloud of injected *grk* RNA. Images were then taken every second for about 300 seconds. This approach usually allowed the capture of the first phase of RNA movement towards

the anterior cortex. The second approach used allowed the visualisation of some particles, which firstly moved to the anterior and then turned towards the oocyte nucleus. Observing these particles was extremely difficult and it has not yet been possible to track many turning particles within the oocyte (see also Discussion of this chapter). In these types of experiment, the oocyte was injected centrally and imaged after approximately 10-20 minutes. By this time, a large quantity of the injected RNA had reached the anterior and could be imaged closely to the oocyte nucleus. However, as *grk* RNA particles had spread from the origin of injection, finding large numbers particles within any given focal plane appeared difficult. To obtain more data on particle movement, another approach was used, incorporating injection of *grk* RNA at the anterior of the oocyte and imaging of particles shortly after injection. All time-lapse images were processed using deconvolution analysis and all particles were tracked manually on screen over the entire 300 time points. The exact position in coordinates of each particles at each time point were then transferred to Excel software and calculations of angles relative to the anterior and oocyte nucleus determined, using the first and last visible position of each particle. Clear changes in direction of movement of particles were incorporated in the analysis.

When particles were imaged from a central position in the oocyte immediately after injection, Most particles moved to the anterior during their rapid-movement phase (Figure 5-2 A-C, see also supplementary movies). Furthermore, the entire cloud of *grk* RNA could be seen moving towards a more anterior position, even when the RNA could not be visualised as particles. Interestingly, when particles were imaged closer towards the anterior cortex of the oocyte, some moved in a diagonal path towards the oocyte nucleus. Rarely, *grk* RNA particles could be observed moving towards the cortex of the oocyte, but unlike in the experiments using *bcd* RNA

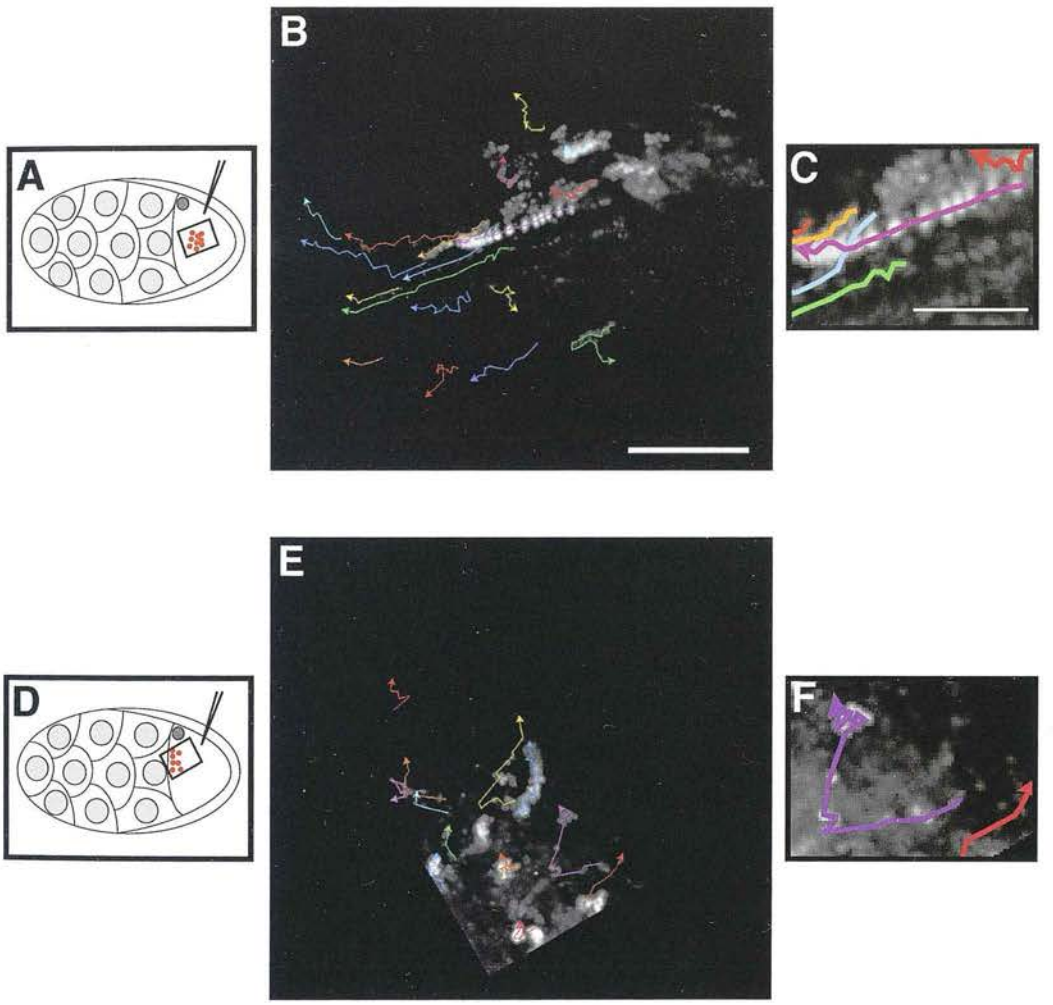

Figure 5-2 Injected *grk* RNA particles move in two distinct phases towards the oocyte nucleus

(A-C) Showing the tracks of *grk* RNA particles immediately after injection into the oocyte.

(A) Illustration showing the site of injection of *grk* RNA and orientation of the image shown in (B).

(B) Image of the movement of *grk* RNA particles during the experiment. Particles are moving anteriorly towards the oocyte cortex. Different coloured arrows are overlayed to represent the different particles.

(C) Showing an enlarged subregion of (B) with a fraction of the particles and their direction of travel.

(D-F)Showing the tracks of *grk* RNA particles when anterior localisation has proceeded.

(D) Illustration of centrally injected *grk* RNA showing region filmed to obtain image (E).

(E) *grk* particles were allowed to move anteriorly and the path subsequently tracked. Dorsal movement can be observed in some particles.

(F) Subregion of (E) showing particles travelling in two phases, first anteriorly, then dorsally.

injections (Cha et al., 2001), these movements towards the cortex were very infrequent (see Figure 5-3 B and D). This type of cortical movement did also not contribute to visible accumulation of larger quantities of *grk* RNA. It can therefore be concluded that, although *grk* RNA particles can move to the cortical regions of the oocyte, this movement only occurs at low frequency. The observations of mostly anteriorly moving *grk* RNA particles in the first set of experiments are consistent with observation of *grk* RNA movement at lower magnification (see also Figure 5-1).

When *grk* RNA was injected into the oocyte either anteriorly and imaged directly after injection, or imaged after the first phase of RNA movement, particles could clearly be observed moving towards the oocyte nucleus, or first moving towards the anterior, then turning and moving toward the oocyte nucleus (Figure 5-2 D-F, see also supplementary movies). In total, 11 particles were observed turning from an anterior movement towards the oocyte nucleus. Interestingly, short intervals of stasis preceded the turning towards the oocyte nucleus, suggestion a possible lag in switching from one phase of movement to the other. Another set of particles imaged could be seen moving diagonally towards the oocyte nucleus. Although these particles had not reached close proximity to the anterior with some particles being about 10 μm away from the anterior, the particles were in a radius of approximately 10-15 μm from the oocyte nucleus. It is therefore possible that the movement captured occurred after these particles had turned. Alternatively, particles injected towards the anterior could already be close enough to the oocyte nucleus and therefore move directly towards this position. Very rarely, particles were observed moving towards the ventroanterior corner, or moving laterally or posteriorly (see Diagram of Figure ure 5-3 B and D). Most particles, however, moved as described

anteriorly or towards the dorsoanterior. These observations were also consistent with further experiments carried out in our lab. In such experiments, performed by Alejandra Clark, a postgraduate student in the Davis lab, oocytes were imaged with the dorsal side up and particles close to the oocyte nucleus were generally seen to move towards it from any position within a close radius (MacDougall et al., 2003).

The results of the experiments described above were used to plot the movement of particles over their entire path (Figure 5-3). To analyse the directionality of the movement of *grk* RNA particles, the angle of movement of particles was plotted in relation to the perpendicular axes of the corresponding egg chamber. Excel Software was used to determine the angle using the first and last coordinates of each particle as reference (for further information, see also Material and Methods chapter of this thesis). To illustrate the directionality of particles, a diagram of circles, representing the axes was used (Figure 5-3 B and D). In the first tracking experiment, the majority of particles moves towards the anterior of the oocyte (Figure 5-3 A and B). When particles were either injected anteriorly and imaged directly, or imaged approximately 15 minutes after injection into the oocyte centre, most particles can be seen moving dorsally as well as anterodorsally and anteriorly. Only a few particles can be observed moving cortically (Figure 5-3 D). It can therefore be concluded that injected *grk* RNA, and, by implication, endogenous *grk* mRNA become localised initially to the anterior and then, by dorsolateral movement to the dorsoanterior corner. Interestingly, the second phase of *grk* RNA particle movement was found to be dependent on Squid, as *sqd* mutant egg chambers did not show dorsal movement of injected *grk* RNA particles (Alejandra Clark, see also MacDougall et al, 2002).

Figure 5-3 Directionality of *grk* RNA particle movement

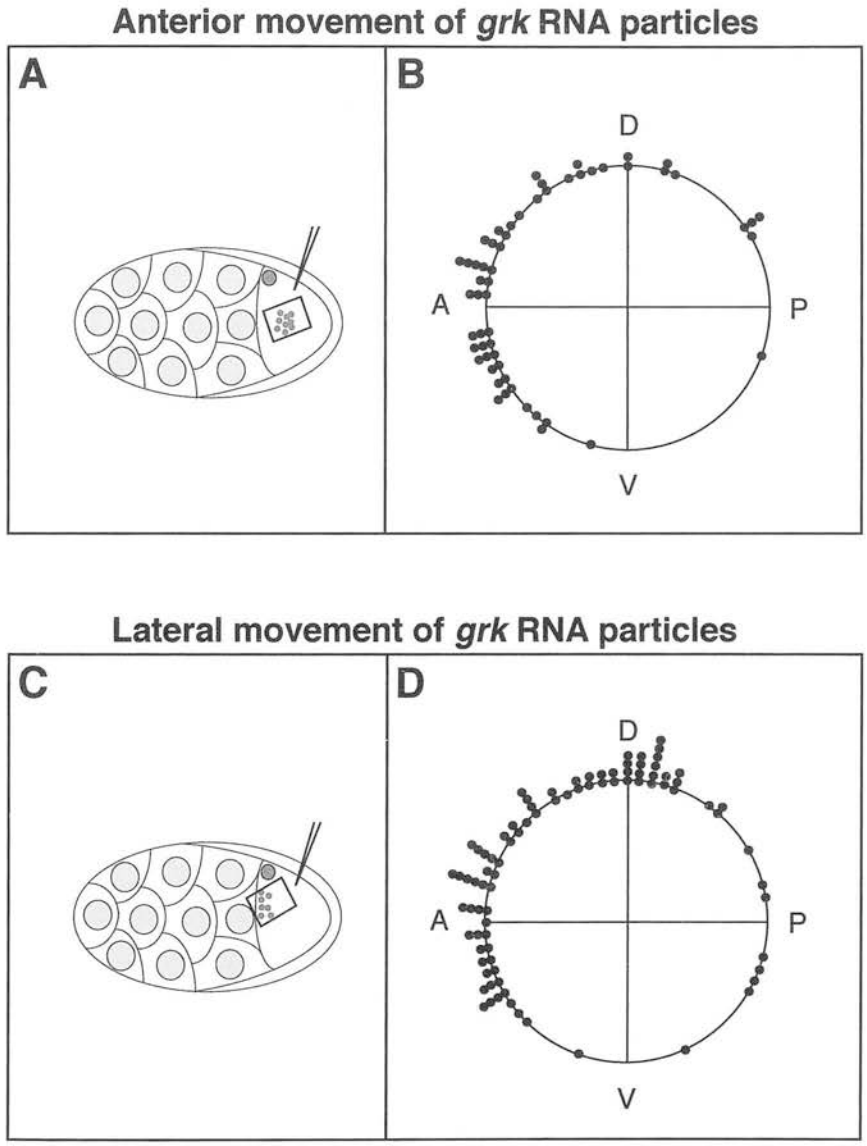

Figure 5-3 *grk* RNA particles move in two distinct phases in the *Drosophila* oocyte

(A and B) Illustration of movement of *grk* RNA particles towards the anterior after injection

(A)Diagram illustrating the injection of *grk* RNA into the oocyte centre.

(B) Diagram showing the direction of *grk* particles movement as analysed from the injection experiments performed at high mignification. The circle represents the four axes of the oocyte with each dot representing the angle of movement. Most particles move toward the anterior, some also move dorsally or anterodorsally with a few particals moving cortically.

(C and D) Illustration of movement of *grk* RNA particles moving laterally.

(C) Showing the position within the oocyte of *grk* RNA particles analysed.

(D) Diagram representing *grk* RNA particles analysed at the anterior of the oocyte. Most particles move dorsally or anterodorsally with only a few moving cortically.

Discussion

When *grk* RNA movement was observed in the oocyte after injection, it was found that the injected *grk* RNA forms particles shortly after injection. When imaged at high resolution at approximately one minute after injection, *grk* RNA had readily assembled into particles. Interestingly, these particles moved with clear anterior or dorso-anterior directionality in most cases. In order to try and reconstruct the entire path of *grk* RNA localisation, high magnification time-lapse cinematography was used in several different approaches. To eliminate the problem of photo damage of the localisation machinery within the oocyte, short time interval experiments were used at different stages of *grk* RNA localisation. Typically, *grk* RNA particles were imaged at different stages for approximately 300 seconds at 1 second time intervals. When *grk* RNA particles were imaged immediately after injection, most particles were found to move anteriorly, with exceptions of some particles moving either laterally, posteriorly or diagonally towards the oocyte nucleus. However, most of injected *grk* RNA moved anteriorly, as could be seen even when particles weren't visible in this particular focal plane.

When *grk* RNA particles were imaged 20 minutes after injection at an anterior position, close to the cortex, some *grk* RNA particles could be observed moving first anteriorly and then turning towards the oocyte nucleus. Interestingly, such particles often remained pausing for a short while before changing their direction. This movement could suggest movement of particles along the cytoskeleton with a switch, such as different population of MTs, contributing to this particular directionality change. However, turning particles could not be observed at high

frequency and only 11 particles in total were seen to move and turn dorso-anteriorly. The infrequency of turning particles could be due to a number of different factors. Firstly, particles were only imaged within a narrow region, as imaging was performed at high resolution in only one focal plane. Such imaging allows the capture of particles within approximately 1μm depth from the plan of focus on either side. If the *grk* particles move further away from the focal plane, they become invisible and cannot be tracked. As particles had to be imaged with very short intervals, typically one second, it was not possible to capture a large region within the oocyte, as the speed of the digital camera and automatic stage did not allow this. When *grk* RNA was injected and imaged immediately, imaging at the centre of the cloud allowed tracking of a reasonable number of particles at a time. Due to the nature of particle movement however, less *grk* RNA could be found after 20 minutes at certain areas of the anterior.

Particles can generally be described as moving and pausing, so not all *grk* RNA particles will reach a certain point away from the site of injection at the same time. This explains in part the lower numbers of particles observed with such experiments. Particles may also turn within different regions along the anterior and around the oocyte nucleus. Therefore, only a small fraction of particles can be observed turning towards the oocyte nucleus within a given region of the oocyte. Further experiments will be needed to investigate whether the majority of particles move indeed in two phases within the oocyte. However, the experiments clearly show that *grk* RNA localises in two steps suggesting some sort of switch within the movement of *grk* RNA. This switch could be regulated by different subpopulations of MTs within the oocyte, along which *grk* RNA particles could be moving, using cytoskeletal localisation machinery and experiments so far implicate that the endogenous *grk*

RNA may utilize such cytoskeletal structures involving the MTs within the oocyte. Different RNAs have previously been shown to localise in a MT dependent manner (for review, see van Eeden and St Johnston, 1999). It is therefore likely that *grk* RNA localisation within the oocyte may utilise similar structures.

The results of this chapter clearly state the significance of the two-step movement of *grk* RNA particles within the oocyte. Firstly, unlike other maternal transcripts, *grk* RNA can recruit all factors required for localisation in the ooplasm. Secondly, localisation occurs in two steps to deliver the RNA at the dorsoanterior corner. As it is currently not resolved where *grk* RNA is synthesized, it can only be suggested that the two phases of movement represent the distinct steps of *grk* localisation, either in the oocyte, or in nurse cell-to oocyte transport and localisation to the dorsoanterior (see also chapter 8 of this thesis). Both phases of movement are clearly distinct from diffusion, as particles display directionality as well as speeds suggesting the possibility that *grk* RNA in the oocyte localises by directed transport along the oocyte cytoskeleton.

6

LOCALISATION OF *GRK* RNA REQUIRES MICROTUBULES AND DYNEIN

Introduction

The localisation of many mRNAs within specific regions of the cytoplasm have previously been shown to require an intact MT cytoskeleton and recent work suggests that directed transport of many transcripts along a polarised cytoskeleton may be the most common mechanism of mRNA localisation (Tekotte and Davis, 2002; Jansen, 2001). In *Saccharomycis cerevisiae*, localisation of *ASH1* mRNA to the bud of a dividing cell is achieved by transport along the Actin cytoskeleton using the class V myosin motor Myo4p (Jansen et al., 1996; Munchow et al., 1999). Furthermore, it has been shown that particles of fluorescently tagged *ASH1* mRNA move within yeast cells, illustrating the Actin based transport of this mRNA in vivo (Bertrand et al., 1998).

The assay to inject fluorescently labelled transcripts into living *Drosophila* embryos based on modifications of previous assays (Glotzer et al., 1997; Lall et al., 1999), which was developed by our lab, revealed that pair-rule and *wg* transcripts require the minus end directed motor protein, dynein, for apical localisation. Transcripts move apically along the polarised MT network towards the minus end with speeds

consistent of dynein based transport (Wilkie and Davis, 2001). It was also shown that the maternal proteins Egl and BicD are recruited by injected pair-rule mRNA, possibly functioning as linkers between dynein and the recruited transcript although direct interaction with RNA is not particularly likely (Bullock and Ish-Horowicz, 2001).

In *Drosophila* oocytes, maternal transcript localisation initiates axes formation. The plus end- directed motor protein Kinesin I has been implicated to play a role in posterior localisation of *osk* mRNA (Brendza et al., 2000; Cha et al., 2002). The localisation of *bcd* mRNA requires Swa, a protein interacting with the dynein light chain in biochemical assays (Schnorrer et al., 2000). *bcd* mRNA also requires Exu protein (St Johnston et al., 1989) for the correct path of localisation of injected *bcd* RNA in living oocytes (Cha et al., 2001).

In comparison with both *bcd* and *osk* RNA, less was known about the mechanism of *grk* RNA localisation in the oocyte at the onset of work for this thesis. *grk* RNA localisation has been shown to require MTs within the oocyte (Pokrywka and Stephenson, 1991) and it recently emerged that Kinesin I is required for the dorsoanterior localisation of *grk* RNA (Brendza et al., 2002). It has been suggested that Kinesin I affects *grk* RNA localisation through the requirement to recycle the minus end directed motor cytoplasmic dynein back to the posterior (Brendza et al, 2002) and further evidence of involvement of dynein in *grk* mRNA localisation comes from overexpression of p50/dynamitin. Dynamitin is part of the dynactin complex, which is required for Dynein processivity (King and Schroer, 2000). In egg chambers overexpressing p50/dynamitin, *grk* localisation is disrupted, further suggesting a role of dynein in *grk* mRNA localisation in the oocyte (Januschke et al.,

2002). However, the path of *grk* RNA had not been visualised directly and it had not been tested whether dynein is directly involved in *grk* RNA localisation. The experiments described in the previous chapters of this thesis provide a powerful tool to test directly the requirement of molecular motors, such as dynein in *grk* RNA localisation in the oocyte.

Results

grk RNA localisation requires the integrity of microtubules, but not the actin cytoskeleton

In order to investigate whether *grk* RNA requires the integrity of the oocyte MTs at any stage of localisation, various experiments were performed using colcemid, a MT depolymerising drug. In the experiment, colcemid was injected at a concentration of both 30 μg/ml as well as 100 μg /ml. There was no difference in the result using the two different concentrations, so 100 μg/ml of colcemid were used in the experiments shown below. Colcemid was also injected either ten minutes prior to *grk* RNA injection, or coinjected in the same needle as *grk* RNA. Both approaches gave similar results and because coinjection minimises damage to the egg chamber, all following results shown are coinjection experiments, unless otherwise stated.

When oocytes were coinjected with colcemid and *grk* RNA, unlocalised distribution of *grk* RNA within the oocyte could be observed (Figure 6-1A). The RNA quickly distributed evenly from the site of injection and no directed movement of RNA could be observed, indicating that colcemid successfully blocks all *grk* RNA localisation within the oocyte. (N=26 localisation: 0%). Some mRNAs have previously been shown to require not just MT integrity, but also an intact Actin network. *osk* RNA has been suggested to require Actin for anchoring at certain stages within the oocyte (Glotzer et al., 1997; Erdelyi et al., 1995).

To investigate whether *grk* RNA also requires the actin cytoskeleton for localisation, egg chambers were injected with the actin depolymerising drug CytochalasinD. When CytochalasinD was coinjected with *grk* RNA at concentrations of 150µg /ml, *grk* RNA localized in a manner indistinguishable from control egg chambers injected only with *grk* RNA (Figure 6-1 B). In the majority of cases, *grk* RNA localised correctly within the time observed previously (N=15 localised 86%). It was technically not possible to use immunostaining against Actin as a positive control following Cytochalasin D injections into cultured egg chambers. However, the same batch of Cytochalasin D was used by other lab members on Blastoderm stage embryos at the same time, where nuclei could be observed to dislocate to the centre of the embryo, due to Actin depolymerisation, ruling out that the Actin depolymerising drug was ineffective. It can therefore be concluded that *grk* RNA localisation and by implication endogenous *grk* transcript localisation, does not require Actin, but does require the integrity of the oocyte MTs.

To analyse whether the integrity of oocyte MTs is required for both steps of *grk* RNA localisation, colcemid injections were also performed 10-30 minutes after *grk* RNA injection. In those experiments, partial localisation of *grk* RNA to the anterior (Figure 6-1 C and D) and the dorso-anterior (Figure 6-1 E and F) had already taken place. When oocytes were injected with the MT depolymerising drug after initial anterior localisation of *grk* RNA, no further localisation to the dorso-anterior corner was observed and *grk* RNA became generally more delocalized (see Figure 6-1 D). However, when dorso-anterior *grk* RNA localisation was already visible at the time of colcemid injection, the result was less clear. Overall, *grk* RNA localisation did not seem to increase further, but the dorsoanterior localisation as well as anterior localisation did not change (Figure 6-1 E and F). So far, the results suggest that *grk*

Figure 6-1 Injections of MT-and Actin depolymerising drugs

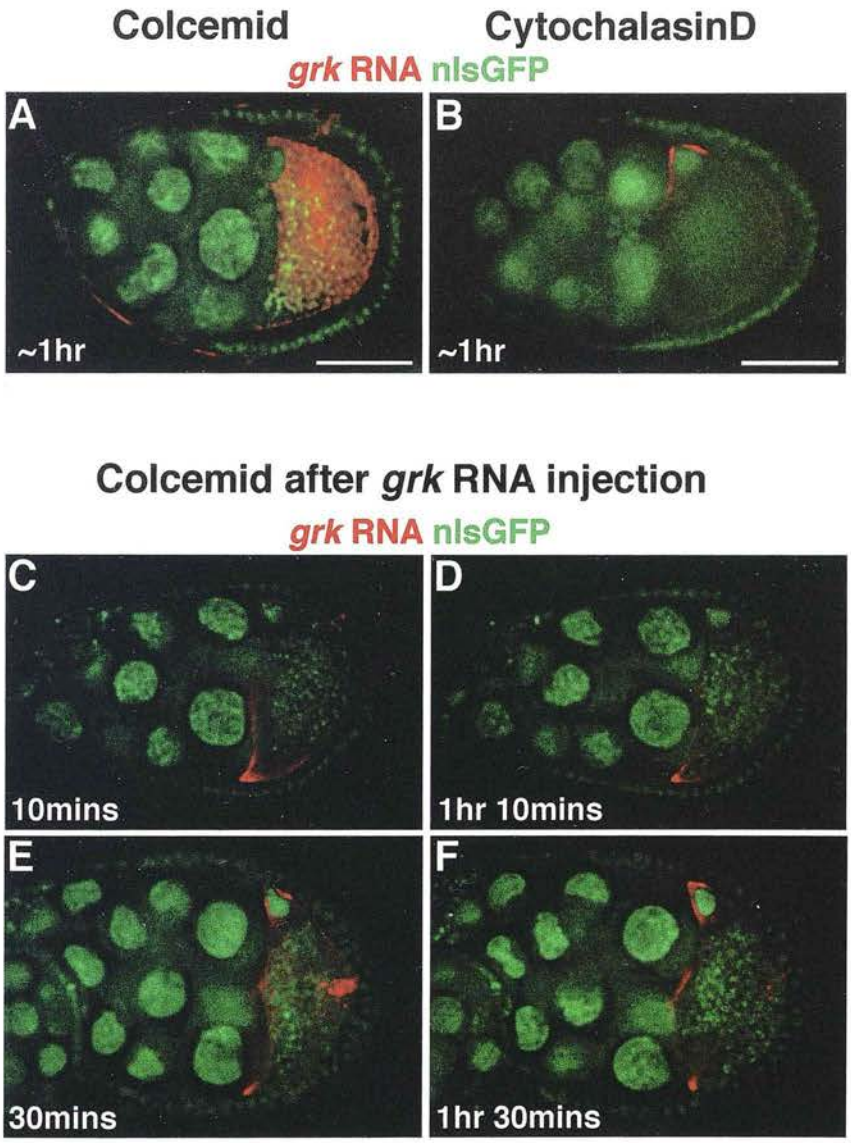

Figure 6-1 *grk* RNA localisation requires microtubules, but not Actin

(A) Coinjection of *grk* RNA and 100µg/ml Colcemid into living stage 9 egg chamber. One hour after injection, *grk* RNA is dispersed within the ooplasm and does not localise.

(B) Coinjection of CytochalasinD 150µg/ml and *grk* RNA. One hour after injection, *grk* localises to the dorsoanterior corner.

(C) Image taken immediately after injection of colcemid 10 minutes after injection of *grk* RNA. The injected RNA has begun to localise anteriorly with very little RNA reaching the dorsoanterior.

(D) Image taken a further hour after (C). *grk* RNA has not localised further.

(E) Image taken immediately after injection with colcemid 30 minutes after injection of *grk* RNA. Dorsoanterior and anterior localisation of *grk* RNA is visible at this stage.

(F) Image taken a further hour after (E). *grk* RNA has not localised further, but still localises dorsoanteriorly.

Scalebars represent 50 µm.

RNA already localised at the dorsoanterior corner may be more resistant to the treatment with MT depolymerising drugs. The depolymerisation of MTs may not be complete and there may still be short MTs within the oocyte, to which *grk* RNA could bind. This would explain, why the dorsoanteriorly localised *grk* RNA, as well as anteriorly localised one are not delocalised by colcemid injection.

Localisation of *grk* RNA requires microtubule polarity

To determine whether correct oocyte MT polarity is required for *grk* RNA localisation, experiments were performed using the previously studied allele of *Mer*, Mer^{ts1}. As shown in chapter 3 of this thesis, the mutant phenotype of Mer^{ts1} oocytes is a result of incorrect MT repolarisation during stages 6-7. Instead of an anterior-posterior MT gradient within the oocyte, Mer^{ts1} mutant oocytes display symmetrical MTs organisation, with the MT minus ends at the posterior, as well as the anterior of the oocyte. Plus ends of these MTs are thought to be located within the centre of the oocyte, as shown using MT polarity markers.

When in vitro transcribed and fluorescently labelled *grk* RNA was injected into the centre of Mer^{ts1} mutant oocytes, *grk* RNA could be seen to localise to both the posterior and anterior cortex of the oocyte (Figure 6-2 A). Interestingly, localisation at the posterior was very tightly associated with the oocyte nucleus (which has not migrated in ~50% of cases of these mutants-see chapter3), similar to the endogenous transcript as shown in RNA in situ hybridisation procedures. Endogenous *grk* mRNA is only localised to the posterior in Mer^{ts1} oocytes (Figure 6-2B). However, when *grk* RNA was injected into the centre of the oocyte of Mer^{ts1} egg chambers, *grk* localised to both poles of the oocyte, which correspond to the location of MT

minus-ends. The anteriorly localised injected *grk* RNA was distributed evenly along the entire anterior cortex, with no visible enrichment in either anterior corner (Figure 6-2 A). These results indicate that the second step of *grk* RNA localisation requires the correct positioning of the oocyte nucleus at the dorsoanterior corner. In Mer^{ts1} mutant oocytes, the second step of localisation of injected *grk* RNA is disconnected and anteriorly localised *grk* RNA is unable to initiate in the second step of localisation.

Dynein is required to localise *grk* RNA in the oocyte

When *grk* RNA was injected into Mer^{ts1} mutant oocytes, the injected RNA moved to the posterior and the anterior cortex, where the minus ends of MTs are thought to be located. It is therefore of importance to test whether the movement of *grk* RNA could be facilitated by MT dependent minus end directed localisation machinery. One important abundant motor protein, which is thought to direct movement along MTs towards the minus end, is cytoplasmic dynein.

Cytoplasmic dynein is a multi-subunit protein known to be required for many processes in *Drosophila*, such as lipid droplet transport and the localisation of transcripts in *Drosophila* embryos (Gross et al., 2000; Wilkie and Davis, 2001). The dynein protein is a heterodimer of a multiple complex consisting of light, intermediate and heavy chain subunits.

In order to find out whether *grk* RNA transport could require the dynein motor protein, an approach was undertaken to affect the protein activity by injecting antibodies against parts of the dynein protein to reduce or eliminate protein activity. Two different monoclonal antibodies against different parts of the dynein heavy chain (see Methods chapter for details, as well as MacDougall et al, 2002) were injected either 10 minutes prior to *grk* RNA injection, or coinjected together with the RNA.

In both cases, localisation was completely abolished within each egg chamber (Figure 6-2 C; N=34, 0% localised). The subsequent experiments were carried out using the anti-Dhc antibody P1H4, kindly provided by Tom Hays (for details, see Material and Methods chapter of this thesis). In order to titrate the reduction of protein activity, various dilutions of the anti Dhc antibody were coinjected together with *grk* RNA to re-establish localisation. When a 1:1 dilution in injection buffer was injected, no localisation was observed. The same result was yielded using a 1:5 and 1:10 dilution of the anti-Dhc antibody (n=15), but further titrations of the antibody could not be used due to the small amount of antibody supplied by Tom Hays (data not shown).

To test whether the antibody injections have a gross effect on the oocyte MTs, Tau GFP egg chambers were injected and MTs visualised 1 hour after injection. The overall MT polarity in the oocyte did not change, so it can be concluded that the injection with the anti-Dhc antibody did not affect the MTs. To exclude that the effect of the dynein antibody was unspecific, a control anti-HA antibody (for details see Methods chapter) was injected into stage 9 oocytes. It did not affect *grk* localisation in the oocyte and *grk* RNA localised normally to the dorsoanterior

corner (Figure 6-2 D; 73% localised, n=11) and it therefore seems likely that a disruption of dynein function by the anti-Dhc antibody is the cause of the inhibition of *grk* RNA localisation, rather than a non-specific effect of the antibody injection.

To investigate whether both steps of *grk* RNA localisation require cytoplasmic dynein, living stage 9 nlsGFP egg chambers were injected firstly with *grk* RNA and then left to undergo anterior localisation of some of the injected *grk* RNA (Figure 6-2 E). After approximately 10 minutes, the antibody against Dhc was injected and the egg chamber subsequently imaged for a further hour. After one hour, *grk* RNA can be seen dispersed within the ooplasm and no anteriorly localised *grk* RNA is visible (Figure 6-2 F). It can therefore be concluded that anterior localisation of injected *grk* RNA in the oocyte requires the function of Dhc. To identify whether dorsoanterior localisation of *grk* RNA also requires Dhc function, stage 9 oocytes were injected with *grk* RNA and then left untreated for approximately 30 minutes, in which most RNA localised anteriorly as well as a fraction of the RNA dorsoanteriorly (Figure 6-2G). The oocyte was then injected with the antibody against Dhc and left for a further hour. When the oocyte was imaged one hour after antibody injection, *grk* RNA had not localised further and the anteriorly localised RNA appeared less strongly attached (Figure 6-2 H). It can therefore be concluded that dynein is required for the second step of *grk* RNA localisation to the dorsoanterior corner. Furthermore, injections with antibodies against Dhc also affect anteriorly localised *grk* RNA (see Figure 6-2 F and H), suggesting the requirement of dynein for both steps of *grk* RNA localisation within the oocyte.

Figure 6-2 *grk* RNA localisation and oocyte MT-polarity

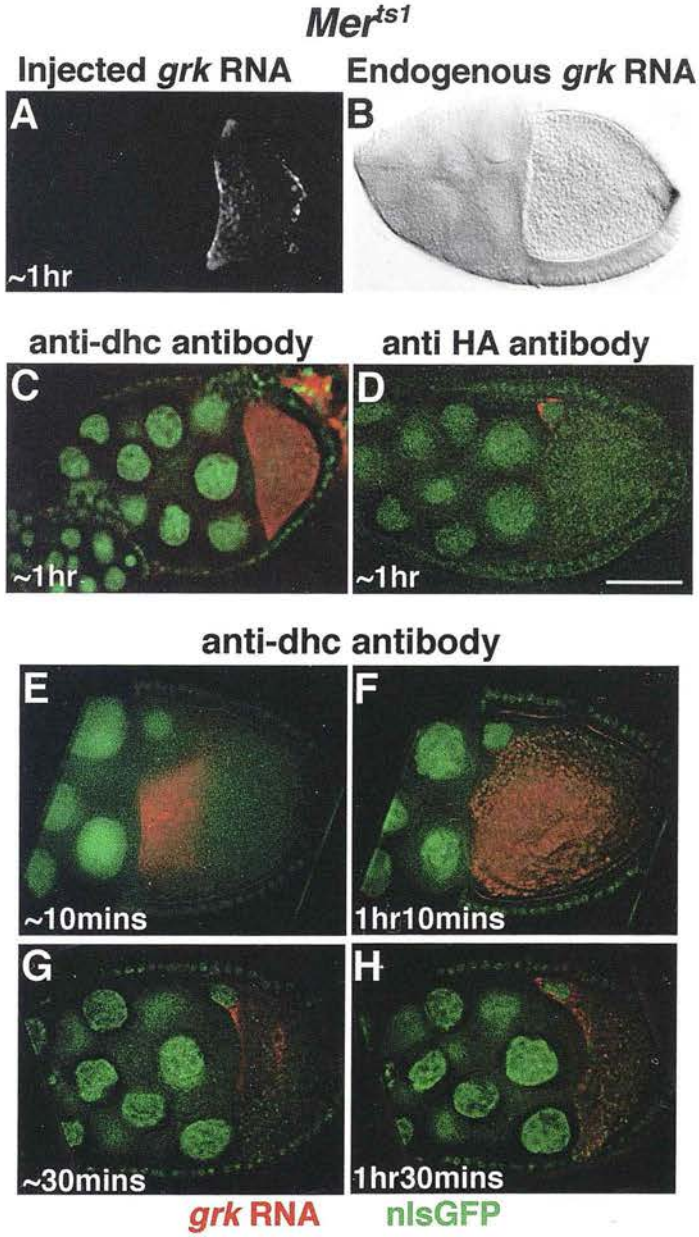

Figure 6-2 *grk* RNA localisation requires MT-polarity and dynein

(A)Showing a *Mer*^{ts1} egg chamber 1 hr after injection with *grk* RNA. *grk* RNA localises closely to the posterior oocyte nucleus (see arrowhead), as well as to the anterior cortex of the oocyte.

(B) In situ hybridisation against *grk* mRNA on a *Mer*^{ts1} egg chamber. *grk* RNA is closely localised at the oocyte nucleus at the posterior of the oocye.

(C) Coinjection of *grk* RNA and P1H4 monoclonal anti-dhc antibody. *grk* RNA fails to localise.

(D) Coinjection of control HA antibody. *grk* RNA localises normally to the dorsoanterior corner.

(E) Injection of anti -dhc antibody 10 mins after *grk* RNA injection. *grk* RNA is anteriorly localised.

(F) Image taken one hour after (E). *grk* RNA is dispersed within the ooplasm and fails to localise.

(G) Injection of anti -dhc antibody 30 mins after *grk* RNA injection. The RNA localises dorsoanteriorly.

(H) Image taken one hour after (G). Most *grk* RNA remains at the dorsoanterior.

grk RNA localisation is less efficient in dynein hypomorphic mutants

The dynein heavy chain (Dhc) is the essential force-generating ATPase subunit of the protein complex. The dynein protein is essential for survival and complete deletion of dynein activity is cell lethal. It is therefore not possible to test the requirement for dynein in *grk* RNA localisation using null allele mutants of dynein. However, hypomorphic alleles of the *dynein heavy chain* (*dhc*) have been found to be viable as transheterozygous. To test whether *grk* RNA can localise in such mutants, the transheterozygous allelic combination $dhc^{6\text{-}6}/dhc^{6\text{-}12}$, which has previously been reported to show oogenesis defects was used (Gepner et al., 1996).

When *grk* RNA was injected into $dhc^{6\text{-}6}/dhc^{6\text{-}12}$ mutant oocytes, it was found that *grk* RNA does localise less efficiently and possibly slower. After one hour, only 21% of stage 9 oocytes show localisation of *grk* RNA to the dorsoanterior corner, whereas 36% show anterior, or weak dorso-anterior localisation (N=14; Figure 6-3 A). The remaining 43% of egg chambers show no localisation after one hour. In wildtype stage 9 egg chambers, approximately 85% of cases will show clear dorsoanterior localisation (N=40; Figure 6-3 B) and the reduction of dorsoanterior localisation in *dhc* mutant oocytes is significant. In order to track the path of localisation of *grk* RNA particles in $dhc^{6\text{-}6}/dhc^{6\text{-}12}$ mutant oocytes, high resolution imaging using time-lapse cinematography was used to visualise particle movement. However, it was not possible during the given timeframe to gain enough data for analysis. It appears that particles form less readily in $dhc^{6\text{-}6}/dhc^{6\text{-}12}$ mutants. These experiments will have to be repeated in the future to be able to analyse whether the speed of movement of *grk*

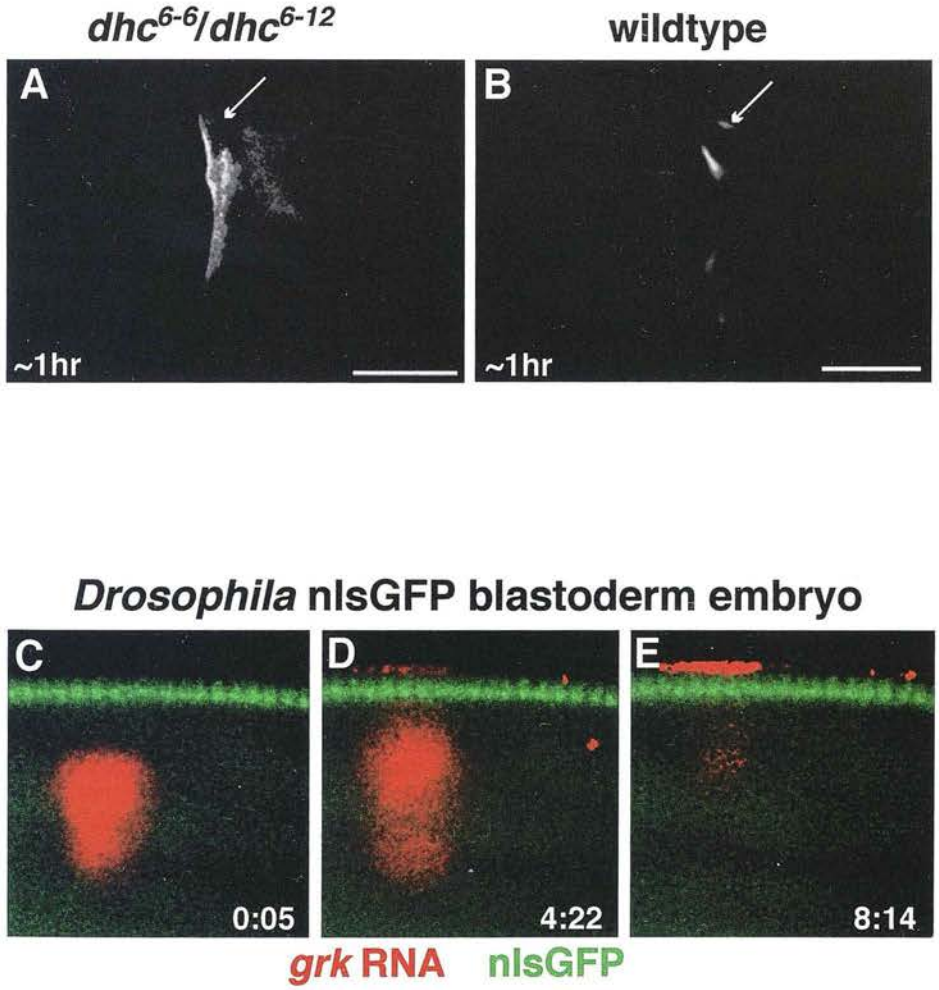

Figure 6-3 Efficiency of *grk* RNA localisation is reduced in *dhc* hypomorphic alleles

(A) A stage 9 hypomorphic *dhc* mutant egg chamber injected with *grk* RNA, showing that the RNA is localised to the anterior after 1hour, with no significant dorsoanterior localisation. The arrowhead indicates the oocyte nucleus.

(B) A wildtype control egg chamber showing a strong dorsoanterior cap of *grk* RNA, 1 hour after injection. The arrowhead again indicates the position of the oocyte nucleus.

(C-E) Time lapse images of a living interphaser 14 blastoderm embryo expressing nlsGFP fusion protein (green) and injected with *grk* RNA(red) at time 0. Exact times are given in minutes and seconds at the right hand bottom corner of each image. Arrowheads indicate visible particles of *grk* RNA. *grk* RNA localises apically (E) as particles in blastoderm embryos.

Table 6a. Particle speed in wild type and *dhc* mutant embryos

GENOYTPE	PARTICLE SPEED	MAXIMUM SPEED
wild type	0.46 ± 0.09 μm/sec (N=21)	0.89 μm/sec
Dhc64C$^{8\text{-}1}$/*Dhc64C*$^{6\text{-}10}$	0.198 ± 0.048 μm/sec (N=78)	0.45 μm/sec
Dhc64C$^{6\text{-}6}$/*Dhc64C*$^{6\text{-}8}$	0.19 ± 0.06 μm/sec (N=82)	0.54 μm/sec

Analysis of speeds of apical localisation particles in wild type and mutant dynein embryos. Speeds of particles were measured from the distance between successive positions of injected RNA particles at 10 second intervals. At least three embryos of each genotype were tested.

RNA particles is indeed slower, or if the dynamics of movement change to explain the observed effect. To overcome the problems using $dhc^{6\text{-}6}/dhc^{6\text{-}12}$ egg chambers, two different *dhc* trans-allelic combinations were analysed using *grk* RNA injections during Blastoderm stage of embryogenesis. It was found that when *grk* RNA was injected into wildtype embryos, the injected RNA localised very similar to injected pair rule transcripts previously characterized (Wilkie and Davis, 2001), (Figure 6-3 C-E). The average speed of *grk* RNA particle movement was 0.46+/-0.09 μm/sec (N=21 particle movement).

When *grk* RNA was injected into the two different allelic combinations $dhc^{8\text{-}1}/dhc^{6\text{-}10}$ and $dhc^{6\text{-}6}/dhc^{6\text{-}8}$, the speed of *grk* RNA particle movement was reduced significantly (Table 6a). Although *grk* RNA is not normally present at this stage in development it can be suggested that it is able to recruit the necessary localisation machinery present in the embryo. The apical transport of pair rule transcripts at this stage has been shown previously to require dynein and it therefore strengthens the conclusion that *grk* RNA localisation in the oocyte also requires dynein dependent localisation machinery. Together with the results of antibody injections it can be suggested that *grk* RNA localisation requires the integrity and correct polarity of MTs within the oocyte and localises in two phases with a speed of 0.19 +/- 0.06 μm /sec (N=82 particle movements). It can therefore be concluded that injected *grk* RNA moves to the anterior and dorsoanterior using dynein-dependent transport to the minus ends of MTs.

Discussion

The localisation of injected *grk* RNA into oocytes has been shown to require the integrity and correct polarity of the oocyte MT network. When MT and Actin depolymerising drugs were injected in combination and prior to *grk* RNA, it was shown that *grk* localisation is likely to be MT dependent, but Actin independent. Furthermore, data so far suggests that MT integrity is required for both steps of *grk* RNA localisation. When MT depolymerising drugs were injected after dorsoanterior localisation of some of the injected *grk* RNA, the already localised RNA at the dorsal cap does not delocalise. These results could be interpreted as follows: The final localisation is either independent of MT integrity and some form of anchoring may occur at this stage, or the depolymerisation through administration of colcemid is not complete. This is likely, as colcemid reduces the length of MTs, but may not depolymerise them completely. As Actin depolymerisation did not show any effect on the dorsal cap formation and stability it seems unlikely at this stage, that simple anchoring at the dorso-anterior is part of the *grk* RNA localisation mechanism. Further experiments would most likely be able to distinguish between these hypotheses.

When *grk* RNA was injected into mutants, which affect the polarity of the oocyte MTs, such as Mer^{ts1}, it was shown that *grk* RNA still localises to minus end of MTs. However, the displacement of the oocyte nucleus in these mutants meant that some *grk* RNA would move to the oocyte nucleus, whereas some moved anteriorly, but failed to then progress to move towards the oocyte nucleus. The data so far presented further supports the suggestion that the second step of *grk* RNA localisation requires

the positioning of the oocyte nucleus in the correct place. Further evidence supporting this hypothesis comes from oocytes mutant for the *kinesin-heavy chain* (*khc*), encoding for the motor unit of Kinesin I. The cytoplasmic plus-end directed motor Kinesin I has been implicated in *osk* RNA localisation (Brendza et al., 2000).

In germline clones of the null allele khc^{27}, 50% of oocytes show a displacement of the oocyte nucleus to the centre of the oocyte in later stages. The cause of this displacement is not fully understood, but it has been suggested that a possible late anchoring defect could be the cause (Brendza et al., 2000). When oocytes of khc^{27} germline clones were injected with *grk* RNA, localisation to the entire anterior cortex could be seen, as well as localisation of a proportion of the *grk* RNA to the displaced oocyte nucleus (Adrian Carr-data not shown). Interestingly, the cloud of *grk* RNA could be observed to concentrate to one side of the oocyte nucleus. Endogenous *grk* RNA has been shown to localise in a similar pattern in RNA in situ hybridisation of khc^{27} mutant oocytes. This provides further evidence that *grk* RNA movement is bi-phasic and it suggests a possible movement along two orthogonal sets of MTs, one set connected with the nucleus, the other one cortical.

It is likely that first, *grk* RNA moves towards the anterior cortex and then a switch occurs from one set of MTs to another. One possibility is that the two MT networks are different biochemically, but it has not been possible so far to identify these MTs in immunofluorescence experiments. High resolution imaging of TauGFP, a MT binding protein fusion to GFP in living oocytes indeed showed a basket of MTs connected with the oocyte nucleus and extending radialy (Alejandra Clark, see also (MacDougall et al., 2003).

Experiments in both oocytes and embryos using antibody injections to disrupt the function of dynein, as well as hypomorphic alleles strongly support dynein dependence as *grk* RNA localisation in the oocyte was reduced and slowed down in hypomorphic mutants of the dynein heavy chain, the motor unit of the protein.

Evidence of reduced particle speed comes from experiments using blastoderm stage embryos of two transallelic combinations of EMS induced hypomorphic alleles of *Dhc64C*. In blastoderm stage embryos of *Drosophila, grk* RNA localises apically to the minus ends of MTs. *grk* RNA has been shown to move in particles whose speed can be measured during the phase of movement towards the apical cytoplasm. In hypomorphic *dhc* mutant embryos, speed of *grk* particles is reduced significantly, suggesting dynein to play a direct role in transport of this RNA in the embryo. As *grk* RNA localisation efficiency is strongly affected in hypormorphic *dhc* mutant oocytes, it is likely that the speed of *grk* RNA particles is also reduced in oocytes, suggesting a conserved mechanism of cytoplasmic RNA transport in the embryo and oocyte. However, particles did not form as readily in the *dhc* mutant oocytes and so far, speeds of *grk* RNA particles in the oocyte could not be measured in this mutant. It will be of interest to investigate whether the formation of *grk* RNA particles is indeed affected by mutation of Dhc.

In the oocyte, *grk* RNA particles have been shown to localise through periods of stasis and fast movement. It will therefore be very interesting to analyse the exact particles behaviour in *dhc* mutants. It will be important to investigate whether processivity of particle movement is affected, or whether the overall speed during the phase of movement is reduced. This will also have to be investigated in the oocyte, but it proves currently very difficult to combine high resolution and high

speed imaging with very short intervals without causing photo induced damage to the oocyte. Technical advances will hopefully overcome this problem in the near future, allowing a more in depth analysis of *grk* RNA localisation dynamics within the oocyte. Future advances in imaging may allow tracking particles in the oocyte in different focal planes, allowing a much more comprehensive analysis of particle behaviour within the oocyte.

7

ANALYSIS OF NURSE CELL TO OOCYTE TRANSPORT OF *GRK* RNA

Introduction

grk mRNA is one of the key maternal components that is localised specifically within the oocyte cytoplasm to initiate asymmetry within the developing egg. Grk protein is a homologue of TGF-α protein and is involved in signalling that initiates the formation of both the anteroposterior and the dorsoventral axis through bidirectional signalling with the surrounding follicle cell layer (Schüpbach et al., 1990; Schüpbach and Roth, 1994). The anterior structures of the future embryo are determined through the positioning of *bcd* mRNA, which is translated after fertilisation and forms a gradient of protein. This gradient in turn activates the hierarchy of patterning genes within the embryo, defining progressively finer positional information. *osk* mRNA is deposited at the posterior of the oocyte in later stage oogenesis and recruits other germline defining factors, such as Vasa protein, Staufen and *nanos* mRNA to the posterior (Curtis et al., 1995; Ephrussi et al., 1991; Ephrussi and Lehmann, 1992). These factors subsequently play a role in the assembly of pole plasm and formation of pole cells in the embryo (Kim-Ha et al., 1991)

During oogenesis, fifteen nurse cells and one oocyte are formed within each egg chamber, which is surrounded by somatically derived columnar epithelial follicle cells (for review see van Eeden and St Johnston, 1999).

As each egg chamber develops in isolation from its neighbouring egg chambers, it is important that the oocyte is provided with all required factors to develop into a polarised egg in a highly reproducible manner. The polyploid nurse cells are connected to each other and the oocyte through actin rich structures, known as ring canals (Spradling, 1993). All the required organelles, proteins and mRNAs are transported from the nurse cells into the oocyte through the ring canals. It is currently believed that most or all mRNAs are transcribed originally within the nurse cells and subsequently transported to the oocyte.

Both *bcd* and *osk* mRNAs have been detected within the nurse cell cytoplasm by RNA in situ hybridisation (Ephrussi et al., 1991; Kim-Ha et al., 1991; Macdonald and Kerr, 1997). Their transport to the oocyte has been suggested to be microtubule dependent, as depolymerising drugs, such as colcemid can trap the mRNA within the nurse cell and prevent localisation of mRNA in the oocyte (Saunders and Cohen, 1999). However, there is so far no direct evidence that *grk* mRNA really is transcribed by the nurse cells and it has been suggested that it may be transcribed within the oocyte by the oocyte nucleus through certain stages of development (Saunders and Cohen, 1999). Experiments using microtubule depolymerising drugs in *Drosophila* feeding experiments did not show any accumulation of *grk* mRNA within the nurse cell cluster, so it was suggested that oocyte transcription during these stages may be utilised. However, expression of an altered *grk* transgene fused to the reporter gene lacZ did show βgal expression within the nurse cells at earlier

stages of oogenesis (Thio et al., 2000). This supported the view that *grk* mRNA may be transcribed by the nurse cells in earlier stages of oogenesis, but would later on, after stage 6 of oogenesis, be transcribed by the oocyte nucleus. There is so far no direct evidence to support either of these suggestions, as it has so far not been possible to visualise the endogenous transcript intermediates or nuclear transcripts by methods of detection, such as in situ hybridisation.

The injection assay described in the previous chapters of this thesis provides a very useful tool to study *grk* mRNA localisation and movement in real time assays. This chapter described attempts to use the injection assay to identify possible mechanisms of nurse cell- to oocyte transport and to gain more insight into the transcriptional regulation of *grk* mRNA during oogenesis.

Results

grk RNA injected into nurse cells localises in the oocyte

To investigate whether *grk* RNA has the ability to localise within the oocyte when injected into the nurse cells, egg chambers were injected with *grk* RNA into various nurse cells, both adjacent and distal to the oocyte. Every attempt was made to inject one nurse cell at a time, but in earlier stage egg chambers, more than one nurse cell was often injected together, as the set up and technical expertise did not always provide complete accuracy. However, this did not seem to affect the morphology or functioning of the egg chamber in most cases. When too much damage to the nurse cell compartments occurred, cell cytoplasm sometimes leaked out of the egg chamber from the injection site. Such damaged egg chambers were not included in the results shown below.

When *grk* RNA was injected into the nurse cells of egg chambers stage 8-10A, the RNA was able to move from the side of injection to the oocyte, where it had the ability to localise (Figure 7-1 A-D, see also supplementary movies). Firstly, *grk* RNA could be observed within the nurse cell cytoplasm close to the nurse cell-oocyte border, presumably being moved through ring canals. This oocyte accumulation was seen after approximately 15-30minutes (Figure 7-1 B-C). Following movement to the oocyte, *grk* RNA then localised at the dorso-anterior corner within the next hour (Figure 7-1 D and J). Interestingly, when earlier stage egg chambers were injected with *grk* RNA into the nurse cells *grk* RNA could also be seen moving to the oocyte and localising (Figure 7-1 F-I; see also supplementary movies). As the oocyte nucleus was still positioned at the posterior of these oocytes,

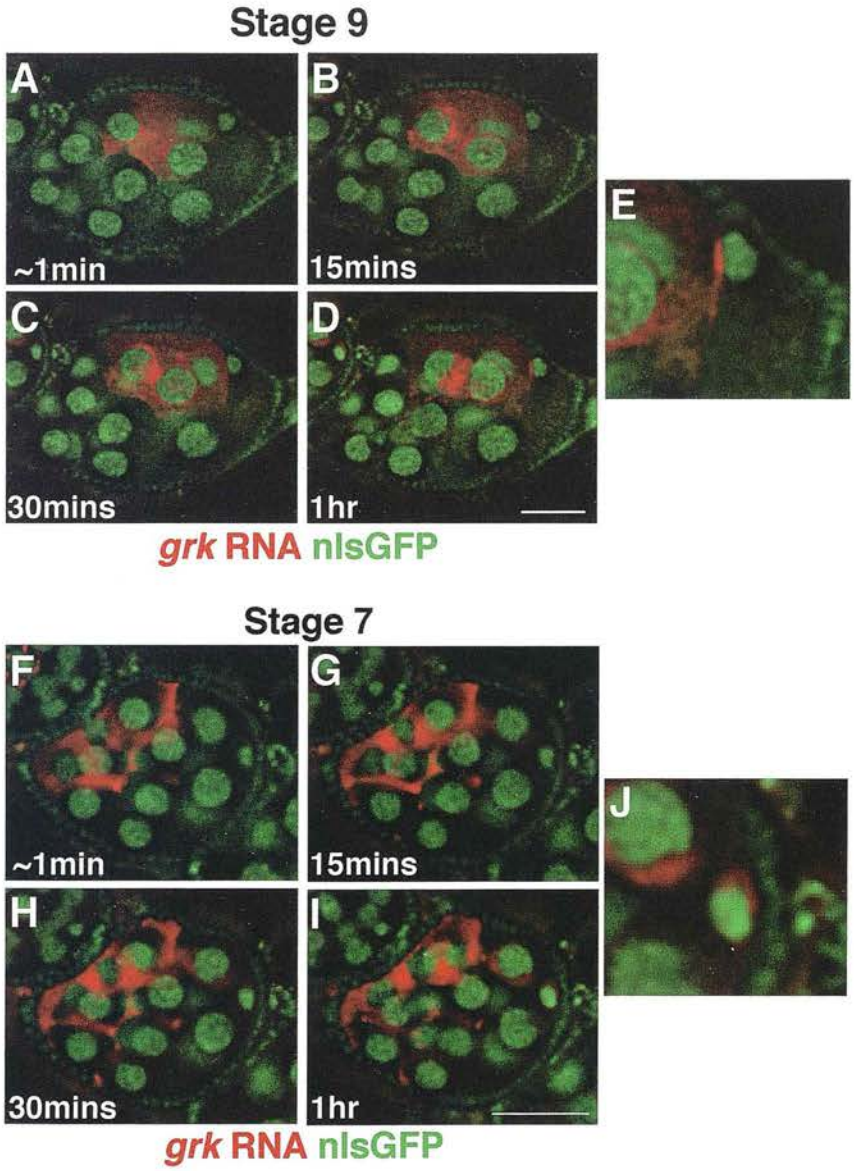

Figure 7-1 nurse cell-injected *grk* RNA localises within the oocyte

(A-E) Injection of *grk* RNA into nurse cells of stage 9 egg chamber.

(A) Showing *grk* RNA within the nurse cells one minute after injection.

(B) Fifteen minutes after injection into nurse cells, *grk* RNA is moving toward the oocyte.

(C) Thirty minutes after injection, *grk* RNA enriches along the anterior cortex of the oocyte.

(D) One hour after injection, *grk* RNA has moved into the oocyte to form a dorsal cap (see also E)

(F) One minute after injection into nurse cells of stage 7 egg chamber. Note the oocyte nucleus at posterior of the oocyte.

(G) Fifteen minutes after injection, *grk* RNA enriches in nurse cells adjacent to the oocyte.

(H) Thirty minutes after injection, a fraction of *grk* RNA can be seen within the ooplasm.

(I) One hour after nurse cell injection, *grk* RNA forms a posterior crescent in the oocyte (see also J).

Arrowheads indicate the oocyte nucleus, scalebars represent 50 μm.

grk RNA was observed localising to the posterior crescent, closely resembling localisation of the endogenous *grk* transcript (Figure 7-1 I and J).

The frequency of localisation in stage 8-10 egg chambers was 50% (N=33), lower than the localisation observed in the oocyte (Table 7a). This may be due to more damage to the morphology of the nurse cells, as they are much smaller than the oocyte and harder to inject into. Furthermore, it is not certain whether an efficient mechanism for *grk* RNA transport exists in nurse cells, as it is yet unclear whether endogenous transcript is transcribed within the nurse cells in vivo. However, the relatively high frequency suggests that the localisation mechanism is in place to move *grk* RNA to the oocyte (see also Conclusions of this chapter).

Nurse cell-oocyte transport of *grk* RNA requires MTs and dynein

The movement of *grk* RNA from the nurse cells to the oocyte could occur by simple diffusion, passive transport with cytoplasmic streaming or by directed transport requiring microtubules. To begin to distinguish between these possibilities, the MT-depolymerising drug colcemid (100μg/ml) was coinjected together with *grk* RNA into nurse cells of stage 8-10 egg chambers. No *grk* RNA was observed moving from the nurse cell compartments to the oocyte and remained close to the site of injection in all cases. (N=33, localisation 0%) (Figure 7-2 A-B). It can therefore be concluded that transport from the nurse cells to the oocyte does indeed require integrity of the nurse cell-oocyte microtubules. It has previously been reported that the network of microtubules extending into the nurse cells has a certain polarity. It has been suggested (Theurkauf et al., 1992; Theurkauf et al., 1993) that microtubules have

Table 7a. Oocyte localisation of nurse cell-injected *grk* RNA

STAGE	INJECTED WITH	LOCALISATION IN OOCYTE
6-7	*grk* RNA	50% (N=4)
8-10	*grk* RNA	50% (N=33)
8-10	*grk* RNA and Colcemid	0% (N=33)
8-10	*grk* RNA and anti-dhc antibody	0% (N=24)*

Percentage of *grk* RNA localisation at the dorsoanterior corner of the oocyte after injection into nurse cells. N equals the number of egg chamber injected.

* Approximately half of all egg chambers injected with *grk* RNA and anti-dhc antibody into nurse cells showed a small fraction of *grk* RNA accumulating within the ooplasm.

plus ends located in the nurse cells and minus ends extending into the oocyte. This arrangement of microtubules would suggest that *grk* RNA transport occurs towards the minus ends of microtubules.

To investigate whether this type of transport requires cytoplasmic dynein, coinjections of *grk* RNA and a monoclonal antibody against part of the N-terminus of the dynein-heavy chain (Dhc) were performed into various nurse cells (for details, see Methods chapter). The antibody, which had previously been used in the oocyte (see results chapter 6) eliminates activity of the dynein-heavy chain, which results in inactivation of the motor unit of the dynein protein complex. None of the injected egg chambers showed transport of *grk* RNA from the nurse cells to the oocyte (N=24) and the injected *grk* RNA remained largely at the injection site (Figure 7-2 D). Although this experiment cannot provide direct proof, it strongly suggest that there is a requirement for cytoplasmic dynein in nurse cell-to-oocyte transport. However, low level accumulation of *grk* RNA within the ooplasm one hour after injection into the nurse cells was sometimes observed (Figure 7-2 E).

As further work carried out in our lab suggests, the accumulation is probably due to diffusion of some of the injected *grk* RNA through the ring canals. The low-level accumulation does not appear to be specific to any RNA injected (Alejandra Clark, personal communication), but may be generally observed with any RNA injected into the nurse cells. Further experiments will need to be carried out to establish more clearly the significance of this observation. It becomes clear from the nurse cell injections so far that the integrity and polarity of the nurse cell-oocyte microtubule network is vital to the correct transport and localisation of *grk* RNA. However, these experiments were not able to distinguish whether *grk* RNA is moved along passively

Figure 7-2 *grk* RNA and colcemid/anti-dhc antibody injections

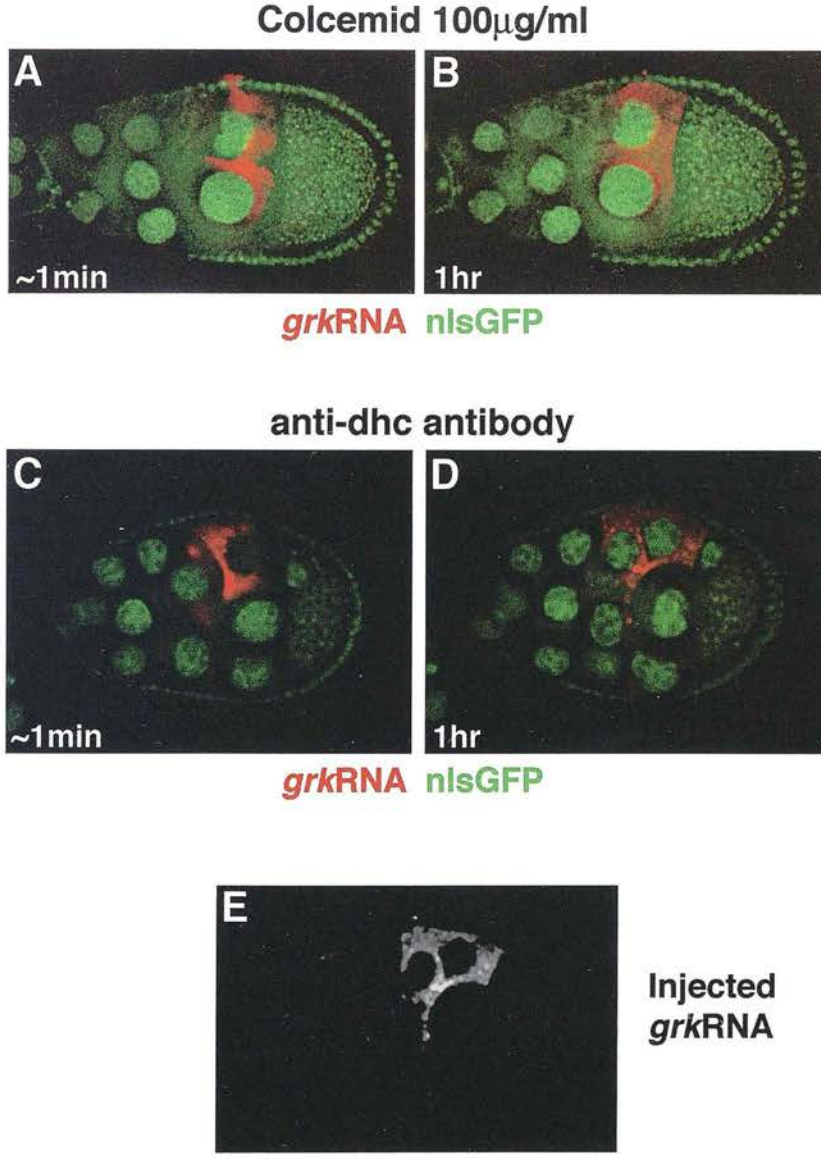

Figure 7-2 nurse cell-oocyte transport of *grk* RNA is dependent on MTs and dynein

(A and B) Coinjection of *grk* RNA and colcemid (100µg/ml) into nurse cells of stage 9 egg chamber.

(A) Showing *grk* RNA one minute after injection into nurse cells.

(B) One hour after coinjection, *grk* RNA does not localise in the oocyte, but remains close to the injection site.

(C to E) Coinjection of *grk* RNA and anti-dhc antibody into nurse cells of a stage 9 egg chamber.

(C) Showing *grk* RNA accumulation in the nurse cells one minute after injection.

(D) One hour after injection, no localisation of *grk* RNA within the oocyte is visible.

(E) Showing the low level accumulation of *grk* RNA within the oocyte from the egg chamber shown in image (D).

with cytoplasmic streaming that requires dynein, or whether *grk* RNA required dynein directly to move from the nurse cells to the oocyte.

Nurse cell injected *grk* RNA assembles into particles which move to the oocyte

To investigate further the mechanism of transport of injected *grk* RNA from nurse cells to the oocyte, high-resolution imaging combined with time-lapse cinematography was performed after injection into various nurse cells. The intervals between images were chosen as one second and typically 300 images were taken per experiment.

When the final images were analysed, *grk* RNA particles were found travelling straight towards the oocyte. (Figure 7-3 A; see also supplementary movie). Particles appeared to be moving towards the actin rich ring canals, where they paused shortly, before entering the oocyte. Different particles were also found to be travelling on what appeared to be the same track-perhaps the same bundle of microtubules. After entering the oocyte, the particles quickly disappeared from the focal plane, but it is possible that they continued their track towards the dorsoanterior corner of the oocyte. Unfortunately, photo induced damage prevented the imaging of the entire path of *grk* RNA particles from the nurse cell, to its destination within the oocyte.

It also proved difficult to find the right focus to visualise the particles on their way from the nurse cell cytoplasm through to the oocyte. The particles observed were travelling at maximum speeds of 1 μm/sec. Additional experiments would be

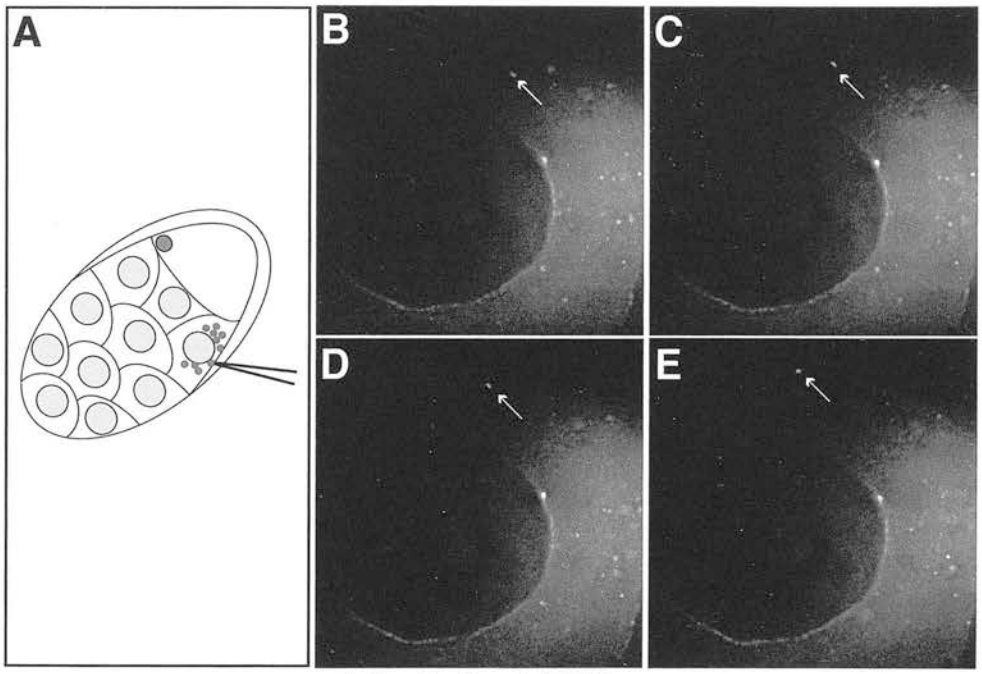

Figure 7-3 *grk* RNA particles show directional nurse cell-to-oocyte movement
(A) Illustration showing orientation of injected egg chamber. *grk* RNA was injected into one adjacent nurse cell. (B-E) High magnification images taken from timelapse movie (see also supplementary data) of the nurse cell-to oocyte area of a stage 9 egg chamber injected with *grk* RNA. Particles of *grk* RNA can be seen moving on a direct path from the nurse cell to the oocyte (See also supplementary movie). Arrowheads indicate particle in phase of movement, which can be seen moving towards the oocyte in (B) to (E).

required to provide more data on particle motility in the nurse cells, which is currently being undertaken in our lab by Alejandra Clark.

So far, the results of this chapter suggest that *grk* RNA transport from the nurse cells to the oocyte is specific to *grk* RNA and requires both integrity and polarity of the nurse cell microtubules. It also suggests that the ability to transport *grk* RNA through the ring canals from the nurse cells to the oocyte is present in egg chambers, raising the question of nurse cell specific transcription of endogenous *grk* mRNA.

Discussion

The experiments above have shown that, the localisation machinery to transport *grk* RNA from the nurse cells to the oocyte is present in stage 6-10 egg chambers (Table 7a). When injected into the nurse cells, *grk* RNA is able to move to the oocyte after a short time, where it could localise to the dorsoanterior corner, similar to the localisation observed after *grk* RNA injection into the oocyte.

Experiments using microtubule-depolymerising drugs in coinjection with *grk* RNA showed that the transport of *grk* RNA from the nurse cells to the oocyte is a microtubule dependent process. Interestingly, this transport did not seem to require cytoplasmic dynein, as antibody injections, which are thought to eliminate dynein activity in the egg chamber did not inhibit *grk* RNA from moving into the oocyte. However, the oocyte specific localisation was not observed at any point when dynein specific antibodies were coinjected with *grk* RNA.

These results suggest that a different mechanism must be present for the nurse cell-to-oocyte transport and the question remains whether this transport might require other motor proteins. In addition, although injections of dynein specific antibodies strongly suggest the requirement for dynein in the process of localisation in the oocyte, this type of experiment does not provide direct evidence for the dynein requirement. Further experiments to strengthen the suggestion of dynein requirement would be needed, possibly in form of particle analysis in the available *dhc* hypomorphic mutants. Further experiments would also have to be carried out to investigate a possible requirement for Kinesin I in the nurse cell-oocyte transport.

Kinesin I has been shown so far to play a role in *osk* mRNA localisation and is thought to be required for cytoplasmic movement within the oocyte. A null allele of kinesin-heavy chain (khc) as germline clones is available and it would be of great interest to analyse particle behaviour during all steps of *grk* transport and localisation in these mutant alleles. However, due to time restrictions this work has not yet been carried out, but will hopefully answer some questions in the near future.

When particles were observed within the nurse cells they were found travelling at a maximum speed of 1 μm/sec. This strongly supports the idea of directed transport as a means of *grk* RNA localisation dynamics. However, it is not yet clear whether *grk* RNA needs to be transported from the nurse cells to the oocyte in vivo. So far, no endogenous *grk* transcripts have been observed within the nurse cells, and it is possible that the *grk* mRNA is actually transcribed within the oocyte during these stages of oogenesis. However, the evidence for localisation machinery capable of transporting *grk* RNA from the nurse cells to the oocyte is clearly in place and this would indicate that at least at some point in oogenesis, *grk* mRNA could be transcribed in the nurse cells and transported into the oocyte where it is required.

The results of this chapter indicate that the nurse cell-to oocyte transport is a microtubule dependent process and particles are found to be travelling on a direct path from the nurse cells to the oocyte, where they are able to localise. Data on particle movement clearly support directed transport of *grk* RNA rather than just diffusion and passive streaming. However, as coinjections of *grk* RNA and antibodies against dynein heavy chain did lead to a low frequency accumulation of *grk* RNA in the oocyte, it cannot be excluded that a degree of diffusion of RNA from the nurse cell to the oocyte can occur. Experiments carried out in our lab also

suggest this accumulation to be non-specific, as other transcripts also accumulated within the ooplasm (Alejandra Clark, personal communication). To identify the actual site of transcription of *grk* mRNA would greatly improve understanding of the processes of mRNA localisation and this will be of major interest for the future.

8

DISCUSSION AND FUTURE PERSPECTIVES

Axis formation in *Drosophila* is initiated during oogenesis through the asymmetric localisation of maternal transcripts to specific sites of the developing oocyte. This thesis provides new insights into the mechanisms of localisation of one of the key maternal mRNAs, *grk* mRNA. The dorsoventral and anteroposterior polarisation of the oocyte are both initiated by Grk signalling, which involves the oocyte and the surrounding somatically derived layer of follicle cells. The localisation of *grk* mRNA and protein to specific sites of the oocyte is essential for correct signalling, but the mechanisms by which transcripts are localised are still not very well understood at the molecular level. Using the in vivo injection assay on cultured oocytes injected with in vitro transcribed and fluorescently labelled transcripts into living egg chambers has provided evidence suggesting multiple steps of *grk* mRNA localisation in the oocyte, requiring both MT integrity and dynein.

Previous work carried out in our lab had shown that pair-rule and *wg* transcripts labelled with different fluorescent UTP analogues injected into living blastoderm stage embryos can localise apically (Wilkie and Davis, 2001). The in vivo injection assay allowed the study of RNA localisation dynamics and real time imaging revealed that the apical localisation of the injected transcripts depends on MTs and

cytoplasmic dynein. It provides therefore a powerful tool for studying the underlying mechanisms of cytoplasmic RNA localisation and does not rely on construction of transgenic reporter constructs and their localisation in fixed material. Adapting the in vivo injection assay for analysis of *grk* mRNA localisation in the oocyte revealed that injected *grk* RNA localises within the oocyte to the dorsoanterior cap. The localisation machinery required for correct localisation is therefore present in the oocyte cytoplasm. Furthermore studies of RNA particle movement in the oocyte has elucidated the entire path of *grk* mRNA localisation from its site of injection to the final localisation site within the oocyte.

grk RNA localisation requires factors present in the ooplasm

In vitro transcribed and labelled *grk* transcripts have been shown to localise correctly within the oocyte of living and cultured oocytes. Furthermore, injected *grk* RNA closely mimics localisation of endogenous transcript. Timelapse cinematography has revealed that the injected RNA moves first to the anterior and then to the dorsoanterior corner where it localises in the characteristic dorsal cap at the site of the oocyte nucleus. The observed localisation is specific to *grk* RNA, as other transcripts injected did not show localisation to the dorsoanterior. The anteriorly localised transcript fs(1)K10 (K10) was analysed for its ability to localise within the oocyte. The 44 nucleotide localisation element of *K10*, The *K10* transport/localisation sequence (*K10tls*), which had previously been shown to localise to the anterior of the oocyte as a transgene (Serano and Cohen, 1995), as well as apically when injected into blastoderm stage embryos (Bullock and Ish-Horowicz, 2001), localised to the anterior cortex of stage 9 oocytes. The efficiency of localisation was reduced, which is probably due to the size of the transcript, which could lead to aggregation of the injected RNA, interfering with its localisation.

When a point mutation was introduced, the K10 transport/localisation sequence remained unlocalised, as well as injected *hb* RNA. *hb* is normally expressed in embryos and the Hb protein is unlocalised (Davis and Ish-Horowicz, 1991). It can so far be concluded that localisation of *grk* RNA to the dorsoanterior of oocytes is specific.

Another embryo-specific transcript, the pair rule transcript *fushi-tarazu* (*ftz*), which had previously been shown to localise apically when injected into embryos, shows low efficiency localisation to the anterior in oocytes. Interestingly, this transcript is not normally present in oocytes, but shows the ability to utilise the oocyte localisation machinery to localise to the anterior cortex. This raises the question of similarities in RNA transport in oocytes and embryos. In the stage 9 oocyte, MTs have reorganised to form an anterior-posterior gradient within the oocyte (Theurkauf et al., 1992) with the minus ends of MTs located along the anterior cortex. In the embryo, where *ftz* transcripts localise apically, the minus ends of MTs are located in the apical cytoplasm and plus ends extending into the basal cytoplasm and yolk (Foe et al., 1993). In the embryo, *ftz* RNA localises via minus-end directed transport along the MTs and similarly localises within the oocyte, possibly also via minus-end directed MT-based transport. *grk* RNA on the other hand localises apically within the embryo, when injected, although it is not present and required in the embryo. This raises the question of what the two systems have in common regarding the machinery that is able to localise the transcripts in both oocyte and embryo. It has recently been suggested that two maternal proteins, Egl and Bic-D may play a role in transport of mRNAs by linking the RNA complex to the motor protein (Bullock and Ish-Horowicz, 2001). It has been shown in the embryo that both Egl and BicD are recruited apically by the injected RNA and that interference with either protein

disrupts transcript localisation. It has not been shown directly whether the two proteins function in a similar way in oocytes, but both have been shown to be required for oocyte selection and are colocalised in the oocyte at the proposed minus- ends of MTs. It would therefore be of interest to analyse the requirement of Egl and Bic-D in *grk* RNA localisation, using the in vivo injection assay. Interference with protein function could be performed using available antibodies, which have effectively been used in the embryo (Bullock and Ish-Horowicz, 2001), as well as existing alleles of *bicD* and *egl*. It can so far be suggested that the transport machinery in both embryo and oocytes utilise the same factors which would explain why both *grk* RNA and *ftz* RNA can be recruited to the minus ends at times of development where they would not normally be present.

grk RNA localises in particles in the oocyte

When imaged using high magnification time-lapse cinematography, injected *grk* RNA could be observed moving as particles within the oocyte towards the anterior and dorsoanterior. The work carried out to form part of this thesis revealed that *grk* RNA localises in a biphasic movement, localising firstly to the anterior before turning to move dorsoanteriorly. The switch from one phase of movement to the next occurred most frequently near the anterior cortex of the oocyte, but did not require the RNA to be localised exclusively at the anterior first. RNA particles have therefore the ability to move dorsolaterally when in the interior of the oocyte near the anterior cortex. The time scope of the experiments carried out did not allow further analysis into the exact positioning of RNA particles at the time of switching from one movement to the next. However, future experiment will hopefully define more clearly the dynamics of particle movement within the oocyte that facilitate the final stage of *grk* RNA localisation at the dorsoanterior corner.

grk RNA localisation in the oocyte is microtubule and dynein dependent

Injected pair-rule and *wg* transcripts in the embryo have been shown to require both MTs as well as cytoplasmic dynein. In the oocyte, *grk* RNA has also been shown to require MT-integrity and polarity, as well as activity of the Dhc. Particles of *grk* RNA in the oocyte were observed travelling with an average speed of 0.25 μm/sec with maximum speeds of up to 1.25 μm/sec (Alejandra Clark). Generally, the movement of *grk* RNA particles is slower than the speed of pair-rule and *wg* RNA particles observed in the embryo, which is on average twice as fast (Wilkie and Davis, 2001). However, *grk* RNA particles in the oocyte appear to go through phases of rapid motion interspersed by periods of stasis.

The fact that *grk* RNA particles pause frequently within the ooplasm would explain the much longer timeframe during which *grk* RNA localises to the final destination. It can be suggested that the different speeds observed in embryos and oocytes do not represent two different mechanisms of localisation, but display the difference in tissues studied and their specificity. Oogenesis occurs over a much longer period of time and there is therefore no need to localise maternal RNAs as quickly as in the blastoderm embryo, where development is extremly rapid and dynamic. Furthermore, transcripts in the embryo have been found to be very unstable with a short half time of 6 minutes in the case of *ftz* mRNA (Edgar et al., 1986), suggesting a requirement for fast transport to the appropriate site within the cytoplasm to deposit the translated protein at the site of function.

Not much is known about stability of *grk* RNA within the oocyte, but it is generally accepted that it is likely to be very different to the embryo, as development is much slower. The half-life of *grk* mRNA in the oocyte is likely to be at least an order of magnitude greater than that of *ftz* in the embryo.

grk RNA localisation in the oocyte has been shown to require the integrity of the oocyte MTs as well as the function of dynein, which has also been shown to be required for apical localisation of transcripts in the embryo. Cytoplasmic dynein is a highly complex and conserved motor protein facilitating minus end directed transport (Hays et al., 1994). Dynein has been shown to participate in a wide range of cellular processes, from mitosis, axonal transport and localisation of the Golgi-complex and endosomal membranes to various processes during development, such as axon guidance, oogenesis and nuclear migration (Holzbaur and Vallee, 1994; Waterman-Storer et al., 1997; Burkhardt et al., 1997; McGrail and Hays, 1997). A direct role for dynein during mRNA localisation in the oocyte had not been shown at the time the work for this thesis was composed, although it has been suggested that *bcd* mRNA may require dynein to localise to the anterior of the oocyte. Swa, a protein required for correct *bcd* mRNA localisation, has been shown to interact with the dynein-light chain in in vitro biochemical assays (Schnorrer et al., 2000).

When the work for this thesis was undertaken, little was known about the requirement of motor proteins in *grk* mRNA localisation in the oocyte. However, very recent data has linked *grk* mRNA localisation to dynein. Overexpression of p50/dynamitin, a subunit required for dynein processivity (King and Schroer, 2000), disrupts *grk* mRNA localisation (Januschke et al., 2002). Furthermore, the plus end directed motor Kinesin I has been shown to be required for the dorsoanterior

localisation of *grk* mRNA, possibly because of a requirement to recycle dynein (Brendza et al., 2002). However, the path of *grk* RNA had not been defined prior to this thesis and no particle tracking had been performed to study *grk* mRNA movement in the oocyte, believed to be the most compulsive way to distinguish between the various hypotheses for localisation.

The difficulties of analysing the requirement for such an abundant cytoplasmic motor protein as dynein lies in the variety of processes relying on function of cytoplasmic dynein. Cytoplasmic dynein function is required for cell viability in several *Drosophila* tissues (Gepner et al., 1996). In hypormorphic alleles of cytoplasmic dynein, endogenous *grk* mRNA had been shown to correctly localise and was therefore not considered to be required for the localisation of this maternal transcript (McGrail and Hays, 1997). Although previous work had shown that correct endogenous *grk* RNA localisation requires MTs (Pokrywka and Stephenson, 1991), the in vivo injection assay in this thesis was able to provide more direct evidence for the requirement of cytoplasmic dynein in *grk* RNA localisation.

Hypomorphic alleles disrupting the heavy chain of dynein localise *grk* RNA slower compared to control egg chambers and in embryos, the speed of *grk* RNA particles localising apically is reduced by over 50% in two different trans-allelic combination of the *dhc* mutant alleles available. *grk* RNA particle formation in the oocytes of *dhc* mutants appeared reduced, so analysis of *grk* RNA particle dynamics in the oocyte could not be performed during the time given for completion of this thesis. However, further technical advances will make it easier in the future to analyse particle movement in oocytes, which will enable further detailed studies to be carried out.

Dorsoanterior localisation of *grk* RNA is achieved by a two-step mechanism

When injected into stage 8-10 cultured oocytes, *grk* RNA could be observed localising firstly to the anterior before finally localising to the dorsoanterior of the oocyte. When *grk* RNA particle movement was analysed in detail using high magnification timelapse cinematography it was found that particles of the injected RNA had the ability to turn from an anterior to a dorsolateral direction. Frequently, the turning of particles was preceded by a short phase of stasis, which can be interpreted as a switching mechanism for the RNA particle, for example leaving one MT and finding a second MT track.

We propose that the two steps of *grk* RNA localisation are mechanistically different and utilise distinct networks of oocyte MTs. Oocyte MTs are complex and high resolution imaging of MTs in the oocyte, using Tau GFP egg chambers, has supported the idea that there are multiple populations of MTs (see MacDougall et al, 2003). It was found that a high number of MT-minus ends are located on one side of the oocyte nucleus during stage 8-10 in egg chambers expressing Nod:lacZ, which is a putative marker for the minus ends of MTs in the oocyte (Clark et al., 1997; Micklem et al., 1997). High resolution imaging of egg chambers expressing a fusion between the bovine MT associated protein Tau and GFP, revealed, that MTs are concentrated around the oocyte nucleus and the anterior cortex of the oocyte with fewer MTs present cortically elsewhere or in the posterior of the oocyte. The concentration of MTs around the oocyte nucleus is much higher than along the anterior cortex of the oocyte, further supporting a model in which there are subpopulations of MTs within the oocyte.

Recent work has also revealed that there are MT-minus ends throughout all parts of the oocyte cortex (Cha et al., 2002) and it is less clear whether there is a simple gradient of MTs from anterior to the posterior, as had been proposed previously (Theurkauf et al., 1992; Theurkauf, 1994).

The data provided in this thesis in the context of previous work suggests that there may be a complex network of different subpopulations of MTs within the oocyte, which may be biochemically distinct, so that they can facilitate the specific localisation of different maternal RNAs to their final localisation site. It can be suggested that the oocyte nucleus has a different network of MTs associated, which specifically allow localisation of *grk* RNA to the dorsoanterior. These MTs would not allow other RNAs from localising to the dorsoanterior, such as *bcd* RNA. As *bcd* has also been shown to localise to minus ends of MTs, this would explain the difference in localisation between *bcd* and *grk* RNA.

In recent work, *bcd* RNA has been shown to localise to the nearest cortex when injected into the oocyte rather than to the anterior when injected into the nurse cells (Cha et al., 2001), which is also in line with experiments carried out in this thesis (see chapter 4 of this thesis). However, when *bcd* RNA is exposed to the nurse cell cytoplasm prior to oocyte injection, it subsequently localises correctly to the anterior (Cha et al., 2001), similarly to the first step of *grk* RNA localisation. Interestingly, *bcd*, but not *grk* mRNA localisation requires g-Tub37C and Dgrip75 (Schnorrer et al., 2002).

If *grk* and *bcd* RNA share part of the localisation path, the question is how the different sites of localisation are achieved. A model proposing the sorting of different transcripts to distinct subsets of MT minus ends in association with

cytoplasmic dynein would deliver an explanation as to why *grk* RNA is transported to a different destination compared to their mRNAs which may also be transported utilising dynein mediated transport. Different transacting factors that recognise RNA signals will most likely play a role in determining which RNAs use which motor protein to achieve localisation along different subpopulations of MTs. So far no transacting factors have been directly identified to interact with *grk* RNA to achieve correct localisation, but it is likely that the hnRNPA1 homologue Squid and K10 are involved in localising *grk* mRNA (Kelley, 1993; Cheung et al., 1992), as analysis of mutant alleles shows mislocalisation of *grk* mRNA to the anterior cortex of the oocyte (Norvell et al., 1999; Serano et al., 1995). Furthermore, experiments in vitro show that Squid protein interacts with the 3'UTR, supporting the view that the nuclear isoform of Squid S may interact with *grk* mRNA to facilitate the dorsoanterior localisation.

It is likely that, in addition to the transacting factors, the different MTs are likely to differ, allowing different kinds of RNA-motor complexes to distinguish between them. Possible modification could include modification of the tubulin itself, as well as association with MT-associating proteins (MAPs). MTs could differ in their stability as well as in the number of tubulin monomers assembled. Furthermore, chemical modification, such as tyrosination and acetylation of the tubulin monomers has been reported and could possibly be used as a means of mRNA sorting (Bulinski et al., 1988). The model proposed would suggest how dynein-dependent motility of RNA and other cargo could lead to delivering different cargoes to distinct minus end destinations.

grk RNA synthesis and nurse cell-to oocyte transport

The in vivo injection assay revealed a two step mechanism for *grk* RNA localisation within the oocyte. The majority of *grk* RNA specifically localises firstly to the anterior of the oocyte and subsequently to the dorsoanterior cap in stage 9 egg chambers, in a similar pattern to endogenous *grk* RNA. Endogenous *grk* mRNA is one of the key maternal transcripts being localised firstly to the posterior of the oocyte and later to the dorsoanterior corner. The experiments carried out in this thesis have shown clear similarities between the injected and endogenous *grk* RNA. Both injected and endogenous *grk* RNA are localised in a similar pattern in the oocyte and high magnification imaging also shows that both are located at the dorsoanterior cap in a punctate pattern. Furthermore, localisation of injected and endogenous *grk* RNA has been shown to be specific and to require the hnRNP A1 homologue, Squid. Finally, both injected and endogenous *grk* RNA has been shown to require MTs as well as dynein (Duncan and Warrior, 2002; Januschke et al., 2002).

During oogenesis in *Drosophila*, the nurse cells produce mRNAs as well as proteins and organelles, which are transported through the ring canals into the oocyte to facilitate oocyte growth and maturation. Whether *grk* RNA is also transcribed by the nurse cells and transported into the oocyte is currently not resolved. Previous work has suggested that *grk* RNA is transcribed in the nurse cells, like *bcd* and *osk,* and is subsequently transported into the oocyte (Thio et al., 2000). Other work carried out suggests that the site of transcription for *grk* mRNA resides in the oocyte nucleus, from where it is exported to the oocyte (Saunders and Cohen, 1999). When *grk* RNA was injected into the nurse cells of living stage 6-10 egg chambers, it clearly

localised within the oocyte approximately one hour after injection, which involved the transport of *grk* RNA into the oocyte prior to localisation. The nurse cell-to –oocyte transport is a MT-dependent process but it is not clear whether it directly requires dynein, as disruption of dynein function only impaired oocyte localisation, but not accumulation of *grk* RNA. High-resolution imaging has revealed that *grk* RNA can form particles, which appear to move directly into the oocyte, presumably through the ring canals. However, it is not clear whether directed transport is the only means of nurse cell-to-oocyte transport and other factors, such as diffusion through the ring canals may play a role as well. Whatever the site of transcription of *grk* RNA, the observed particle motility in both oocyte and the nurse cells are clearly significant. The Two-step mechanism of *grk* RNA particle movement observed in the oocyte could resemble the two steps of nurse cell-to–oocyte transport, if *grk* RNA is transcribed in the nurse cells. Otherwise, the same two-step mechanism is able to localise *grk* RNA to the dorsoanterior if it is transcribed by the oocyte nucleus. It is possible that the transcriptional regulation of *grk* mRNA is more complex and *grk* mRNA may indeed be transcribed by both the nurse cells and the oocyte during different stages of oogenesis. So far, in situ hybridisation has not revealed the site of transcription, but experiments are currently carried out in our lab, which will hopefully shed light on this question in the near future.

grk mRNA localisation requires cis-acting localisation elements

For most RNAs, all the *cis*-acting sequences necessary for RNA localization that have been mapped reside in the 3'UTR. The only exception are *yemanuclein-alpha* mRNA, which accumulates in the early oocyte of *Drosophila, grk* mRNA and *Ash1*mRNAin *S. cerevisiae* (see Introduction of this thesis) (Capri M, 1997;

Chartrand et al., 1999; Gonzalez et al., 1999; Saunders and Cohen, 1999; Thio et al., 2000). Different steps in the localisation of a transcript are often mediated by separate *cis*-acting elements.

Previous work has identified certain sequences within the 3' and 5'UTR sequence as well as the coding region of *grk* RNA, which are required for correct localisation of the transcript within the oocyte (Thio et al., 2000; Saunders and Cohen, 1999). All injections performed so far for this thesis have used the entire cDNA fragment of *grk* RNA, but currently more work, carried out in our lab is trying to map more precisely the cis-acting sequences required for *grk* RNA localisation. The in vivo injection assay provides a powerful tool to identify the relevant sequences very rapidly. Injection and direct analysis of the localisation dynamics of *grk* fragments is hugely faster and more powerful than producing transgenic reporter constructs and assaying them by in situ hybridisaiton. The work currently under way will hopefully lead to a much better understanding of the localisation mechanism of one of the key maternal transcripts required for oocyte polarity in *Drosophila*. This has general implications on how different RNAs transported by the same motors specify their localisation site through a complex network of cis acting sequences and trans-acting factors which allow the RNA protein complex to utilise different networks of MTs for their transport. Furthermore, this work is likely to be applicable to various other cargos transported by the two families of motors in the cell, namely dynein and Kinesin.

9

REFERENCES

Arking, R. (1975). Temperature sensitive cell-lethal mutants of *Drosophila*: Isolation and characterization. Genetics *80*, 519-537.

Arn, E. A., Cha, B. J., Theurkauf, W. E., and Macdonald, P. M. (2003). Recognition of a *bicoid* mRNA localization signal by a protein complex containing Swallow, Nod, and RNA binding proteins. Dev Cell *4*, 41-51.

Barkai, N., and Shilo, B. Z. (2002). Modeling pattern formation: counting to two in the *Drosophila* egg. Curr Biol. *12(14)*, 493-5

Bashirullah, A., Halsell, S. R., Cooperstock, R. L., Kloc, M., Karaiskakis, A., Fisher, W. W., Fu, W., Hamilton, J. K., Etkin, L. D., and Lipshitz, H. D. (1999). Joint action of two RNA degradation pathways controls the timing of maternal transcript elimination at the midblastula transition in *Drosophila* melanogaster. Embo J *18*, 2610-20.

Beach DL, S. E., Bloom K. (1999). Localization and anchoring of mRNA in budding yeast. Curr. Biol *9*, 569-78.

Bergsten, S. E., and Gavis, E. R. (1999). Role for mRNA localization in translational activation but not spatial restriction of nanos RNA.
Development *126*, 659-69.

Berleth, T., Burri, M., Thoma, G., Bopp, D., Richstein, S., Frigerio, G., Noll, M., and Nüsslein-Volhard, C. (1988). The role of localization of *bicoid* RNA in organizing the anterior pattern of the *Drosophila* embryo. EMBO J. *7*, 1749-1756.

Bertrand, E., Chartrand, P., Schaefer, M., Shenoy, S. M., Singer, R. H., and Long, R. M. (1998). Localization of *ASH1* mRNA particles in living yeast. Mol Cell *2*, 437-45.

Bolivar, J., Huynh, J. R., Lopez-Schier, H., Gonzalez, C., St Johnston, D., and Gonzalez-Reyes, A. (2001). Centrosome migration into the *Drosophila* oocyte is independent of BicD and egl, and of the organisation of the microtubule cytoskeleton.
Development *128*, 1889-97.

Bratu, D., Cha, B., Mhlanga, M.M, Kramer, F.R,Tyagi, S. (2003). Visualizing the distribution and transport of mRNAs in living cells. Proc Natl Acad Sci USA *100*, 13308-13.

Brendza, R., Serbus, L., Saxton, W., and Duffy, J. (2002). Posterior localization of Dynein and dorsal-ventral axis formation depend on Kinesin in *Drosophila* oocytes.
Curr Biol *12*, 1541.

Brendza, R. P., Serbus, L. R., Duffy, J. B., and Saxton, W. M. (2000). A function for kinesin I in the posterior transport of *oskar* mRNA and Staufen protein.
Science *289*, 2120-2.

Bulinski J.C., Piperno G. (1988). Posttranslational modifications of alpha tubulin: detyrosination and acetylation differentiate populations of interphase microtubules in cultured cells. J Cell Biol. 1988 *106*, 1213-20.

Bullock, S. L. and Ish-Horowicz, D. (2001). Conserved signals and machinery for RNA transport in *Drosophila* oogenesis and embryogenesis. Nature *414*, 611-616.

Burkhardt, J. K., Echeverri, C. J., Nilsson, T., and Vallee, R. B. (1997). Overexpression of the dynamitin (p50) subunit of the dynactin complex disrupts dynein-dependent maintenance of membrane organelle distribution. J Cell Biol *139*, 469-84.

Capri M, S. M., Thomas-Delaage M, Ait-Ahmed O. (1997). Implication of a 5' coding sequence in targeting maternal mRNA to the *Drosophila* oocyte. Mech Dev *68*, 91-100.

Castagnetti, S., Hentze, M. W., Ephrussi, A., and Gebauer, F. (2000). Control of *oskar* mRNA translation by Bruno in a novel cell-free system from *Drosophila* ovaries. Development *127*, 1063-1068.

Cha, B., Koppetsch, B. S., and Theurkauf, W. E. (2001). In Vivo Analysis of *Drosophila bicoid* mRNA Localization Reveals a Novel Microtubule-Dependent Axis Specification Pathway. Cell *106*, 35-46.

Cha, B. J., Serbus, L. R., Koppetsch, B. S., and Theurkauf, W. E. (2002). Kinesin I-dependent cortical exclusion restricts pole plasm to the oocyte posterior. Nat Cell Biol *4*, 592-8.

Chang, J. S., Tan, L., Wolf, M. R., and P., S. (2001). Functioning of the *Drosophila orb* gene in *gurken* mRNA localization and translation. Development *128*, 3169-77.

Chartrand, P., Meng, X. H., Singer, R. H., and Long, R. M. (1999). Structural elements required for the localization of *ASH1* mRNA and of a green fluorescent protein reporter particle in vivo. Current Biology *9*, 333-336.

Cheung, H. K., Serano, T. L., and Cohen, R. S. (1992). Evidence for a highly selective RNA transport system and its role in establishing the dorsoventral axis of the *Drosophila* egg. Development *114*, 653-61.

Chou, T. B., and Perrimon, N. (1992). Use of a yeast site-specific recombinase to produce female germline chimeras in *Drosophila*. Genetics *131*, 643-653.

Clark, I., Giniger, E., Ruohola-Baker, H., Jan, L. Y., and Jan, Y. N. (1994). Transient posterior localization of a kinesin fusion protein reflects anteroposterior polarity of the *Drosophila* oocyte. Current Biology *4*, 289-300.

Clark, I. E., Jan, L. Y., and Jan, Y. N. (1997). Reciprocal localization of Nod and kinesin fusion proteins indicates microtubule polarity in the *Drosophila* oocyte, epithelium, neuron and muscle. Development *124*, 461-470.

Clements, D., Friday, R. V., and Woodland, H. R. (1999). Mode of action of VegT in mesoderm and endoderm formation. Development *126*, 4903-11.

Colon-Ramos, D. A., Salisbury, J. L., Sanders, M. A., Shenoy, S. M., Singer, R. H., Garcia-Blanco, M. A. (2003). Asymmetric distribution of nuclear pore complexes and the cytoplasmic localization of beta2-tubulin mRNA in Chlamydomonas reinhardtii. Dev Cell *4*, 941-52.

Curtis, D., Apfeld, J., and Lehmann, R. (1995). nanos is an evolutionarily conserved organizer of anterior-posterior polarity. Development *121*, 1899-910.

Dahanukar, A., Walker, J. A., and Wharton, R. P. (1999). Smaug, a novel RNA-binding protein that operates a translational switch in *Drosophila*. Mol Cell *4*, 209-18.

Dahanukar, A., and Wharton, R. P. (1996). The Nanos gradient in *Drosophila* embryos is generated by translational regulation. Genes Dev *10*, 2610-20.

Davis, I. (2000). Visualising fluorescence in *Drosophila* - optimal detection in thick specimens. In Protein Localisation by Fluorescence Microscopy: A Practical Approach, V. J. Allan, ed. (Oxford: OUP), pp. 131-162.

Davis, I., Francis-Lang, H., and Ish Horowicz, D. (1993). Mechanisms of intracellular transcript localization and export in early *Drosophila* embryos.
Cold Spring Harbor Symposia On Quantitative Biology *58*, 793-798.

Davis, I., Girdham, C. H., and O Farrell, P. H. (1995). A nuclear GFP that marks nuclei in living *Drosophila* embryos - maternal supply overcomes a delay in the appearance of zygotic fluorescence. Developmental Biology *170*, 726-729.

Davis, I., and Ish-Horowicz, D. (1991). Apical localization of pair-rule transcripts requires 3' sequences and limits protein diffusion In the *Drosophila* blastoderm embryo.
Cell *67*, 927-940.

Deng, W. M., and Ruohola-Baker, H. (2000). Laminin A is required for follicle cell-oocyte signaling that leads to establishment of the anterior-posterior axis in *Drosophila*.
Current Biology *10*, 683-686.

Deshler, J. O., Highett, M. I., Abramson, T., and Schnapp, B. J. (1998). A highly conserved RNA-binding protein for cytoplasmic mRNA localization in vertebrates. Curr Biol *8*, 489-96.

Ding, D., Parkhurst, S. M., Halsell, S. R., and Lipshitz, H. D. (1993). Dynamic Hsp83 RNA localization during *Drosophila* oogenesis and embryogenesis. Mol Cell Biol *13*, 3773-81.

Dollar, G., Struckhoff, E., Michaud, J., and Cohen, R. S. (2002). Rab11 polarization of the *Drosophila* oocyte: a novel link between membrane trafficking, microtubule organization, and *oskar* mRNA localization and translation. Development *129*, 517-26.

Driever, W., and Nüsslein-Volhard, C. (1988). A gradient of bicoid protein in *Drosophila* embryos. Cell *54*, 83-93.

Dubowy, J., and Macdonald, P. M. (1998). Localization of mRNAs to the oocyte is common in *Drosophila* ovaries. Mech Dev *70*, 193-5.

Duffy, J. B., Harrison, D. A., and Perrimon, N. (1998). Identifying loci required for follicular patterning using directed mosaics. Development *125*, 2263-2271.

Duncan, J. E., and Warrior, R. (2002). The cytoplasmic Dynein and Kinesin motors have interdependent roles in patterning the *Drosophila* oocyte. Curr Biol *12*, 1982-91.

Edgar, B. A., Weir, M. P., Schubiger, G., and Kornberg, T. (1986). Repression and turnover pattern of *fushi tarazu* RNA in the early *Drosophila* embryo. Cell *47*, 747-54.

Ehrenberg, N. (1998). Characterisation of *l(1)ts594*, a temperature-sensitive mutation disrupting mRNA localisation and polarity during *Drosophila* oogenesis. Diploma Thesis, University of Cologne

Ephrussi, A., Dickinson, L. K., and Lehmann, R. (1991). Oskar organizes the germ plasm and directs localization of the posterior determinant nanos. Cell *66*, 37-50.

Ephrussi, A., and Lehmann, R. (1992). Induction of germ cell formation by oskar. Nature *358*, 387-392.

Erdelyi, M., Michon, A. M., Guichet, A., Glotzer, J. B., and Ephrussi, A. (1995). Requirement for *Drosophila* cytoplasmic tropomyosin in *oskar* mRNA localization. Nature *377*, 524-7.

Farina KL, S. R. (2002). The nuclear connection in RNA transport and localization. Trends Cell Biol. *12*, 466-472.

Foe, V. E., Odell, G. M., and Edgar, B. A. (1993). Mitosis and morphogenesis in the *Drosophila* embryo: Point and counterpoint. In the development of *Drosophila melanogaster*, M. Bate and A. Martinez-Arias, eds.
New York: Cold Spring Harbour Laboratory Press, pp. 149-300.

Forbes, A., and Lehmann, R. (1998). Nanos and Pumilio have critical roles in the development and function of *Drosophila* germline stem cells. Development *125*, 679-690.

Forrest K.M., G. E. R. (2003). Live Imaging of endogenous RNA reveals a diffusion and entrapment mechanism for *nanos* mRNA localization in *Drosophila*.
Curr Biol *13*, 1159-1168.

Francis-Lang, H., Davis, I., and Ish-Horowicz, D. (1996). Asymmetric localization of *Drosophila* pair-rule rranscripts from displaced nuclei - evidence for directional nuclear export. Embo Journal *15*, 640-649.

Fujimura, M., and Takamura, K. (2000). Characterization of an ascidian DEAD-box gene, *CiDEAD1*: specific expression in the germ cells and its mRNA localization in the posterior-most blastomeres in early embryos. Dev.Genes.Evol. *210*, 64-72.

Gavis, E. R., and Lehmann, R. (1994). Translational regulation of nanos by RNA localization. Nature *369*, 315-318.

Gepner, J., Li, M., Ludmann, S., Kortas, C., Boylan, K., Iyadurai, S. J., McGrail, M., and Hays, T. S. (1996). Cytoplasmic dynein function is essential in *Drosophila* melanogaster. Genetics *142*, 865-78.

Ghabrial, A., Ray, R. P., and Schupbach, T. (1998). *okra* and *spindle-B* encode components of the RAD52 DNA repair pathway and affect meiosis and patterning in *Drosophila* oogenesis. Genes Dev *12*, 2711-23.

Gillespie, D. E., and Berg, C. A. (1995). Homeless is required for RNA localization in *Drosophila* oogenesis and encodes a new member of the De-H family of RNA-dependent ATPases. Genes & Development *9*, 2495-2508.

Glotzer, J. B., Saffrich, R., Glotzer, M., and Ephrussi, A. (1997). Cytoplasmic flows localize injected *oskar* RNA in *Drosophila* oocytes. Current Biology *7*, 326-337.

Gonzalez, I., Buonomo, S. B., Nasmyth, K., and von Ahsen, U. (1999). ASH1 mRNA localization in yeast involves multiple secondary structural elementsand ash1 protein translation. Curr Biol *9*, 337-40.

Gonzalez-Reyes, A., Elliott, H., and St Johnston, D. (1997). Oocyte determination and the origin of polarity in *Drosophila*: the role of the *spindle* genes. Development *124*, 4927-37.

Gonzalez-Reyes, A., Elliott, H., and St Johnston, D. (1995). Polarization of both major body axes in *Drosophila* by Gurken-Torpedo signaling. Nature *375*, 654-658.

Gonzalez-Reyes, A., and St Johnston, D. (1998). The *Drosophila* AP axis is polarised by the cadherin-mediated positioning of the oocyte. Development *125*, 3635-44.

Gonzalez-Reyes, A., and St Johnston, D. (1994). Role of oocyte position in establishment of anterior-posterior polarity In *Drosophila*. Science *266*, 639-642.

Gonzalez-Reyes, A., and St Johnston, D. S. (1998). Patterning of the follicle cell epithelium along the anterior-posterior axis during *Drosophila* oogenesis.
Development *125*, 2837-2846.

Goode, S., Melnick, M., Chou, T. B., and Perrimon, N. (1996 a). The neurogenic genes *egghead* and *brainiac* define a novel signaling pathway essential for epithelial morphogenesis during *Drosophila* oogenesis. Development *122*, 3863-3879.

Goode, S., Morgan, M., Liang, Y. P., and Mahowald, A. P. (1996 b). *brainiac* encodes a novel, putative secreted protein that cooperates with Grk TGF alpha in the genesis of the follicular epithelium. Developmental Biology *178*, 35-50.

Gross, S. P., Welte, M. A., Block, S. M., and Wieschaus, E. F. (2000). Dynein-mediated cargo transport in vivo. A switch controls travel distance. J Cell Biol *148*, 945-56.

Grunert, S., and St Johnston, D. (1996). RNA localization and the development of asymmetry during *Drosophila* oogenesis.
Current Opinion In Genetics & Development *6*, 395-402.

Gunkel, N., Yano, T., Markussen, F. H., Olsen, L. C., and Ephrussi, A. (1998). Localization-dependent translation requires a functional interaction between the 5' and 3' ends of oskar mRNA. Genes Dev *12*, 1652-64.

Hachet, O., and Ephrussi, A. (2001). *Drosophila* Y14 shuttles to the posterior of the oocyte and is required for *oskar* mRNA transport. Curr Biol *11*, 1666-74.

Havin, L., Git, A., Elisha, Z., Oberman, F., Yaniv, K., Schwartz, S. P., Standart, N., and Yisraeli, J. K. (1998). RNA-binding protein conserved in both microtubule- and microfilament- based RNA localization. Genes Dev *12*, 1593-8.

Hawkins, N. C., Van Buskirk, C., Grossniklaus, U., and Schüpbach, T. (1997). Post-transcriptional regulation of gurken by encore is required for axis determination in *Drosophila*. Development *124*, 4801-10.

Hays, T. S., Porter, M. E., McGrail, M., Grissom, P., Gosch, P., Fuller, M. T., and McIntosh, J. R. (1994). A cytoplasmic dynein motor in *Drosophila:* identification and localization during embryogenesis. J Cell Sci *107*, 1557-69.

Hazelrigg (1990). The exuperantia gene is required for Drosophila spermatogenesis as well as anteroposterior polarity of the developing oocyte, and encodes overlapping sex-specific transcripts. Genetics *126*, 607-617.

Holzbaur, E. L., and Vallee, R. B. (1994). DYNEINS: molecular structure and cellular function. Annu Rev Cell Biol *10*, 339-72.

Hoogenraad CC, A. A., Howell SA, Dortland BR, De Zeeuw CI, Willemsen R, Visser P, Grosveld F, Galjart N. (2001). Mammalian Golgi-associated Bicaudal-D2 functions in the dynein-dynactin pathway by interacting with these complexes. Embo J *20*, 4041-4054.

Hoogenraad CC, W. P., Schiefermeier N, Stepanova T, Galjart N, Small JV, Grosveld F, De Zeeuw CI, Akhmanova A. (2003). Bicaudal D induces selective dynein-mediated microtubule minus end-directed transport. Embo J *22*, 6004-6015.

Hyde, C. E., and Old, R. W. (2000). Regulation of the early expression of the *Xenopus nodal-related 1* gene, *Xnr1*. Development *127*, 1221-29.

Jansen, R. P. (2001). mRNA localization: message on the move.
Nat Rev Mol Cell Biol *2*, 247-56.

Jansen, R. P., Dowzer, C., Michaelis, C., Galova, M., and Nasmyth, K. (1996). Mother cell-specific HO expression in budding yeast depends on the unconventional myosin myo4p and other cytoplasmic proteins. Cell *84*, 687-97.

Januschke, J., Gervais, L., Dass, S., Kaltschmidt, J. A., Lopez-Schier, H., Johnston, D. S., Brand, A. H., Roth, S., and Guichet, A. (2002). Polar transport in the *Drosophila* oocyte requires Dynein and Kinesin I cooperation. Curr Biol *12*, 1971-81.

Johnstone, O., and Lasko, P. (2001). Translational regulation and RNA localization in *Drosophila* oocytes and embryos. Annu Rev Genet *35*, 365-406.

Kelley, R. L. (1993). Initial organization of the Drosophila dorsoventral axis depends on an RNA-binding protein encoded by the squid gene. Genes Dev. *7*, 948-960.

Kim-Ha, J., Kerr, K., and Macdonald, P. M. (1995). Translational regulation of *oskar* mRNA by Bruno, an ovarian RNA-binding protein, is essential. Cell *81*, 403-412.

Kim-Ha, J., Smith, J. L., and MacDonald, P. M. (1991). *oskar* mRNA is localized to the posterior pole of the *Drosophila* oocyte. Cell *66*, 23-35.

King, R. C. (1970). Ovarian Development in *Drosophila* melanogaster.
New York: Academic Press

King, S. J., and Schroer, T. A. (2000). Dynactin increases the processivity of the cytoplasmic dynein motor. Nat Cell Biol *2*, 20-4.

Kloc, M., Bilinski, S., Pui-Yee Chan, A., and Etkin, L. D. (2000). The targeting of Xcat2 mRNA to the germinal granules depends on a cis-acting germinal granule localization element within the 3'UTR. Dev.Biol. *217*, 221-29.

Kloc, M., and Etkin, L. D. (1998). Apparent continuity between the messenger transport organizer and late RNA localization pathways during oogenesis in Xenopus. Mechanisms Of Development *73*, 95-106.

Kloc, M., Zearfoss, N. R., and Etkin, L. D. (2002). Mechanisms of subcellular mRNA localization. Cell *108*, 533-44.

Koch, E. A., and Spitzer, R. H. (1983). Multiple effects of colchicine on oogenesis in *Drosophila*: induced sterility and switch of potential oocyte to nurse-cell developmental pathway. Cell Tissue Res. *228*, 21-32.

Kofron, M., Demel, T., Xanthos, J., Lohr, J., and Sun, B. (1999). Mesoderm induction in *Xenopus* is a zygotic event regulated by maternal VegT via *TGF* β growth factors. Development *126*, 5759-70.

Ku, M., and Melton, D. A. (1993). Xwnt-11: a maternally expressed *Xenopus* wnt gene. Development *119*, 1161-73.

LaJeunesse, D. R., McCartney, B. M., and Fehon, R. G. (1998). Structural analysis of *Drosophila* merlin reveals functional domains important for growth control and subcellular localization. Journal of Cell Biology *141*, 1589-1599.

Lall, S., Francis-Lang, H., Flament, A., Norvell, A., Schüpbach, T., and Ish-Horowicz, D. (1999). Squid hnRNP protein promotes apical cytoplasmic transport and localization of *Drosophila* pair-rule transcripts. Cell *98*, 171-80.

Lane, M. E., and Kalderon, D. (1995). Localization and functions of protein kinase A during *Drosophila* oogenesis. Mech Dev *49*, 191-200.

Lane, M. E., and Kalderon, D. (1994). RNA localization along the anteroposterior axis of the *Drosophila* oocyte requires PKA-mediated signal transduction to direct normal microtubule organization. Genes & Development *8*, 2986-2995.

Larkin, M. K., Holder, K., Yost, C., Giniger, E., and Ruohola-Baker, H. (1996). Expression of constitutively active Notch arrests follicle cells at a precursor stage during *Drosophila* oogenesis and disrupts the anterior-posterior axis of the oocyte. Development *122*, 3639-3650.

Lie, Y. S., and Macdonald, P. M. (1999). Apontic binds the translational repressor Bruno and is implicated in regulation of *oskar* mRNA translation. Development *126*, 1129-38.

Lie, Y. S., and Macdonald, P. M. (1999). Translational regulation of *oskar* mRNA occurs independent of the cap and poly(A) tail in *Drosophila* ovarian extracts. Development *126*, 4989-96.

Lin, H., Yue, L., and Spradling, A. C. (1994). The *Drosophila* fusome, a germline-specific organelle, contains membrane skeletal proteins and functions in cyst formation. Development *120*, 947-955.

Lipshitz, H. D., and Smibert, C. A. (2000). Mechanisms of RNA localization and translational regulation. Curr Opin Genet Dev *10*, 476-88.

Long, R. M., Chartrand, P., Gu, W., Meng, X. H., Schaefer, M. R., and Singer, R. H. (1997). Characterization of transport and localization of ASH1 mRNA in yeast. Molecular Biology Of the Cell *8*, 2060-2060.

Macdonald, P. M., and Kerr, K. (1997). Redundant RNA recognition events in bicoid mRNA localization. Rna *3*, 1413-20.

Macdonald, P. M., Luk, S. K., and Kilpatrick, M. (1991). Protein encoded by the *exuperantia* gene is concentrated at sites of *bicoid* mRNA accumulation in *Drosophila* nurse cells but not in oocytes or embryos. Genes Dev *5*, 2455-66.

Macdonald, P. M., and Struhl, G. (1988). cis-acting sequences responsible for anterior localization of *bicoid* mRNA in *Drosophila* embryos. Nature *336*, 595-8.

MacDougall, N., Clark, A., MacDougall, E., and Davis, I. (2003). *Drosophila gurken* (TGFalpha) mRNA Localizes as Particles that Move within the Oocyte in Two Dynein-Dependent Steps. Dev Cell *4*, 307-19.

MacDougall, N., Lad, Y., Wilkie, G., Francis-Lang, H., Sullivan, W., and Davis, I. (2001). Merlin, the *Drosophila* homologue of Neurofibromatosis-2, is specifically required in posterior follicle cells for axis formation in the oocyte. Development *128*, 665-673.

Mach, J. M., and Lehmann, R. (1997). An Egalitarian-BicaudalD complex is essential for oocyte specification and axis determination in *Drosophila*.
Genes & Development *11*, 423-435.

Mangeat, P., Roy, C., and Martin, M. (1999). ERM proteins in cell adhesion and membrane dynamics. Trends Cell Biol *9*, 187-192.

Markussen FH, M. A., Breitwieser W, Ephrussi A. (1995). Translational control of oskar generates short OSK, the isoform that induces pole plasma assembly. Development *121*, 3723-32.

McCartney, B. M., and Fehon, R. G. (1996). Distinct cellular and subcellular patterns of expression imply distinct functions for the *Drosophila* homologues of moesin and the neurofibromatosis 2 tumor suppressor, merlin. J Cell Biol *133*, 843-852.

McCartney, B. M., Kulikauskas, R. M., LaJeunesse, D. R., and Fehon, R. G. (2000). The neurofibromatosis-2 homologue, Merlin, and the tumor suppressor expanded function together in *Drosophila* to regulate cell proliferation and differentiation. Development *127*, 1315-1324.

McGrail, M., and Hays, T. S. (1997). The microtubule motor cytoplasmic dynein is required for spindle orientation during germline cell divisions and oocyte differentiation in *Drosophila*. Development *124*, 2409-19.

Michael, W. M., Choi, M., and Dreyfuss, G. (1995). A nuclear export signal in hnRNP A1: a signal-mediated, temperature- dependent nuclear protein export pathway. Cell *83*, 415-22.

Micklem, D. R., Adams, J., Grunert, S., and St Johnston, D. (2000). Distinct roles of two conserved Staufen domains in oskar mRNA localization and translation. Embo J *19*, 1366-77.

Micklem, D. R., Dasgupta, R., Elliott, H., Gergely, F., Davidson, C., Brand, A., Gonzalez-Reyes, A., and St Johnston, D. (1997). The *mago nashi* gene is required for the polarisation of the oocyte and the formation of perpendicular axes in *Drosophila*.
Current Biology *7*, 468-478.

Mosquera, L., Forristall, C., Zhou, Y., and King, M. L. (1993). A mRNA localized to the vegetal cortex of Xenopus oocytes encodes a protein with a nanos-like zinc finger domain.
Development *117*, 377-86.

Mowry, K. L., and Cote, C. A. (1999). RNA sorting in Xenopus oocytes and embryos.
Faseb J 13, 435-45.

Munchow, S., Sauter, C., and Jansen, R. P. (1999). Association of the class V myosin Myo4p with a localised messenger RNA in budding yeast depends on She proteins.
J Cell Sci *112*, 1511-8.

Neuman-Silberberg, F. S., and Schüpbach, T. (1993). The *Drosophila* dorsoventral patterning gene *gurken* produces a dorsally localized RNA and encodes a TGF alpha-like protein. Cell *75*, 165-174.

Neuman-Silberberg, F. S., and Schüpbach, T. (1996). The *Drosophila* TGF-alpha-like protein Gurken: expression and cellular localization during *Drosophila* oogenesis.
Mech Dev *59*, 105-113.

Newmark, P. A., Mohr, S. E., Gong, L., and Boswell, R. E. (1997). mago nashi mediates the posterior follicle cell-to-oocyte signal to organize axis formation in *Drosophila*.
Development *124*, 3197-3207.

Nilson, L. A., and Schüpbach, T. (1999). EGF receptor signaling in *Drosophila* oogenesis. Curr Top Dev Biol *44*, 203-243.

Nishida, H., and Sawada, K. (2001). *macho-1* encodes a localized mRNA in ascidian eggs that specifies muscle fate during embryogenesis. Nature *409*, 724-29.

Norvell, A., Kelley, R. L., Wehr, K., and Schüpbach, T. (1999). Specific isoforms of Squid, a *Drosophila* hnRNP, perform distinct roles in *gurken* localization during oogenesis. Genes Dev *13*, 864-876.

Nüsslein-Volhard, C., and Wieschaus, E. (1980). Mutations affecting segment number and polarity in *Drosophila*. Nature *287*, 795--801.

Olsen, L. C., Aasland, R., and Fjose, A. (1997). A *vasa*-like gene in zebrafish identifies putative primordial germ cells. Mech.Dev. *66*, 95-105.

Palacios, I. M., St Johnston, D. (2001). Getting The Message Across: The Intracellular Localization of mRNAs in Higher Eukaryotes. Annu. Rev. Cell Dev. Biol. *17*, 569-614.

Palacios, I. M. (2002). RNA processing: splicing and the cytoplasmic localisation of mRNA. Curr Biol *12*, R50-2.

Palacios, I. M., and Johnston, D. S. (2002). Kinesin light chain-independent function of the Kinesin heavy chain in cytoplasmic streaming and posterior localisation in the Drosophila oocyte. Development *129*, 5473-85.

Pankratz, M. J., and Jäckle, H. (1993). Blastoderm segmentation. In the development of *Drosophila melanogaster*, M. Bate and A. Martinez-Arias, eds.
(New York: Cold Spring Harbour Laboratory Press).

Pare, C., and Suter, B. (2000). Subcellular localization of Bic-D:GFP is linked to an asymmetric oocyte nucleus. J Cell Sci. *113*, 2119-27.

Peri, F., and Roth, S. (2000). Combined activities of Gurken and decapentaplegic specify dorsal chorion structures of the *Drosophila* egg. Development *127*, 841-50.

Perrimon, N. (1994). Signalling pathways initiated by receptor protein tyrosine kinases in *Drosophila*. Curr Opin Cell Biol *6*, 260-266.

Perrimon, N., Smouse, D., and Miklos, G. L. (1989). Developmental genetics of loci at the base of the X chromosome of *Drosophila* melanogaster. Genetics *121*, 313-331.

Pinol-Roma, S., Swanson, M., Gorlach, M., Burd, C., Matunis, M., Matunis, E., Michael, M., and Dreyfuss, G. (1990). Recent studies on hnRNP complexes. Mol Biol Rep *14*, 85.

Pokrywka, N. J., and Stephenson, E. C. (1991). Microtubules mediate the localization of *bicoid* RNA during *Drosophila* oogenesis. Development *113*, 55-66.

Riechmann, V., Gutierrez, G. J., Filardo, P., Nebreda, A. R., and Ephrussi, A. (2002). Par-1 regulates stability of the posterior determinant Oskar by phosphorylation.
Nat Cell Biol *4*, 337-42.

Robinson, D. N., and Cooley, L. (1997). Genetic analysis of the actin cytoskeleton in the *Drosophila* ovary. Annu. Rev. Cell Dev. Biol. *13*, 147-70.

Roegiers, F., and Jan, Y. N. (2000). Staufen: a common component of mRNA transport in oocytes and neurons? Trends Cell Biol *10*, 220-4.

Rongo, C., Gavis, E. R., and Lehmann, R. (1995). Localization of *oskar* RNA regulates *oskar* translation and requires Oskar protein. Development *121*, 2737-46.

Ross, A. F., Oleynikov, Y., Kislauskis, E. H., Taneja, K. L., and Singer, R. H. (1997). Characterization of a beta-actin mRNA zipcode-binding protein. Molecular and Cellular Biology *17*, 2158-2165.

Roth, S., Neuman-Silberberg, F. S., and Schüpbach, T. (1995). Dorsoventral signaling in *Drosophila* oogenesis. J. Cell. Biochem. *19A*, 326.

Ruohola, H., Bremer, K. A., Baker, D., Swedlow, J. R., Jan, L. Y., and Jan, Y. N. (1991). Role of neurogenic genes in establishment of follicle cell fate and oocyte polarity during oogenesis in *Drosophila*. Cell *66*, 433-449.

Ruohola-Baker, H., Jan, L. Y., and Jan, Y. N. (1994). The role of gene cassettes in axis formation during *Drosophila* oogenesis. Trends In Genetics *10*, 89-94.

Saffman, E. E., Styhler, S., Rother, K., Li, W., Richard, S., and Lasko, P. (1998). Premature translation of *oskar* in oocytes lacking the RNA-binding protein bicaudal-C. Mol. Cell Biol. *18*, 4855-4862.

Sapir, A., Schweitzer, R., and Shilo, B. Z. (1998). Sequential activation of the EGF receptor pathway during *Drosophila* oogenesis establishes the dorsoventral axis. Development *125*, 191-200.

Satou, Y. (1999). *posterior end mark 3* (*pem-3*), an ascidian maternally expressed gene with localized mRNA encodes a protein with *Caenorhabditis elegans* MEX-3-like KH domains. Dev. Biol. *212*, 337-50.

Saunders, C., and Cohen, R. S. (1999). The role of oocyte transcription, the 5'UTR, and translation repression and derepression in *Drosophila gurken* mRNA and protein localization. Molecular Cell *3*, 43-54.

Schnorrer, F., Bohmann, K., and Nüsslein-Volhard, C. (2000). The molecular motor dynein is involved in targeting swallow and *bicoid* RNA to the anterior pole of *Drosophila* oocytes. Nat Cell Biol 2, 185-90.

Schnorrer, F., Luschnig, S., Koch, I., and Nüsslein-Volhard, C. (2002). gamma-Tubulin37C and gamma-tubulin ring complex protein 75 are essential for *bicoid* RNA localization during *Drosophila* oogenesis. Dev Cell *3*, 685-96.

Schüpbach, T., Clifford, R. J., Manseau, L. J., and Price, J. V. (1990). Signalling pathways in *Drosophila* oogenesis. J. Cell. Biochem. *14*, 41.

Schüpbach, T., and Roth, S. (1994). Dorsoventral patterning in *Drosophila* oogenesis. Curr Opin Genet Dev *4*, 502-507.

Schüpbach, T., and Wieschaus, E. (1986). Germline autonomy of maternal-effect mutations altering the embryonic body pattern of *Drosophila*. Dev Biol *113*, 443-8.

Serano, T. L., and Cohen, R. S. (1995). A small predicted stem-loop structure mediates oocyte localization of *Drosophila K10* mRNA. Development *121*, 3809-18.

Serano, T. L., Karlin-McGinness, M., and Cohen, R. S. (1995). The role of fs(1)K10 in the localization of the mRNA of the TGF alpha homolog *gurken* within the *Drosophila* oocyte. Mech Dev *51*, 183-92.

Shilo, B., Golembo, M., Kritchman, N., Gabay, L., and Reich, A. (1998). The *Drosophila* EGF receptor (DER) signaling pathway. Dev. Biol. *198*, 162.

Shisa, J. A., Pitt, J. N., and Priess, J. R. (2001). Analysis of RNA associated with P-granules in germs cells of *C.elegans* adults. Development *128*, 1287-98.

Shulman, J. M., Benton, R., and St Johnston, D. (2000). The *Drosophila* homolog of *C. elegans* PAR-1 organizes the oocyte cytoskeleton and directs *oskar* mRNA localization to the posterior pole. Cell *101*, 377-88.

Sil, A., and Herskowitz, I. (1996). Identification of asymmetrically localized determinant, Ash1p, required for lineage-specific transcription of the yeast HO gene. Cell *84*, 711-22.

Simmonds, A. J., dosSantos, G., Livne-Bar, I., and Krause, H. M. (2001). Apical localization of *wingless* transcripts is required for wingless signaling. Cell *105*, 197–207.

Siomi, H., and Dreyfuss, G. (1995). A nuclear localization domain in the hnRNP A1 protein. J Cell Biol *129*, 551-60.

Smibert, C. A., Lie, Y. S., Shillinglaw, W., Henzel, W. J., and Macdonald, P. M. (1999). Smaug, a novel and conserved protein, contributes to repression of *nanos* mRNA translation in vitro. Rna *5*, 1535-47.

Smibert, C. A., Wilson, J. E., Kerr, K., and Macdonald, P. M. (1996). smaug protein represses translation of unlocalized *nanos* mRNA in the *Drosophila* embryo. Genes Dev *10*, 2600-9.

Spradling, A. C. (1993). Developmental genetics of oogenesis. In The development of *Drosophila melanogaster*, M. Bate and A. M. Martinez Arias, eds. (New York: Cold Spring Harbour Laboratory Press), pp. 1-70.

Spradling, A. C., de Cuevas, M., Drummond-Barbosa, D., Keyes, L., Lilly, M., Pepling, M., and Xie, T. (1997). The *Drosophila* germarium: stem cells, germ line cysts, and oocytes. Cold Spring Harbor Symp. Quant. Biol. *62*, 25-34.

St Johnston, D. (1995). The intracellular localization of messenger RNAs. Cell *81*, 161-170.

St Johnston, D., Beuchle, D., and Nüsslein-Volhard, C. (1991). *staufen*, a gene required to localize maternal RNAs in the *Drosophila* egg. Cell *66*, 51-63.

St Johnston, D., Driever, W., Berleth, T., Richstein, S., and Nüsslein-Volhard, C. (1989). Multiple steps in the localization of bicoid RNA to the anterior pole of the *Drosophila* oocyte. Development *107*, 13-19.

St Johnston, R. D., and Nüsslein-Volhard, C. (1992). The origin of pattern and polarity in the *Drosophila* embryo. Cell *68*, 201-219.

Stephenson, E. C., Chao, Y.C., Fackelthal, J.D. (1988). Molecular analysis of the *swallow* gene of *Drosophila* melanogaster. Genes Dev. *2*, 1655-1665.

Styhler, S., Nakamura, A., Swan, A., Suter, B., and Lasko, P. (1998). vasa is required for Gurken accumulation in the oocyte, and is involved in oocyte differentiation and germline cyst development. Development *125*, 1569-78.

Sundell, C. L., and Singer, R. H. (1990). *Actin* mRNA localizes in the absence of protein synthesis. Journal Of Cell Biology *111*, 2397-2403.

Suzuki, T. (1970). Temperature-Sensitive mutations in *Drosophila* melanogaster. Science *170*, 695-706.

Swalla, B. J., and Jeffery, W. R. (1996). Localization of ribosomal protein L5 mRNA in myoplasm during ascidian development. Dev. Genet. *19*, 258-67.

Takizawa, P. A., Sil, A., Swedlow, J. R., Herskowitz, I., and Vale, R. D. (1997). Actin-dependent localization of an RNA encoding a cell-fate determinant in yeast. Nature *389*, 90-3.

Takizawa, P. A., and Vale, R. D. (2000). The myosin motor, Myo4p, binds *Ash1* mRNA via the adapter protein, She3p. Proc Natl Acad Sci U S A *97*, 5273-8.

Tekotte, H., and Davis, I. (2002). Intracellular mRNA localization: motors move messages. Trends Genet *18*, 636-42.

Theurkauf, W. E. (1994). Microtubules and cytoplasm organization during *Drosophila* oogenesis. Developmental Biology *165*, 352-360.

Theurkauf, W. E., Alberts, B. M., Jan, Y. N., and Jongens, T. A. (1993). A central role for microtubules in the differentiation of *Drosophila* oocytes. Development *118*, 1169-1180.

Theurkauf, W. E., and Hazelrigg, T. I. (1998). In vivo analyses of cytoplasmic transport and cytoskeletal organization during *Drosophila* oogenesis: Characterization of a multi-step anterior localization pathway. Development *125*, 3655-66.

Theurkauf, W. E., Jingens, T., Jongsen, Y. N., and Alberts, B. M. (1993). A central role for microtubules in *Drosophila* oocyte differentiation. Molecular Biology Cell *4*, 5a.

Theurkauf, W. E., Smiley, S., Wong, M. L., and Alberts, B. M. (1992). Reorganization of the cytoskeleton during *Drosophila* oogenesis - implications for axis specification and intercellular transport. Development *115*, 923-936.

Thio, G. L., Ray, R. P., Barcelo, G., and Schüpbach, T. (2000). Localization of *gurken* RNA in *Drosophila* oogenesis requires elements in the 5' and 3' regions of the transcript. Developmental Biology *221*, 435-446.

Thomsen, G. H., and Melton, D. A. (1993). Processed Vg1 protein is an axial mesoderm inducer in *Xenopus*. Cell *74*, 433-41.

Tinker, R., Silver, D., and Montell, D. J. (1998). Requirement for the vasa RNA helicase in *gurken* mRNA localization. Developmental Biology *199*, 1-10.

Tomancak, P., Guichet, A., Zavorszky, P., and Ephrussi, A. (1998). Oocyte polarity depends on regulation of gurken by Vasa. Development *125*, 1723-32.

Torres IL, L.-S. H., St Johnston D. (2003). A Notch/Delta-dependent relay mechanism establishes anterior-posterior polarity in *Drosophila*. Developmental Cell *5*, 547-558.

Turunen, O., Sainio, M., Jaaskelainen, J., Carpen, O., and Vaheri, A. (1998). Structure-function relationships in the ezrin family and the effect of tumor-associated point mutations in neurofibromatosis 2 protein. Biochem Biophys Acta *1387*, 1-16.

van Eeden, F., and St Johnston, D. (1999). The polarisation of the anterior-posterior and dorsal-ventral axes during *Drosophila* oogenesis.
Current Opinion in Genetics and Development *9*, 396-404.

van Eeden, F. J., Palacios, I. M., Petronczki, M., Weston, M. J., and St Johnston, D. (2001). Barentsz is essential for the posterior localization of oskar mRNA and colocalizes with it to the posterior pole. Journal of Cell Biology *154*, 511-23.

Vaughan, T. J., James, P. S., Pascall, J. C., and Brown, K. D. (1992). Expression of the genes for TGF alpha, EGF and the EGF receptor during early pig development. Development *116*, 663-9.

Waterman-Storer, C. M., Karki, S. B., Kuznetsov, S. A., Tabb, J. S., Weiss, D. G., Langford, G. M., and Holzbaur, E. L. (1997). The interaction between cytoplasmic dynein and dynactin is required for fast axonal transport. Proc Natl Acad Sci U S A *94*, 12180-5.

Webster, P. J., Liang, L., Berg, C. A., Lasko, P., and Macdonald, P. M. (1997). Translational repressor Bruno plays multiple roles in development and is widely conserved. Genes & Development *11*, 2510-21.

Wieschaus, E. (1978). The uses of mosaics to study oogenesis in *Drosophila melanogaster*. In Subtelny, Sussex, 1978, pp. 23-43.

Wieschaus, E., Marsh, J. L., and Gehring, W. J. (1978). *fs(1)K10*, a germline-dependent female sterile mutation causing abnormal chorion morphology in *Drosophila* melanogaster. Roux Arch. dev. Biol. *184*, 75-82.

Wilhelm, J. E., Mansfield, J., Hom-Booher, N., Wang, S., Turck, C. W., Hazelrigg, T., and Vale, R. D. (2000). Isolation of a ribonucleoprotein complex involved in mRNA localization in *Drosophila* oocytes. Journal of Cell Biology *148*, 427-40.

Wilkie, G. S., and Davis, I. (2001). *Drosophila wingless* and pair-rule transcripts localize apically by dynein-mediated transport of RNA particles. Cell *105*, 209-19.

Yisraeli, J. K., Sokol, S., and Melton, D. A. (1990). A two-step model for the localization of maternal mRNA in *Xenopus* oocytes: involvement of microtubules and microfilaments in the translocation and anchoring of Vg1 mRNA. Development *108*, 289-98.

Yoon, C., Kawakami, K., and Hopkins, N. (1997). Zebrafish *vasa* homologue RNA is localized to the cleavage planes of 2-and 4-cell-stage embryos and is expressed in the primordial germ cells. Development *124*, 3157-65.

Yoshida, S., Marikawa, Y., and Satoh, N. (1996). *posterior end mark*, a novel maternal gene encoding a localized factor in the ascidian embryo. Development *122*, 2005-12.

Yue, L., and Spradling, A. (1992). *hu-li tai shao (hts):* a gene required for ring canal formation during *Drosophila* encodes a hololog of adducin.
In A. Conf. Dros. Res. 33, pp. 10.

Zhou, Y., and King, M. L. (1996). Localization of *Xcat-2* RNA, a putative germ plasm component, to the mitochondrial cloud In *Xenopus* stage-I oocytes.

Development *122*, 2947-2953.

10

APPENDIX

A: *Drosophila* Flystocks

The flystocks used in this thesis are listed below. The wildtype strain used was *Oregon-R (OrR)* or yw^{67g}, unless otherwise stated. The genetic markers and balancer chromosomes are described in Lindsley and Zimm, 1992.

Oregon R	Umea Drosophila stock centre, U-#W0670
yw^{67g}	(Helen Francis-Lang and William Sullivan)
Mer^{1}/*FM7c*	Richard Fehon
Mer^{2}/*FM7c*	Richard Fehon
Mer^{3}/*FM7c*	Richard Fehon
Mer^{4}/*FM7c*	Richard Fehon
UAS Mer^{+} *5.5/TM3 Sb*	Richard Fehon
w; (Pw^{+}, *HS mer GFPRS*)	Richard Fehon
P(cos mer^{+}*)/TM3 Sb*	Richard Fehon
Mer^{ts1}*/FM7c kept at 29°C*	Richard Fehon
Mer^{ts1}/ Mer^{ts1} kept at 21°C	Richard Fehon
yw; nlsGFPM;nlsGFPN	Davis et al., 1995
Sqd^{1}*/Df(3)urd*	David Ish-Horowicz
$Dhc64C^{6-6}$	Gepner et al., 1996
$Dhc64C^{6-8}$	Gepner et al., 1996
$Dhc64C^{8-1}$	Gepner et al., 1996
$Dhc64C^{6-10}$	Gepner et al., 1996
$Dhc64C^{6-12}$	Gepner et al., 1996

B: Primers used for sequencing of *Mer*^{ts1}

All primers listed are shown 3' to 5'.

M1 CGAATTGCGATTCGCGG

M2 CTGTTCGACCTGGTGTG

M3 GGCCAACGATGCACTTC

M4 TACAGCAGCGGCTTGAG

M5 CTACGGTTAAGGCACTC

M6 GAATTCGAGCAGGCGAG

M7 GCGTTAGCTTATCGCGC

M8 GTGTCGACGTACTGCAG

M9 CGAACGCATT CAACATCTGG GC

C: Movielegends

The supplementary time lapse movies are recorded on a CD placed inside the back cover of the thesis, and can be viewed using Quicktime Player or equivalent software.

Movie1. Showing a stage 9 egg chamber expressing nlsGFP (green) and injected with *grk* RNA (red) into the oocyte centre and imaged using timelapse cinematography. The images were recorded at 1 minute intervals for a total of one hour.

Movie 2. Showing a stage 9 egg chamber from a homozygous Mer^{ts1} female kept at the restrictive temperature. The egg chamber is expressing TauGFP (green), which associates with the microtubules in oocyte and nurse cells. *grk* RNA (red) was injected centrally into the oocyte and imaged over 1 hour in intervals of two minutes. Note: The oocyte nucleus is misplaced at the posterior of the oocyte.

Movie3. Trail of injected *grk* RNA moving to the anterior. 300 images were captured at intervals of one second and each frame was overlayed with the next to visualise the trail of each particle visibly over time. Note: The anterior cortex is on the left of the picture (see also Figure 5-2).

Movie 4. Trail of injected *grk* RNA in particles moving to the anterior and then dorsolaterally. Images were taken at ten second intervals and each frame was overlayed to illustrate the directionality of particle movement. Note: The oocyte nucleus is at the top of the image window (see also Figure 5-2).

Movie 5. Showing injection into the nurse cells of a stage 9 nlsGFP (green) expressing egg chamber. *grk* RNA (red) can be seen moving into the oocyte where it forms a cap at the dorsoanterior.

Movie 6. Showing injection of *grk* RNA (red) into the nurse cells of a stage 7 egg chamber expressing nlsGFP (green). *grk* RNA moves into the oocyte and localises to the posterior of the oocyte nucleus. Note: At this stage, prior to migration to the dorsoanterior, the oocyte nucleus can be seen posteriorly in the oocyte.

Movie 7. High magnification injection of *grk* RNA into the nurse cell adjacent to the oocyte. Some particles can be seen moving straight towards the oocyte, many of them appearing to use the same trail.

D: Publications

Nina Ehrenberg, Diploma thesis, December 1998: on CD, which also contains the Quicktime movies, placed inside the back cover of the thesis

MacDougall et al., 2001 Merlin, the Drosophila homologue of Neurofibromatosis 2 is specifically required in the posterior follicle for axis formation in the oocyte Development Vol 128 (5) p 665-673

MacDougall et al., 2003 *Drosophila gurken* (TGFalpha) mRNA Localizes as Particles that Move within the Oocyte in Two Dynein-Dependent Steps Dev Cell Vol4(3) p 307-319

Development

Volume 128 (4) February 2001

biology
www.biologists.com

INFORMATION ABOUT THE JOURNAL

The aim of **Development** is to act as a forum for all research that offers a genuine insight into mechanisms of development. *Manuscripts will be considered primarily with respect to this aim.*
Studies on both plant and animal development are welcome and can be focused upon any aspect of the developmental process, at all levels of biological organization from the molecular and cellular to the tissue levels.

DEVELOPMENT (ISSN 0950-1991) is a continuation of *Journal of Embryology and Experimental Morphology* (ISSN 0022-0752)

What Development offers

- Wide international circulation
- Fast publication – average 7 weeks from acceptance
- Fast editorial processing
- No page charges
- 50 free reprints
- Free colour reproduction (at the editor's discretion)
- With the cooperation of the author, **Development** can also offer very rapid publication provided that the author does not require to see proofs.

Development on-line offers

- Free access to Contents and Abstracts up to 5 weeks ahead of hard copy publication
- Free full-text searching across all three Company journals
- Free access to citation and reference lists - all Medline/PubMed linked
- Full text and high resolution images in Adobe Acrobat PDF back to 1994, available to subscribers

Visit our Website (www.biologists.com) to see what **Development on-line** has to offer and for details of on-line subscriptions.

Subscriptions

Published by The Company of Biologists Limited, Bidder Building, 140 Cowley Road, Cambridge CB4 0DL, UK, and distributed by Mercury Airfreight International Ltd, 2323 Randolph Avenue, Avenel, New Jersey 07001, USA.

One volume (128) of 24 issues (twice monthly) will be published in 2001. The subscription price includes air-speeded delivery to most countries.

USA, Canada and Mexico

Institutional: Paper only US$2250. On-line only US$2035. Combined US$2585.
Individual: Paper only US$430. On-line only US$125. Combined US$465.

(Periodicals postage paid at Rahway, N.J.)

UK and Rest of the World

Institutional: Paper only £1334. On-line only £1210. Combined £1535.
Individual: Paper only £256. On-line only £74. Combined £277.

Individual rates apply only when payment is made by personal cheque or credit card and is sent direct to the Company.

Orders must be accompanied by payment or credit card authorization with details, payable to The Company of Biologists Limited, and sent to the address above. Please contact the above address for reduced prices for society members.

Address changes

SUBSCRIBERS send changes to: Subscription Dept, The Company of Biologists Limited, 140 Cowley Rd, Cambridge CB4 0DL, UK.
POSTMASTER send address corrections to: Development, c/o Mercury Airfreight International Ltd, 2323 Randolph Avenue, Avenel, New Jersey 07001, USA.

Copyright and reproduction

Disclaimer to authors and readers

Responsibility for:

- the accuracy of statements of fact;
- the authenticity of scientific findings or observations;
- expressions of scientific or other opinion;
- any other material published in this Journal

rests solely with the author(s) of the article in which such statements etc appear, and that no responsibility for such matters is assumed by the Journal, its owners, publishers or staff (including referees).

Experimental animals

Care and use of experimental animals must comply with all relevant local animal welfare laws, guidelines and policies, and a statement of such compliance should be provided to the Journal editor.

Research materials

A condition of publication of a paper in this Journal is that authors will make available all propagatable research materials (including monoclonal antibodies, DNA probes and constructs, and genetic strains of all organisms) and, where possible, non-propagatable materials (for example, serum antibodies) to other scientists for bona fide research purposes.

Electronic manipulation of images

If a figure has been subjected to significant electronic manipulation, the specific nature of the enhancements must be noted in the legend or in the Materials and Methods.

Cover picture

Merlin mutant ovariole from a *Drosophila melanogaster* ovary, showing β-spectrin heavy chain staining at the apical surface of cells in red (antibody from Graham Thomas) and DNA (DAPI staining) in cyan. Fluorescence images of stage 7 and 8 egg chambers are superimposed onto a DIC image of the same ovariole. Merlin is required only in the posterior follicle cells to initiate axis formation in the oocyte and to maintain posterior follicle cell morphology. For further details see article by N. MacDougall, Y. Lad, G. Wilkie, H. Francis-Lang, W. Sullivan and I. Davis in *Development* **128(6)**, 665-673.

Development 128, 665-673 (2001)
Printed in Great Britain © The Company of Biologists Limited 2001
DEV7846

Merlin, the *Drosophila* homologue of neurofibromatosis-2, is specifically required in posterior follicle cells for axis formation in the oocyte

Nina MacDougall[1], Yatish Lad[1,*], Gavin S. Wilkie[1], Helen Francis-Lang[2,‡], William Sullivan[2] and Ilan Davis[1,§]

[1]Wellcome Centre for Cell Biology, ICMB, King's Buildings, University of Edinburgh, Edinburgh EH9 3JR, UK
[2]Department of Molecular, Cell and Developmental Biology, 322 Sinsheimer Labs, University of California, Santa Cruz 95064, USA.
*Present address: Centre for Inflammation Research, Medical School, University of Edinburgh, Teviot Place, Edinburgh EH8 9AG, UK
‡Present address: Exelixis, 170 Harbor Avenue, PO Box 511, S. San Francisco, CA 94083-0511, USA
§Author for correspondence (e-mail: ilan.davis@ed.ac.uk)

Accepted 21 December 2000; published on WWW 7 February 2001

SUMMARY

In *Drosophila*, the formation of the embryonic axes is initiated by Gurken, a transforming growth factor α signal from the oocyte to the posterior follicle cells, and an unknown polarising signal back to the oocyte. We report that *Drosophila* Merlin is specifically required only within the posterior follicle cells to initiate axis formation. *Merlin* mutants show defects in nuclear migration and mRNA localisation in the oocyte. Merlin is not required to specify posterior follicle cell identity in response to the Gurken signal from the oocyte, but is required for the unknown polarising signal back to the oocyte. Merlin is also required non-autonomously, only in follicle cells that have received the Gurken signal, to maintain cell polarity and limit proliferation, but is not required in embryos and larvae. These results are consistent with the fact that human Merlin is encoded by the gene for the tumour suppressor neurofibromatosis-2 and is a member of the Ezrin-Radixin-Moesin family of proteins that link actin to transmembrane proteins. We propose that Merlin acts in response to the Gurken signal by apically targeting the signal that initiates axis specification in the oocyte.

Key words: *Drosophila* oogenesis, *Merlin*, *gurken*, *bicoid*, *oskar*, TGFα, mRNA localisation, Oocyte microtubules, Embryonic axis formation, Tumour suppressor, ERM, Cell signalling

INTRODUCTION

The embryonic axes of *Drosophila* are established during oogenesis through the localisation of specific mRNAs to different regions of the oocyte cytoplasm. This process is initiated through bi-directional signalling between the oocyte and the overlying follicle cells (Schüpbach, 1987). While the localised mRNAs and some of the signalling components have been studied in detail, many of the genes involved in these processes are still unknown (Nilson and Schüpbach, 1999; van Eeden and St Johnston, 1999).

grk mRNA is localised in early oocytes in a posterior crescent between the nucleus and the follicle cells (Neuman-Silberberg and Schüpbach, 1993), thus targeting the Grk transforming growth factor α (TGFα) signal only to the adjacent follicle cells. The Grk signal is probably the ligand for Torpedo/DER, an epidermal growth factor receptor (EGFR) (Gonzalez-Reyes et al., 1995; Neuman-Silberberg and Schüpbach, 1993). Grk instructs 200 terminal follicle cells to adopt posterior instead of default anterior fates (Gonzalez-Reyes and St Johnston, 1998). Posterior, anterior and main body follicle cells originate from the same group of cells that divides five or six times before stage 6 and has equivalent columnar epithelial morphology up to stage 9 (Gonzalez-Reyes and St Johnston, 1998). However, anterior and posterior follicle cells express distinct cell fate markers (Deng and Bownes, 1998; Fasano and Kerridge, 1988; Micklem et al., 1997).

Once the Grk signal is received, an unknown signal is sent from the posterior follicle cells back to the oocyte, repolarising the oocyte microtubules (MTs). MT organisation and polarity have been visualised in fixed material with anti-Tubulin antibodies (Theurkauf et al., 1992) and β-galactosidase (βgal) fusions to MT-dependent motor domains (Clark et al., 1994; Clark et al., 1997) as well as a TauGFP fusion in living oocytes (Micklem et al., 1997). Before stage 7, a microtubule organising centre (MTOC) is located at the posterior of the oocyte, where the minus ends of MTs are localised. At stage 7, the posterior MTOC disassembles, a diffuse anterior MTOC forms and plus ends of MTs are found at the posterior. The polarity of MTs determines the site of localisation of different mRNAs in the oocyte. *bicoid* (*bcd*) mRNA is localised to the anterior of the oocyte, leading to a morphogenetic gradient of Bcd protein in the embryo (Driever and Nüsslein-Volhard, 1988). *osk* mRNA is localised at the posterior of the oocyte and embryo and specifies the future germ cells (Ephrussi et al., 1991).

The Grk signal also initiates formation of the dorsoventral (DV) axis when the oocyte nucleus moves from the posterior to the dorsoanterior corner. *grk* transcripts then become tightly

localised near the nucleus, so that Grk signalling instructs only the overlying follicle cells to adopt dorsal fates (Nilson and Schüpbach, 1999; van Eeden and St Johnston, 1999). The specification of appropriate populations of follicle cells along the DV axis leads to the secretion of egg shell structures such as the dorsal appendages. Later in development the embryonic DV axis is formed by signalling from ventral follicle cells, which leads to the formation of a graded nuclear-cytoplasmic distribution of Dorsal protein (Anderson, 1998).

Although the posterior polarising signal remains unidentified, a number of known genes are required for the process. Protein kinase A (PKA) is likely to be part of the machinery that receives the signal in the oocyte (Lane and Kalderon, 1994; Perrimon, 1994) but is not specific to this process. Mago nashi (Mago) is required for oocyte repolarisation and has an independent function in *osk* mRNA localisation. However, Mago is a novel nuclear protein that is ubiquitous in the egg chamber, and its role in signalling is unknown (Micklem et al., 1997; Newmark et al., 1997). Notch-Delta signalling is required among the posterior follicle cells to limit the number of polar posterior follicle cells that express Fasciclin III; it is also required earlier in oogenesis (Larkin et al., 1996). Notch is required for the specification of posterior follicle cell identity (Gonzalez-Reyes and St Johnston, 1998), and is therefore required indirectly for the generation of the polarising signal to the oocyte (Ruohola et al., 1991), rather than being directly involved in the signal itself. Two other neurogenic proteins, Brainiac (Brn) and Egghead (Egh) are required in the oocyte for follicle cell integrity, and it has been suggested that both proteins may interact with Notch and EGF-signalling (Goode et al., 1996a; Goode et al., 1996b). However, it is not known whether they are required for the polarising signal. Laminin A is a component of the extracellular matrix that is expressed and required in the posterior follicle cells for the polarising signal (Deng and Ruohola-Baker, 2000). A better understanding of the events associated with the polarising signal awaits the identification of the signal itself.

Here, we identify a new allele of *Mer* by screening a collection of temperature sensitive (ts) lethal alleles for defects in *grk* mRNA localisation and we show that Merlin functions in axis specification during oogenesis. *Drosophila Mer* was previously cloned by degenerate PCR (McCartney and Fehon, 1996) and mutations isolated by reverse genetic methods (Fehon et al., 1997). The human homologue is a tumour suppressor called neurofibromatosis-2 (NF2), which encodes Merlin (Moesin Ezrin Radixin Related Protein) (McCartney and Fehon, 1996). Merlin and Ezrin-Radixin-Moesin (ERM) proteins are members of the 4.1 family of proteins thought to link actin to transmembrane proteins (Mangeat et al., 1999; Tsukita et al., 1994) and *Drosophila* Merlin is apically localised in follicle cells (McCartney and Fehon, 1996). We show that Merlin is required only within the posterior follicle cells for mRNA localisation and axis specification in the oocyte. Merlin functions downstream of the Grk signal from the oocyte, but is only required if the posterior follicle cells receive the Grk signal. Merlin has no role in Notch-Delta signalling between the follicle cells, but is required upstream of the unknown polarising signal back to the oocyte. Merlin is also required non-autonomously in posterior follicle cells to limit their proliferation and maintain their polarity. We propose that Merlin functions by apically targeting the unknown polarising signal that initiates axis specification.

MATERIALS AND METHODS

Fly stocks

The collection of ts lethals was generated by EMS mutagenesis and subsequent selecting for male lethality at 29°C and viability at 21° (H. F.-L. and W. S., unpublished observations). $Merlin^{ts1}$ (Mer^{ts1}) stocks (yw^{67g},Mer^{ts1}) were maintained at 18°C or 21°C, and mutant phenotypes analysed by shifting newly eclosed adult flies to 29°C on fresh food. For analysis of follicle cell and MT markers, Mer^{ts1} females were crossed to males from the following stocks: posterior follicle cell marker (*yw; 998/12/TM6b*: P. Deak, M. Bownes and D. Glover), border cell markers (*yw; 459/2/TM6b*: P. Deak, M. Bownes and D. Glover), anterior follicle cell marker (*L53b*: S. Kerridge), polar follicle cell *marker (w; P(w+)8523/CyO*: M. Heck, A. Spradling) and MT markers (*yw;Nod-lacZ* and *yw;Kin-lacZ, Tau-GFP*: D. St Johnston). The F_1 male progeny were then back crossed to Mer^{ts1} females.

Generation and detection of FRT/FLP follicle cell clones

Clones were induced by mitotic recombination at high frequency only in follicle cells using *en-Gal4,UAS-FLP* (Duffy et al., 1998) at 29°C in Mer^3,*FRT/nlsGFP,FRT* (Davis et al., 1995) (FRT19A from S. Luschnig). Mer^3 Clones were identified by the lack of nlsGFP expression.

X-ray-induced germline clones

To create homozygous Mer^{ts1} germline clones, $ovoD^1$ males were mated to homozygous yw^{67g},Mer^{ts1} females for two days and transferred to fresh food for 8 hours. The larvae (40-48 hours old) were exposed to 1000 rads of X-rays and allowed to recover at 21°C. 1000 surviving F1 females were crossed to yw^{67g} males in single pair matings, shifted to 29°C for three days, and their ovaries dissected, fixed and stored in methanol at –20°C. 10 females (1%) containing Mer^{ts1} germline clones were identified by the lack of male progeny, and their ovaries studied. 50 (5%) females with wild-type recombinant chromosomes were identified by the presence of male progeny and discarded.

In situ hybridisation

Ovaries were dissected and fixed in 3.7% formaldehyde in PBS with 0.1% Tween20 (PBT) and in situ hybridisation carried out using standard methods (Tautz and Pfeifle, 1989) with our previously described modifications (Wilkie and Davis, 1998; Wilkie et al., 1999). Mounting and imaging were performed as previously described (Davis, 2000).

X-Gal staining

For X-gal staining of the enhancer trap and other transgenic lines expressing βgal fusion proteins, ovaries were dissected and fixed in 0.05% glutaraldehyde in PBT for 15 minutes, and stained for 2 hours to overnight at 37°C using standard methodology.

Protein localisation

Actin

Ovaries were dissected and fixed without methanol and incubated in a 1:40 dilution of Texas-red-phalloidin (Molecular probes) in PBS overnight at 4°C and washed with PBT.

Centrosomes and spectrin

Ovaries were blocked in 2% BSA in PBS with 0.1% TritonX-100 (PBTX) for 2 hours at room temperature, washed several times in PBT and incubated with anti γ-tubulin monoclonal antibody (1:10,000

Sigma) or anti β_H-spectrin (1:200) in PBTX with 2% BSA overnight at 4°C, followed by AlexaFluor594- and AlexaFluor488-coupled secondary antibodies, respectively (Molecular Probes).

RESULTS

Identification of a temperature-sensitive mutation that disrupts mRNA localisation and oocyte nuclear migration

To identify new genes required for axis specification, we screened a collection of X-linked ts lethal mutations generated by selecting for male lethality at 29°C and viability at 21°C. We collected homozygous female progeny at 21°C from 73 viable ts lethal lines, shifted to 29°C for 3 days and performed *grk* RNA in situ hybridisation on ovaries. In wild type or yw^{67g} controls at 29°C or in all strains at 21°C, the oocyte nucleus migrates correctly to the antero-dorsal corner of the oocyte with *grk* mRNA localising between the nucleus and the overlying future dorsal follicle cells (Fig. 1A). In one line, yw^{67g},*l(1)ts594* {*l(1)ts594*}, 55% (n=89) of oocyte nuclei fail to migrate and *grk* mRNA localises at the posterior after stage 8 (Fig. 1B). The remaining 45% of cases were similar to wild type, *l(1)ts594* at 21°C (Fig. 1A) and the same genetic background yw^{67g} (*yw*) chromosome at 29°C. In all subsequent

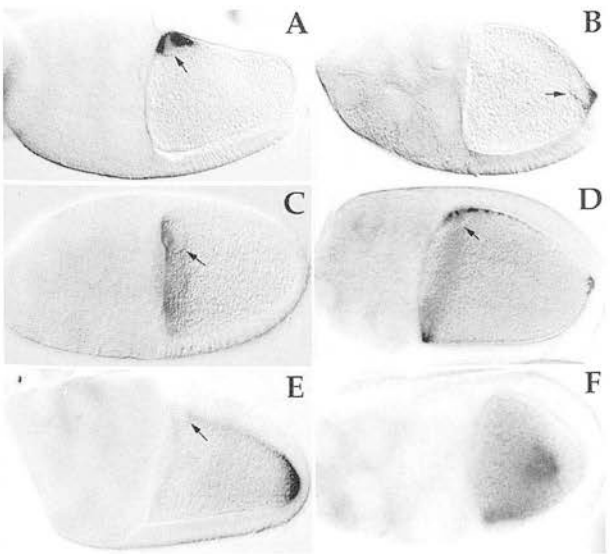

Fig. 1. Mutations in *Mer* disrupt mRNA localisation and nuclear migration in the oocyte. (A) Control showing the oocyte nucleus and *grk* mRNA at the dorso-anterior corner of the oocyte. (B) *Mer* mutant showing *grk* mRNA at the posterior near the oocyte nucleus (55% of cases). The other 45% of cases are the same as the control (not shown). (C) Control showing normal *bcd* mRNA localisation in an anterior ring. (D) *Mer* mutant showing some *bcd* mRNA abnormally localised at the posterior (83% of cases). (E) Control showing normal *osk* mRNA localisation at the posterior. (F) *Mer* mutant showing *osk* mRNA diffusely localised at the centre of the oocyte (89% of cases). The oocyte nucleus is in a different focal plane. (A,C,E) stage 10 Mer^{ts1} mutant 21°C, similar to wild type and *yw* strains at 29°C (not shown). (B,D) stage 10 and (F) stage 9 Mer^{ts1} mutants at 29°C. In situ hybridisation to detect *grk* (A,B), *bcd* (C,D) and *osk* (E,F) mRNA. Arrows indicate the oocyte nucleus.

experiments, similar controls were carried out, showing that the phenotype was not due to the temperature shift itself or the genetic background.

We also performed in situ hybridisation on *l(1)ts594* ovaries to detect *bicoid* (*bcd*) and *oskar* (*osk*) mRNA. We found that in 83% (n=47) of stage 9 or 10A mutants at 29°C, *bcd* mRNA is localised at the posterior as well as its normal accumulation in an anterior ring (Fig. 1C,D). In 89% (n=32) of stage 9 and 10A mutants, *osk* mRNA is mislocalised at the centre of the oocyte (Fig. 1F) instead of its normal posterior localisation (Fig. 1E).

To test whether the defects in the oocyte are primarily due to a defect in MT organisation, we examined MT polarity. We used Kin:βgal, a plus end-directed MT motor fusion that leads to βgal accumulation at the posterior of the oocyte (Clark et al., 1994). We also used Nod:βgal, a MT motor fusion that leads to βgal accumulation at the anterior, where the minus ends of MTs are thought to localise (Clark et al., 1997). The βgal motor fusions indicate that prior to stage 7, there is an MTOC at the posterior (data not shown). In wild-type oocytes after stage 7, the posterior MTOC disassembles, a diffuse MTOC appears at the anterior (Fig. 2A) with MT plus ends at the posterior (Fig. 2C). Prior to stage 7, *l(1)ts594* mutant oocytes show a similar MT organization to wild type (data not shown), but after stage 7, the MTOC fails to disassemble at the posterior and a second diffuse MTOC forms at the anterior (Fig. 2B). This leads to a symmetric organization of MTs, with their plus ends at the centre of the oocyte (Fig. 2D) and minus ends at the anterior and posterior (Fig. 2B). We also examined the overall distribution of MTs using a maternally expressed TauGFP line showing the highest concentration of MTs at the anterior cortex of wild-type oocytes (Micklem et al., 1997). We observed a similar Tau-GFP distribution in *l(1)ts594* oocytes at 21°C (Fig. 2E). In *l(1)ts594* at 29°C Tau-GFP showed an abnormally high level at the posterior, consistent with a failure to disassemble the posterior MTOC (Fig. 2F). We conclude that the mislocalisation of mRNA and failure of the oocyte nucleus to relocate in *l(1)ts594* oocytes are due primarily to defects in MT organisation.

l(1)ts594 is a strong loss-of-function allele of *Mer*

In order to determine the gene mutated in *l(1)ts594*, we mapped the mutation. Complementation analysis against deficiencies showed that the mutation lies in one of two gaps in the available deficiencies on the X chromosome, 18A2-A5 or 18D1-18E1-2 and recombination mapping showed that the lethality and oocyte phenotype both map to 18D-18E. Complementation analysis with all the available alleles in the region showed that three lethal alleles of *Merlin* (Mer^1, Mer^2 *and* Mer^4) (LaJeunesse et al., 1998) failed to complement the lethality of *l(1)ts594* at 29°C. A fusion of the *Mer* full-length cDNA with GFP and a cosmid containing a genomic DNA fragment including *Mer* are both able to fully complement the lethality, oocyte nuclear migration defects and mRNA mislocalisation of *l(1)ts594* (data not shown), suggesting that *l(1)ts594* is a ts allele of *Mer*.

Mer is the closest *Drosophila* homologue of human Merlin, a member of the ERM/4.1 family encoded by the NF2 tumour suppressor (Mangeat et al., 1999). ERM proteins are thought to link actin with transmembrane proteins at the cell membrane (Turunen et al., 1998) and may play a role in signalling (Mangeat et al., 1999). We sequenced the entire coding regions

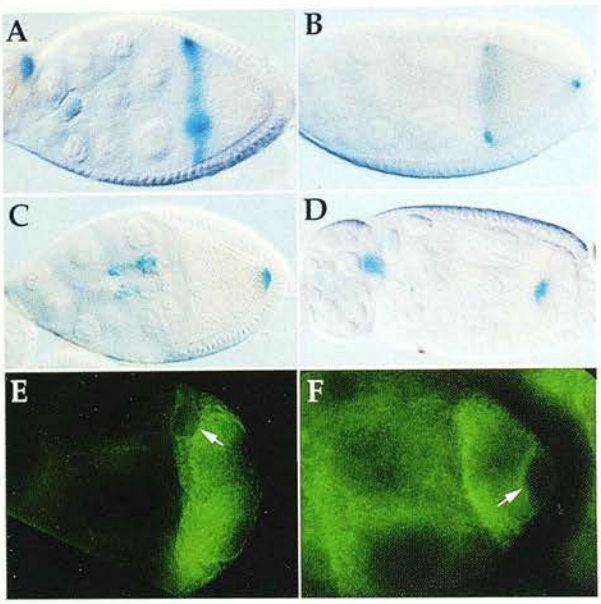

Fig. 2. Mutations in *Mer* disrupt microtubule (MT) organisation in the oocyte. (A,B) Minus ends of MTs visualised with Nod:βgal protein that marks the MT organising centre (MTOC). (A) Stage 9 control showing normal Nod:βgal localisation along the anterior cortex. (B) Stage 9 *Mer* mutant, showing Nod:βgal localisation at the posterior, owing to a failure of the posterior MTOC to disassemble. (C,D) Plus ends of MTs visualised with Kin:βgal expression. (C) Late stage 9 control showing Kin:βgal localised at the posterior of the oocyte. (D) Stage 9 *Mer* mutant showing abnormal Kin:βgal localisation in the centre of the oocyte. (E,F) MTs visualised in living egg chambers using Tau-GFP. Arrows indicate the nuclei. (E) Stage 9 control anterior-posterior gradient of MTs. (F) Stage 9 Mer^{ts1} mutant showing a symmetric array of MTs at the anterior and posterior cortex. (A,C,E) Mer^{ts1} 21°C. (B,D,F) Mer^{ts1} 29°C.

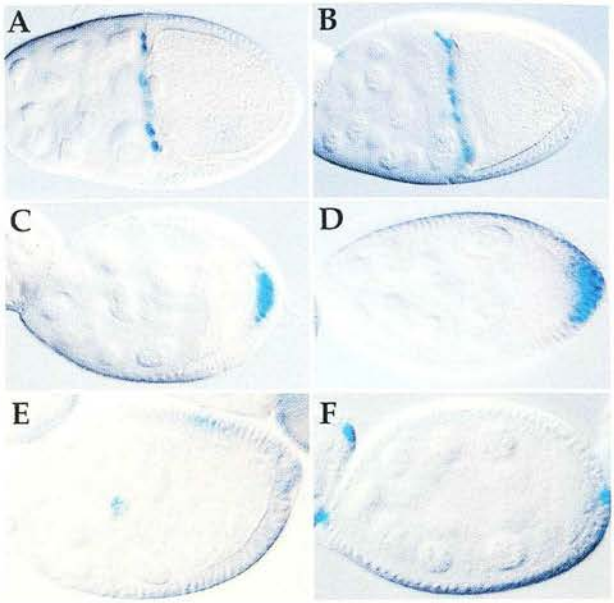

Fig. 3. Mutations in *Mer* do not disrupt follicle cell identity. (A-F) X-Gal staining of different *lacZ* lines crossed into control and Mer^{ts1} egg chambers. (A) Stage 10 control, expressing βgal protein in anterior follicle cells. (B) Mer^{ts1} egg chamber showing indistinguishable anterior follicle cells to A and no expression in posterior follicle cells. (C) Stage 9 control, expressing βgal in the posterior follicle cells. (D) Mer^{ts1} mutant showing normal posterior expression. Note the thicker layer of posterior follicle cells (also see Fig. 4) (E) Mer^{ts1} mutant showing normal expression of a border cell marker. (F) Mer^{ts1} mutant showing normal expression of polar posterior and polar anterior follicle cell marker.

of *Mer* in *l(1)ts594* and in the genetic background yw^{67g} chromosome. Two closely mapping non-conservative amino acid changes (F113L and I125F) were found in the conserved N-terminal domain involved in binding to transmembrane proteins (LaJeunesse et al., 1998). No modifications were detected in the C-terminal domain that has a putative regulatory role. We conclude that *l(1)ts594* is an allele of *Mer* and renamed it Mer^{ts1}.

To determine whether the phenotype we observed in Mer^{ts1} mutants was typical of existing loss-of-function *Mer* alleles, we studied the oogenesis phenotype of various other allelic combinations of *Mer*. We found similar defects in all the allelic combinations studied. Flies homozygous for Mer^{ts1}, and flies with Mer^{ts1} over a null allele (LaJeunesse et al., 1998) (Mer^{ts1}/Mer^{4}) showed almost identical phenotypes. Mer^{ts1} over a weak allele (Fehon et al., 1997) (Mer^{ts1}/Mer^{3}) showed a slightly reduced frequency of the oogenesis phenotype (data not shown). From these results, and the fact that a *Mer* transgene fully complements the Mer^{ts1} phenotype (data not shown), we conclude that Mer^{ts1} is a very strong loss-of-function allele, similar to a null.

Merlin is not required in the germline, or for Grk or Notch signalling

Merlin protein has previously been shown to be expressed in the oocyte and in posterior follicle cells (McCartney and Fehon, 1996), but its function was only studied later in development (LaJeunesse et al., 1998; McCartney et al., 2000). To determine where Merlin functions in egg chambers, we generated homozygous Mer^{ts1} germline clones using X-rays in females raised at the restrictive temperature (29°C). We analysed 10 Mer^{ts1} oocytes surrounded by $Mer^{ts1}/+$ follicle cells (see Materials and Methods), and they all showed normal mRNA localisation and lead to normal eggs (data not shown). We conclude that Merlin is not required in the germline derived nurse cells or oocyte.

To test whether Merlin is required within the somatically derived posterior follicle cells to receive the Grk signal from the oocyte, we studied the expression of different follicle cell markers in *Mer* egg chambers. The results show that Mer^{ts1} posterior follicle cells receive the Grk signal correctly, as they express posterior and not anterior markers (Fig. 3A-D). We conclude that Merlin is not required for any aspect of Grk signalling or its reception in the posterior follicle cells. Merlin is also not required for Notch signalling among the posterior follicle cells, which is required to specify the correct number of posterior cells (Gonzalez-Reyes and St Johnston, 1998).

We also tested whether Merlin is required for the formation or identity of other types of follicle cells by analysing markers for different follicle cell populations in Mer^{ts1}. These included a marker for border cells, stalk cells and polar follicle cells. Our results show that Merlin is not required for the correct

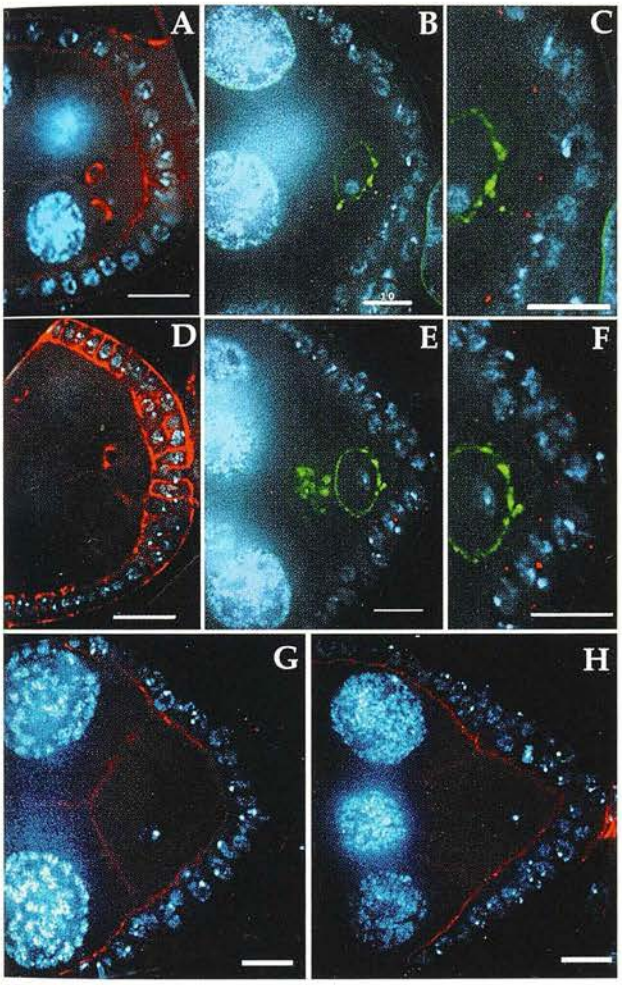

Fig. 4. *Mer* mutations disrupt posterior follicle cell organisation. (A,D) Follicle cell morphology visualised by phalloidin-rhodamine staining of actin (red) and DAPI staining of DNA (blue). (A) Control showing a columnar monolayer of follicle cells. (D) Mer^{ts1} mutant showing a double layer of follicle cells only at the posterior. (B,C,E,F) The polarity of follicle cells in control and Mer^{ts1} egg chambers showing centrosomes (γ-tubulin, red), the nuclear envelope (wheat germ agglutinin (WGA), green) and DNA (DAPI staining, blue). (B) Control showing that follicle cell centrosomes usually point to the apical surface, adjacent to the oocyte. (C) A higher magnification view of the posterior part of (B). (E) Mer^{ts1} egg chamber showing follicle cell centrosomes pointing both apically and basally. The oocyte nucleus has failed to migrate. WGA also stains the yolk particles, the boundary of the oocyte and outer edge of the follicle cells. (F) A higher magnification view of the posterior part of E. The centrosomes are not visible in some cells, as they are located in another focal plane. (G,H) Apical polarity visualised with anti-spectrin β heavy chain (β_H-spectrin) antibody (red) and DNA (blue). (G) Control showing apical localisation of β_H-spectrin in follicle cells. (H) Mer^{ts1} mutant showing normal apical β_H-spectrin in follicle cells adjacent to the oocyte, but no detectable β_H-spectrin in the outer layer of posterior follicle cells. Scale bars: 10 μm.

specification or development of any subgroup of follicle cells, and is not required for Notch signalling among the follicle cells, which limits the number of polar follicle cells to two (Fig. 3E,F). Merlin is therefore likely to be required for cell

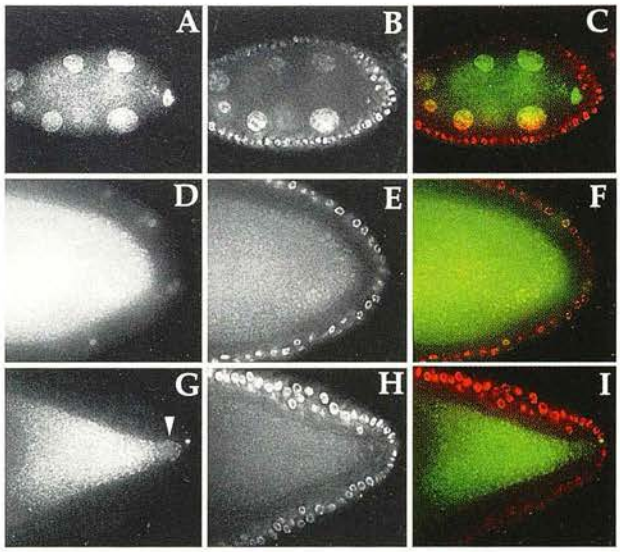

Fig. 5. Merlin is required non-autonomously in the posterior follicle cells to maintain their monolayer columnar morphology. (A-I) Examples of mosaic egg chambers with homozygous mutant *Mer* clones lacking nlsGFP expression. (A,D,G) nlsGFP expression (green in C,F,I). (B,E,H) DAPI staining showing all nuclei in the egg chambers (red in C,F,I). (A-C) Stage 8 in which all the follicle cells are Mer^3, but the germline is $Mer^3/+$, showing an identical phenotype to egg chambers from Mer^3 mothers. The nucleus has failed to migrate. (D-F) Stage 10 with four very small patches of $Mer^3/+$ follicle cells at the posterior in a homozygous Mer^3 mutant background. The few $Mer^3/+$ cells rescue the *Mer* mutant phenotype in all the neighbouring follicle cells and also rescue the nuclear migration phenotype. (G-I) Stage 10 with one $Mer^3/+$ follicle cell at the posterior in a Mer^3 mutant background. The single *Mer*/+ cell is able to rescue the mutant phenotype in the neighbouring follicle cells, but fails to rescue the nuclear migration phenotype. Arrowhead marks the oocyte nucleus.

communication between the follicle cells and oocyte, downstream of Grk and upstream of the unknown polarising signal from the posterior follicle cells to the oocyte.

Merlin acts as a tumour suppressor in posterior follicle cells and is required for their polarity

We observed that the posterior follicle cells in fixed (Figs 3D-F, 4D-F,H) and living (data not shown) *Mer* egg chambers often have a slightly disrupted morphology. To study these defects in more detail, we covisualised actin and DNA to highlight each cell and its boundaries (Fig. 4A,D). Posterior follicle cells in controls have a uniform columnar appearance characteristic of epithelial sheets (Fig. 4A). However, after stage 6, Mer^{ts1} egg chambers have a double layer of follicle cells only at the posterior where follicle cells are in contact with the oocyte (Fig. 4D). To determine whether the double layer of posterior follicle cells is due to overproliferation, we counted the number of cells using three-dimensional microscopy and found a twofold increase in the number of posterior follicle cells, but no changes in other follicle cells (data not shown).

To determine whether the overproliferation of posterior follicle cells is accompanied by polarity defects, we studied MT polarity by covisualising DNA, the nuclear envelope and centrosomes (Fig. 4B,C,E,F). In control egg chambers, most

centrosomes lie on the apical side of each nucleus, where the minus ends of MTs are found (Fig. 4B,C). In contrast, Mer^{ts1} posterior follicle cells mostly loose the apical-basal polarity of their MTs (Fig. 4E,F).

To investigate whether other aspects of the apical-basal polarity of the posterior follicle cells are also disrupted, we studied the distribution of β-spectrin heavy chain (β_H-spectrin) in *Mer* mutants (Fig. 4G,H). β_H-Spectrin is normally restricted to the apical side of follicle cells within a Spectrin-based membrane skeleton (Fig. 4G) (Zarnescu and Thomas, 1999). In Mer^{ts1} mutants β_H-spectrin is apically localised in the cells adjacent to the oocyte, but not detected in the second layer of follicle cells (Fig. 4H). These results suggest that in *Mer* mutants, the apical surface of posterior follicle cells contacts the oocyte correctly, and is probably competent to send and receive signals to the oocyte.

To determine whether the defects in cell proliferation and polarity in *Mer* egg chambers are dependent on receiving the Grk signal, we examined the follicle cells of *Mer, grk* double mutants. We found that even a hypomorphic allele of *grk* (grk^{2E12}) suppresses the *Mer* posterior follicle cell phenotype entirely (data not shown). We conclude that Merlin is required only in cells that receive the Grk signal and is not a constitutive factor required for cell polarity and proliferation.

Merlin is required non-autonomously in posterior follicle cells

To test directly whether Merlin is required only in posterior follicle cells, we used genetic mosaic analysis with the FRT/FLP system to make clones of homozygous *Mer* follicle cells located at posterior, anterior or central positions (Fig. 5A-I). We found that Merlin is required only in the posterior follicle cells for their correct morphology and migration of the oocyte nucleus. We produced *Mer* clones using Mer^3,FRT/*nlsGFP*,FRT; *en-Gal4,UASFLP* females. Mer^3 is a homozygous viable but sterile allele (Fehon et al., 1997) and *en-Gal4,UASFLP* expresses FLP recombinase at very high levels only in the follicle cells (Duffy et al., 1998). We examined a total of 43 egg chambers with Mer^3 clones, of which 29 were particularly revealing and analysed in detail. Of these, one egg chamber had follicle cells that were entirely Mer^3 (Fig. 5A-C), and three egg chambers had large mutant clones covering all the posterior (data not shown). These egg chambers showed a strong *Mer* phenotype indistinguishable from non-mosaic homozygous Mer^3 mutants. 21 egg chambers had large anterior or main body follicle cell clones without a *Mer* phenotype (data not shown). We conclude that Merlin is required only in posterior follicle cells.

To test whether Merlin is required cell autonomously to limit the proliferation and polarity of posterior follicle cells, we studied four egg chambers in which the follicle cells were Mer^3, except for one or more very small Mer^3/+ clones in the posterior follicle cells. Such egg chambers showed complete rescue of the Mer^3 phenotype when sufficient Mer^3/+ cells were present (Fig. 5D-F), indicating that Merlin acts cell non-autonomously among the posterior follicle cells. One of these clones had a single Mer^3/+ cell at the posterior tip surrounded by Mer^3 cells, showing that a single Mer^3/+ cell is able to rescue the overproliferation phenotype up to a distance of about six cell diameters (Fig. 5G-I). While the single Mer^3/+ cell was not able to rescue the oocyte nuclear migration defect, several small Mer^3/+ clones were sufficient to do so. We conclude that Merlin is required non-autonomously in the posterior follicle cells to limit their proliferation.

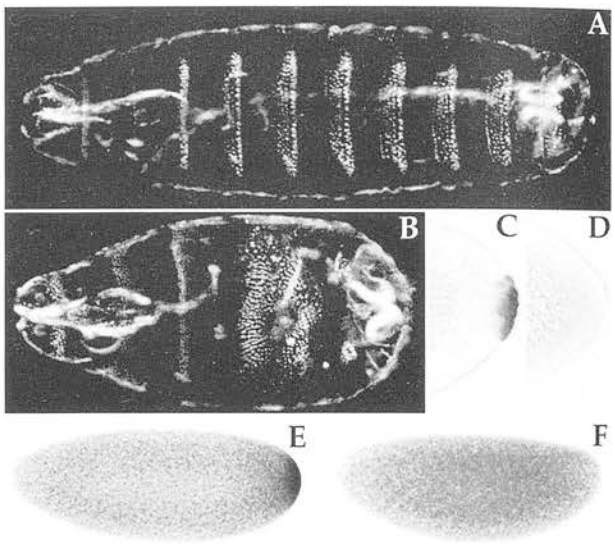

Fig. 6. *Mer* mutations disrupt *osk* mRNA localisation in some embryos, leading to abdominal defects and a lack of pole cells. (A,B) Cuticle preparations from Mer^{ts1} mutant eggs. (A) Normal cuticle of hatched eggs (79%). (B) Abdominal defects in unhatched eggs (21%). (C,D) Vasa antibody staining of pole cells in Mer^{ts1} embryos. (C) Normal numbers of pole cells (52% of cases). (D) Pole cells are absent (48% of cases). (E,F) *osk* mRNA localisation. (E) Control pre-blastoderm embryo showing normal posterior *osk* mRNA localisation. (F) Mer^{ts1} embryo showing unlocalised *osk* mRNA (50% of cases).

Merlin is not required during embryogenesis

To test whether Merlin is required for embryogenesis we analysed the hatch rate of eggs laid by Mer^{ts1} mothers. At 29°C, 74% of eggs (n=100) hatch and develop normally until third instar larvae, compared with a hatch rate of 94% for Mer^{ts1} at 21°C and yw^{67g} at 29°C (a difference of 21%). All the unhatched embryos have abdominal cuticle defects similar to *osk* alleles (Fig. 6B), while the eggs that hatch have normal cuticles (Fig. 6A). We found that *osk* mRNA is mislocalised in 51% of embryos (n=104) (Fig. 6F) and 48% of embryos (n=103) show missing pole cells (Fig. 6D), explaining why many of the resulting flies have few germ cells (data not shown). These results are consistent with the fact that *osk* alleles are known to disrupt pole cell formation more readily than abdominal patterning (Lehmann and Nüsslein-Volhard, 1986).

Initially, it was surprising that most *Mer* eggs hatch, since mislocalised *bcd* mRNA would be expected to disrupt AP axis specification and cause embryonic lethality. However, we found that *bcd* mRNA, which was mislocalised at the posterior, partially or completely relocalised in older egg chambers (Fig. 7A-D). Consequently, Mer^{ts1} embryos have completely normal *bcd* localisation (Fig. 7E,F). The near normal hatch rate of *Mer* eggs was also initially surprising because 55% (n=89) of *Mer* mutants have misplaced oocyte nuclei and mislocalised *grk* mRNA, which would lead to embryonic lethality. However, we

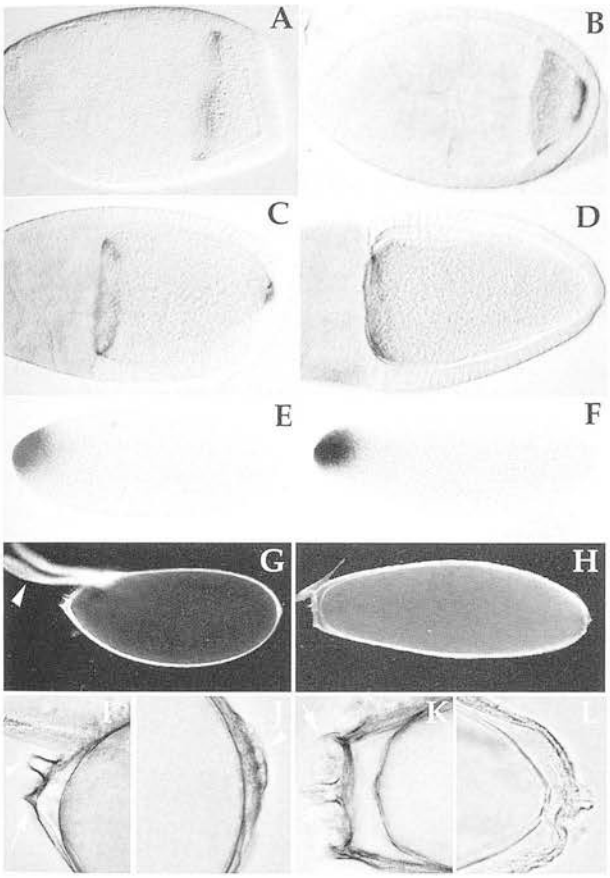

Fig. 7. Mutant *Mer* mothers lay eggs with normal *bcd* mRNA localisation, but some dorsoventral defects. (A-F) *bcd* mRNA in *Mer* and control egg chambers and embryos. (A) Stage 9 control showing normal *bcd* mRNA localisation in an anterior ring. (B) Stage 9 Mer^{ts1} mutant showing *bcd* mislocalisation at the posterior. (C) Stage 10B Mer^{ts1} mutant showing a reduced level of *bcd* mRNA at the posterior. (D) Stage 11 Mer^{ts1} mutant showing no *bcd* mRNA localisation at the posterior. (E) Control pre-blastoderm embryo showing *bcd* mRNA localisation at the anterior. (F) Pre-blastoderm Mer^{ts1} embryo showing indistinguishable anterior *bcd* mRNA localisation to controls. (G,I,J) Control Mer^{ts1} at 21°C showing the same structures as wild type eggs or *yw* eggs at 29°C (not shown). (G) Egg with dorsal appendages (arrowhead). (I) Higher power anterior view of dorsally positioned micropyle (arrowhead) and centrally placed operculum (arrow). (J) High power posterior view of dorsally placed aeropyle (arrowhead). (H,K,L) Egg from Mer^{ts1} female at 29°C. (H) Egg showing a lack of dorsal appendages and a torpedo-like shape (11% of cases). The other 89% are normal (not shown). Females retain many of the defective eggs (not shown). (K) High power anterior view showing a centrally located micropyle (arrowhead) and a symmetric ringed operculum (arrow). (L) High power posterior view showing an enlarged aeropyle.

found that only 11% (n=158) of eggs laid by Mer^{ts1} mothers have strong dorsoventral defects (Fig. 7H,K,L), and the other defective egg chambers degenerate in females after stage 10A (data not shown). It is likely that egg chambers with mislocalised *osk* mRNA also degenerate in the mothers, explaining why there is a lower percentage of *osk* mRNA localisation defects in embryos compared with oocytes.

We conclude that *Mer* eggs hatch at a slightly lower frequency than controls because of abdominal and dorsoventral defects that originate during oogenesis, rather than a direct requirement for Merlin in embryos. Therefore, Merlin is not required for embryogenesis and much of larval development.

DISCUSSION

We have shown that Merlin is required for the signal that initiates axis specification. Merlin is also required non-autonomously for signalling among the posterior follicle cells that limits their proliferation and maintains their polarity. Merlin is not required for other signals within the posterior follicle cells or in other parts of egg chambers and embryos.

Taking our data in the context of previous work, we propose that Merlin is involved in apical targeting of the unknown signal that initiates axis specification in the oocyte. Merlin is a member of the ERM/4.1 family of proteins and, in *Drosophila*, it is localised to the apical membrane of follicle cells and in the germline (McCartney and Fehon, 1996). ERM family members are thought to function as linkers between the cytoskeleton and the apical membrane, and they are probably required for apical targeting of signals, maintenance of epithelial adhesion, apical-basal polarity and to limit cell proliferation (Vaheri et al., 1997).

The overproliferation of the posterior follicle cells is consistent with overproliferation of mutant *Mer* cells seen in imaginal discs and with the function of human Merlin as a tumour suppressor causing neurofibromatosis-2. The changes in cell polarity we observe are also common in many other types of tumours. Interestingly, as in other *Drosophila* tissues (LaJeunesse et al., 1998), the *Mer* phenotypes we have studied are more similar in character to benign tumours seen in individuals with neurofibromatosis-2 than to the aggressive tumours produced in the mouse model (McClatchey et al., 1998). However, it is not known whether Merlin is required during mammalian oogenesis. We speculate that human Merlin may function in a similar non-autonomous manner in response to particular signals such as TGFα, which is known to be expressed in mammalian oocytes (Vaughan et al., 1992). Indeed, many parallels may exist between mammalian and fly oogenesis in respect of communication between the oocyte and follicle cells (Deng et al., 1997).

Is Merlin directly involved in signals that initiate axis specification?

We have shown that Merlin has a more specific and restricted function than previously thought, as it is required only in cells that receive the posterior Grk signal, despite being expressed more widely in egg chambers (McCartney and Fehon, 1996). Interestingly, the dorso-anterior follicle cells do not require Merlin, despite receiving the Grk signal.

Our data show that Merlin is required downstream of Grk but upstream of the unknown polarising signal. We propose that the effect of Merlin on the polarising signal is not indirectly due to the overproliferation and subtle changes in the polarity of the posterior follicle cells. β_H-Spectrin is correctly distributed in *Mer* follicle cells adjacent to the oocyte, despite the centrosomes being disorganised and the second layer of follicle cells showing mislocalised β_H-spectrin. Therefore, the inner layer of posterior follicle cells are probably competent to

send the polarising signal in *Mer* mutants. Furthermore, some *Mer* egg chambers were found in which the polarising signal was not received, despite the posterior follicle cells showing no apparent defects in their proliferation or polarity (data not shown). We also found that *brn* mutant egg chambers show a similar specific morphological disruption of posterior follicle cells to that seen in *Mer* mutants (Goode et al., 1996a; Goode et al., 1996b) but *brn* mutations do not lead to any defects in oocyte axis specification (data not shown). Therefore, the morphological disruption of the posterior follicle cells in itself is not likely to be responsible for perturbing the unknown signal to the oocyte. Instead, we propose that Merlin may have a more direct role in targeting the polarising signal to the apical surface of posterior follicle cells.

What signals are disrupted by *Mer* mutations?

Since many genes involved in signalling among the follicle cells and between the oocyte and follicle cells are unknown, it is difficult to be certain which signals might be disrupted by *Mer* mutations. Nevertheless, our data conclusively rule out a role for Merlin in a number of known signalling processes. Merlin is not required for receiving the Grk signal via Torpedo, an EGF-like receptor, by the posterior or dorso-anterior follicle cells. Merlin is also not required for lateral inhibition via Notch-Delta signalling among the posterior follicle cells, that determines the correct number of posterior, polar posterior follicle cells and stalk cells between egg chambers. Nor is Merlin required for many kinds of essential signalling pathways throughout embryogenesis. Merlin is unlikely to play a direct role in the presumptive Egh/Brn signal from the oocyte, as these proteins are required in the oocyte and not in the follicle cells. Nevertheless, it is intriguing that the posterior follicle cells of *N*, *brn* or *egh* mutant egg chambers all show a similar overproliferation phenotype to *Mer* egg chambers. While it is possible that N, Egh or Brn are in some way related in function to Merlin, further experiments will have to be performed to explore these issues.

Our results show that Merlin is required for two distinct processes involving signalling, but we cannot distinguish whether the two processes depend on a single signal or two distinct signals. For example, the restriction of posterior follicle cell proliferation could require the same unknown signal that initiates MT repolarisation in the oocyte. Both processes could depend on the same signal secreted into the space between the follicle cells and oocyte. Indeed, it is intriguing that *Merlin* egg chambers have MT polarity defects in both the oocyte and the posterior follicle cells. However, further progress awaits the identification of the signal or signals involved.

The identity of the polarising signal is unknown, but some genes are known to be required for the signal, including PKA (Lane and Kalderon, 1995), Mago (Micklem et al., 1997) and Laminin A. Merlin is unlikely to be required for PKA and Mago functions as they are required in the oocyte. In contrast, Laminin A is expressed and required in posterior follicle cells as a component of the extracellular matrix (Deng and Ruohola-Baker, 2000). It is tempting to speculate that Merlin and Laminin A could be functionally linked as specialised structural components required specifically in the posterior follicle cells for the transduction of the polarising signal.

It is interesting to ask how many additional components are required for axis specification in the oocyte but it is not possible to estimate this number from our results. However, the fact that we identified even one mutation required for this process out from only 73 ts alleles, strongly argues that there are many more unrecognised genes required for axis formation.

We thank Rick Fehon for discussions of unpublished observations. We also thank Catherine Rabouille, Rick Fehon, Andrew Jarman, Daniel St Johnston, Hildegard Tekotte and David Ish-Horowicz for comments on the manuscript, and Rick Fehon, Debiao Zhan and Mary Bownes, Peter Deak and David Glover, Stefan Luschnig, Margarete Heck and Alan Spradling, Daniel Kalderon, Graham Thomas, Daniel St Johnston and the Bloomington stock centre for fly stocks and antibodies. We thank Gill MacKay for unpublished observations. This work was supported by a Wellcome Trust career development fellowship and Lister senior fellowship to I. D., a Darwin Trust studentship to N. M., Wellcome Trust studentship to Y. L., MRC studentship to G. W., a Human Frontiers fellowship to H. F. L. and an NIH grant (GM46409) to W. S.

REFERENCES

Anderson, K. V. (1998). Pinning down positional information: dorsal-ventral polarity in the *Drosophila* embryo. *Cell* **95**, 439-442.

Clark, I., Giniger, E., Ruohola-Baker, H., Jan, L. Y. and Jan, Y. N. (1994). Transient posterior localization of a kinesin fusion protein reflects anteroposterior polarity of the *Drosophila* oocyte. *Curr. Biol.* **4**, 289-300.

Clark, I. E., Jan, L. Y. and Jan, Y. N. (1997). Reciprocal localization of Nod and kinesin fusion proteins indicates microtubule polarity in the *Drosophila* oocyte, epithelium, neuron and muscle. *Development* **124**, 461-470.

Davis, I. (2000). Visualising fluorescence in *Drosophila* – optimal detection in thick specimens. In *Protein Localisation by Fluorescence Microscopy: A Practical Approach*. Vol. 218 (ed. V. J. Allan), pp. 131-162. Oxford: Oxford University Press.

Davis, I., Girdham, C. H. and O Farrell, P. H. (1995). A nuclear GFP that marks nuclei in living *Drosophila* embryos – maternal supply overcomes a delay in the appearance of zygotic fluorescence. *Dev. Biol.* **170**, 726-729.

Deng, W. M., Zhao, D., Rothwell, K. and Bownes, M. (1997). Analysis of P[gal4] insertion lines of *Drosophila* melanogaster as a route to identifying genes important in the follicle cells during oogenesis. *Mol. Hum. Reprod.* **3**, 853-862.

Deng, W. M. and Bownes, M. (1998). Patterning and morphogenesis of the follicle cell epithelium during *Drosophila* oogenesis. *Int. J. Dev. Biol.* **42**, 541-552.

Deng, W. M. and Ruohola-Baker, H. (2000). Laminin A is required for follicle cell-oocyte signaling that leads to establishment of the anterior-posterior axis in *Drosophila*. *Curr. Biol.* **10**, 683-686.

Driever, W. and Nüsslein-Volhard, C. (1988). A gradient of bicoid protein in *Drosophila* embryos. *Cell* **54**, 83-93.

Duffy, J. B., Harrison, D. A. and Perrimon, N. (1998). Identifying loci required for follicular patterning using directed mosaics. *Development* **125**, 2263-2271.

Ephrussi, A., Dickinson, L. K. and Lehmann, R. (1991). Oskar organizes the germ plasm and directs localization of the posterior determinant nanos. *Cell* **66**, 37-50.

Fasano, L. and Kerridge, S. (1988). Monitoring positional information during oogenesis in adult *Drosophila*. *Development* **104**, 245-253.

Fehon, R. G., Oren, T., Lajeunesse, D. R., Melby, T. E. and McCartney, B. M. (1997). Isolation of mutations in the *Drosophila* homologues of the human Neurofibromatosis 2 and yeast CDC42 genes using a simple and efficient reverse-genetic method. *Genetics* **146**, 245-252.

Gonzalez-Reyes, A., Elliott, H. and St Johnston, D. (1995). Polarization of both major body axes in *Drosophila* by Gurken-Torpedo signaling. *Nature* **375**, 654-658.

Gonzalez-Reyes, A. and St Johnston, D. S. (1998). Patterning of the follicle cell epithelium along the anterior-posterior axis during *Drosophila* oogenesis. *Development* **125**, 2837-2846.

Goode, S., Melnick, M., Chou, T. B. and Perrimon, N. (1996a). The

neurogenic genes egghead and brainiac define a novel signaling pathway essential for epithelial morphogenesis during *Drosophila* oogenesis. *Development* **122**, 3863-3879.

Goode, S., Morgan, M., Liang, Y. P. and Mahowald, A. P. (1996b). brainiac encodes a novel, putative secreted protein that cooperates with Grk TGF alpha in the genesis of the follicular epithelium. *Dev. Biol.* **178**, 35-50.

LaJeunesse, D. R., McCartney, B. M. and Fehon, R. G. (1998). Structural analysis of *Drosophila* merlin reveals functional domains important for growth control and subcellular localization. *J. Cell Biol.* **141**, 1589-1599.

Lane, M. E. and Kalderon, D. (1994). RNA localization along the anteroposterior axis of the *Drosophila* oocyte requires PKA-mediated signal transduction to direct normal microtubule organization. *Genes Dev.* **8**, 2986-2995.

Lane, M. E. and Kalderon, D. (1995). Localization and functions of protein kinase A during *Drosophila* oogenesis. *Mech. Dev.* **49**, 191-200.

Larkin, M. K., Holder, K., Yost, C., Giniger, E. and Ruohola-Baker, H. (1996). Expression of constitutively active Notch arrests follicle cells at a precursor stage during *Drosophila* oogenesis and disrupts the anterior-posterior axis of the oocyte. *Development* **122**, 3639-3650.

Lehmann, R. and Nüsslein-Volhard, C. (1986). Abdominal segmentation, pole cell formation, and embryonic polarity require the localized activity of oskar, a maternal gene in *Drosophila*. *Cell* **47**, 141-152.

Mangeat, P., Roy, C. and Martin, M. (1999). ERM proteins in cell adhesion and membrane dynamics. *Trends Cell Biol.* **9**, 187-192.

McCartney, B. M. and Fehon, R. G. (1996). Distinct cellular and subcellular patterns of expression imply distinct functions for the *Drosophila* homologues of moesin and the neurofibromatosis 2 tumor suppressor, merlin. *J. Cell Biol.* **133**, 843-852.

McCartney, B. M., Kulikauskas, R. M., LaJeunesse, D. R. and Fehon, R. G. (2000). The neurofibromatosis-2 homologue, Merlin, and the tumor suppressor expanded function together in *Drosophila* to regulate cell proliferation and differentiation. *Development* **127**, 1315-1324.

McClatchey, A. I., Saotome, I., Mercer, K., Crowley, D., Gusella, J. F., Bronson, R. T. and Jacks, T. (1998). Mice heterozygous for a mutation at the NF2 tumor suppressor locus develop a range of highly metastatic tumors. *Genes Dev.* **12**, 1121-1133.

Micklem, D. R., Dasgupta, R., Elliott, H., Gergely, F., Davidson, C., Brand, A., Gonzalez-Reyes, A. and St Johnston, D. (1997). The *mago nashi* gene is required for the polarisation of the oocyte and the formation of perpendicular axes in *Drosophila*. *Curr. Biol.* **7**, 468-478.

Neuman-Silberberg, F. S. and Schüpbach, T. (1993). The *Drosophila* dorsoventral patterning gene gurken produces a dorsally localized RNA and encodes a TGF alpha-like protein. *Cell* **75**, 165-174.

Newmark, P. A., Mohr, S. E., Gong, L. and Boswell, R. E. (1997). *mago nashi* mediates the posterior follicle cell-to-oocyte signal to organize axis formation in *Drosophila*. *Development* **124**, 3197-3207.

Nilson, L. A. and Schüpbach, T. (1999). EGF receptor signaling in *Drosophila* oogenesis. *Curr. Top. Dev. Biol.* **44**, 203-243.

Perrimon, N. (1994). Signalling pathways initiated by receptor protein tyrosine kinases in *Drosophila*. *Curr. Opin. Cell Biol.* **6**, 260-266.

Ruohola, H., Bremer, K. A., Baker, D., Swedlow, J. R., Jan, L. Y. and Jan, Y. N. (1991). Role of neurogenic genes in establishment of follicle cell fate and oocyte polarity during oogenesis in *Drosophila*. *Cell* **66**, 433-449.

Schüpbach, T. (1987). Germ line and soma cooperate during oogenesis to establish the dorsoventral pattern of egg shell and embryo in *Drosophila melanogaster*. *Cell* **49**, 699-707.

Tautz, D. and Pfeifle, C. (1989). A non-radioactive in situ hybridization method for the localization of specific RNAs in *Drosophila* embryos reveals translational control of the segmentation gene hunchback. *Chromosoma* **98**, 81-85.

Theurkauf, W. E., Smiley, S., Wong, M. L. and Alberts, B. M. (1992). Reorganization of the cytoskeleton during *Drosophila* oogenesis – implications for axis specification and intercellular transport. *Development* **115**, 923-936.

Tsukita, S., Oishi, K., Sato, N., Sagara, J. and Kawai, A. (1994). ERM family members as molecular linkers between the cell surface glycoprotein CD44 and actin-based cytoskeletons. *J. Cell Biol.* **126**, 391-401.

Turunen, O., Sainio, M., Jaaskelainen, J., Carpen, O. and Vaheri, A. (1998). Structure-function relationships in the ezrin family and the effect of tumor-associated point mutations in neurofibromatosis 2 protein. *Biochim. Biophys. Acta* **1387**, 1-16.

Vaheri, A., Carpen, O., Heiska, L., Helander, T. S., Jaaskelainen, J., Majander-Nordenswan, P., Sainio, M., Timonen, T. and Turunen, O. (1997). The ezrin protein family: Membrane-cytoskeleton interactions and disease associations. *Curr. Opin. Cell Biol.* **9**, 659-666.

van Eeden, F. and St Johnston, D. (1999). The polarisation of the anterior-posterior and dorsal-ventral axes during *Drosophila* oogenesis. *Curr. Opin. Genet. Dev.* **9**, 396-404.

Vaughan, T. J., James, P. S., Pascall, J. C. and Brown, K. D. (1992). Expression of the genes for TGF alpha, EGF and the EGF receptor during early pig development. *Development* **116**, 663-669.

Wilkie, G. and Davis, I. (1998). High resolution and sensitive mRNA in situ hybridisation using fluorescent tyramide signal amplification. *Tech. Tips Online* **t01458** (http://www.biomednet.com/db/tto).

Wilkie, G., Shermoen, A., O'Farrell, H. and Davis, I. (1999). Transcribed genes are localized according to chromosomal position within polarized *Drosophila* embryonic nuclei. *Curr. Biol.* **9**, 1263-1266.

Zarnescu, D. C. and Thomas, G. H. (1999). Apical spectrin is essential for epithelial morphogenesis but not apicobasal polarity in *Drosophila*. *J. Cell Biol.* **146**, 1075-1086.

SUBMISSION OF MANUSCRIPTS

Manuscripts covering all areas of developmental biology will be considered. Experimental papers will be given the highest priority. Manuscripts that are entirely descriptive will only be accepted if they are of particularly high quality and offer novel insight into developmental mechanisms (see also Information about the Journal).

Length of manuscript

Manuscripts including text and figure legends, but excluding references, should not exceed 7,000 words plus 4 page equivalents of figures and tables. Manuscripts longer than this will only be accepted at the editors' discretion.

Where to send

Manuscripts should be sent to the most appropriate editor (see list of addresses opposite). If you need advice, please contact the Editorial Office, or Editor in Chief.
Please supply your address, and telephone, fax and e-mail numbers, for all correspondence about your manuscript.
For Customs purposes, please mark all packages as 'No Commercial Value', otherwise charges are levied.

What to send

Please send 3 unstapled copies of the manuscript and figures with the completed 'Preparation of manuscripts' check list. Copies of the figures must be of suitable standard for reviewers to judge the quality of the work (photocopies of photographs are not acceptable). The original illustrations and electronic files should *not* be included initially. These should be sent with your revised manuscript, when requested, i.e. after editor's and referees' comments have been incorporated.

Movies

Authors may submit moving images to accompany the Web version of their article. Please provide three copies of these movies on disk, and if possible the URL of a Web page where they can be viewed, **at submission**. Movies should be in QuickTime or MPEG format and should not exceed 5 MB. If you cannot generate files in one of these formats, please contact our webmaster at webmaster@biologists.com.

Proofs

Authors will receive one set of proofs, which should be corrected and returned to the Editorial Office (a photocopy should be made and retained by the author). No alteration should be made to proofs other than those needed to correct printer's errors. All corrections, including those to figures, must be marked on the proof.

Reprints

Authors will receive 50 reprints free of charge.

Colour plates

These can be reproduced free of charge at the discretion of the editor. Any charge for excessive use of colour will also be at the editor's discretion.

Development Editorial Office (for accepted manuscripts and information only)
Production editors: Thelma Burrell and Lindsay Roberts
The Company of Biologists Ltd, Bidder Building, 140 Cowley Road, Cambridge, CB4 0DL, UK
Tel: +44 1223 420007 Fax: +44 1223 423353
E-mail: dev@biologists.com

EDITORS

Contents

Volume 128 (4) February 2001

The Company of Biologists Limited, Bidder Building, 140 Cowley Road, Cambridge CB4 0DL, UK
ISSN: 0950-1991

Developmental Cell, Vol. 4, 307–319, March, 2003, Copyright ©2003 by Cell Press

Drosophila gurken (TGFα) mRNA Localizes as Particles that Move within the Oocyte in Two Dynein-Dependent Steps

Nina MacDougall, Alejandra Clark, Eilidh MacDougall, and Ilan Davis*
Wellcome Trust Centre for Cell Biology
ICMB
King's Buildings
University of Edinburgh
Mayfield Road
Edinburgh EH9 3JR
Scotland
United Kingdom

Summary

In *Drosophila* oocytes, *gurken* mRNA localization orientates the TGF-α signal to establish the anteroposterior and dorsoventral axes. We have elucidated the path and mechanism of *gurken* mRNA localization by time-lapse cinematography of injected fluorescent transcripts in living oocytes. *gurken* RNA assembles into particles that move in two distinct steps, both requiring microtubules and cytoplasmic Dynein. *gurken* particles first move toward the anterior and then turn and move dorsally toward the oocyte nucleus. We present evidence suggesting that the two steps of *gurken* RNA transport occur on distinct arrays of microtubules. Such distinct microtubule networks could provide a general mechanism for one motor to transport different cargos to distinct subcellular destinations.

Introduction

mRNA localization provides an efficient posttranscriptional method of targeting many kinds of proteins to their sites of function in a wide range of organisms (Jansen, 2001; Kloc et al., 2002; Lipshitz and Smibert, 2000; Palacios and Johnston, 2001). In a variety of cases, mRNA localization is thought to involve polarized transport of mRNA by cytoskeletal motors (Tekotte and Davis, 2002). However, only in a few cases has transport been demonstrated by real-time imaging of directed movement of RNA. For example, *ASH1* mRNA localizes to the buds of dividing yeast cells, thus suppressing mating-type switching in the daughter cell (Bobola et al., 1996). The movement of *ASH1* mRNA indirectly tagged with GFP has been visualized directly (Bertrand et al., 1998) and requires Myosin V and actin. She2 and She3 act as linkers between Myosin and the RNA (Jansen et al., 1996; Long et al., 2000; Munchow et al., 1999; Takizawa and Vale, 2000). In the *Drosophila* blastoderm embryo, *wingless* (*wg*) and pair-rule apical transport of RNA particles has been visualized directly with injected fluorescently labeled RNA. Apical transcript localization in the embryo requires cytoplasmic Dynein (Dynein), the major minus end-directed microtubule (MT) motor (Wilkie and Davis, 2001). Egalitarian (Egl) and Bicaudal-D (BicD) may act as linkers between pair-rule RNA and the Dynein motor complex (Bullock and Ish-Horowicz, 2001).

In *Drosophila* oocytes, mRNA localization plays a central role in axis specification, but the role of cytoskeletal motor proteins has not been tested directly by observation of the movement of mRNA. The embryonic axes are preformed during oogenesis through the sorting of different mRNAs to distinct regions of the oocyte (Jansen, 2001). *gurken* (*grk*) mRNA localization plays a key role in breaking the initial symmetry of the oocyte by restricting the Grk-transforming growth factor-α (TGF-α) signal to particular groups of overlying follicle cells (Gonzalez-Reyes et al., 1995; Neuman-Silberberg and Schüpbach, 1993). There are two rounds of Grk signals at different times during oogenesis, both of which are received by Torpedo, an EGF receptor in the follicle cells (Nilson and Schüpbach, 1999). In stage 6, *grk* mRNA and Grk protein are localized at the posterior of the oocyte, thus instructing a group of follicle cells to become posterior in identity. These cells then send a signal back to the oocyte that initiated the formation of the anteroposterior axis. The signal leads to the repolarization of the oocyte MTs and the migration of the oocyte nucleus to the dorsoanterior corner of the oocyte (Gonzalez-Reyes and St Johnston, 1998). Before stage 7 an MT-organizing center (MTOC) is located at the posterior of the oocyte, the site at which most MT minus ends are localized (Clark et al., 1994, 1997; Micklem et al., 1997; Theurkauf et al., 1992). By stage 8, the posterior MTOC disassembles and a diffuse MTOC forms in the anterior. The anterior MTOC has been visualized with Nod-LacZ, a putative MT minus end marker (Clark et al., 1997), and Centrosomin, a centrosome component (Brendza et al., 2000), as well as the MT-nucleating components, γ-Tubulin37C (γTub37C) and γ-Tubulin ring complex protein 75 (Dgrip75) (Schnorrer et al., 2002). Plus ends of MTs, visualized with Kinesin-LacZ (Kin-LacZ), are found at the posterior of the oocyte (Clark et al., 1994). This results in an anteroposterior gradient of MT concentration, with the highest concentration at the anterior, which has been visualized with Tau-GFP (Micklem et al., 1997), a fusion containing the MT binding protein Tau. The second round of Grk signaling initiates dorsoventral axis formation in stage 9, when *grk* mRNA and protein are localized in an anterodorsal cap near the oocyte nucleus. The overlying dorsal follicle cells are instructed by the Grk signal to adopt dorsal fates, leading later to secretion of correct eggshell structures, such as the dorsal appendages (Nilson and Schüpbach, 1999; van Eeden and St Johnston, 1999).

The breaking of the initial axial symmetry of the oocyte involves several other localized transcripts in addition to *grk*. *bicoid* (*bcd*) mRNA is localized to the extreme anterior cortex of the oocyte, leading to a morphogenetic gradient of Bcd protein when it is translated in the embryo (Driever and Nüsslein-Volhard, 1988). *oskar* (*osk*) mRNA is localized at the extreme most-posterior part of the oocyte and embryo and specifies the future

*Correspondence: ilan.davis@ed.ac.uk

germ cells and posterior structures through recruitment of many other localized posterior components by the Osk protein (Ephrussi et al., 1991). While the functions of *grk*, *bcd*, and *osk* have been studied in detail, the mechanism of localization of these transcripts is not as well understood (Tekotte and Davis, 2002). *osk* mRNA localization to the posterior requires actin and Tropomyosin, probably for anchoring at the posterior (Erdelyi et al., 1995), a crucial step in pole plasm assembly (Vanzo and Ephrussi, 2002). The MT plus end motor, Kinesin I (Kin I), is probably required for transport of *osk* mRNA along MTs to their plus ends (Brendza et al., 2000), for its exclusion from the lateral cortex (Cha et al., 2001), and for all cytoplasmic movements in the oocyte (Palacios and Johnston, 2002). *osk* mRNA localization is also likely to require cytoplasmic movements to deliver it to the posterior (Glotzer et al., 1997). Surprisingly, Kin light chain is not required for this process (Palacios and Johnston, 2002). However, the path of movement of *osk* mRNA has not been visualized directly either in wild-type or Kin mutants. *bcd* mRNA localization to the anterior requires Swa, which interacts with Dynein in yeast two-hybrid assays (Schnorrer et al., 2000), but the role of Dynein in *bcd* mRNA localization has not yet been tested directly. *bcd* localization also requires Exu protein (St Johnston et al., 1989) for the correct path of localization of injected *bcd* RNA in living oocytes (Cha et al., 2001). Exu-GFP fusion protein has been visualized in particles that move within the oocyte (Theurkauf and Hazelrigg, 1998), but it remains unclear whether Exu and *bcd* mRNA coassemble in the same particles (Wilhelm et al., 2000).

In comparison with *bcd* and *osk*, less is known about the mechanism of localization of *grk* mRNA within the oocyte. Like *bcd* and *osk*, *grk* mRNA may be transcribed at early stages in nurse cells (Thio et al., 2000), but, in later stages, *grk* mRNA may be transcribed in the oocyte nucleus (Saunders and Cohen, 1999). *grk* mRNA localization requires MTs (Pokrywka and Stephenson, 1991). Kin I is required for the localization of *grk* mRNA to the dorsoanterior corner, possibly because of a requirement to recycle Dynein back to the posterior (Brendza et al., 2002). Overexpression of p50/dynamytin, a subunit of the dynactin complex that is required for Dynein processivity (King and Schroer, 2000), disrupts *grk* RNA localization, suggesting a possible role for Dynein in *grk* mRNA localization (Januschke et al., 2002). However, as in the cases of *bcd* and *osk* mRNAs, the path of *grk* mRNA has not been defined, and it has not been tested directly whether Dynactin, Dynein, and Kinesin are required for active transport of *grk* as opposed to cytoplasmic streaming or diffusion and for the anchoring of *grk* or a factor required for its localization.

Here, we have observed the path of movement and elucidated the mechanism of *grk* RNA localization in the oocyte by studying its movement in real-time in living egg chambers. Injected *grk* RNA assembles into discrete particles that move first to the anterior cortex and then turn and move dorsally toward the oocyte nucleus. Both steps involve transport to the minus ends of MTs mediated by Dynein. We propose and show some supporting evidence for the view that the two steps of *grk* movement take place on two distinct arrays of MTs, the first orientated toward the anterior and the second associated with the oocyte nucleus.

Results

Injected *grk* Transcripts Localize in Cultured Egg Chambers like Endogenous *grk* mRNA to the Anterodorsal Corner of the Oocyte

To investigate the path and mechanism of *grk* mRNA localization, we developed a rapid real-time injection assay for *grk* RNA localization in living oocytes cultured in oxygen-rich halocarbon oil. About 1 hr after injection, fluorescently labeled *grk* transcripts localize to a very similar site to the endogenous transcripts. The assay is based on previous procedures used to inject fluorescently labeled mRNA into embryos (Bullock and Ish-Horowicz, 2001; Wilkie and Davis, 2001) and on our modifications of previous methods used to inject mRNA into living egg chambers or embryos (Glotzer et al., 1997; Lall et al., 1999). We used time-lapse cinematography with low-powered objectives to capture the movement and localization of *grk* RNA over the entire oocyte (Experimental Procedures).

In stage 8 of oogenesis, endogenous *grk* transcripts are localized in the oocyte in an anterior ring with an enrichment at the dorsoanterior corner near the oocyte nucleus. By early stage 9 the majority of *grk* RNA is located in the dorsoanterior corner, with a small amount present in the entire anterior region. Fluorescently labeled *grk* RNA injected into oocytes of stage 8–10B egg chambers is correctly localized in 81% of cases ($n = 96$). Localization efficiency is higher in stages 8–9 (87%, $n = 47$) and stage 10A (83%, $n = 35$) than in stage10B (57%, $n = 14$). *grk* transcripts localize correctly approximately 1 hr after injection into any part of the oocyte, including the extreme posterior end (Figures 1A–1F).

The time-lapse movies we captured suggest that the localization of *grk* RNA occurs in two steps (Figure 1 and Supplemental Movie S1 at http://www.developmentalcell.com/cgi/content/full/4/3/307/DC1). The RNA begins to move toward the anterior soon after its injection (Figure 1B). Thirty minutes after injection, the RNA is strongly localized along the entire anterior but begins to be enriched at the dorsoanterior corner (Figure 1C). Between 30 and 60 min after injection, *grk* RNA becomes progressively much more concentrated in the dorsoanterior corner, and the anterior signal is diminished (Figure 1D). These results suggest that *grk* mRNA first moves to the anterior and then to the dorsoanterior corner, rather than being degraded everywhere other than at the dorsoanterior corner. In contrast, we find that injected fluorescent *bcd* RNA fails to correctly localize to the anterior cortex when injected into the oocyte (data not shown), in agreement with previous studies (Cha et al., 2001). We conclude that, unlike for *bcd*, all the machinery required for *grk* mRNA localization is present within the oocyte cytoplasm.

In addition to localizing at the dorsoanterior corner, injected *grk* RNA also accumulates at a lower level in the opposite side of the oocyte, at the ventroanterior corner (Figures 1E and 1F). To determine whether this additional site of localization is also found in the case of endogenous *grk* mRNA, we used high-resolution fluorescent in situ hybridization methods (Wilkie et al, 1999; Wilkie and Davis, 2001) (detailed protocol available by

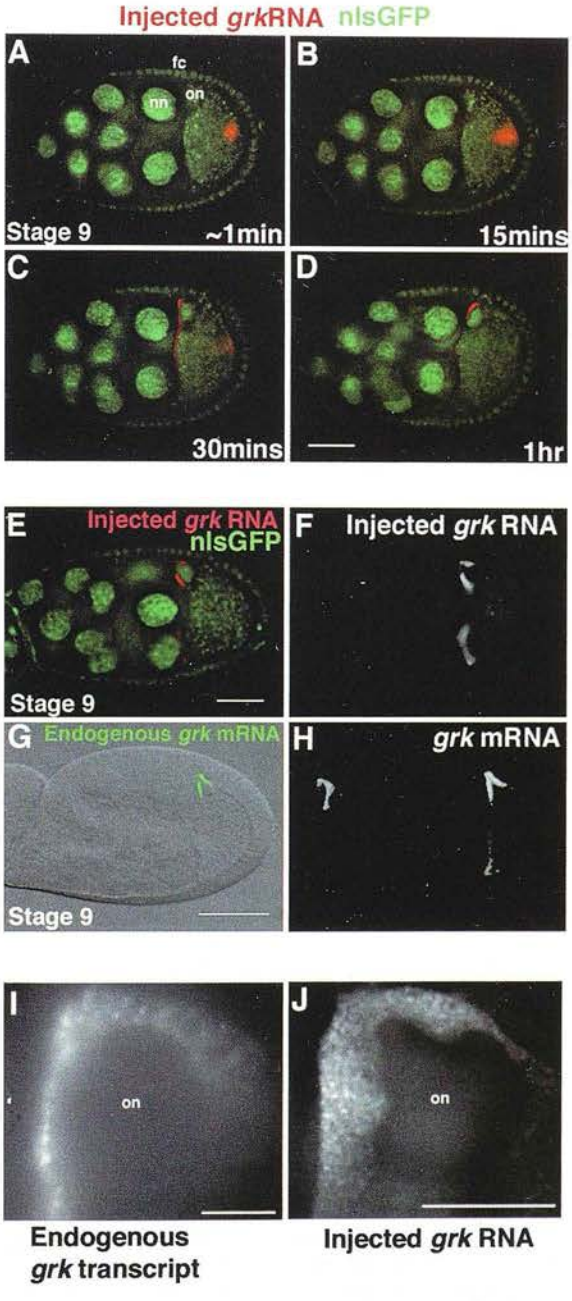

Figure 1. Injected *grk* RNA, like Endogenous *grk* Transcripts, Localizes to the Dorsoanterior Corner of the Oocyte

(A–D) Time-lapse movie of the movement of injected Alexa Fluor 546-UTP-labeled *grk* RNA in a living stage 9 egg chamber expressing nlsGFP.

(A) One minute after the injection of the *grk* RNA in the posterior of the oocyte. fc, follicle cells; nn, nurse cell nuclei; on, oocyte nucleus.

(B) Fifteen minutes after the injection, the RNA has begun to move toward the anterior.

(C) Thirty minutes after the injection, much of the RNA is localized to the anterior of the oocyte.

(D) One hour after the injection, the RNA is predominantly localized at the dorsoanterior cap.

(E–H) Stage 9 egg chambers showing a comparison of the final distribution of injected *grk* RNA and endogenous *grk* transcripts. In both cases, the majority of the RNA has accumulated at the oocyte nucleus, and a fraction of the RNA has accumulated at the ventroanterior corner.

(E and F) Living stage 9 egg chamber injected with *grk* RNA.

(G and H) Endogenous *grk* transcripts visualized by in situ hybridization in a fixed stage 9 egg chamber.

(I and J) High-magnification comparison of the distribution of injected *grk* RNA and endogenous *grk* transcripts showing that both are localized in a punctate manner in a dorsoanterior cap around the oocyte nucleus (on). The scale bars represent 50 μm in lower-powered images and 10 μm in high-powered images in this and all other figures. In this and all subsequent figures, the oocyte is orientated with dorsal up and posterior to the right, unless otherwise stated.

request) and three-dimensional imaging of entire fixed egg chambers (Davis, 2000). We modified the in situ procedure to allow greater probe penetration and increased signal to noise ratio (Experimental Procedures). In stage 9 egg chambers, endogenous *grk* mRNA shows a pattern of accumulation very similar to that of the injected RNA, with the majority of the RNA in a dorsoanterior cap and some RNA concentrated in the ventroanterior corner (Figures 1G and 1H). The translation of the ventroanterior RNA is presumably repressed. We also found that high-resolution imaging of endogenous *grk* transcripts and injected *grk* RNA showed that both are localized in a punctate pattern in the dorsoanterior corner (Figures 1I and 1J). We conclude that injected *grk* RNA localizes to the same site as endogenous *grk* mRNA approximately 1 hr after injection.

To test whether *grk* is specific in its ability to localize to the dorsoanterior corner, we injected the anteriorly localized transcript, *fs(1)K10 (K10)*. A 44 nt *K10* small stem loop, previously shown to localize to the anterior region as a transgene in oocytes (Serano and Cohen, 1995) and apically when injected as part of a larger RNA into blastoderm embryos (Bullock and Ish-Horowicz, 2001), localizes anteriorly when injected into the oocyte, albeit less efficiently than *grk* RNA (26% anteriorly localized, 64% unlocalized, n = 15; Figure 2A). In contrast, a mutant *K10* stem loop previously shown not to localize as a transgene in oocytes and when injected into blastoderm embryos (Bullock and Ish-Horowicz, 2001; Serano and Cohen, 1995) fails to localize when injected into oocytes (0% anteriorly localized, n = 9; Figure 2B). In contrast, *hb* RNA, which is not normally found in the oocyte and is unlocalized in embryos (Davis and Ish-Horowicz, 1991), becomes evenly distributed when injected into the oocyte (0% localization, n = 12; Figure 2D). We conclude that the anterodorsal localization of injected *grk* RNA is specific.

Endogenous *grk* transcripts require the transacting protein Squid (*Drosophila* hnRNP A1) for correct anterodorsal localization (Kelley, 1993). We injected *grk* RNA into *squid* mutant egg chambers and found that injected *grk* RNA, like the endogenous transcripts, localizes to the entire anterior cortex, instead of the dorsoanterior corner (75% anteriorly localized, 25% unlocalized, n = 8; Figure 2C). In no case was injected *grk* RNA specifically enriched in the dorsoanterior corner of *squid* mutant oocytes. We conclude that our injection assay for *grk* RNA reflects faithfully the specificity of endogenous *grk* mRNA localization.

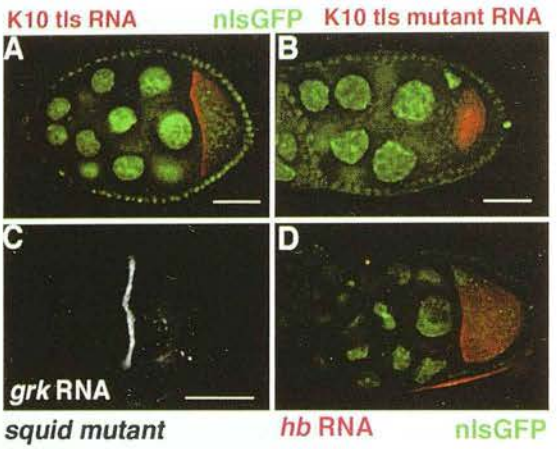

Figure 2. Dorsoanterior Localization of *grk* RNA Is Specific

(A) Stage 9 egg chamber injected with the *K10tls* (44 nt *K10* localization element). The RNA localizes to the anterior in 26% of injected oocytes.

(B) Stage 9 egg chamber injected with a mutated *K10tls* previously shown to disrupt localization. In all cases the RNA does not localize and remains near the injection site.

(C) Stage 9 *squid*^{1}/*Df(3)urd* oocyte injected with *grk* RNA. The RNA localizes tightly to the anterior and fails to form a dorsoanterior cap.

(D) Stage 9 egg chamber injected with *hb* RNA. *hb* RNA does not localize and diffuses throughout the ooplasm.

Injected *grk* RNA Assembles into Particles that Move in Two Phases

To determine the precise path of injected *grk* RNA movement, we imaged the movement of injected RNA in the oocyte at higher resolution at a time-lapse interval of one frame per second. Unlike in the blastoderm embryo, injected RNA in the oocyte appears diffuse at low resolution and moves with less well-defined directionality (Wilkie and Davis, 2001). However, by imaging at higher magnification and time resolution than in the embryo, we can readily resolve RNA into discrete particles that move in specific directions in the oocyte. These particle-tracking experiments confirm the two-step path of *grk* RNA localization observed with low-powered imaging. The RNA particles are usually apparent within 30–60 s of injection. Twenty-seven percent of the particles move in distinct, usually anterior or dorsal, paths in the plane of observation, 42% of the particles move rapidly into different focal planes and cannot be tracked, and the other 31% do not move substantial distances during the period of observation of 300 s (n = 265 particles) (Figure 3). Our observations suggest that all the particles eventually move to their correct destination, but, at any one time, particles go through periods of rapid motion interspersed by periods of stasis. During the periods of rapid motion, average speeds of 0.25 ± 0.013 μm/s and maximum speeds of 1.25 μm/s were observed. These speeds are approximately half of those observed in the embryo for *grk*, *wg*, and pair-rule RNA particle movements (this paper and Wilkie and Davis, 2001), probably because the particles pause more frequently in the oocyte than in the embryo. The speeds and paths taken by *grk* particles are entirely consistent with active transport, rather than diffusion and anchoring (Figure 3).

We were unable to track the particles at high resolution through their entire path of localization, as they eventually move out of the plane of focus and imaging at high power for long periods or through many focal sections causes an inhibition of the motility. This is probably due to photo-induced damage of the cellular machinery required for localization. Therefore, we were only able to image the movement of the RNA particles over short portions of their paths for 300 time points (5 min in total). Nevertheless, tracking the speed and direction of movement of many particles after injection of *grk* RNA at different sites in the oocyte has allowed us to reconstruct their entire route between the site of injection and their final destination.

To map the path of movement of *grk* RNA particles fully, we performed three kinds of particle-tracking experiments (Figure 3 and Supplemental Movies S2–S4 http://www.developmentalcell.com/cgi/content/full/4/3/307/DC1). In the first, we tracked the particles immediately after the injection of *grk* RNA in the center. In most cases, the particles move through the center toward the anterior of the oocyte (n = 214 particles; Figure 3A–3C), although, in some cases, the particles adopted diagonal routes directly to the oocyte nucleus. Unlike in *bcd* RNA injection experiments (Cha et al., 2001), we only sometimes observed particles moving toward the cortex (Figure 3B), and these appear to eventually move anteriorly from the cortex (data not shown). In the second type of particle-tracking experiment, we injected *grk* RNA in the center of the oocyte, waited for approximately 20 min, and then imaged the movement of particles at the anterior of the oocyte (n = 51; Figures 3D–3F). Near the anterior, some particles still move toward the anterior, while others move dorsally toward the nucleus. Interestingly, 11 particles were observed to move anteriorly, pause for a short period, and then make a sharp turn toward the dorsal corner (Figures 3E and 3F). In the third kind of particle-tracking experiment, we followed the movement of particles immediately after injection of *grk* RNA near the oocyte nucleus. In such experiments the oocyte was orientated with the dorsoanterior corner and nucleus uppermost, nearest the objective lens and out of focus. Particles near the oocyte nucleus generally move toward the nucleus (n = 17; Figures 3G–3I).

We plotted the angle of movement of the particles over their entire path (Figures 3J–3L). We found that, in the first particle-tracking experiment, the majority of particles moved toward the anterior (Figure 3J), and, in the second tracking experiment, the majority either moved anteriorly or dorsally (Figure 3K). In the third kind of particle-tracking experiment, the majority of the particles moved toward the oocyte nucleus (Figure 3L). To further test whether the turning of *grk* RNA particles we observe toward the dorsoanteriorly located nucleus is specific, we compared the direction of movement of *grk* particles in *squid* mutant and control egg chambers. In *squid* mutants *grk* RNA particles move less frequently to the dorsoanterior and more frequently to the ventral side than in controls (Figure 3M). We conclude that injected *grk* RNA and, by implication, endogenous *grk*

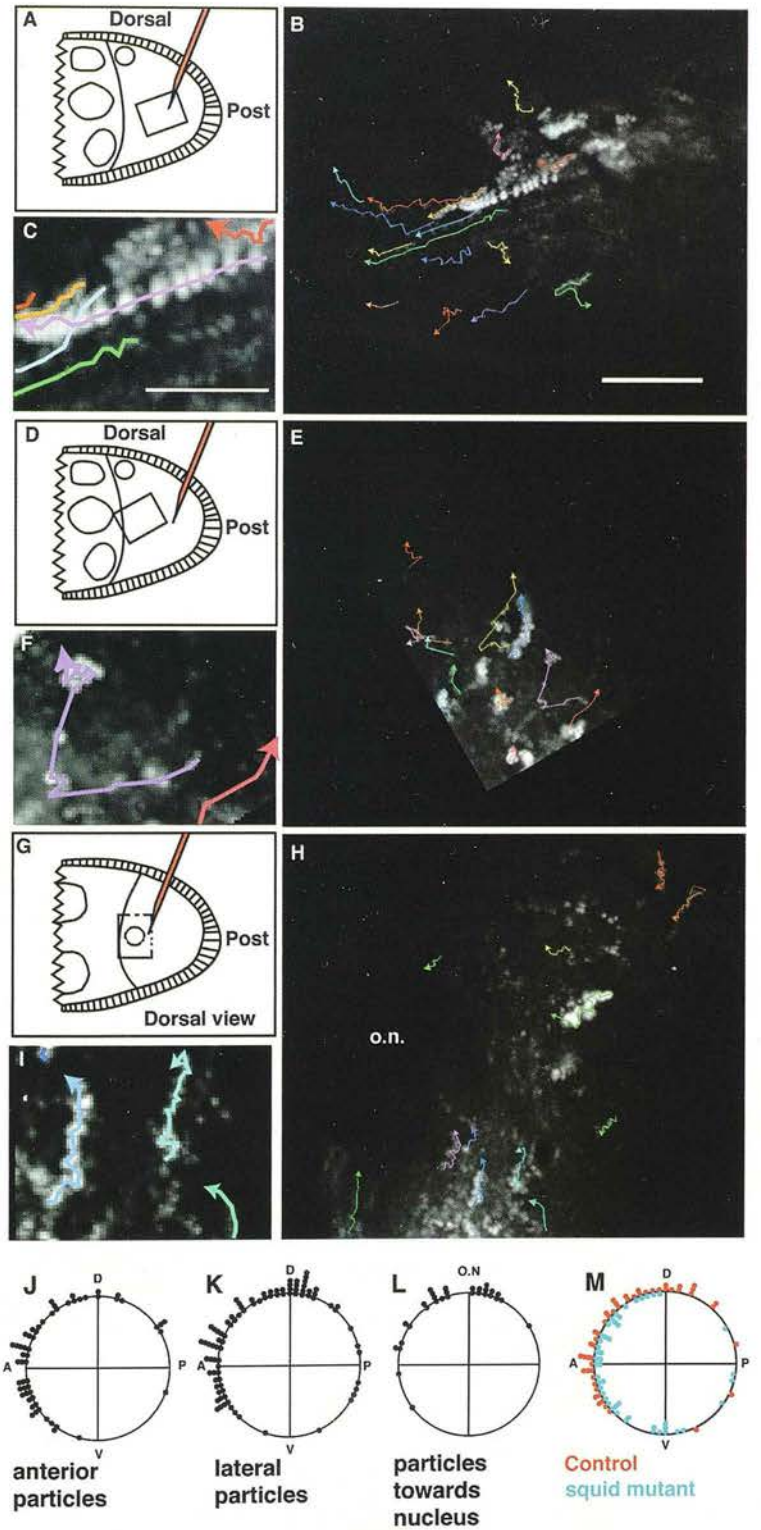

Figure 3. Injected *grk* RNA Assembles into Particles that Move First Anteriorly and then Dorsally Toward the Oocyte Nucleus

(A–C) The tracks of *grk* RNA particles and their direction of movement immediately after injection into the middle of the oocyte of a stage 9 egg chamber.

(A) Diagram showing the site of injection of *grk* RNA and orientation of the images acquired.

(B) Tracks of the path of movement of RNA particles identified by lines of various colors. The arrows indicate the direction of travel of the particles.

(C) An enlarged subregion of (B) showing some of the particles and their position over time.

(D) Diagram of another stage 9 egg chamber in which *grk* RNA was injected centrally into the oocyte.

(E) *grk* particles were allowed to move anteriorly for 30 min before their movement was tracked over time. Some particles travel anteriorly, but many travel dorsally (colored lines with arrows).

(F) An enlarged subregion of (E) showing a particle that travels in two phases, first anteriorly and then dorsally.

(G) Diagram of a stage 9 egg chamber in dorsal view (oocyte nucleus uppermost) injected with *grk* RNA in a broad region close to the oocyte nucleus.

(H) Particles close to the nucleus and their position and direction of movement over time (colored lines with arrows). Most particles move toward the oocyte nucleus.

(I) Enlargement of a subregion of (H) showing some particles moving toward the oocyte nucleus.

(J–L) Diagrams showing the direction of movement of *grk* RNA particles, illustrated as colored lines with arrows in (B), (E), and (H), respectively, and additional corresponding examples. The circles in (J) and (K) represent the angle of movement with respect to the four axes: D, dorsal; V, ventral; A, anterior; P, posterior. The circle in (L) represents the angle of movement relative to the oocyte nucleus (o.n.).

(J) Most particles move toward the anterior, some particles also move dorsally or anterodorsally, and a few move cortically.

(K) Most particles move dorsally or anteriorly, and a few moving cortically.

(L) Most particles move toward the oocyte nucleus.

(M) A comparison of the direction of movement of *grk* RNA particles in control (red) and *squid* (blue) mutant oocytes after injection halfway between the middle and the anterior of the oocytes. In the *squid* mutants most particles move anteriorly, but a few move dorsally or ventrally. In the control oocyte many particles move dorsally, but only one moves ventrally.

RNA become localized through an initial movement to the anterior through the center of the oocyte and then through a Squid-dependent dorsal movement from any part of the anterior toward the dorsoanterior corner.

grk mRNA Localization Requires MTs and Dynein

To investigate whether *grk* RNA localization requires an intact cytoskeleton, we coinjected or preinjected actin or MT inhibitors with *grk* RNA. Preinjection or coinjection

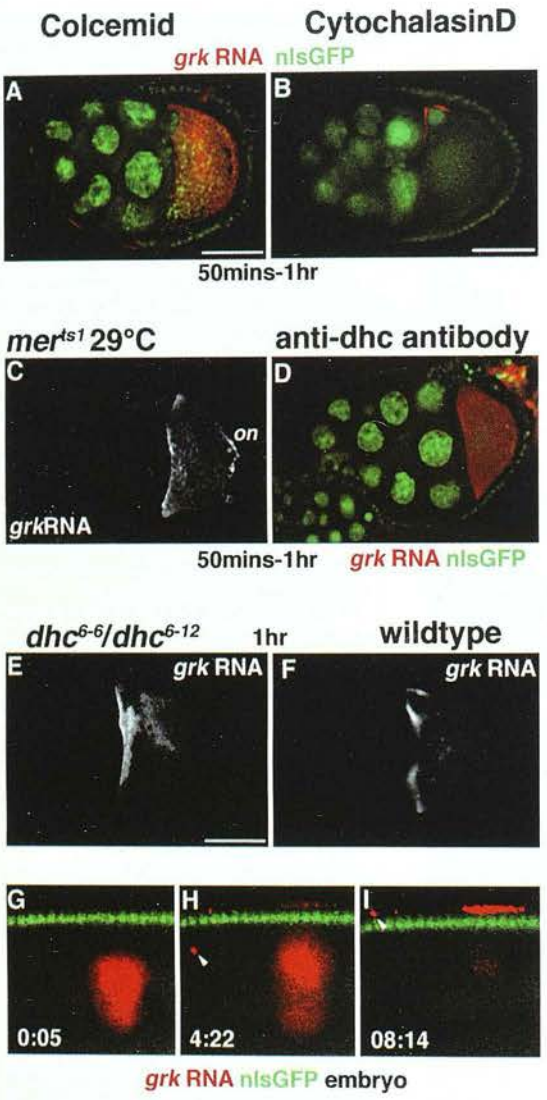

Figure 4. The First Step of *grk* RNA Localization Requires MTs and Dynein

(A) A stage 9 egg chamber 1 hr after coinjection of *grk* RNA and the MT-destabilizing drug, Colcemid (100 μg/ml). The RNA fails to localize within the oocyte.

(B) A stage 9 egg chamber 1 hr after coinjection of *grk* RNA and 150 μg/ml Cytochalasin D. *grk* RNA localizes to the dorsoanterior cap near the oocyte nucleus with normal kinetics.

(C) *merlin*^{ts1} mutant egg chamber 50 min after injection of *grk* RNA into the center of the oocyte. *grk* localizes to both the anterior and posterior of the oocyte, where minus ends of MTs are thought to localize. Note the oocyte nucleus at the posterior of the oocyte (on).

(D) A stage 9 egg chamber coinjected with *grk* RNA and P1H4 monoclonal anti-Dhc antibody (T. Hays). In all cases, *grk* RNA fails to localize within the oocyte.

(E) A stage 9 hypomorphic *dhc* mutant egg chamber injected with *grk* RNA, showing that the RNA is localized to the anterior after 1 hr (see text).

(F) A wild-type control egg chamber showing a strong dorsoanterior cap of *grk* RNA, 1 hr after injection.

(G–I) Time-lapse images of a living interphase 14 blastoderm embryo expressing nlsGFP fusion protein (green) and injected with *grk* RNA (red) at time 0. The time at which the images were captured after injection are shown in minutes and seconds in the bottom left hand corner of each panel. The arrowheads in (H) and (I) show an RNA particle, which formed from diffuse RNA at a second simultaneous site of injection of smaller quantities of RNA (not visible in [G]). In embryos, injected *grk* RNA localizes as particles with similar kinetics to *wg* and pair-rule RNA.

of Colcemid, an MT-depolymerizing drug, leads to an unlocalized distribution of *grk* RNA in the oocyte (100 μg/ml Colcemid, 0% localized, n = 26; 30 μg/ml Colcemid, 0% localized, n = 13; Figure 4A). In contrast, the actin-depolymerizing drug, Cytochalasin D, does not disrupt *grk* RNA localization to the dorsoanterior corner (86% localized, n = 15; Figure 4B). We conclude that *grk* RNA localization is dependent on intact MTs, but not on actin integrity.

To determine whether *grk* RNA localization is dependent on correct MT polarity, we injected *grk* RNA into *merlin* mutant egg chambers, which we previously showed fail to reorganize their MT at stage 7 of oogenesis (MacDougall et al., 2001). In *merlin* egg chambers, the posterior MTOC fails to disassemble and persists in later stages. In 50% of cases, the oocyte nucleus fails to migrate to the anterior and remains at the posterior of the oocyte. Our results show that, in *merlin* egg chambers, injected *grk* RNA localizes to the posterior near the misplaced oocyte nucleus, in addition to localizing along the entire anterior cortex (100% localized, n = 4; Figure 4C). We interpret these results as indicating that, in *merlin* mutants, the two steps of *grk* localization are disconnected, so that the RNA that completes the first step is not able to move from the anterior to the misplaced posterior nucleus, but the second step can occur in the absence of the first step. We conclude that *grk* mRNA localization depends on MT polarity and is normally targeted to minus ends of MTs at the anterior and near the oocyte nucleus.

The major minus end-directed MT-dependent motor in eukaryotic cells is Dynein. To test whether *grk* mRNA localization depends on Dynein, we injected *grk* RNA into egg chambers with reduced Dynein heavy chain (Dhc) activity. Dhc is the essential force-generating ATPase subunit of the large Dynein motor complex. Coinjection of either of two monoclonal antibodies against Dhc together with *grk* RNA is sufficient to completely inhibit the localization of *grk* RNA (0% localized, n = 34; Figure 4D), as is preinjection of either of the antibodies 10 min before *grk* RNA (data not shown). In contrast, injection of anti-Dynein antibody into Tau-GFP embryos does not alter the previously described (Micklem et al., 1997) anteroposterior gradient of MT (data not shown). Furthermore, injection of a control anti-HA antibody does not affect the localization of injected *grk* RNA (73% localized, n = 11). We conclude that a disruption of Dynein function by the anti-Dynein antibody is the cause of the inhibition of *grk* mRNA localization, rather than nonspecific effects of antibody injections or an indirect disruption of MT distribution.

We also studied the localization of injected *grk* RNA in hypomorphic semiviable *dhc* allelic combinations (Gepner et al., 1996). Injected *grk* RNA localizes more slowly in *dhc* mutant oocytes (Figures 4E and 4F). After 1 hr, 85% (n = 40) stage 9 wild-type oocytes injected with *grk* RNA were found to localize correctly in an anterodorsal cap near the nucleus. In contrast, only 21% of

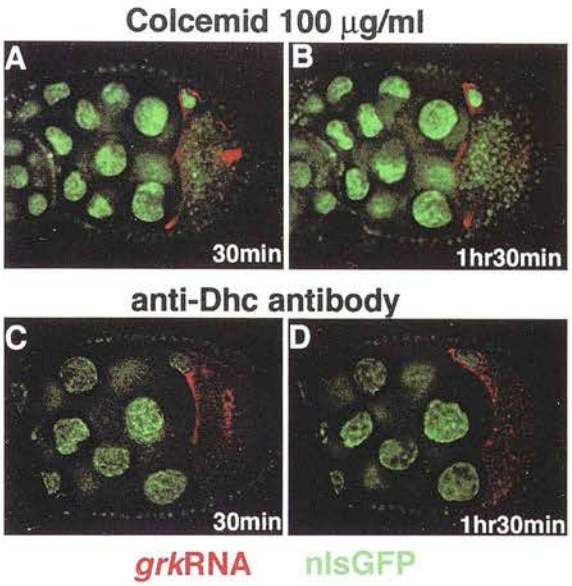

Figure 5. The Second Step of *grk* RNA Localization Requires MTs and Dynein

(A) A stage 9 egg chamber injected with Colcemid (100 μg/ml) approximately 30 min after *grk* RNA injection.

(B) One hour after Colcemid injection, no further localization of *grk* RNA occurs, but the RNA already at the anterior and in the dorsoanterior cap remains localized.

(C) A stage 9 egg chamber injected with anti-Dhc antibody P1H4 30 min after injection with *grk* RNA, which has partly localized to the anterior and near the oocyte nucleus.

(D) One hour after injection of the anti-Dhc, *grk* RNA is still only partly localized.

dhc mutant egg chambers injected with *grk* RNA show localization to a dorsoanterior cap similar to wild-type, 36% show anterior and a weak dorsoanterior localization, and 43% show no localization after 1 hr (n = 14; Figure 4E). We interpret the *dhc* mutants as causing a reduction in the efficiency of Dhc function, while we interpret the anti-Dhc antibody experiments as representing a complete knockout of Dhc function, equivalent to a null allele. We therefore conclude that injected *grk* RNA moves to the anterior using Dynein-dependent transport to the minus ends of MTs.

We were unable to determine the speed of movement of *grk* RNA particles in the *dhc* allelic combinations, as RNA particles appeared to form less readily in the mutant egg chambers than in controls. Instead, to test whether the *grk* RNA particle movement is reduced in *dhc* alleles, we injected *grk* RNA into *dhc* mutant embryos. We found that, in control embryos, the localization of injected *grk* RNA (Figures 5A–5C) was very similar to that of *wg* and pair-rule transcripts previously characterized in embryos (Wilkie and Davis, 2001). Injected *grk* RNA particles localize in control embryos at an average speed of 0.46 ± 0.09 μm/sec (n = 21 particle movements). In two different allelic combinations of *dhc* mutants (dhc^{8-1}/dhc^{6-10} and dhc^{6-6}/dhc^{6-8}), the speed of movement of *grk* particles is reduced to 0.198 ± 0.048 μm/sec (n = 78 particle movements) and 0.19 ± 0.06 μm/sec (n = 82 particle movements), respectively. We conclude that, despite not normally being present in the embryo, *grk* RNA is able to recruit all the machinery required for Dynein-dependent apical localization. These data also strengthen the conclusion that *grk* RNA localizes by a Dynein-dependent mechanism in the oocyte.

To test the dependence of the dorsoanterior movement of *grk* RNA on Dynein, we injected *grk* RNA and waited for approximately 30 min, until the RNA completed most of the first step, and then injected Colcemid or antibodies against Dhc. Either Colcemid (Figures 5D and E) or anti-Dhc (Figures 5F and 5G) injection after completion of the first step does not strongly affect the distribution of RNA that is already localized at the anterior, but the anterior RNA is unable to continue on the second step to the dorsoanterior corner. We interpret these results as follows. Colcemid reduces the length of MTs but does not depolymerize MTs completely. Anteriorly localized RNA (that has completed only the first step) remains bound to the short MTs at the anterior but is unable to move dorsally because the MTs leading to the dorsoanterior corner are also much shortened.

An Anterior Network of MTs Surrounds the Oocyte Nucleus and Contains a High Concentration of MT Minus Ends in a Dorsoanterior Cap

The existence of two distinct MT- and Dynein-dependent steps of *grk* RNA localization in the oocyte suggests that the two steps could involve movement along two distinct MT networks. Previous experiments in stage 9 oocytes do not address this question directly but show that MTs exist in an anteroposterior gradient, with high concentrations in the anterior and low concentrations at the posterior (see Introduction).

To attempt to visualize the different networks of MTs on which the two steps of *grk* RNA localization could occur, we improved the resolution and sensitivity of detection of minus ends of MTs with the Nod-LacZ marker using immunodetection with fluorescent secondary antibodies (see Experimental Procedures), instead of histochemical detection with X-gal staining (Clark et al., 1997). Our results show that there is a concentration of minus ends all over the anterior of the oocyte, as previously reported (Clark et al., 1997), but also a particularly high concentration in a dorsoanterior cap around the nucleus (Figure 6A). Minus ends of MTs are also found along the entire anterior cortex, with lower concentrations in the middle of the anterior "plate" as well as some minus ends at the junction of the follicle cells and oocyte (Figure 6B). Nod-LacZ distribution is therefore different from that of *grk* mRNA, as it is likely to mark all minus ends of MTs, whereas *grk* mRNA mostly localizes at the dorsoanterior cap.

To further study the distinction between *grk* RNA and Nod-LacZ distribution, we crossed the Nod-LacZ marker into a *squid* mutant background (see Experimental Procedures) previously shown to disrupt *grk* mRNA disrtribution (this paper and Norvell et al., 1999). In contrast to *grk* mRNA, Nod-LacZ distribution in *squid* mutants is indistinguishable from that in control egg chambers (data not shown and Figure 6). We conclude that, while Nod-LacZ is a marker for all minus ends of MTs

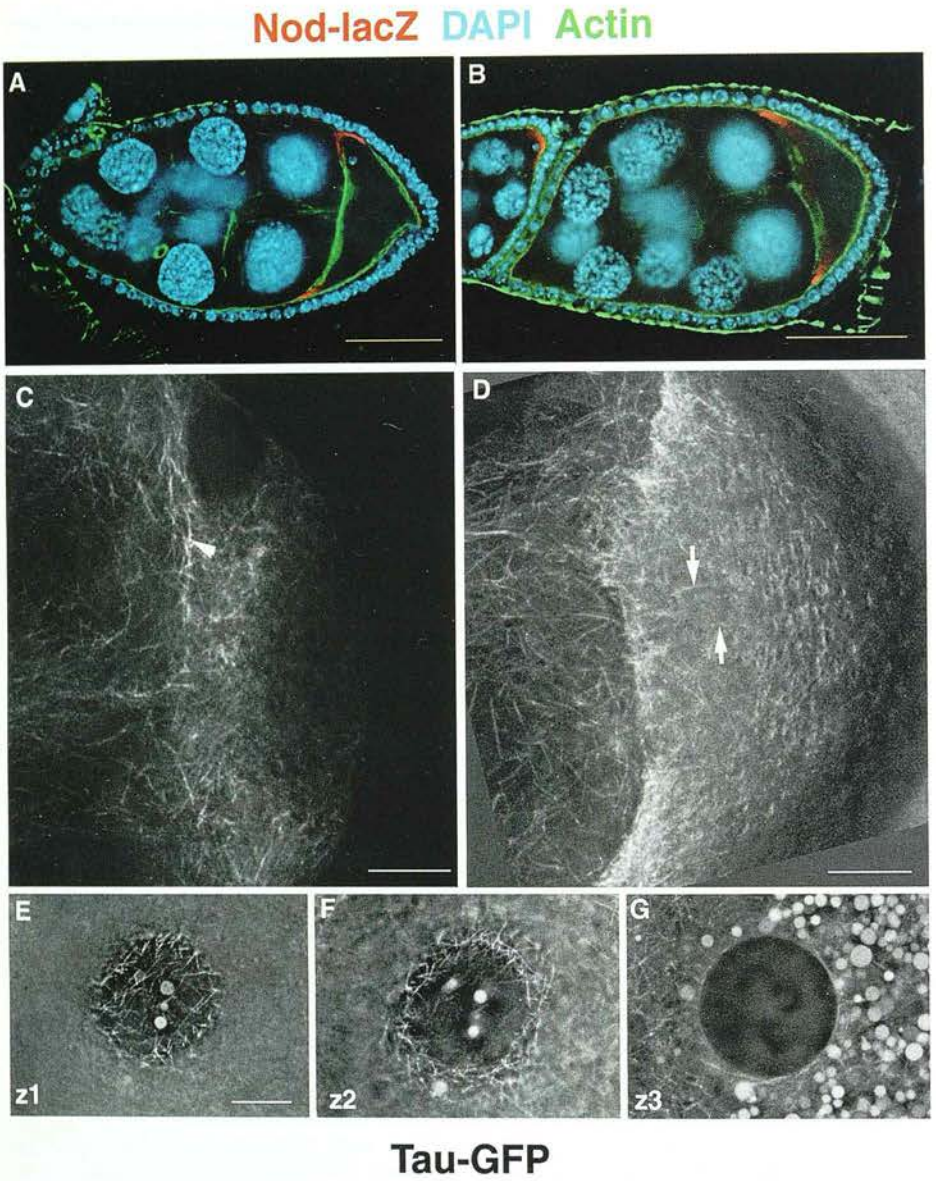

Figure 6. A Network of MTs Is Associated with the Oocyte Nucleus, with MT Minus Ends at a Dorsoanterior Cap

(A–B) Stage 9 Nod-LacZ egg chambers stained with polyclonal anti β-galactosidase antibody visualized by fluorescent secondary antibody (red). Phalloidin-Alexa 488 staining (green) and DAPI staining (cyan) visualize actin and DNA, respectively.

(A) Nod-LacZ, the putative MT minus end marker, is strongly localized at the dorsoanterior cap (where the condensed DNA of the oocyte nucleus can be seen in the DAPI channel) and more weakly in a ventroanterior cap.

(B) Another similar egg chamber orientated with the dorsal side pointing out of the page, showing an anterior cortical ring of Nod-LacZ as well as fainter Nod-LacZ accumulation in the center of the anterior. Note that the red channel is more strongly contrasted in (B) than in (A).

(C–G) Tau-GFP egg chambers revealing MT distribution around the oocyte nucleus and in the anterior region in stage 9 oocytes.

(C) A network of MTs can be visualized surrounding the oocyte nucleus and near the anterior of the oocyte.

(D) A cross-section through the center of a similar Tau-GFP egg chamber revealing some MT arrays deep in the anterior of the oocyte.

(E–G) A high-powered image of three different focal planes (Z1–Z3) of the oocyte nucleus in a Tau-GFP egg chamber (dorsal pointing out of the page). Z2 is 1.5 μm deeper than Z1, and Z3 is 4 μm deeper than Z2. The MTs form a basket around the nucleus (E and F) and extend into the oocyte (G). Note that single MTs are more clearly visible on the surface than in the interior of the oocyte and in the nurse cells that lack the autofluorescence of the yolk. Long segments of MTs are only occasionally visualized, when they lie in the plane of focus ([C], arrowheads; [D], arrows).

in the oocyte, Squid is required for *grk* RNA to localize specifically to a subset of minus ends at the dorsoanterior corner.

We also studied the distribution of MTs in living specimens using the Tau-GFP marker, which decorates MTs, by improving the imaging of MTs near the surface (see

Experimental Procedures) at a higher magnification and resolution than previously described (Januschke et al., 2002; Micklem et al., 1997). A highly convoluted array of MTs exists in the anterior of the oocyte (Figure 6C). Optical sectioning through the nucleus reveals that this anterior array of MTs forms a basket around the oocyte nucleus (Figures 6C and 6E–6G). MTs could also be visualized in the center of the anterior (Figure 6D). These results support, but do not demonstrate conclusively, the existence of two distinct networks of MTs, one forming a basket surrounding the oocyte nucleus, with the MT minus ends at the dorsoanterior cap, and the other with the minus ends at the diffuse anterior MTOC and the plus ends extending toward the posterior. While many MTs appear very short because they do not lie in the plane of observation, some long MTs are observed, which could provide tracks on which *grk* RNA travel anteriorly during the first step, or dorsally during the second step, of localization (Figures 6C and 6D).

Discussion

We have shown that, like *wg* and pair-rule transcripts in the embryo (Bullock and Ish-Horowicz, 2001; Wilkie and Davis, 2001), injected *grk* RNA is able to recruit all the factors required for its correct localization within the cytoplasm of stage 9 oocytes or blastoderm embryos. *grk* RNA assembles into particles that move in two distinct steps within the oocyte to the dorsoanterior corner of the oocyte. The particles first move through the interior of the oocyte to the anterior and then turn and move toward the nucleus and become localized to a dorsoanterior cap. The switch from step one to two occurs most frequently near the anterior, but can also occur in the interior of the oocyte. Both steps of *grk* RNA movement require MTs and Dynein. We propose that the two steps are mechanistically distinct and occur on different networks of MTs.

We have shown that *grk* RNA particle movements in the oocyte are Dynein dependent, as is the apical localization of injected *grk* (this paper), *wg*, and pair-rule RNA particles in the embryo (Wilkie and Davis, 2001). The differences in speeds of particle movements observed in the embryo and oocyte are most likely due to inherent differences in the tissues, rather than an indication of fundamentally different mechanisms of motility. We suggest that the slower speeds of RNA particle movements observed in the oocyte are due to greater frequencies of particle pausing as well as the fact that all known developmental processes are much slower in the oocyte than in the embryo. Furthermore, it is generally accepted that the in vivo speeds of molecular motors can vary considerably from their speeds in vitro because of availability of accessory factors and in vivo regulation.

We were able to study the movement of *grk* RNA only in oocytes whose MTs have already undergone repolarization (stage 8 and later), as injection into the smaller, earlier stages causes a severe disruption of cytoplasmic position and is more difficult to interpret. Nevertheless, we anticipate that, before stage 7, injected *grk* RNA would most likely localize to the posterior, where the minus ends of MTs are located. There are many reasons to think that endogenous *grk* mRNA localization occurs by similar mechanisms to those we have defined for injected *grk* RNA. First, injected and endogenous *grk* RNA localize to very similar sites in the oocyte and are localized to a similar punctate distribution in the dorsoanterior corner. Second, *grk* is the only RNA that is known to localize dorsoanteriorly when injected into the oocyte; others tested localize anteriorly (*K10*) or do not localize (*bcd*, mutant *K10*, and *hb*). Third, injected and endogenous *grk* RNA are mislocalized in precisely the same way in *squid* mutants. Fourth, both injected and endogenous *grk* RNA localization depend on MTs and Dynein (Duncan and Warrior, 2002; Januschke et al., 2002).

It is currently not resolved where *grk* RNA is synthesized. One view is that *grk* is transcribed in the nurse cells, like *bcd* and *osk*, and is subsequently transported into the oocyte (Thio et al., 2000). Another view is that it is transcribed by the oocyte nucleus (Saunders and Cohen, 1999). It seems most likely that *grk* is synthesized at different sites at different times of oogenesis: in early stages, it is synthesized by the nurse cells and, in late stages, by the oocyte nucleus. Whatever the site of synthesis of *grk* RNA, our description of the path of movement and mechanism of movement of injected *grk* RNA is likely to be relevant to endogenous *grk* transcripts. If *grk* is transcribed in the nurse cells, then the two-step movement provides a Dynein-dependent mechanism for delivering *grk* RNA to the dorsoanterior corner from its site of entry into the oocytes. Alternatively, if *grk* RNA is synthesized by the oocyte nucleus, then the same two steps would deliver *grk* RNA to the dorsoanterior corner after export out of the oocyte nucleus.

The Oocyte Contains Distinct Networks of MTs, Each of which Has Its Own Specific Minus Ends

We have analyzed the organization of MTs in the oocyte with high-resolution imaging of Tau-GFP and Nod-LacZ distributions in the oocyte. We detect a particularly high concentration of MT minus ends at the dorsoanterior corner as well as in the anterior cortex and entire anterior. The presence of an MT network associated with the oocyte nucleus explains why a higher concentration of MTs are found in the anterior than in the posterior (Micklem et al., 1997), despite the diffuse nature of the MTOC in the oocyte. A distinct network of MTs associated with the oocyte nucleus also explains why, in *merlin* mutant oocytes, we observed injected *grk* RNA accumulating at the posterior, where the oocyte nucleus is located. We also detect a high concentration of MT minus ends in an anterior ring in addition to a lower concentration all over the anterior. Considering all our results in the context of the previously published data on MT distribution in the oocyte leads us to propose the following model for MT organization in the oocyte (Figure 7). In addition to MTs with their minus ends at the diffuse anterior MTOC (Figure 7, green) and their plus ends at the posterior (Clark et al., 1994, 1997; Micklem et al., 1997), there are some other MTs with their minus ends throughout all parts of the cortex (Figure 7, cyan) (Cha et al., 2001, 2002). We propose that, in addition to these networks, there is also a distinct network of MTs that

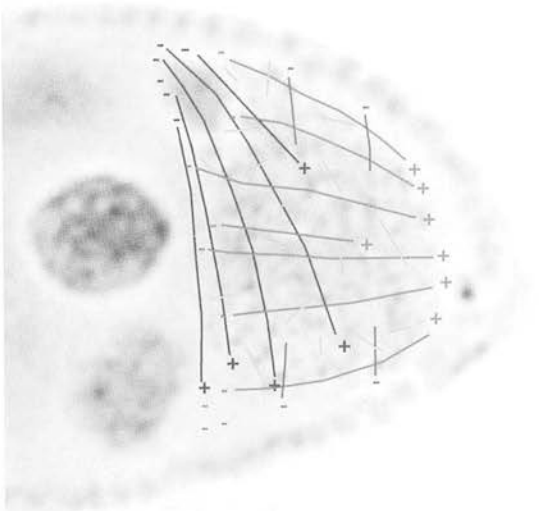

Figure 7. Model for the Organization of MTs in the Oocyte

Four classes of MTs are drawn in red, blue, green, and yellow over a black and white inverted image of an nlsGFP egg chamber. Green MTs have their plus ends at the posterior and minus end all over the anterior; we propose that they are used to transport *grk* RNA during the first step of its localization. Blue MTs have their minus ends at the cortex and are proposed to be used by Kin I to exclude *osk* RNA from the cortex (see text). Red MTs are specifically associated with the oocyte nucleus forming a high concentration of minus ends in the dorsoanterior cap. We propose that only the second step of *grk* localization, but not anterior localization of *bcd* and *K10* RNAs, occurs on these MTs. Yellow MTs have no orientation, and their minus ends occur throughout the entire oocyte. Magenta MT minus ends are part of an array in the anterior.

are specifically associated with the oocyte nucleus (Figure 7, red). These MTs form a loose basket surrounding the nucleus and radiate throughout the anterior and partly into the middle of the oocyte. Our observations of Tau-GFP and previous work (Cha et al., 2001) suggest that there are many other MTs that are more loosely organized throughout much of the oocyte (Figure 7, yellow).

The organization of MTs we propose provides a good explanation for why the *grk* particle movements we observe occur in two distinct steps. We propose that, during the first step of movement of *grk* particles to the anterior of the oocyte, the RNA is likely to be moving on MTs whose plus ends are at the posterior of the oocyte and whose minus ends are along the entire anterior. The second step of movement of the particles is likely to occur on the MT network that forms a basket around the nucleus, with the MT minus ends at the dorsoanterior corner and the plus ends extending toward the anterior and, also, partly into the middle of the oocyte. This model for MT organization fits well with the fact that many *grk* RNA particles were observed to make sharp turns at the anterior, and some in the interior, of the oocyte.

A Model for Sorting Different Transcripts to Distinct Subsets of MT Minus Ends with the Same Dynein Motor

Our model showing that distinct classes of MTs exist within the oocyte begs the question, how does Dynein-dependent transport deliver *grk* RNA to a very different destination from other RNAs in the oocyte, which may also be transported to the minus ends of MTs by Dynein? We propose that different RNAs that are transported to the minus ends of MTs by the same Dynein motors could move on distinct networks of MTs. This would explain why the destination of injected *bcd* RNA (which is thought to require Dynein for its localization [Schnorrer et al., 2000]), depends on whether it is preexposed to nurse cell cytoplasm (Cha et al., 2001). *bcd* RNA injected into the oocyte moves to the nearest cortex along MTs whose minus ends are at the cortex. However, *bcd* RNA that is preexposed to nurse cell cytoplasm is able to move from the posterior to the anterior of the oocyte, apparently in a similar route to that in step 1 of *grk* localization, which we have defined (Cha et al., 2001). Step 2 of *grk* RNA particle movement is not shared with *bcd* RNA and could occur along the MT network that is specifically associated with the oocyte nucleus. Interestingly, *bcd*, but not *grk*, mRNA localization requires γ-Tub37C and Dgrip75 (Schnorrer et al., 2002).

It is most likely that specific transacting factors that recognize RNA signals are responsible for determining which RNAs use which motors and also which distinct MT network is utilized during the Dynein-dependent transport to different destinations. For example, in nerve cells, the choice of cytoplasmic destination of cargo transported by Kinesin is determined by the presence or absence of a protein called GRIP (Setou et al., 2002). Such key transacting factors are likely to also include Squid (Kelley, 1993) and K10 (Cheung et al., 1992), since, in mutants of these genes, *grk* mRNA is localized in the anterior, rather than the dorsoanterior corner (Norvell et al., 1999; Serano et al., 1995). However, in addition to the transacting factors, the different MTs are likely to differ in some way, allowing the different kinds of RNA-motor complexes to distinguish among them. Such differences could include chemical modifications of tubulin or different tubulin isoforms as well as distinct populations of MT-associated proteins (MAPs). It is also possible that γTub37C and Dgrip75 (Schnorrer et al., 2002) could be involved in selectively nucleating a subset of MTs used for *bcd*, but not *grk*, mRNA localization.

Dynein-dependent motility of RNA and other cargo to the minus ends of MTs is likely to be a widely deployed mechanism within cells. Selective utilization of different MT networks would provide a nice way to sort different cellular components that are transported by the same Dynein motor to a variety of distinct minus ends in the same cell. Our rapid and efficient real-time assays for mRNA localization will allow us to begin to define the *cis*-acting signals and *trans*-acting factors that determine which subset of MTs are selected by different RNA cargos that utilize the same motors.

Experimental Procedures

Fly Strains

Stocks were raised on standard cornmeal-agar medium at 25°C. RNA was injected into wild-type (Oregon R) egg chambers or those of a strain with four copies of the nlsGFP transgene (yw; nlsGFPM; nlsGFPN) (Davis et al., 1995) and *sqd*^{1}*/Df(3)urd* (Norvell et al., 1999). *yw, mer*^{ts1} females were dissected after shifting homozygous females to the restrictive temperature for 3 days (MacDougall et al.,

2001) prior to injection. *dhc64C* mutants were from T. Hays (Gepner et al., 1996). The semiviable allelic combinations used ($dhc^{6\text{-}6}/dhc^{6\text{-}12}$) are slightly more severe than the viable allelic combinations of $dhc^{8\text{-}1}/dhc^{6\text{-}10}$ and $dhc^{6\text{-}6}/dhc^{6\text{-}8}$, in which the speed of apical mRNA transport in the blastoderm embryo is reduced (Wilkie and Davis, 2001).

RNA In Situ Hybridization

In situ hybridization was performed as previously described (Wilkie et al., 1999) by fluorescent tyramide detection (NEN LifeSciences). *grk* probes were fragmented in carbonate buffer (Cox et al., 1984) to allow greater probe penetration. Ovaries were prepared for hybridization as described in MacDougall et al. (2001).

Synthesis of Fluorescently Labeled, Capped RNA

RNA was transcribed in vitro as previously described (Wilkie and Davis, 2001) from plasmids containing *grk* cDNA (G. Schüpbach), *hb* cDNA (B. Edgar), *K10 tls* (transport localization signal), or *K10 mutant tls* (R. Cohen and S. Bullock).

Injection of RNA and Inhibitors

Prior to injection, egg chambers were dissected directly onto coverslips in Series 95 halocarbon oil (KMZ Chemicals). Egg chambers were separated into individual ovarioles or egg chambers for injection. Oocytes were microinjected with Femtotip needles (Eppendorf). RNAs were injected at concentrations of 250–500 ng/μl, and Colcemid (Sigma) was injected at concentrations of 100 μg/ml or 30 μg/ml. Anti-Dynein antibodies (T. Hays or D. Sharp) were spot dialyzed as previously described (Wilkie and Davis, 2001).

Immunolocalization of Proteins

Ovaries were dissected and prepared for DAPI, phalloidin, and antibody stainings as previously described (MacDougall et al., 2001), with the following modifications. Ovaries were dissected directly into 3.7% formaldehyde in PBS with 0.1% Triton X and fixed for 20 min. Incubation in a polyclonal rabbit anti β-galactosidase antibody (ICN) at 1:10,000 dilution was performed overnight at 4°C. After three 20 min washes in PBS with 0.1% Triton X, ovaries were incubated with an Alexa Fluor 546-coupled secondary antibody (Molecular Probes) for three hours at room temperature.

Four-Dimensional Imaging and Deconvolution

Fixed egg chambers were mounted in Vectashield (Vector Laboratories). Tau-GFP fluorescence was imaged by placing a breathable membrane (YSI) over the egg chambers after dissection in halocarbon oil on a coverslip, as previously described (Davis, 2000). Imaging was performed on a widefield DeltaVision microscope (Applied Precision) based closely on an original design by John Sedat and David Agard. The microscope consists of an Olympus IX70 inverted microscope with a 12 bit cooled CCD camera (Coolsnap HQ; Roper). Images were acquired with 20×/0.75 NA or 100×/1.4 NA objective lenses selected for symmetric point spread functions and spherical aberration corrected. Out of focus light was reassigned to its point of origin by iterative deconvolution (Davis, 2000). Up to five egg chambers were imaged in parallel, by repeat visiting with a highly accurate XYZ motorized stage.

Particle Tracking

Particles were tracked with a 100×/1.4 NA objective lens and time-lapse intervals of 1 s. Moving particles were manually tracked with DeltaVision (Applied Precision) and Metamorph (Universal Imaging Corporation) image analysis software. The speeds of movement of particles were calculated in micrometers per second according to the distance traveled in each time interval. A vector was taken between the first and last points of each tracked particle to calculate the overall direction of movement. The directions traveled were then calculated with reference to the anteroposterior and dorsoventral axes or the center of the nucleus, as determined by low-magnification imaging in brightfield images or nlsGFP. The directions of movement of particles moving anteriorly and then dorsolaterally were calculated with vectors representing the anterior and lateral phases separately. The directions and speeds of all particles tracked were calculated and plotted with Microsoft Excel. The dorsoanterior phase of the movement toward the nucleus was more difficult to observe, as the particles were spread over a wide range of planes of focus after moving from the site of injection to the anterior of the oocyte. Two approaches were used to identify the dorsoanterior phase of movement. Particles were either injected at the anterior and imaged directly or injected in the center of the oocyte and imaged 20 min later, when they had moved to the anterior. In all cases, particles were analyzed from at least two different egg chambers.

Acknowledgments

We thank David Ish-Horowicz, Catherine Rabouille, Simon Bullock, Isabelle Kos, Veronique Van De Bor, Renald Delanoue, and Hildegard Tekotte for their constructive comments on the manuscript. This work was funded by a Lister Fellowship, a Wellcome Trust Senior Fellowship to I.D., and Darwin Trust, Edinburgh University, and Wellcome Trust studentships to N.M., A.C., and E.M., respectively.

Received: September 16, 2002
Revised: January 10, 2003

References

Bertrand, E., Chartrand, P., Schaefer, M., Shenoy, S.M., Singer, R.H., and Long, R.M. (1998). Localization of ASH1 mRNA particles in living yeast. Mol. Cell *2*, 437–445.

Bobola, N., Jansen, R.P., Shin, T.H., and Nasmyth, K. (1996). Asymmetric accumulation of Ash1p in postanaphase nuclei depends on a myosin and restricts yeast mating-type switching to mother cells. Cell *84*, 699–709.

Brendza, R., Serbus, L., Saxton, W., and Duffy, J. (2002). Posterior localization of Dynein and dorsal-ventral axis formation depend on Kinesin in *Drosophila* oocytes. Curr. Biol. *12*, 1541.

Brendza, R.P., Serbus, L.R., Duffy, J.B., and Saxton, W.M. (2000). A function for kinesin I in the posterior transport of *oskar* mRNA and Staufen protein. Science *289*, 2120–2122.

Bullock, S.L., and Ish-Horowicz, D. (2001). Conserved signals and machinery for RNA transport in *Drosophila* oogenesis and embryogenesis. Nature *414*, 611–616.

Cha, B., Koppetsch, B.S., and Theurkauf, W.E. (2001). In vivo analysis of *Drosophila bicoid* mRNA localization reveals a novel microtubule-dependent axis specification pathway. Cell *106*, 35–46.

Cha, B.J., Serbus, L.R., Koppetsch, B.S., and Theurkauf, W.E. (2002). Kinesin I-dependent cortical exclusion restricts pole plasm to the oocyte posterior. Nat. Cell Biol. *4*, 592–598.

Cheung, H.K., Serano, T.L., and Cohen, R.S. (1992). Evidence for a highly selective RNA transport system and its role in establishing the dorsoventral axis of the Drosophila egg. Development *114*, 653–661.

Clark, I., Giniger, E., Ruohola-Baker, H., Jan, L.Y., and Jan, Y.N. (1994). Transient posterior localization of a kinesin fusion protein reflects anteroposterior polarity of the *Drosophila* oocyte. Curr. Biol. *4*, 289–300.

Clark, I.E., Jan, L.Y., and Jan, Y.N. (1997). Reciprocal localization of Nod and kinesin fusion proteins indicates microtubule polarity in the *Drosophila* oocyte, epithelium, neuron and muscle. Development *124*, 461–470.

Cox, K.H., DeLeon, D.V., Angerer, L.M., and Angerer, R.C. (1984). Detection of mRNAs in sea urchin embryos by in situ hybridization using asymmetric RNA probes. Dev. Biol. *101*, 485–502.

Davis, I. (2000). Visualising fluorescence in *Drosophila*—optimal detection in thick specimens. In Protein Localisation by Fluorescence Microscopy: A Practical Approach, V.J. Allan, ed. (Oxford: OUP), pp. 131–162.

Davis, I., Girdham, C.H., and O'Farrell, P.H. (1995). A nuclear GFP that marks nuclei in living *Drosophila* embryos—maternal supply overcomes a delay in the appearance of zygotic fluorescence. Dev. Biol. *170*, 726–729.

Davis, I., and Ish-Horowicz, D. (1991). Apical localization of pair-rule transcripts requires 3′ sequences and limits protein diffusion in the *Drosophila* blastoderm embryo. Cell *67*, 927–940.

Driever, W., and Nüsslein-Volhard, C. (1988). A gradient of bicoid protein in *Drosophila* embryos. Cell *54*, 83–93.

Duncan, J.E., and Warrior, R. (2002). The cytoplasmic Dynein and Kinesin motors have interdependent roles in patterning the *Drosophila* oocyte. Curr. Biol. *12*, 1982–1991.

Ephrussi, A., Dickinson, L.K., and Lehmann, R. (1991). Oskar organizes the germ plasm and directs localization of the posterior determinant nanos. Cell *66*, 37–50.

Erdelyi, M., Michon, A.M., Guichet, A., Glotzer, J.B., and Ephrussi, A. (1995). Requirement for *Drosophila* cytoplasmic tropomyosin in *oskar* mRNA localization. Nature *377*, 524–527.

Gepner, J., Li, M., Ludmann, S., Kortas, C., Boylan, K., Iyadurai, S.J., McGrail, M., and Hays, T.S. (1996). Cytoplasmic dynein function is essential in *Drosophila* melanogaster. Genetics *142*, 865–878.

Glotzer, J.B., Saffrich, R., Glotzer, M., and Ephrussi, A. (1997). Cytoplasmic flows localize injected *oskar* RNA in *Drosophila* oocytes. Curr. Biol. *7*, 326–337.

Gonzalez-Reyes, A., Elliott, H., and St Johnston, D. (1995). Polarization of both major body axes in *Drosophila* by Gurken-Torpedo signaling. Nature *375*, 654–658.

Gonzalez-Reyes, A., and St Johnston, D.S. (1998). Patterning of the follicle cell epithelium along the anterior-posterior axis during *Drosophila* oogenesis. Development *125*, 2837–2846.

Jansen, R.P. (2001). mRNA localization: message on the move. Nat. Rev. Mol. Cell Biol. *2*, 247–256.

Jansen, R.P., Dowzer, C., Michaelis, C., Galova, M., and Nasmyth, K. (1996). Mother cell-specific HO expression in budding yeast depends on the unconventional myosin myo4p and other cytoplasmic proteins. Cell *84*, 687–697.

Januschke, J., Gervais, L., Dass, S., Kaltschmidt, J.A., Lopez-Schier, H., Johnston, D.S., Brand, A.H., Roth, S., and Guichet, A. (2002). Polar transport in the *Drosophila* oocyte requires Dynein and Kinesin I cooperation. Curr. Biol. *12*, 1971–1981.

Kelley, R.L. (1993). Initial organization of the Drosophila dorsoventral axis depends on an RNA-binding protein encoded by the *squid* gene. Genes Dev. *7*, 948–960.

King, S.J., and Schroer, T.A. (2000). Dynactin increases the processivity of the cytoplasmic dynein motor. Nat. Cell Biol. *2*, 20–24.

Kloc, M., Zearfoss, N.R., and Etkin, L.D. (2002). Mechanisms of subcellular mRNA localization. Cell *108*, 533–544.

Lall, S., Francis-Lang, H., Flament, A., Norvell, A., Schupbach, T., and Ish-Horowicz, D. (1999). Squid hnRNP protein promotes apical cytoplasmic transport and localization of *Drosophila* pair-rule transcripts. Cell *98*, 171–180.

Lipshitz, H.D., and Smibert, C.A. (2000). Mechanisms of RNA localization and translational regulation. Curr. Opin. Genet. Dev. *10*, 476–488.

Long, R.M., Gu, W., Lorimer, E., Singer, R.H., and Chartrand, P. (2000). She2p is a novel RNA-binding protein that recruits the Myo4p-She3p complex to ASH1 mRNA. EMBO J. *19*, 6592–6601.

MacDougall, N., Lad, Y., Wilkie, G., Francis-Lang, H., Sullivan, W., and Davis, I. (2001). Merlin, the *Drosophila* homologue of Neurofibromatosis-2, is specifically required in posterior follicle cells for axis formation in the oocyte. Development *128*, 665–673.

Micklem, D.R., Dasgupta, R., Elliott, H., Gergely, F., Davidson, C., Brand, A., Gonzalez-Reyes, A., and St Johnston, D. (1997). The *mago nashi* gene is required for the polarisation of the oocyte and the formation of perpendicular axes in *Drosophila*. Curr. Biol. *7*, 468–478.

Munchow, S., Sauter, C., and Jansen, R.P. (1999). Association of the class V myosin Myo4p with a localised messenger RNA in budding yeast depends on She proteins. J. Cell Sci. *112*, 1511–1518.

Neuman-Silberberg, F.S., and Schüpbach, T. (1993). The *Drosophila* dorsoventral patterning gene *gurken* produces a dorsally localized RNA and encodes a TGF alpha-like protein. Cell *75*, 165–174.

Nilson, L.A., and Schüpbach, T. (1999). EGF receptor signaling in *Drosophila* oogenesis. Curr. Top. Dev. Biol. *44*, 203–243.

Norvell, A., Kelley, R.L., Wehr, K., and Schüpbach, T. (1999). Specific isoforms of Squid, a *Drosophila* hnRNP, perform distinct roles in *gurken* localization during oogenesis. Genes Dev. *13*, 864–876.

Palacios, I.M., and Johnston, D.S. (2001). Getting the message across: the intracellular localization of mRNAs in higher eukaryotes. Annu. Rev. Cell Dev. Biol. *17*, 569–614.

Palacios, I.M., and Johnston, D.S. (2002). Kinesin light chain-independent function of the Kinesin heavy chain in cytoplasmic streaming and posterior localisation in the Drosophila oocyte. Development *129*, 5473–5485.

Pokrywka, N.J., and Stephenson, E.C. (1991). Microtubules mediate the localization of *bicoid* RNA during *Drosophila* oogenesis. Development *113*, 55–66.

Saunders, C., and Cohen, R.S. (1999). The role of oocyte transcription, the 5′UTR, and translation repression and derepression in *Drosophila gurken* mRNA and protein localization. Mol. Cell *3*, 43–54.

Schnorrer, F., Bohmann, K., and Nüsslein-Volhard, C. (2000). The molecular motor dynein is involved in targeting swallow and *bicoid* RNA to the anterior pole of *Drosophila* oocytes. Nat. Cell Biol. *2*, 185–190.

Schnorrer, F., Luschnig, S., Koch, I., and Nusslein-Volhard, C. (2002). *γ-Tubulin37C* and *γ-tubulin ring complex protein 75* are essential for *bicoid* RNA Localization during *Drosophila* oogenesis. Dev. Cell *3*, 685–696.

Serano, T.L., and Cohen, R.S. (1995). A small predicted stem-loop structure mediates oocyte localization of Drosophila K10 mRNA. Development *121*, 3809–3818.

Serano, T.L., Karlin-McGinness, M., and Cohen, R.S. (1995). The role of fs(1)K10 in the localization of the mRNA of the TGF alpha homolog gurken within the *Drosophila* oocyte. Mech. Dev. *51*, 183–192.

Setou, M., Seog, D.H., Tanaka, Y., Kanai, Y., Takei, Y., Kawagishi, M., and Hirokawa, N. (2002). Glutamate-receptor-interacting protein GRIP1 directly steers kinesin to dendrites. Nature *417*, 83–87.

St Johnston, D., Driever, W., Berleth, T., Richstein, S., and Nüsslein-Volhard, C. (1989). Multiple steps in the localization of bicoid RNA to the anterior pole of the *Drosophila* oocyte. Development *107*, 13–19.

Takizawa, P.A., and Vale, R.D. (2000). The myosin motor, Myo4p, binds Ash1 mRNA via the adapter protein, She3p. Proc. Natl. Acad. Sci. USA *97*, 5273–5278.

Tekotte, H., and Davis, I. (2002). Intracellular mRNA localization: motors move messages. Trends Genet. *18*, 636–642.

Theurkauf, W.E., and Hazelrigg, T.I. (1998). In vivo analyses of cytoplasmic transport and cytoskeletal organization during *Drosophila* oogenesis: characterization of a multi-step anterior localization pathway. Development *125*, 3655–3666.

Theurkauf, W.E., Smiley, S., Wong, M.L., and Alberts, B.M. (1992). Reorganization of the cytoskeleton during *Drosophila* oogenesis—implications for axis specification and intercellular transport. Development *115*, 923–936.

Thio, G.L., Ray, R.P., Barcelo, G., and Schüpbach, T. (2000). Localization of gurken RNA in *Drosophila* oogenesis requires elements in the 5′ and 3′ regions of the transcript. Dev. Biol. *221*, 435–446.

van Eeden, F., and St Johnston, D. (1999). The polarisation of the anterior-posterior and dorsal-ventral axes during *Drosophila* oogenesis. Curr. Opin. Genet. Dev. *9*, 396–404.

Vanzo, N.F., and Ephrussi, A. (2002). Oskar anchoring restricts pole plasm formation to the posterior of the *Drosophila* oocyte. Development *129*, 3705–3714.

Wilhelm, J.E., Mansfield, J., Hom-Booher, N., Wang, S., Turck, C.W.,

Hazelrigg, T., and Vale, R.D. (2000). Isolation of a ribonucleoprotein complex involved in mRNA localization in *Drosophila* oocytes. J. Cell Biol. *148*, 427–440.

Wilkie, G.S., and Davis, I. (2001). *Drosophila wingless* and pair-rule transcripts localize apically by dynein-mediated transport of RNA particles. Cell *105*, 209–219.

Wilkie, G.S., Shermoen, A.W., O'Farrell, P.H., and Davis, I. (1999). Transcribed genes are localized according to chromosomal position within polarized *Drosophila* embryonic nuclei. Curr. Biol. *9*, 1263–1266.